Complexity

Finite-time Control of Complex Systems and Their Applications 2021

Lead Guest Editor: Xiaodi Li
Guest Editors: Jianquan Lu, Oh-Min Kwon, and Sabri Arik

Finite-time Control of Complex Systems and Their Applications 2021

Complexity

Finite-time Control of Complex Systems and Their Applications 2021

Lead Guest Editor: Xiaodi Li
Guest Editors: Jianquan Lu, Oh-Min Kwon, and Sabri Arik

Contents

Terminal Sliding-Mode Control of Uncertain Robotic Manipulator System with Predefined Convergence Time
Yang Wang, Mingshu Chen, and Yu Song
Research Article (16 pages), Article ID 9991989, Volume 2021 (2021)

Finite-Time Impulsive Control of Financial Risk Dynamic System with Chaotic Characteristics
Li Ziyan, Tao Ke, Xia Qing, Xie Chengrong, and Xu Yuhua
Research Article (8 pages), Article ID 5207154, Volume 2021 (2021)

Hindawi
Complexity
Volume 2022, Article ID 6279373, 14 pages
https://doi.org/10.1155/2022/6279373

Research Article

A Novel Highly Nonlinear Quadratic System: Impulsive Stabilization, Complexity Analysis, and Circuit Designing

Arthanari Ramesh,[1] **Alireza Bahramian**,[2] **Hayder Natiq**,[3] **Karthikeyan Rajagopal**,[4] **Sajad Jafari**,[2,5] **and Iqtadar Hussain**[6,7]

[1]*Centre for Materials Research, Chennai Institute of Technology, Chennai, India*
[2]*Department of Biomedical Engineering, Amirkabir University of Technology (Tehran Polytechnic), Tehran, Iran*
[3]*Information Technology Collage, Imam Ja'afar Al-Sadiq University, 10001 Baghdad, Iraq*
[4]*Centre for Nonlinear Systems, Chennai Institute of Technology, Chennai, India*
[5]*Health Technology Research Institute, Amirkabir University of Technology (Tehran Polytechnic), Tehran, Iran*
[6]*Mathematics Program, Department of Mathematics, Statistics and Physics, College of Arts and Sciences, Qatar University, 2713 Doha, Qatar*
[7]*Statistical Consulting Unit, College of Arts and Science, Qatar University, Doha, Qatar*

Correspondence should be addressed to Karthikeyan Rajagopal; rkarthiekeyan@gmail.com

Received 20 June 2021; Revised 16 February 2022; Accepted 17 February 2022; Published 30 March 2022

Academic Editor: M. De Aguiar

This work introduces a three-dimensional, highly nonlinear quadratic oscillator with no linear terms in its equations. Most of the quadratic ordinary differential equations (ODEs) such as Chen, Rossler, and Lorenz have at least one linear term in their equations. Very few quadratic systems have been introduced and all of their terms are nonlinear. Considering this point, a new quadratic system with no linear term is introduced. This oscillator is analyzed by mathematical tools such as bifurcation and Lyapunov exponent diagrams. It is revealed that this system can generate different behaviors such as limit cycle, torus, and chaos for its different parameters' sets. Besides, the basins of attractions for this system are investigated. As a result, it is revealed that this system's attractor is self-excited. In addition, the analog circuit of this oscillator is designed and analyzed to assess the feasibility of the system's chaotic solution. The PSpice simulations confirm the theoretical analysis. The oscillator's time series complexity is also investigated using sample entropy. It is revealed that this system can generate dynamics with different sample entropies by changing parameters. Finally, impulsive control is applied to the system to represent a possible solution for stabilizing the system.

1. Introduction

Chaos is a complex behavior that has been investigated in nature and mathematics [1]. It refers to the systems' sensitivity to their initial conditions and parameters [2]. Nonlinear systems such as ordinary differential equations (ODEs) can generate chaotic behavior [3]. Therefore, they can have applications in modeling natural systems with chaotic behaviors such as neurons [4]. Besides, using coupling methods, these systems can investigate collective behaviors of neuronal networks [5]. It is good to mention that sometimes these dynamical systems are used in their nonchaotic mode to model some behaviors of natural systems like central pattern generators (neurons that make rhythms for locomotions) [6]. ODEs chaotic systems have been categorized based on their equilibrium points types and locations [7]. In this way, chaotic systems' attractors can be divided into two groups: ones that have at least one equilibrium point in their basin of attraction (self-excited attractors) [8] and ones that have no equilibrium point in their basin of attraction (hidden attractor(s)) [9]. Besides, the systems' equilibrium points are interesting nonlinear dynamics properties for researchers. For example, systems have been introduced and investigated with a line of

equilibria [9] or just one stable equilibrium [10]. Besides, two main groups of systems can be defined based on the equations' time dependency: autonomous systems in which no term as a function of time exists in their equations [11] and nonautonomous systems in which a term dependent to the time can be found in their equations (forced systems) [12]. Besides, forcing systems can lead nonchaotic oscillators to systems that have the capability of generating chaos. For instance, using this technique, two-dimensional systems that cannot generate chaotic time series can demonstrate chaotic attractors [13]. These nonautonomous systems are also capable of generating hidden attractors [14]. Another method to make a system chaotic is considering delays in the equations of the system. For instance, a system with just one equation can make chaos if it has a time delay in its equation [15]. On the other hand, systems with four dimensions or more can generate hyperchaotic behaviors. For instance, a four-dimensional jerk system implicated with memristors has shown the potential of demonstrating hyperchaos [16]. Besides these features, multistability refers to the existence of several attractors (at least two ones) for different initial values for a system without parameters' changing [17]. In addition to the mentioned properties, some other features are defined for chaotic systems based on the topology and shapes of attractors [18]. Some strange attractors with different symmetries' types were reported [19]. Besides, the systems with several wings' attractors (multiscrolls) have grabbed researchers' interest [20]. For instance, it is investigated how the strange multiscrolls attractor for a system can emerge and how its shape can be preserved [21]. In addition, the systems that their attractors look like known objects were also reported. For instance, chaotic systems have been introduced to look like a Persian carpet [22] or a peanut [23].

Among different ODE systems, quadratic ones are mainly focused on by some researchers interested in finding elegant systems [2]. One reason is that these systems can have simpler equations [24]. Lorenz equations, the first introduced chaotic system, are one of these classes and have just quadratic terms. Some quadratic systems were introduced whose equations' terms are lower than that of the Lorenz equations [24]. Various dynamics of a quadratic system were studied in [25]. Most of the quadratic systems have at least one linear term in one of their equations [26]. Few systems have been introduced with no linear term in their equations [27]. Xu and Wang introduced such a system built by just nonlinear quadratic terms for the first time [28]. As another example of the pure nonlinear systems category, a multistable system can be mentioned with heterogeneous attractors [29]. Here, an oscillator with absolute nonlinear terms is introduced to generate various types of nonlinear dynamics' behaviors such as torus and chaos.

The chaotic feasibility of nonlinear ODEs systems always has been a question. Designing analog circuits for chaotic systems has been a hot topic recently. Electrical circuits simulated with PSpice or implemented physically are tools to assess ODE systems' chaotic behaviors. For example, an electrical circuit was introduced to regenerate the chaotic signals with a multiscroll dynamic [30]. In another instance, analog electrical circuits of a system with multistability were impacted [23]. Using memristors to model chaotic dynamics is one of the hot topics; for instance, a five-dimensional system with three linear dimensions was implicated using two memristors [1]. Besides, chaotic systems' implication using digital circuits like field-programmable gate array (FPGA) has been carried out to assess the possibility of implicating chaotic systems. For instance, a jerk system feasibility with strange coexisting attractors was assessed with FPGA [31]. In another example, the chaotic time series of a system with coexisting attractors and strange fixed points' curves was regenerated using FPGA [23]. One of the applications of these circuits is random number generation [32]. Other applications can be secure communications [33] and image encryption [34]. In this work, the system's analog circuit is designed with PSpice, and the results of simulations are reported.

The complexity of chaotic systems' signals has recently become an exciting subject for researchers [35]. For instance, the complexities of a system with hidden attractors (for time series of its different parameters' values) were calculated and discussed [36]. Sample entropy is a feature for comparing the complexity of time series repetitively [37]. In this method, the philosophy of calculating complexity is based on the possibility of predicting the future of the signals based on their previous samples [37]. This method has some advantages in comparison with other methods of measuring complexity. For instance, it is less dependent on the length of time series than approximated entropy [37]. Here, sample entropy is used for calculating the complexities of the oscillator's signals for different ranges of the introduced system's parameters.

Controlling chaotic oscillators has been an interesting topic [38]. Various methods have been proposed to control the chaotic dynamics [39, 40]. Impulsive control is a method of stabilizing nonlinear systems such as the ones with infinite [41, 42] or finite delays [43], delayed neural networks [44] (that also includes exponentially stabilization [45] and fixed time control [46]), stochastic delayed systems [47], or singularly perturbed models [48]. For instance, it was used for stabilizing systems whose states are not measurable [49]. In another example, an event-based version of this method was used for controlling Chua-coupled systems [50]. This method also has been used for synchronization among nonlinear systems [51], switched complex networks [52, 53], high-dimensional Kuramoto systems [54], and fuzzy neural networks [55]. Some advanced methods of impulsive control have been introduced, for instance, versions with adaptable frequencies [56]. In this paper, an impulsive-based method for controlling the introduced pure nonlinear system is implicated as a possible solution for stabilizing its equilibrium points.

In the next section, the system's equations whose terms are all nonlinear quadratic are presented (Section 2). Also, the oscillator's bifurcation and Lyapunov diagrams for different parameters' values are analyzed. Besides, the basin of attractions of the pure nonlinear oscillator is plotted and discussed. Section 3 explains the design of the introduced pure nonlinear oscillator's analog circuit and its

simulations with PSpice. The next part assesses the complexity of the oscillator's signals for various parameter values (Section 4). Applying the impulsive control method (Section 5) to the proposed system helps to enhance its applications. The simulations' results are concluded in the final part (Section 6).

2. The Highly Nonlinear System: Analytical and Numerical Analysis

The construction of chaotic dynamics is an unknown subject that attracted lots of attention [3, 57]. After revealing some counterexamples for the hypothesis of a relation between saddle equilibrium points and chaotic attractors [58, 59], many works have been focused on studying chaotic flows with unique properties [60, 61]. They have tried to understand the construction of chaotic attractors. Some examples are chaotic flows with different equilibrium points [62, 63] and special attractors [64]. So, a pure nonlinear chaotic flow is proposed here, and its various dynamics are investigated. The oscillator can be described by three-dimension equations that are coupled as follows:

$$\begin{aligned}\dot{x} &= 1.3z^2 - y^2 + a\dot{y}\\ &= y^2 - x^2\dot{z}\\ &= y^2 - x^2 + 0.1z^2 + b,\end{aligned} \tag{1}$$

where x, y, and z are the system's variables when a and b are considered parameters. The system is symmetric with the change of variables $(x, y, x, t) \longrightarrow (-x, -y, -z, -t)$. So any attractor of system (1) has a twin in reversed time and is symmetric to the origin of the main attractor. The system's equilibrium points are as follows:

$$\begin{aligned}0 &= 1.3z^2 - y^2 + a,\\ X &= \pm\sqrt{-13b + a},\\ 0 &= y^2 - x^2 \longrightarrow Y = \pm\sqrt{-13b + a},\\ 0 &= y^2 - x^2 + 0.1z^2 + b,\\ Z &= \pm\sqrt{-10b}.\end{aligned} \tag{2}$$

Considering these eight fixed points, the system's Jacobian and eigenvalues are as follows:

$$J = \begin{bmatrix} 0 & -2Y & 2.6Z \\ -2X & 2Y & 0 \\ -2X & 2Y & 0.2Z \end{bmatrix} \longrightarrow |\lambda I - J| = 0 \longrightarrow \begin{bmatrix} \lambda & 2Y & -2.6Z \\ 2X & \lambda - 2Y & 0 \\ 2X & -2Y & \lambda - 0.2Z \end{bmatrix} \longrightarrow$$
$$\lambda((\lambda - 2Y)(\lambda - 0.2Z) - 0) - 2Y(2X(\lambda - 0.2Z)) - 2.6Z(-4XY - (2X(\lambda - 2Y))) = 0. \tag{3}$$

The types of equilibria when $a = 0.5$ and $b = -2.3$ are shown in Table 1 (considering eigenvalues for each equilibrium).

The system's attractors for different parameters' values have been presented in Figure 1. Figures 1(a)–1(d) demonstrate periods 1, 2, 4 and chaotic behaviors of the oscillator.

The Lyapunov exponent and bifurcation diagrams for different parameters' set are calculated to investigate more about possible behaviors that the introduced system can present. Firstly the b parameter is fixed ($b = -2.3$), and Lyapunov and bifurcation diagrams for a range of a are plotted (Figure 2). Figure 2(a) demonstrates two Lyapunov exponents that have higher values than the rest. The third Lyapunov exponent's values are always negative and have a higher absolute value than the two others. For the two Lyapunov with higher values, the system's behavior is periodic when one is zero and the other is negative. For the situation that one of them is zero and another is positive, the system's behavior is chaotic. When both are zero, the system's behavior is the torus. Figure 2(a) demonstrates all of the mentioned situations; therefore, the system has the capability of having limit cycles, torus, and chaotic solutions. Figure 2(b) is the bifurcation diagram for the same range of a. Period windows can be seen in Figure 2(b). In the bifurcation diagram, a period-doubling route to chaos can be observed by decreasing parameter a.

In the next step, parameter a is fixed, and the oscillator's behaviors for various b are investigated. Figure 3 reveals the Lyapunov exponent and bifurcation diagrams when $a = 0.5$ and the b's value changes. For better visualization, the Lyapunov exponent with the largest absolute value (its value is always negative) is not plotted in Figure 3(a). The system's different behaviors from different limit cycles' periods to torus and chaos can be seen based on the previously explained situations of the two larger Lyapunov exponents (Figure 3(a)). An inverse route of the period-doubling route to chaos can be observed in the bifurcation diagram by increasing b (Figure 3(b)).

The basin of attractions when the oscillator's parameters are set $a = 0.5$ and $b = 2.3$ are plotted for a range of initial values (Figure 4). Two surfaces each containing four equilibrium points are plotted. Studying the basin of attraction of the oscillator shows that the oscillator has only one attractor. Figures 4(a) and 4(b) show the parts of plates that $Z = \sqrt{23}$ and $Z = -\sqrt{23}$, respectively. The equilibrium points ($X = +\sqrt{30.4}$, $Y = +\sqrt{30.4}$, $Z = +\sqrt{23}$) and ($X = -\sqrt{30.4}$, $Y = -\sqrt{30.4}$, $Z = -\sqrt{23}$) are located at the edge of the unstable region and the basin of attraction. The type of both of them is unstable (spiral). It can be seen that some equilibrium points exist in the system's attractor's basin of attraction. Therefore, the system's attractor is self-excited.

In the next section, an analog circuit of the system is implicated for the system when it is in its chaotic mode.

Table 1: The pure nonlinear system's equilibrium points and their related eigenvalues when $a = 0.5$ and $b = -2.3$ are set. The equilibria types are determined based on their eigenvalues.

Equilibrium points	Eigenvalues	Types
$X = +\sqrt{30.4},\ Y = +\sqrt{30.4},\ Z = +\sqrt{23}$	$\lambda_{1,2} \approx 7.0371 \pm 2.5182i,\ \lambda_3 \approx -2.0879$	Unstable (spiral)
$X = -\sqrt{30.4},\ Y = +\sqrt{30.4},\ Z = +\sqrt{23}$	$\lambda_{1,2} \approx -0.5447 \pm 2.9365i,\ \lambda_3 \approx 13.0757$	Unstable (spiral)
$X = +\sqrt{30.4},\ Y = -\sqrt{30.4},\ Z = +\sqrt{23}$	$\lambda_{1,2} \approx -5.2642 \pm 15.0219i,\ \lambda_3 \approx 0.4603$	Unstable (spiral)
$X = +\sqrt{30.4},\ Y = +\sqrt{30.4},\ Z = -\sqrt{23}$	$\lambda_1 \approx 22.3613,\ \lambda_2 \approx -11.8532,\ \lambda_3 \approx -0.44$	Unstable (saddle)
$X = -\sqrt{30.4},\ Y = -\sqrt{30.4},\ Z = +\sqrt{23}$	$\lambda_1 \approx -22.3613,\ \lambda_2 \approx 11.8532,\ \lambda_3 \approx 0.44$	Unstable (saddle)
$X = +\sqrt{30.4},\ Y = -\sqrt{30.4}, Z = -\sqrt{23}$	$\lambda_{1,2} \approx 0.5447 \pm 2.9365i,\ \lambda_3 \approx -13.0757$	Unstable (spiral)
$X = -\sqrt{30.4},\ Y = +\sqrt{30.4}, Z = -\sqrt{23}$	$\lambda_{1,2} \approx 5.2642 \pm 15.0219i,\ \lambda_3 \approx -0.4603$	Unstable (spiral)
$X = -\sqrt{30.4},\ Y = -\sqrt{30.4}, Z = -\sqrt{23}$	$\lambda_{1,2} \approx -7.0371 \pm 2.5182i,\ \lambda_3 \approx 2.0879$	Unstable (spiral)

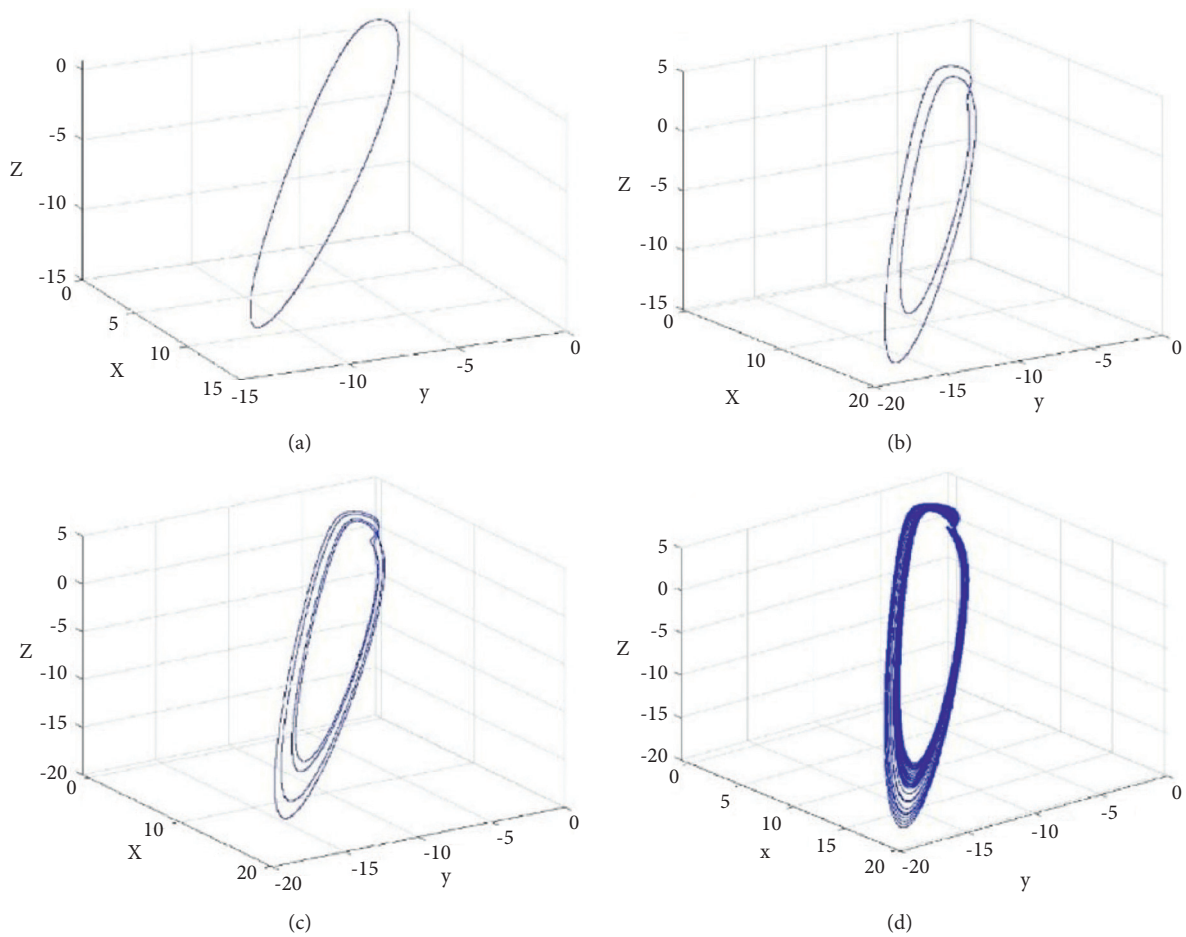

Figure 1: The systems' attractors for a's different values when $b = -2.3$. (a) For $a = 3$, period 1 can be seen in the system's attractor. (b) For $a = 2$, period 2 can be seen in the system's attractor. (c) For $a = 1.5$, period 3 can be seen in the system's attractor. (d) When $a = 1.1$, the oscillator's behavior is chaotic.

3. Analog System's Circuit, Design, and PSpice Implication

The pure nonlinear system's analog circuit in the chaotic mode is designed. Simple elements such as resistors and Op-Amps are used in its designed circuit. Its circuit's schematic is demonstrated in Figure 5. AD633/AD as an analog device is used for multiplying variables together. The values of capacitors and resistors are tuned to compensate for the mentioned coefficient. To avoid the analog devices' saturation,

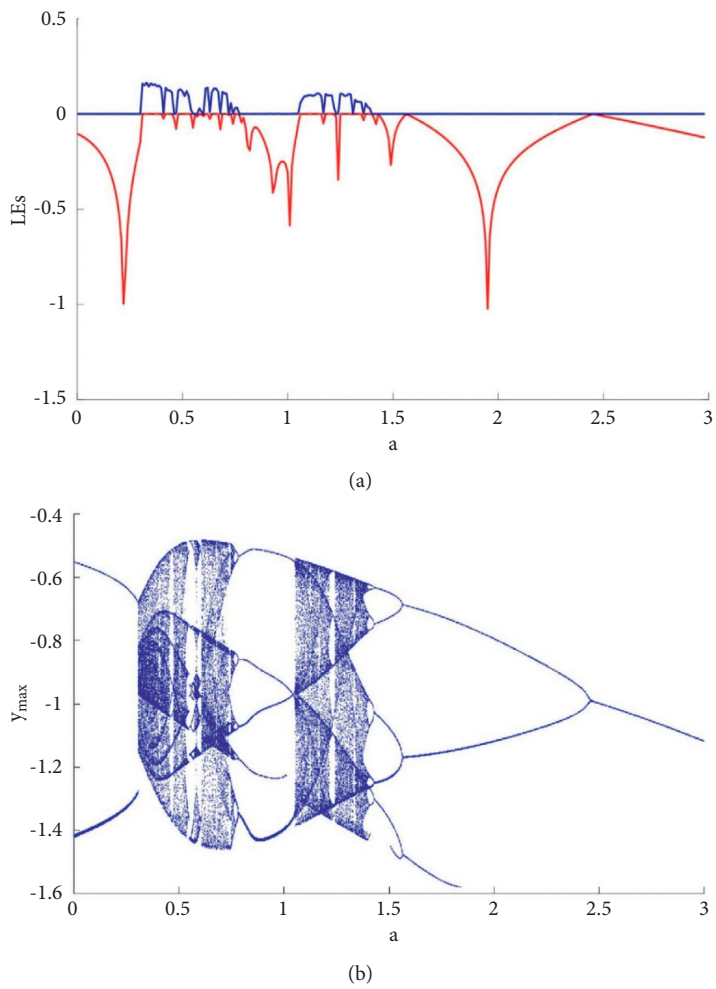

Figure 2: Lyapunov exponents and bifurcation diagrams for different a values. (a) The systems' two larger Lyapunov exponents are plotted. Periodic behaviors (one Lyapunov exponent negative and one zero), torus behaviors (when both Lyapunov exponents are zero), and chaotic behavior (one Lyapunov exponent is zero and another one is positive) can be seen in the diagram. (b) The bifurcation diagram of the system is plotted when the period-doubling route to chaos (from right to left) and period windows can be observed in the diagram.

$x = 10X$, $y = 10Y$, $z = 10Z$, and $t = 0.1T$ are considered. Therefore, the system's equations can be rewritten as follows:

$$\begin{aligned}
\frac{\mathrm{d}(10X)}{\mathrm{d}(0.1T)} &= 1.3(10z)^2 - (10Y)^2 + a \longrightarrow \frac{\mathrm{d}X}{\mathrm{d}T} = 1.3Z^2 - Y^2 + \frac{a}{100}, \\
\frac{\mathrm{d}(10Y)}{\mathrm{d}(0.1T)} &= (10Y)^2 - (10X)^2 \longrightarrow \frac{\mathrm{d}Y}{\mathrm{d}T} = Y^2 - X^2, \\
\frac{\mathrm{d}(10z)}{\mathrm{d}(0.1T)} &= (10Y)^2 - (10X)^2 + 0.1(10z)^2 + b \longrightarrow \frac{\mathrm{d}Z}{\mathrm{d}T} = Y^2 - X^2 + 0.1Z^2 + \frac{b}{100}.
\end{aligned} \tag{4}$$

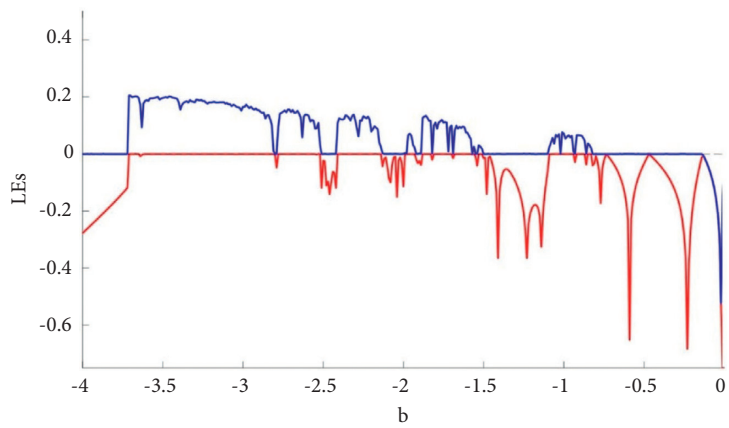

(a)

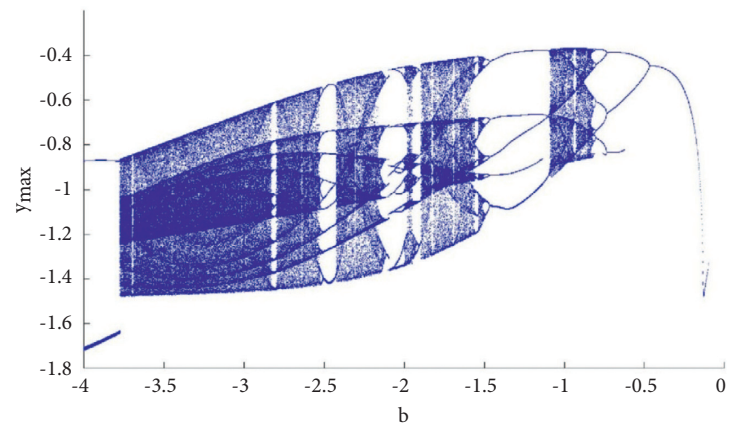

(b)

Figure 3: Lyapunov exponents and bifurcation diagrams when a value is fixed ($a = 0.5$). (a) For a range of b, the two largest Lyapunov exponents are potted. Based on these Lyapunov exponents' values, the system's behaviors (torus when both are zero, chaos when one is zero and another is positive, and periodic when one is negative and another is zero) for each specific value of b can be determined. (b) Bifurcation diagrams of the system for the b's same range. Period-doubling route to chaos (from right side to the left) and periodic windows can be seen in the diagram.

The new version of the system's equation (Eq. (4)) is designed by analog elements (Figure 5). The values of the analog elements are as follows: $R1 = 10K\Omega$, $R2 = 10K\Omega$, $R3 = 10K\Omega$, $R4 = 10K\Omega$, $R5 = 1K\Omega$, $R6 = 10K\Omega$ $R7 = 10K\Omega$, $R8 = 10K\Omega$, $R9 = 10K\Omega$, $R10 = 1K\Omega$, $R11 = 10K\Omega$, $R12 = 1K\Omega$ and $R13 = 1K\Omega$, $R14 = 1K\Omega$, $R15 = 13K\Omega$, $R16 = 1K\Omega$, $R17 = 1K\Omega$, $C1 = 10n\text{F}$, $C2 = 10n\text{F}$, $C3 = 10n\text{F}$. Finally, the implicated system's equation to simulate in PSpice can be written as follows:

$$\begin{aligned}
\frac{dX}{dT} &= \left(\frac{C1}{R1}\right)\left(\frac{R15}{R14}\right)\left(0.1Z^2\right) - \left(\frac{C1}{R2}\right)\left(\frac{R11}{R10}\right)\left(\frac{R13}{R12}\right)\left(0.1Y^2\right) + \left(\frac{C1}{R2}\right)V1,\\
\frac{dY}{dT} &= \left(\frac{C2}{R4}\right)\left(\frac{R11}{R10}\right)\left(0.1Y^2\right) - \left(\frac{C2}{R5}\right)\left(0.1X^2\right),\\
\frac{dZ}{dT} &= \left(\frac{C3}{R7}\right)\left(\frac{R11}{R10}\right)\left(0.1Y^2\right) - \left(\frac{C3}{R7}\right)\left(0.1X^2\right) + \left(\frac{R17}{R16}\right)\left(\frac{C3}{R9}\right)\left(0.1Z^2\right) + \left(\frac{C3}{R9}\right)V2.
\end{aligned} \tag{5}$$

The circuit simulation in PSpice when $a = 0.5$ and $b = -3.7$ is demonstrated in Figure 5. All elements that are used are analog. The outputs of the designed analog circuit compared to Matlab simulations are demonstrated in Figure 6.

4. The Pure Nonlinear System's Complexity Analysis

Defining the complexity of the time series based on their predictability results in the definition of sample entropy

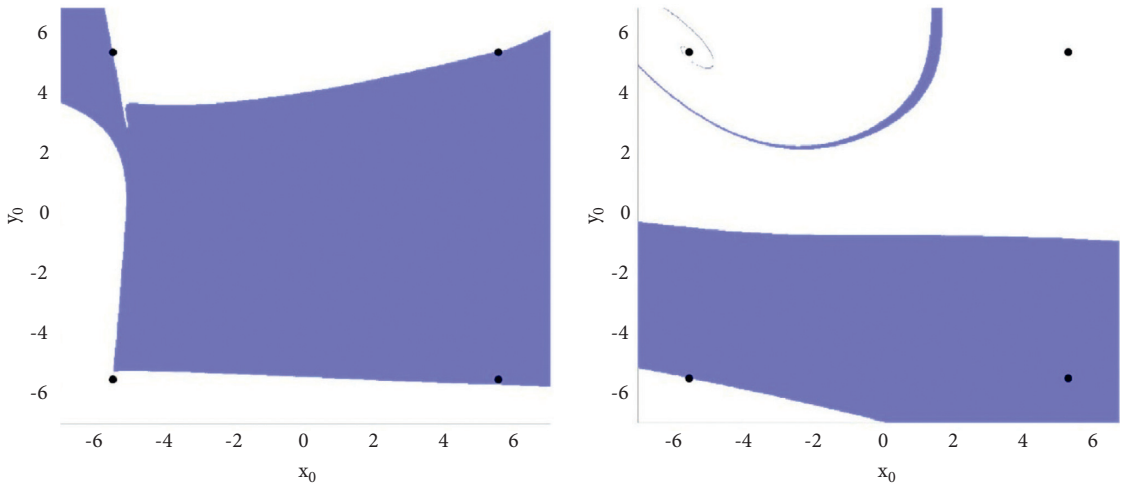

Figure 4: The system's basin of attractions ($a = 0.5$ and $b = 2.3$). According to our best search, the system has just one attractor. Different initial values of the systems are attracted to the attractor or have unbounded responses. White color is considered for plotting in both (a) and (b) parts for the initial values with unbounded responses. Regions that are attracted to the attractor are plotted with blue color. (a) and (b) are responsible for plates that $Z = \sqrt{23}$ and $Z = -\sqrt{23}$, respectively. Because some equilibrium points can be found in blue regions, the system can be categorized in the self-excited class.

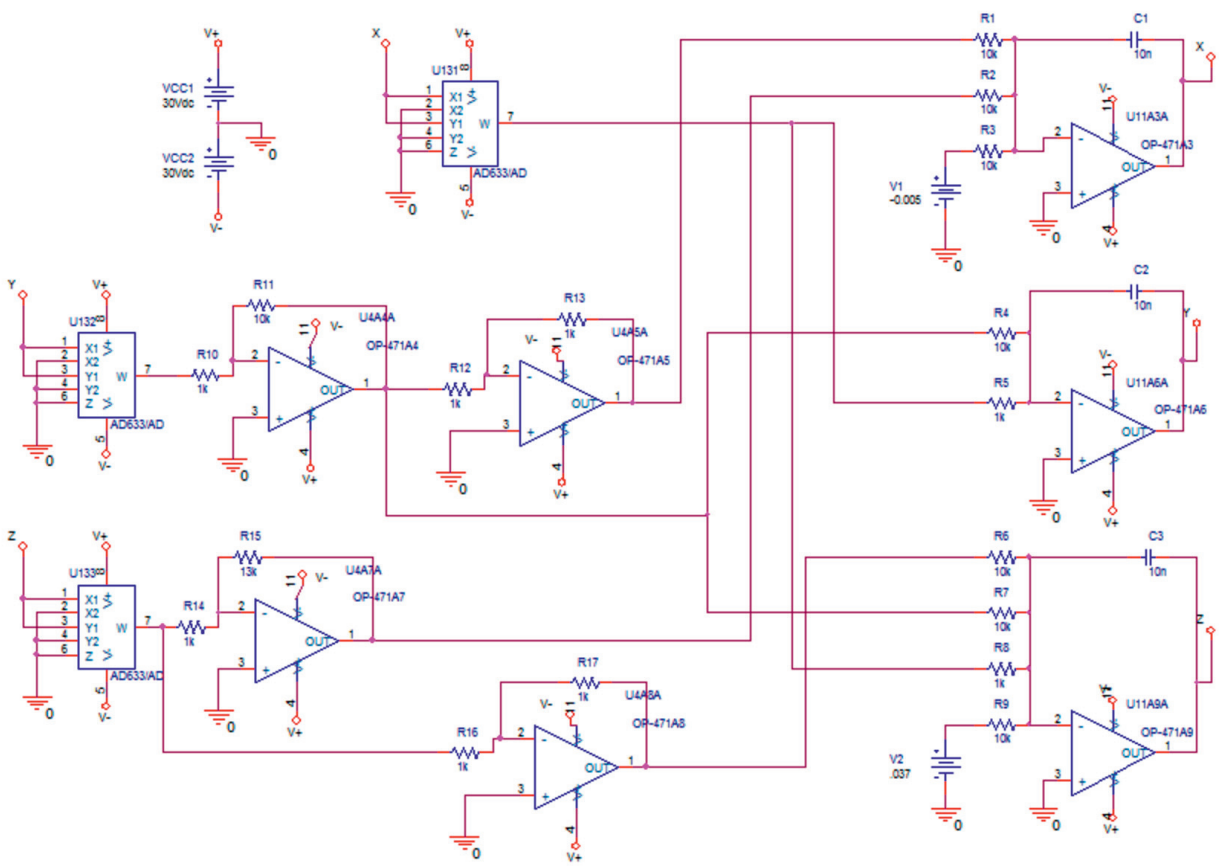

Figure 5: Schematic of the pure nonlinear system's designed circuit. In the designed circuits, all used elements are analogs. Op-Amps are used as integrators. Besides, they are also used for regulating the coefficients of nonlinear terms. Capacitors and resistors are the other analog elements in the circuit. The circuit is simulated in PSpice software.

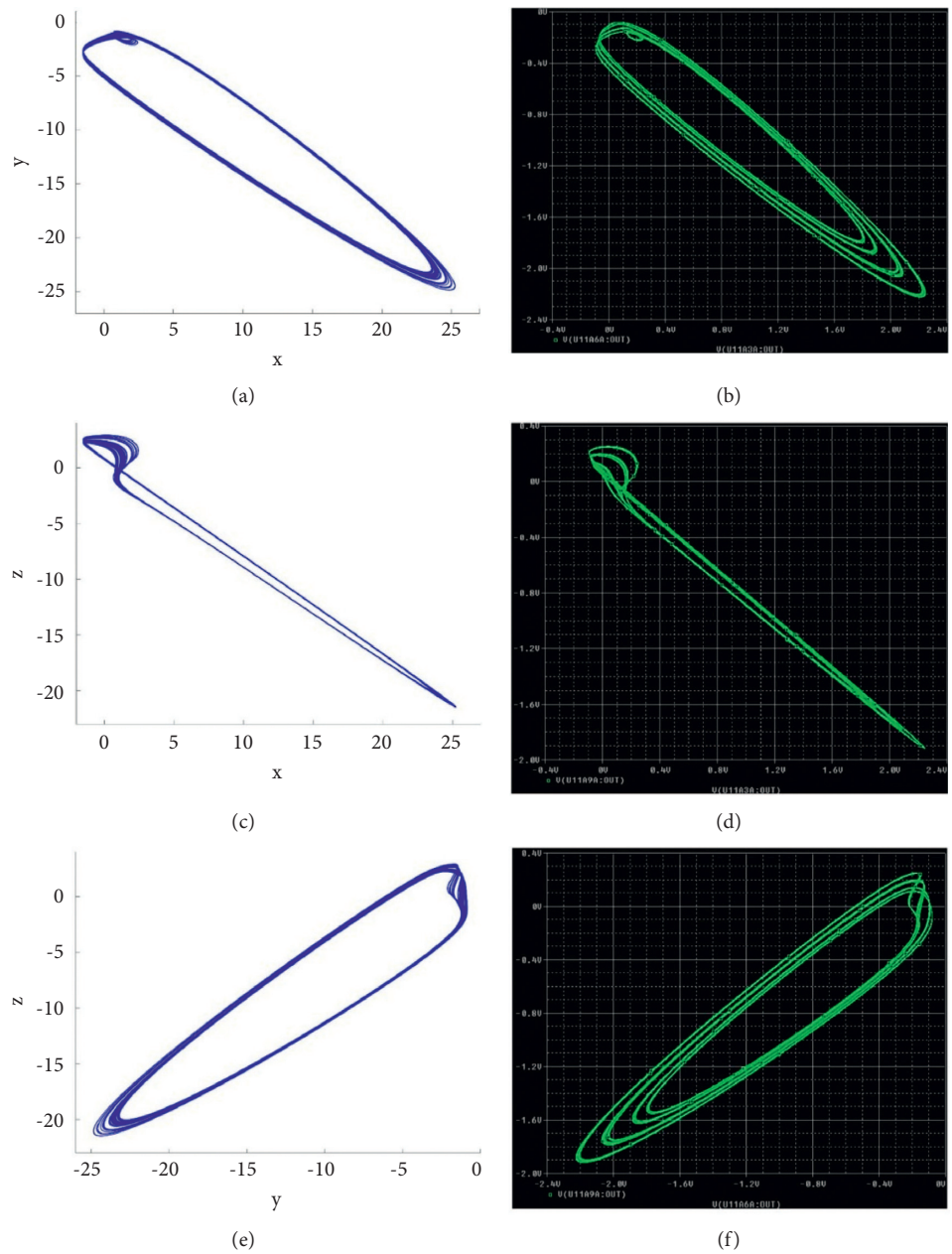

Figure 6: The results of Matlab and PSpice simulations for the system's attractor when $a = 0.5$ and $b = -3.7$. (a), (c), and (e) are related to the Matlab simulations when (b), (d), and (f) are generated by the analog circuit designed in PSpice. (a, b) The attractor's projection in the XY plane, (c, d) the attractor's shadow in the XZ plane, and (e, f) the attractor's projection in the surface of the YZ.

(SaEn). Accepting this definition, SaEn is applied to estimate the complexity of the system's time series, as reviewed in the Introduction section. SaEn tries to measure the predictability of $(t+1)th$ samples of time series when the previous samples $(1, 2, \ldots, t)$ are observed. The algorithm of calculating SaEn can be read in [37]. To calculate the algorithm of SaEn, $m = 2$ and $r = 0.2$ are considered. The algorithm is applied to the oscillator's attractors (the x variable time series) for ranges of the parameters (a and b). The initial conditions are considered $(0, 0, 0)$ and the transient time parts of the time series are emitted before calculating SaEn. The results of SaEn values can be observed in Figure 7. The attractor is a fixed point in parameters that SaEn values are zero. A trend can be seen that increasing a, at first, causes an increase in SaEn and then decreases it. In comparison with Figure 2, generally chaotic states of the system have more sample entropy values than periodic ones. Besides, a trend also can be observed that decreasing b parameter values increases SaEn values. Comparing this trend with the bifurcation diagram reveals that the chaotic regions generally have more complexity.

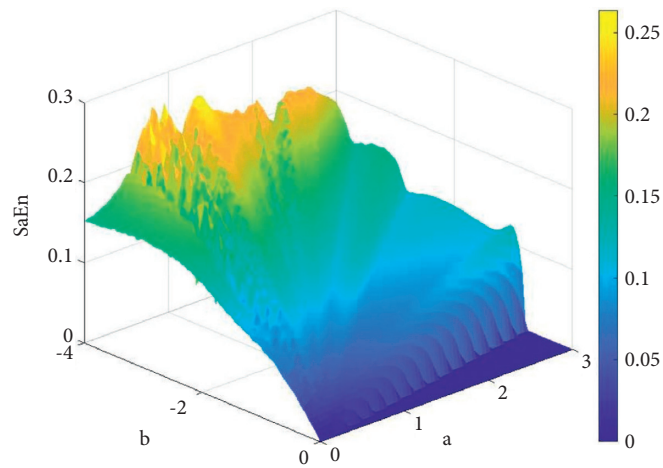

Figure 7: The sample entropy is used for assessing the oscillator's signals complexities for a range of the system's parameters. A trend can be seen that decreasing b and increasing a values result in increasing the sample entropy.

5. Impulsive Control

Here, the pure nonlinear oscillator is controlled using impulsive control. In the first step, the system under impulsive control can be described as follows [65–67]:

$$\begin{aligned} \dot{X} &= f(t, X) \\ &= AX + \Phi(X), \\ \Delta X &= X(t^{+}) - X(t^{-}) \\ &= U(k, X), \\ t &= T_k, \\ k &= 1, 2, \ldots \end{aligned} \tag{6}$$

When $f: R_{+} \times R^{n} \longrightarrow R^{n}$ is continuous, $U: R^{n} \times R^{n} \longrightarrow R^{n}$ is continuous; $X \in R^{n}$ is the vector of state variables; and $0 < T_1 < T_2 < \ldots < T_K < T_{K+1} < \ldots, T_{K \longrightarrow \infty}$ *as* $k \longrightarrow \infty$. AX, in general, represents linear terms of systems when $\Phi(X)$ contains nonlinear terms.

Definition 1. Assuming $V: R_{+} \times R^{n} \longrightarrow R_{+}$, then V is said to belong to the class V_0, if

(1) V is continuous in $(T_{k-1}, T_k] \times R^{n}$ and for each $X \in R^{n}$, $k = 1, 2, \ldots, (t, Y) \longrightarrow (T_k^{+}, X)$ $\lim V(t, Y) = V(T_k^{+}, X)$ exists

(2) V is locally Lipschitzian in X

Definition 2. For $(t, X) \in (T_{i-1}, T_i]] \times R^{n}$, it is considered:

$$\begin{aligned} D^{+}V(t, X) \triangleq h \longrightarrow 0 + \limsup \frac{1}{h} [V(t + h, X \\ + hf(t, X)) - V(t, X)]. \end{aligned} \tag{7}$$

Definition 3 (comparison system). Let $V \in V0$ and assume that

$$D^{+}V(t, X) \leq g(t, V(t, X)),\ t \neq T_k;\ \text{and}\ V(t, X + U(k, X)) \leq \Psi k(V(t, X)),\ t = T_k, \tag{8}$$

where $g: R_{+} \times R_{+} \longrightarrow R$ is continuous and $\Psi k: R_{+} \longrightarrow R_{+}$ is nondecreasing. Then the following system is the comparison system of Eq. (6):

$$\begin{aligned} \omega &= g(t, \omega),\ t \neq T_k \omega(T_k^{+}) \\ &= \Psi k(\omega(T_k))\omega(T_0^{+}) \\ &= \omega 0 \geq 0. \end{aligned} \tag{9}$$

Theorem 1. *These three conditions are assumed:*

(1) $V: R^{n} \times R^{n} \longrightarrow R_{+}$, $V \in V0$, $K(t)D^{+}V(t, X) + D^{+}K(t)V(t, X) \leq g(t, K(t)V(t, X))$, $t \triangleq \tau k$, *when* g *is continuous in* $(T_{k-1}, T_k] \times R^{n}$ *for each* $x \in R^{n}$, $k = 1, 2, \ldots, (t, y) \longrightarrow (T_k^{+}, x) \lim g(t, y) = g(T_k^{+}, x)$ *exists.* $K(t) \geq m > 0$, $t \longrightarrow T_k^{-} \lim K(t) = K(T_k)$, $t \longrightarrow T_k^{+} \lim K(t)$ *exists,* $k = 1, 2, \ldots, D^{+}K(t) = h \longrightarrow 0^{+} \limsup (1/h)[K(t + h) - K(t)]$

(2) $K(T_k + 0)V(T_k + 0, X + U(k, X)) \leq \Psi k(K(T_k)\ V(T_k, X))$, $k = 1, 2, \ldots$

(3) $V(t, 0) = 0$ *and* $\alpha(|X|) \leq V(t, X)$ *on* $R_{+} \times R^{n}$, *when* $\alpha(\cdot) \in \aleph$ *(continuous strictly increasing function class* $\alpha: R_{+} \longrightarrow R_{+}$ *so that* $\alpha(0) = 0$*) are satisfied. Next, the global asymptotic stability for the trivial solution* $\omega = 0$ *of the comparison system implies global asymptotic stability of impulsive system (6) trivial solution*

Theorem 2. *Let $g(t, \omega) = \dot{\lambda}(t)\omega, \Psi k(\omega) = d_k\omega, d_k \geq 0$ for all $k \geq 1$. consequently, system (6) origin is global asymptotically stable if Theorem 1 conditions and the following conditions are held:*

(1) $\lambda(t)$ is nondecreasing, $t \longrightarrow T_k^+ \lim \lambda(t) = \lambda(T_k)$, $t \longrightarrow T_k^+ \lim \lambda(t) = \lambda(T_k^+)$ exists, for all $k = 1, 2, \ldots$

(2) $\sup_i [d_I \exp(\lambda(T_{i+1}) - \lambda(T_i^+))] = \varepsilon_0 < \infty$

(3) There exists a $r > 1$ such that $\lambda(T_{2k+3}) + \lambda(T_{2k+2}) + \ln(rd_{2k+2} + d_{2k+1}) \leq \lambda(T_{2k+2}^+) + \lambda(T_{2k+2}^+)$ is held for all $d_{2k+2}d_{2k+1} \neq 0$, $k = 1, 2, \ldots$, or there exists an $r > 1$ so that $\lambda(T_{k+1}) + \ln(rd_k) \leq \lambda(T_k^+)$ for all k

(4) $V(t, 0) = 0$ and there exists $\alpha(\cdot)$ in class N such that $\alpha(\|X\|) \leq V(t, X)$

Theorem 3. *The origin of the introduced pure nonlinear chaotic system is asymptotically stable if there exists a $\xi > 1$ and a differentiable at $t \neq T_k$, and nonincreasing function $K(t)$ which satisfies the following:*

$$-\frac{\dot{K}(t)}{K(t)} \leq q + r \leq \frac{1}{(1+\varepsilon)\Delta 2}\ln\left(\left(\frac{K(T_{2i}^+)K(T_{2i-1}^+)}{K(T_{2i+1})K(T_{2i})\xi d^2}\right)\right) \text{ or}$$

$$-\frac{\dot{K}(t)}{K(t)} \leq q + r \leq \frac{1}{\max(\Delta 1, \Delta 2)}\ln\left(\frac{K(T_i^+)}{K(T_{i+1})\xi\, d}\right),$$

$$r = \begin{cases} 0, \; if \quad P = I, \\ 2M\sqrt{\dfrac{\lambda_2}{\lambda_1}} \; if \quad P \neq I, \end{cases} \tag{10}$$

q is the $(A + P^{-1}A^TP)$ largest eigenvalue assuming P is a positive definite symmetric matrix and $\lambda_1 > 0$ and $\lambda_2 > 0$ are the smallest and the largest eigenvalues of P, respectively. $\rho(A)$ denote the spectral radius of A: $d = \rho^2(I + B)$. M for the pure nonlinear chaotic system considered so that $|x_{(t)}| < M, |y_{(t)}| < M, |z_{(t)}| < M.K(t)$. It is as in Theorem 1, T_i: $i = 1, 2, \ldots$ are varying but satisfy the following:

$$\begin{aligned} \Delta 1 &= \sup_{1\leq j<\infty}\left(T_{2j+1} - T_{2j}\right) < \infty, \\ \Delta 2 &= \sup_{1\leq j<\infty}\left(T_{2j} - T_{2j-1}\right) < \infty. \end{aligned} \tag{11}$$

Furthermore, for a given constant ε,

$$T_{2j+1} - T_{2j} \leq \varepsilon\left(T_{2j} - T_{2j-1}\right) \; \forall j \in 1, 2, \ldots, \infty. \tag{12}$$

This theorem's proof can be seen in [66].

Remark 1. Theorem 3 also gives an estimate for the upper bound. $\Delta 1_{max}$ and $\Delta 2_{max}$ of impulsive intervals are given by

$$\begin{aligned} \Delta 1 &= \frac{1}{(1+\varepsilon)(q + 2|a\alpha|)}\ln\left(\frac{K(T_{2i}^+)K(T_{2i-1}^+)}{K(T_{2i+1})K(T_{2i})\xi d^2}\right), \\ \Delta 2 &= \varepsilon\Delta 1. \end{aligned} \tag{13}$$

The introduced pure nonlinear system when $a = 0.5$ and $b = 2.3$ are set is considered. According to the second section, this system has eight equilibrium points. Assuming (x^*, y^*, z^*) as an equilibrium point of the system, the system equations considering $x_1 = x - x^*$, $y_1 = y - y^*$, $z_1 = z - z^*$ can be rewritten as follows:

$$\begin{aligned} \dot{x_1} &= 1.3z_1^2 + 2.6z^*z_1 + 1.3z^{*2} - y_1^2 - 2y^*y_1 - y^{*2} + a, \\ \dot{y_1} &= y_1^2 + 2y^*y_1 + y^{*2} - x_1^2 - 2x^*x_1 - x^{*2}, \\ \dot{z_1} &= y_1^2 + 2y^*y_1 + y^{*2} - x_1^2 - 2x^*x_1 - x^{*2} + 0.1z_1^2 + 0.2z^*z_1 + 0.1z^{*2} + b. \end{aligned} \tag{14}$$

Equilibrium $(x^* = +\sqrt{30.4}, y^* = -\sqrt{30.4}, z^* = -\sqrt{23})$ is considered to be stabilized. Without losing generosity for stabilizing equilibrium points of the system, the same method can be applied to the other equilibria of the pure nonlinear system. In this way, considering (6) and (12), for the equilibrium point $(x^* = +\sqrt{30.4}, y^* = -\sqrt{30.4}, z^* = -\sqrt{23})$, equations can be rewritten as follows:

$$\dot{X} = AX + \Phi(X),$$

$$A = \begin{pmatrix} 0 & -2y^* & 2.6z^* \\ -2x^* & 2y^* & 0 \\ -2x^* & 2y^* & 0.2z^* \end{pmatrix}$$

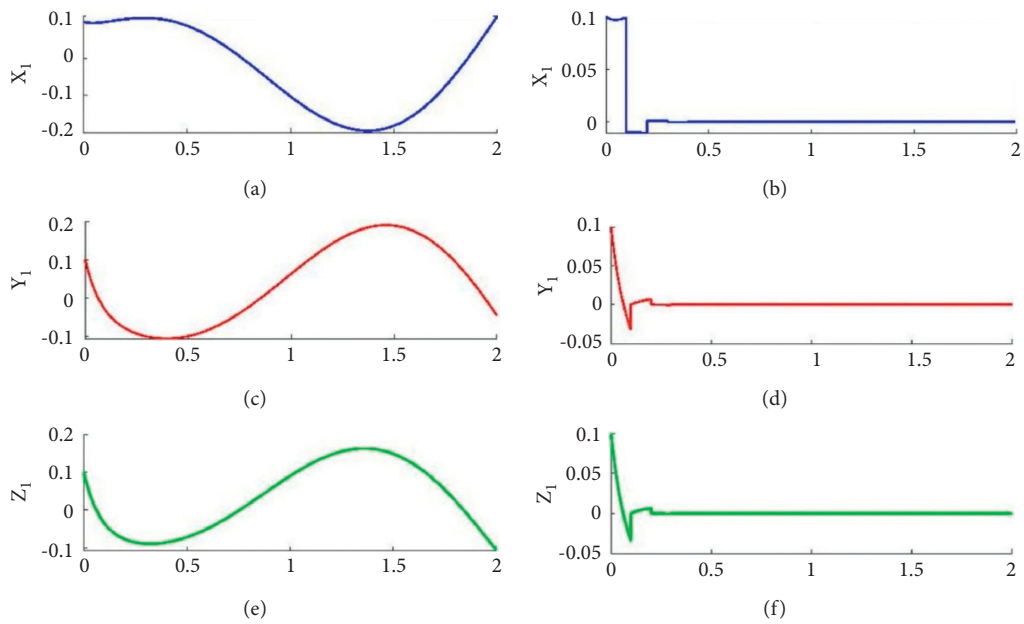

Figure 8: For the initial condition $(0.1, 0.1, 0.1)$, time series of x_1, y_1, and z_1 of the system demonstrated in Equation (12) are plotted in (a), (b), and (c), respectively. The transient signals of, x_1, y_1, and z_1 for this system under the impulsive controller (Equation (13)) are plotted in (d), (e), and (f), respectively.

$$
\begin{aligned}
&= \begin{pmatrix} 0 & 2\sqrt{30.4} & -2.6\sqrt{23} \\ -2\sqrt{30.4} & -2\sqrt{30.4} & 0 \\ -2\sqrt{30.4} & -2\sqrt{30.4} & -0.2\sqrt{23} \end{pmatrix}, \\
\Phi(X) &= \begin{bmatrix} 1.3z_1^2 - y_1^2 \\ y_1^2 - x_1^2 \\ y_1^2 - x_1^2 + 0.1z_1^2 \end{bmatrix}, \\
U(k, X) &= BX, \\
t &= T_k, k = 1, 2, \ldots
\end{aligned} \tag{15}
$$

Considering $K(t) = 1$, $\varepsilon = 1$, $\xi = 1.1$, $B = \begin{pmatrix} s = -1.1 & 0 & 0 \\ 0 & -1 & 0 \\ 0 & 0 & -1 \end{pmatrix}$ and $P = I$, then $d = (s+1)^2 = 0.01$, $q = 23.86$ $(T_{2j+1} - T_{2j}) = (T_{2j} - T_{2j-1}) = \Delta < (\Delta 1 = \Delta 2 = -\ln(\xi\ d)/q = 0.1890 \longrightarrow (\Delta \text{ is considered } 0.1))$. The stabilized system numerical simulations are plotted in Figure 8. Figures 8(a)–8(c) demonstrate the time series of x_1, y_1, and z_1, respectively, for the oscillator described in Eq. 12. The time series of x_1, y_1, and z_1 for the stabilized system using the impulsive controller (based on Eq. 13) are demonstrated in Figures 8(d)–8(f), respectively.

6. Conclusion

Here, a pure nonlinear 3D system was presented. It was observed that the system could generate periodic, torus, and chaotic time series. Analytical analysis revealed that the oscillator has eight unstable equilibrium points for a set of parameters. The basin of attraction diagrams showed for this set of parameters that the system attractor is self-excited. The pure nonlinear system's feasibility was investigated with an analog circuit built by simple elements like capacitors and Op-Amps. Changing parameters' values revealed that the system could generate time series with a wide range of complexities. A possible solution to system stabilization was described by using the impulsive controller on the system. For this system, when both constants (parameters a and b) were equal to zero, the system had an unbounded solution. According to the authors' best knowledge, no pure nonlinear quadratic system has been introduced before with no constant values in its equations. Therefore, searching for such a system can be interesting for future research.

Data Availability

All the numerical simulation parameters are mentioned in the respective text part, and there are no additional data requirements for the simulation results.

Conflicts of Interest

The authors declare that there are no conflicts of interest.

Acknowledgments

This work was funded by the Center for Nonlinear Systems, Chennai Institute of Technology, India, vide funding number CIT/CNS/2021/RP-015.

References

[1] H. Bao, M. Chen, H. Wu, and B. Bao, "Memristor Initial-Boosted Coexisting Plane Bifurcations and its Extreme Multi-Stability Reconstitution in Two-Memristor-Based Dynamical System," *Science China Technological Sciences*, vol. 63, pp. 1–11, 2019.

[2] Z. Faghani, F. Nazarimehr, S. Jafari, and J. C. Sprott, "Simple chaotic systems with specific analytical solutions," *International Journal of Bifurcation and Chaos*, vol. 29, no. 9, Article ID 1950116, 2019.

[3] F. Nazarimehr and J. C. Sprott, "Investigating chaotic attractor of the simplest chaotic system with a line of equilibria," *The European Physical Journal - Special Topics*, vol. 229, no. 6-7, pp. 1289–1297, 2020.

[4] M. Chen, J. Qi, H. Wu, Q. Xu, and B. Bao, "Bifurcation analyses and hardware experiments for bursting dynamics in non-autonomous memristive fitzhugh-nagumo Circuit," *Science China Technological Sciences*, vol. 63, pp. 1–10, 2020.

[5] A. Bahramian, F. Parastesh, V.-T. Pham, T. Kapitaniak, S. Jafari, and M. Perc, "Collective behavior in a two-layer neuronal network with time-varying chemical connections that are controlled by a Petri net," *Chaos: An Interdisciplinary Journal of Nonlinear Science*, vol. 31, no. 3, Article ID 033138, 2021.

[6] A. Bahramian, A. Nouri, F. Towhidkhah, H. Azarnoush, and S. Jafari, "Introducing a nonlinear coupling for central pattern generator: improvement on robustness by expanding basin of attraction and performance by decreasing the transient time," *Journal of Vibration and Control*, vol. 26, no. 7-8, pp. 377–386, 2020.

[7] V.-T. Pham, S. Jafari, C. Volos, X. Wang, and S. M. R. H. Golpayegani, "Is that really hidden? The presence of complex fixed-points in chaotic flows with no equilibria," *International Journal of Bifurcation and Chaos*, vol. 24, no. 11, Article ID 1450146, 2014.

[8] Z. Wei, I. Moroz, J. C. Sprott, A. Akgul, and W. Zhang, "Hidden hyperchaos and electronic circuit application in a 5D self-exciting homopolar disc dynamo," *Chaos: An Interdisciplinary Journal of Nonlinear Science*, vol. 27, no. 3, Article ID 033101, 2017.

[9] J. C. Sprott and B. Munmuangsaen, "Comment on "A hidden chaotic attractor in the classical Lorenz system"," *Chaos, Solitons & Fractals*, vol. 113, pp. 261-262, 2018.

[10] M. Molaie, S. Jafari, J. C. Sprott, and S. M. R. H. Golpayegani, "Simple chaotic flows with one stable equilibrium," *International Journal of Bifurcation and Chaos*, vol. 23, no. 11, Article ID 1350188, 2013.

[11] C. Feng, Q. Huang, and Y. Liu, "Jacobi analysis for an unusual 3D autonomous system," *International Journal of Geometric Methods in Modern Physics*, vol. 17, no. 04, Article ID 2050062, 2020.

[12] A. Giakoumis, C. Volos, A. J. M. Khalaf et al., "Analysis, synchronization and microcontroller implementation of a new quasiperiodically forced chaotic oscillator with megastability," *Iranian Journal of Science and Technology, Transactions of Electrical Engineering*, vol. 44, no. 1, pp. 31–45, 2020.

[13] K. Sun and J. C. Sprott, "Periodically forced chaotic system with signum nonlinearity," *International Journal of Bifurcation and Chaos*, vol. 20, no. 05, pp. 1499–1507, 2010.

[14] B. Bao, J. Luo, H. Bao, C. Chen, H. Wu, and Q. Xu, "A simple nonautonomous hidden chaotic system with a switchable stable node-focus," *International Journal of Bifurcation and Chaos*, vol. 29, no. 12, Article ID 1950168, 2019.

[15] T. Banerjee, D. Biswas, and B. C. Sarkar, "Design and analysis of a first order time-delayed chaotic system," *Nonlinear Dynamics*, vol. 70, no. 1, pp. 721–734, 2012.

[16] H. G. Wu, Y. Ye, B. C. Bao, M. Chen, and Q. Xu, "Memristor initial boosting behaviors in a two-memristor-based hyper-chaotic system," *Chaos, Solitons & Fractals*, vol. 121, pp. 178–185, 2019.

[17] C. Li, G. Chen, J. Kurths, T. Lei, and Z. Liu, "Dynamic transport: from bifurcation to multistability," *Communications in Nonlinear Science and Numerical Simulation*, vol. 95, Article ID 105600, 2021.

[18] W. J. Sanders, "The topology of chaos: alice in stretch and squeezeland," *Mathematics Teacher*, vol. 96, p. 218, 2003.

[19] M. Hua, S. Yang, Q. Xu, M. Chen, H. Wu, and B. Bao, "Symmetrically Scaled Coexisting Behaviors in Two Types of Simple Jerk Circuits," *Circuit World*, vol. 47, 2020.

[20] S. Zhang, J. Zheng, X. Wang, and Z. Zeng, "Multi-scroll hidden attractor in memristive HR neuron model under electromagnetic radiation and its applications," *Chaos: An Interdisciplinary Journal of Nonlinear Science*, vol. 31, no. 1, Article ID 011101, 2021.

[21] E. C. Díaz-González, J.-A. López-Rentería, E. Campos-Cantón, and B. Aguirre-Hernández, "Maximal unstable dissipative interval to preserve multi-scroll attractors via multi-saturated functions," *Journal of Nonlinear Science*, vol. 26, pp. 1833–1850, 2016.

[22] J. P. Singh, J. Koley, K. Lochan, and B. K. Roy, "Presence of megastability and infinitely many equilibria in a periodically and quasi-periodically excited single-link manipulator," *International Journal of Bifurcation and Chaos*, vol. 31, no. 2, Article ID 2130005, 2021.

[23] A. Sambas, S. Vaidyanathan, E. Tlelo-Cuautle et al., "A 3-D multi-stable system with a peanut-shaped equilibrium curve: circuit design, FPGA realization, and an application to image encryption," *IEEE Access*, vol. 8, pp. 137116–137132, 2020.

[24] V. P. Thoai, M. S. Kahkeshi, V. V. Huynh, A. Ouannas, and V.-T. Pham, "A nonlinear five-term system: symmetry, chaos, and prediction," *Symmetry*, vol. 12, no. 5, p. 865, 2020.

[25] M. D. Vijayakumar, A. Bahramian, H. Natiq, K. Rajagopal, and I. Hussain, "A chaotic quadratic bistable hyperjerk system with hidden attractors and a wide range of sample entropy: impulsive stabilization," *International Journal of Bifurcation and Chaos*, vol. 31, Article ID 2150253, 2021.

[26] J. Kengne, S. Jafari, Z. T. Njitacke, M. Yousefi Azar Khanian, and A. Cheukem, "Dynamic analysis and electronic circuit implementation of a novel 3D autonomous system without linear terms," *Communications in Nonlinear Science and Numerical Simulation*, vol. 52, pp. 62–76, 2017.

[27] V. T. Pham, S. Jafari, C. Volos, and L. Fortuna, "Simulation and experimental implementation of a line-equilibrium system without linear term," *Chaos, Solitons & Fractals*, vol. 120, pp. 213–221, 2019.

[28] Y. Xu and Y. Wang, "A new chaotic system without linear term and its impulsive synchronization," *Optik*, vol. 125, no. 11, pp. 2526–2530, 2014.

[29] Z. T. Njitacke, R. L. T. Mogue, G. D. Leutcho, T. Fonzin Fozin, and J. Kengne, "Heterogeneous multistability in a novel system with purely nonlinear terms," *International Journal of Electronics*, pp. 1–17, 2020.

[30] V. Carbajal-Gómez, E. Tlelo-Cuautle, R. Trejo-Guerra, C. Sánchez-López, and J. Munoz-Pacheco, "Experimental synchronization of multiscroll chaotic attractors using current-feedback operational amplifiers," *Nonlinear Science Letters B: Chaos, Fractal, Synchronization*, vol. 1, pp. 37–42, 2011.

[31] F. Hellmann, P. Schultz, P. Jaros et al., "Network-induced multistability through lossy coupling and exotic solitary states," *Nature Communications*, vol. 11, pp. 592–599, 2020.

[32] E. Tlelo-Cuautle, A. Dalia Pano-Azucena, O. Guillén-Fernández, and A. Silva-Juárez, "Synchronization and applications of fractional-order chaotic systems," *Analog/Digital Implementation of Fractional Order Chaotic Circuits and Applications*, pp. 175–201, Springer, Cham, Switzerland, 2020.

[33] E. Tlelo-Cuautle, O. Guillén-Fernández, J. de Jesus Rangel-Magdaleno, A. Melendez-Cano, J. C. Nuñez-Perez, and L. G. de la Fraga, "FPGA implementation of chaotic oscillators, their synchronization, and application to secure communications," *Recent Advances in Chaotic Systems and Synchronization*, pp. 301–328, Academic Press, Cambridge, MA, USA, 2019.

[34] E. Tlelo-Cuautle, J. D. Díaz-Muñoz, A. M. González-Zapata et al., "Chaotic image encryption using hopfield and hindmarsh-rose neurons implemented on FPGA," *Sensors*, vol. 20, no. 5, p. 1326, 2020.

[35] H. Natiq, S. Banerjee, and M. R. M. Said, "Cosine chaotification technique to enhance chaos and complexity of discrete systems," *The European Physical Journal - Special Topics*, vol. 228, no. 1, pp. 185–194, 2019.

[36] L. Liu, C. Du, L. Liang, and X. Zhang, "A high Spectral Entropy (SE) memristive hidden chaotic system with multi-type quasi-periodic and its circuit," *Entropy*, vol. 21, no. 10, p. 1026, 2019.

[37] J. S. Richman and J. R. Moorman, "Physiological time-series analysis using approximate entropy and sample entropy," *American Journal of Physiology. Heart and Circulatory Physiology*, vol. 278, pp. H2039–H2049, 2000.

[38] J. N. Weiss, A. Garfinkel, M. L. Spano, and W. L. Ditto, "Chaos and chaos control in biology," *Journal of Clinical Investigation*, vol. 93, no. 4, pp. 1355–1360, 1994.

[39] T. Kapitaniak, L. Kocarev, and L. O. Chua, "Controlling chaos without feedback and control signals," *International Journal of Bifurcation and Chaos*, vol. 3, no. 2, pp. 459–468, 1993.

[40] E. Ott, C. Grebogi, and J. A. Yorke, "Controlling chaos," *Physical Review Letters*, vol. 64, no. 11, pp. 1196–1199, 1990.

[41] X. Li, T. Caraballo, R. Rakkiyappan, and X. Han, "On the stability of impulsive functional differential equations with infinite delays," *Mathematical Methods in the Applied Sciences*, vol. 38, no. 14, pp. 3130–3140, 2015.

[42] X. Yang, X. Li, X. Li, Q. Xi, and P. Duan, "Review of stability and stabilization for impulsive delayed systems," *Mathematical Biosciences and Engineering*, vol. 15, no. 6, pp. 1495–1515, 2018.

[43] X. Li, J. Shen, and R. Rakkiyappan, "Persistent impulsive effects on stability of functional differential equations with finite or infinite delay," *Applied Mathematics and Computation*, vol. 329, pp. 14–22, 2018.

[44] Z. Yang, W. Zhou, and T. Huang, "Input-to-state stability of delayed reaction-diffusion neural networks with impulsive effects," *Neurocomputing*, vol. 333, pp. 261–272, 2019.

[45] X. Li, D. O'Regan, and H. Akca, "Global exponential stabilization of impulsive neural networks with unbounded continuously distributed delays," *IMA Journal of Applied Mathematics*, vol. 80, no. 1, pp. 85–99, 2015.

[46] J. Hu, G. Sui, X. Lv, and X. Li, "Fixed-time control of delayed neural networks with impulsive perturbations," *Nonlinear Analysis Modelling and Control*, vol. 23, no. 6, pp. 904–920, 2018.

[47] D. Peng, X. Li, R. Rakkiyappan, and Y. Ding, "Stabilization of stochastic delayed systems: event-triggered impulsive control," *Applied Mathematics and Computation*, vol. 401, Article ID 126054, 2021.

[48] X. Li, J. Shen, H. Akca, and R. Rakkiyappan, "LMI-based stability for singularly perturbed nonlinear impulsive differential systems with delays of small parameter," *Applied Mathematics and Computation*, vol. 250, pp. 798–804, 2015.

[49] M. Li, H. Chen, and X. Li, "Exponential stability of nonlinear systems involving partial unmeasurable states via impulsive control," *Chaos, Solitons & Fractals*, vol. 142, Article ID 110505, 2021.

[50] X. Tan, J. Cao, and X. Li, "Event-based impulsive control for nonlinear systems and its application to synchronization of Chua's circuit," *IMA Journal of Mathematical Control and Information*, vol. 37, pp. 82–104, 2018.

[51] X. Li, H. Zhu, and S. Song, "Input-to-state stability of nonlinear systems using observer-based event-triggered impulsive control," *IEEE Transactions on Systems Man Cybernetics Systems*, vol. 51, 2020.

[52] D. Yang, X. Li, and J. Qiu, "Output tracking control of delayed switched systems via state-dependent switching and dynamic output feedback," *Nonlinear Analysis: Hybrid Systems*, vol. 32, pp. 294–305, 2019.

[53] D. Yang, X. Li, J. Shen, and Z. Zhou, "State-dependent switching control of delayed switched systems with stable and unstable modes," *Mathematical Methods in the Applied Sciences*, vol. 41, no. 16, pp. 6968–6983, 2018.

[54] S. Peng, J. Zhang, J. Zhu, J. Lu, and X. Li, "Exact exponential synchronization rate of high-dimensional Kuramoto models with identical oscillators and digraphs," 2021, https://arxiv.org/abs/2102.03817.

[55] P. Wang, X. Li, N. Wang, Y. Li, K. Shi, and J. Lu, "Almost periodic synchronization of quaternion-valued fuzzy cellular neural networks with leakage delays," *Fuzzy Sets and Systems*, vol. 426, 2021.

[56] Y. Zhao, X. Li, and J. Cao, "Global exponential stability for impulsive systems with infinite distributed delay based on flexible impulse frequency," *Applied Mathematics and Computation*, vol. 386, Article ID 125467, 2020.

[57] F. Nazarimehr, S. Jafari, G. Chen et al., "A tribute to J. C. Sprott," *International Journal of Bifurcation and Chaos*, vol. 27, no. 14, Article ID 1750221, 2017.

[58] Z. Wei, "Dynamical behaviors of a chaotic system with no equilibria," *Physics Letters A*, vol. 376, no. 2, pp. 102–108, 2011.

[59] X. Wang and G. Chen, "A chaotic system with only one stable equilibrium," *Communications in Nonlinear Science and Numerical Simulation*, vol. 17, no. 3, pp. 1264–1272, 2012.

[60] A. Sambas, S. Vaidyanathan, T. Bonny et al., "Mathematical model and FPGA realization of a multi-stable chaotic dynamical system with a closed butterfly-like curve of equilibrium points," *Applied Sciences*, vol. 11, no. 2, p. 788, 2021.

[61] Z. Wang, Z. Wei, K. Sun et al., "Chaotic flows with special equilibria," *The European Physical Journal - Special Topics*, vol. 229, no. 6-7, pp. 905–919, 2020.

[62] Q. Wan, Z. Zhou, W. Ji, C. Wang, and F. Yu, "Dynamic analysis and circuit realization of a novel no-equilibrium 5D memristive hyperchaotic system with hidden extreme multistability," *Complexity*, vol. 2020, Article ID 7106861, 2020.

[63] S. Nag Chowdhury and D. Ghosh, "Hidden attractors: a new chaotic system without equilibria," *The European Physical Journal - Special Topics*, vol. 229, no. 6-7, pp. 1299–1308, 2020.

[64] X. Zhang and C. Wang, "Multiscroll hyperchaotic system with hidden attractors and its circuit implementation," *International Journal of Bifurcation and Chaos*, vol. 29, no. 9, Article ID 1950117, 2019.

[65] X. He, C. Li, X. Pan, and M. Peng, "Impulsive control and Hopf bifurcation of a three-dimensional chaotic system," *Journal of Vibration and Control*, vol. 20, no. 9, pp. 1361–1368, 2014.

[66] J. Sun and Y. Zhang, "Impulsive control of Lorenz systems," in *Proceedings of the Fifth World Congress on Intelligent Control and Automation*, pp. 71–73, IEEE, Hangzhou, China, June 2004.

[67] X. Li, X. Yang, and T. Huang, "Persistence of delayed cooperative models: impulsive control method," *Applied Mathematics and Computation*, vol. 342, pp. 130–146, 2019.

Hindawi
Complexity
Volume 2021, Article ID 1957510, 9 pages
https://doi.org/10.1155/2021/1957510

Research Article

Adaptive Super-Twisting Sliding Mode Control of Permanent Magnet Synchronous Motor

Chao Lu and Jing Yuan

School of Information Engineering, Suqian University, Suqian 223800, China

Correspondence should be addressed to Chao Lu; lchao@sqc.edu.cn

Received 29 June 2021; Revised 2 August 2021; Accepted 17 August 2021; Published 31 August 2021

Academic Editor: Xiaodi Li

The work has developed an innovative speed loop controller for the permanent magnet synchronous motor (PMSM) system. The main advantage of the presented method lies in the fact that the boundary of the lumped disturbance is not required. Under this case, the severe chattering caused by the inappropriate choice of parameters can be avoided. Finally, the simulation and experimental consequences are given to demonstrate the efficiency of the proposed algorithm used to control a PMSM system subject to the lumped disturbance.

1. Introduction

Owing to its superiorities of high control precision, high energy conversion rate, and low rotor inertia, permanent magnet synchronous motor (PMSM) has been applied to numerous fields, such as aerospace, new energy vehicle, industrial robot, and so on [1–3]. Nowadays, in actual industrial applications, the control strategies of the PMSM speed regulation system mostly adopt a classical proportional-integral (PI) controller. It is noted that the structure of such a controller is uncomplicated, and its parameters are easy to be modified [4, 5]. Nevertheless, the scheme for PI is a linear method. With the system running for a long time and emerging external disturbances, the system parameters will fluctuate nonlinearly. Therefore, the strategy based on PI cannot meet the qualifications of high performance of the servo system.

In order to settle the defects of the traditional PI controller, the nonlinear control plans are employed in the speed controller. With the evolution of control technologies, multifarious nonlinear control algorithms have been presented by scholars. Abundant schemes are feasible in the PMSM servo system among them, such as fuzzy control [6, 7], adaptive control [8, 9], fractional-order control [10, 11], disturbance observer [12–14], sliding mode control (SMC) [15, 16], intelligent control [17–19], and so on. By applying these algorithms to PMSM servo systems, the performances of PMSM servo systems have been noteworthily improved.

Among the aforementioned algorithms, the SMC method, which can guarantee excellent tracking performance despite parameters or model uncertainties, has been widely used in nonlinear systems owing to its strong robustness and fast dynamic response [20, 21]. Nonetheless, the chattering phenomenon is the main factor that hinders the further development of SMC. To cripple the chattering effect, different methods have been adopted, which can be summarized as the following three types [22–24]:

(i) The discontinuous control functions are substituted by "saturation" or "sigmoid ones."

(ii) The higher-order SMC techniques are used.

(iii) The controllers with dynamical gains are utilized.

By adopting these ideas, the modified SMC approaches have been successfully applied in many fields. Feng et al. [25] proposed a new reaching law, which achieved the expected goal of impairing chattering. The author in [26] used a super-twisting algorithm as the loop of the speed controller to fulfill high performance and attenuate

chattering. In [27], an adaptive first-order sliding mode controller was proposed and evaluated for the control of an electro-pneumatic actuator. However, the above research studies neglect the problem of uncertainty boundary which determines the choice of control parameters. In order to solve the aforementioned problem, the authors in [28, 29], respectively, proposed adaptive sliding mode plans. In [28], the boundary of disturbance is required in advance, and the adoption of a low-pass filter brings about some disadvantages such as time delay. In [29], the gain may be large, which leads to chattering. Everything has two sides, and these articles have own advantages and disadvantages. However, to some extent, they have promoted the development of control technology.

Motivated by the aforementioned observations, the main work of this paper concentrates on the design of the speed controller. The main contributions are outlined as follows. By combining the super-twisting algorithm and the adaptive technique, a novel speed loop controller is developed such that the requirements for the high performance of the PMSM servo system are satisfied. Particularly, the super-twisting algorithm can make the motor have superior starting characteristics and reduce the chattering effect. Also, the adaptive law can effectively handle the issue that the disturbance boundary cannot be obtained beforehand.

The remainder of the paper is organized as follows. In Section 2, the traditional model of surface-mounted PMSM is introduced, and the model uncertainties are analyzed. In Section 3, the design of the proposed ASMC controller and its stability analysis are presented. In Section 4, simulation and experimental results are shown to demonstrate the effectiveness of the proposed control strategy. The conclusions are drawn in Section 5.

2. Preliminaries

In this section, to facilitate the proposal of the new method, some preliminaries are introduced, including PMSM models and basic perturbation boundary analysis.

2.1. Model of PMSM System. In order to establish the mathematical model of surface-mounted PMSM in the coordinate system, it should be required to make the following assumptions:

(a) The saturation of the motor core is ignored.

(b) The eddy current and hysteresis loss in the motor are excluded.

(c) The current of the motor is a symmetrical three-phase sine wave current.

Based on the above three assumptions, the surface-mounted PMSM mathematical model in the rotor speed coordinate system is expressed as follows [30]:

$$\begin{cases} L_s \dfrac{\mathrm{d}i_d}{\mathrm{d}t} = -Ri_d + P_n L_s \omega i_q + U_d, \\ L_s \dfrac{\mathrm{d}i_q}{\mathrm{d}t} = -Ri_q - P_n L_s \omega i_d + U_q - P_n \varphi_f \omega, \\ J \dfrac{\mathrm{d}\omega}{\mathrm{d}t} = -B\omega + 1.5 P_n \varphi_f i_q - T_L. \end{cases} \tag{1}$$

To carry out the static decoupling of the axis current, we usually make i_d equivalent to 0, since the magnetic flux is completely offered by the permanent magnet when $i_d = 0$. The current on the straight axis is 0, which makes the motor be without armature reaction of the straight axis (i.e., the straight axis does not contribute torque). All the current of the motor is used to obtain electromagnetic torque, which is equivalent to a separately excited DC motor. Only by controlling the value, the torque of the motor can be controlled, which naturally realizes the static state of the motor decoupling. Consequently, the mathematical model of the motor can be simplified as

$$\begin{cases} L_s \dfrac{\mathrm{d}i_q}{\mathrm{d}t} = -Ri_q + U_q - P_n \varphi_f \omega, \\ J \dfrac{\mathrm{d}\omega}{\mathrm{d}t} = -B\omega + 1.5 P_n \varphi_f i_q - T_L, \end{cases} \tag{2}$$

where i_q and i_d represent the current component of the motor stator current on the d and q axes, respectively; U_d is the stator d-axis voltage and U_q is the stator q-axis voltage; T_L is the load torque; J is the rotational inertia; ω is the mechanical angular velocity of the motor; B is friction coefficient; φ_f is the motor flux linkage; and P_n represents motor pole pairs.

By formula (2), the relationship between angular velocity ω and i_q is as follows:

$$\dot{\omega} = -\frac{B}{J}\omega + \frac{1.5 P_n \varphi_f}{J} i_q^* + d_0(t), \tag{3}$$

where i_q^* is the reference current of q axis and $d_0(t) = -(T_L/J) - ((1.5 P_n \varphi_f)/J)(i_q^* - i_q)$ can be considered as the lumped disturbance.

2.2. Analysis of Lumped Disturbance Boundary. PMSM speed control is essentially the tracking problem of the actual servo system output signals and the given reference signals. As a result, the speed error is defined as

$$\sigma = \omega - \omega_r, \tag{4}$$

where ω_r is given reference mechanical angular velocity. Differentiating (4) yields

$$\dot{\sigma} = \dot{\omega} - \dot{\omega}_r\,. \tag{5}$$

Substituting (2) in the above equation produces

$$\dot{\sigma} = -\frac{B}{J}\sigma + d(t) + \frac{1.5P_n\varphi_f}{J}i_q^*, \tag{6}$$

where $k_t = 1.5P_n\varphi_f$ is the torque constant and $d(t) = -(T_L/J) - (k_t/J)(i_q^* - i_q) - (B/J)\omega_r$.

Although the mathematical model established only takes into account the external load disturbance mentioned in Section 2.1, it is usually accompanied by the parameter variation during the motor operation. Considering various disturbance, the motor model is further improved as

$$\dot{\sigma} = \left(-\frac{B}{J}\sigma + d(t) + \Delta\varpi\right) + \left(\frac{1.5P_n\varphi_f}{J} + \Delta\rho\right)i_q^*. \tag{7}$$

Then, we denote $\varpi_0(x,t) = -(B/J)\sigma + d(t)$, $\rho_0(x,t) = (k_t\varphi_f/J)$, where $\Delta\varpi$ is the sum of parameter variables and load disturbances and $\Delta\rho$ is the parameter variable. Considering that the change of parameter variable is smaller in comparison with the change of parameter itself, it is assumed that

$$\frac{|\Delta\rho(x,t)|}{\rho_0(x,t)} = \xi(x,t) \le \xi_1 < 1, \tag{8}$$

where ξ_1 is a constant of bounded but unknown value. In addition, we assume $|\varpi_0(x,t)| \le \delta_1|\sigma|^{1/2}$. Meanwhile, $\Delta\varpi$ is not a pulse signal, that is to say,

$$|\Delta\dot{\varpi}(x,t)| \le \delta_2, \tag{9}$$

where δ_2, δ_2 are random positive numbers, but their values are unknown.

After meeting the above hypothesis, (6) can be rewritten in the following form:

$$\dot{\sigma} = \varpi_0(x,t) + \Delta\varpi + \underbrace{\left(1 + \frac{\Delta\rho(x,t)}{\rho_0(x,t)}\right)}_{\rho_1(x,t)} u, \tag{10}$$

where $u = \rho_0(x,t)i_q$.

From (7), it is derived that

$$1 - \xi_1 \le \rho_1(x,t) \le 1 + \xi_1. \tag{11}$$

3. Structure of Speed Controller

In general, PMSM adopts the scheme of magnetic field orientation control (FOC), where the system is a double closed-loop structure. The sliding mode controller is a speed loop designed outside the PMSM system. In this part, the super-twisting controller is firstly designed. Then, the adaptive law is applied to the designed super-twisting controller.

3.1. Designing Super-Twisting Controller. By using high-order sliding mode related theory, the following super-twisting controller is given:

$$u = -\lambda_m\sqrt{|\sigma|}\operatorname{sign}(\sigma) - \int \frac{u_1}{2}\operatorname{sign}(\sigma)\mathrm{d}\tau, \tag{12}$$

where λ_m and u_1 are gains of the controller.

Since it is difficult to obtain the precise information about boundary, we usually assume that the lumped disturbance is bounded. However, the gains of the super-twisting controller depend on the upper and lower values of the boundary in the process of experiment. In order to solve this problem, we firstly need to prove that the lumped disturbance is bound at the mathematical level.

Therefore, we denote $u_* = \Delta\rho(x,t) + \rho_1 v$. Taking the derivative of u_*, one can obtain

$$\dot{u}_* = -\frac{u_1\rho_1(x,t)}{2}\operatorname{sign}(\sigma) + \Delta\dot{\varpi} + \dot{\rho}_1 v, \tag{13}$$

where $\dot{v} = -(u_1/2)\operatorname{sign}(\sigma)$.

Additionally, ε_{λ_m} and ε_{u_1}, respectively, represent their borders. There exist constant parameters ε_λ and ε_{u_1} such that $\varepsilon_\lambda = \lambda_m - \lambda_m^* < 0$ and $\varepsilon_{u_1} = u_1 - u_1^* < 0$. Then, it is not difficult for us to deduce

$$\left|\dot{\rho}_1(x,t)v\right| \le \frac{\dot{\rho}_1(x,t)}{2}\int_t^0 u_1\mathrm{d}\tau \le \frac{\dot{\rho}_1(x,t)}{2}u_1^* t \le \delta_3, \tag{14}$$

where $\delta_3 > 0$ is a constant of bounded but unknown value. Based on the above analysis, it is easy to obtain the lumped disturbance of the system as follows:

$$|\dot{\psi}(x,t)| = \Delta\dot{\varpi}(x,t) + \dot{\rho}_1(x,t)v \le \delta_2 + \delta_3 = \delta_4, \tag{15}$$

where δ_4 is unknown positive number and $\psi(x,t)$ is the lumped disturbance.

So far, we do not know the boundary value of each disturbance, but they have satisfied the bound for all possible disturbances. Therefore, the problem is simplified to the design of adaptive law such that the sliding variables $\sigma \longrightarrow 0$ and $\dot{\sigma} \longrightarrow 0$ are satisfied in finite time in the case of unknown boundary value.

3.2. Main Results. In general, the controller gains will be selected in very large values to improve the robustness of the system, but this leads to chattering of the system, which is not tolerated in some systems. In order to solve this problem, the adaptive law method can be used to dynamically adjust the controller gain online. According to the relevant theory, the designed adaptive law is formulated in the following theorem.

Theorem 1. *For a positive constant λ_M, when $\lambda_m \le \lambda_M$, $\dot{\lambda}_m = \eta, \dot{u}_1 \ge 2\varepsilon\eta$; when $\lambda_m > \lambda_M$,*

$$\begin{aligned} \dot{\lambda}_m &= \phi\sqrt{\frac{\gamma}{2}}\operatorname{sign}(|\sigma| - \mu), \\ \dot{u}_1 &\ge 2\varepsilon\phi\sqrt{\frac{\gamma}{2}}\operatorname{sign}(|\sigma| - \mu). \end{aligned} \tag{16}$$

Proof.

$$\begin{bmatrix} \dfrac{\mathrm{d}\left(|\sigma|^{1/2}\mathrm{sign}(\sigma)\right)}{\mathrm{d}t} \\ \dot{u}_* \end{bmatrix} = \frac{1}{\left||2\sigma|^{1/2}\mathrm{sign}(\sigma)\right|}\begin{bmatrix} -\lambda_m\rho_1|\sigma|^{1/2}\mathrm{sign}(\sigma) + u_* + \varpi_1 \\ -\dfrac{u_1\rho_1}{2|\sigma|^{1/2}\mathrm{sign}(\sigma)}|\sigma|^{1/2}\mathrm{sign}(\sigma) + \dot{\chi}(x,t) \end{bmatrix}$$
$$= \frac{1}{2|\sigma|^{1/2}\mathrm{sign}(\sigma)}\begin{bmatrix} -ab_1 & 1 \\ -\beta b_1 & 0 \end{bmatrix}\begin{bmatrix} |\sigma|^{1/2}\mathrm{sign}(\sigma) \\ \omega_* \end{bmatrix} + \frac{1}{2|\sigma|^{1/2}\mathrm{sign}(\sigma)}\begin{bmatrix} 1 & 0 \\ 0 & 2|\sigma|^{1/2}\mathrm{sign}(\sigma) \end{bmatrix}\begin{bmatrix} a_1 \\ \dot{\chi}(x,t) \end{bmatrix}. \tag{17}$$

Based on the above analysis, we know that

$$\varpi_0 = t_1|\sigma|^{1/2}\mathrm{sign}(\sigma),$$
$$\dot{\chi}(x,t) = \frac{t_2}{2}\frac{|\sigma|^{1/2}\mathrm{sign}(\sigma)}{\left||\sigma|^{1/2}\mathrm{sign}(\sigma)\right|}, \tag{18}$$

where $t_1 = (0, \delta_1], t_2 = (0, \delta_2]$.

Then, in view of (17), (16) can be rewritten as

$$\begin{bmatrix} \dfrac{\mathrm{d}\left(|\sigma|^{1/2}\mathrm{sign}(\sigma)\right)}{\mathrm{d}t} \\ \dot{u}_* \end{bmatrix} = \frac{1}{\left||2\sigma|^{1/2}\mathrm{sign}(\sigma)\right|}\begin{bmatrix} -(\lambda_m\rho_1 - t_1) & 1 \\ -(u_1\rho_1 - t_2) & 0 \end{bmatrix}\begin{bmatrix} |\sigma|^{1/2}\mathrm{sign}(\sigma) \\ \omega_* \end{bmatrix}. \tag{19}$$

For the convenience of expression, we denote $\begin{bmatrix} \zeta_1 \\ \zeta_2 \end{bmatrix} = \begin{bmatrix} |\sigma|^{1/2}\mathrm{sign}(\sigma) \\ u_* \end{bmatrix}$. To prove the stability of the system, we consider the following Lyapunov function:

$$V(\zeta_1, \zeta_2, \lambda_m, u_1) = V_0 + \frac{1}{2\xi_1}(\lambda_m - \lambda_m^*)^2 + \frac{1}{2\xi_2}(u_1 - u_1^*)^2, \tag{20}$$

where

$$V_0(\zeta) = \left(\lambda + 4\varepsilon^2\right)\zeta_1^2 + \zeta_1^2 - 4\varepsilon\zeta_1\zeta_2 = \zeta^T P\zeta, \tag{21}$$

$$P = \begin{bmatrix} \lambda + 4\varepsilon^2 & -2\varepsilon \\ -2\varepsilon & 1 \end{bmatrix}, \quad \varepsilon > 0. \tag{22}$$

Obviously, the matrix P is positive definite matrix when the parameter λ is greater than 0. By taking the derivative of $V_0(\zeta)$ in (20), one can derive

$$\dot{V}_0(\zeta) = \dot{\zeta}^T P\zeta + \zeta^T P\dot{\zeta} \le \zeta^T \widetilde{Q}\zeta. \tag{23}$$

To stabilize the system, the symmetric matrix Q must be positive definite. Hence, the characteristic value of matrix Q needs to be greater than 0. Hence, we enforce

$$u_1 = 2\varepsilon\lambda_m. \tag{24}$$

In view of (22), it is easy to show that

$$V_0(z) \le -rV_0^{1/2}(z), \tag{25}$$

where

$$r = \frac{\varepsilon\lambda_{\min^{1/2}}(P)}{\lambda_{\max}(P)}. \tag{26}$$

Based on the finite-time Lyapunov stability theorem, taking the derivative of $V(\zeta_1, \zeta_2, \lambda_m, u_1)$ in (19) gives

$$\begin{aligned}\dot{V}(\zeta,\lambda_m,u_1) &= \dot{\zeta}P\zeta + \zeta^T P\dot{\zeta} + \frac{1}{\gamma_1}\varepsilon_{\lambda_m}\dot{\lambda}_m + \frac{1}{\gamma_2}\varepsilon_{u_1}\dot{u}_1 \\ &\le -\frac{1}{|\zeta_1|}\zeta^T\widetilde{Q}\zeta + \frac{1}{\gamma_1}\varepsilon_n\lambda_m + \frac{1}{\gamma_2}\varepsilon_{u_1}\dot{u}_1 \\ &\le -rV_0^{1/2} + \frac{1}{\gamma_1}\varepsilon_{\lambda_m}\dot{\lambda}_m + \frac{1}{\gamma_2}\varepsilon_{u_1}\dot{u}_1 \\ &= -rV_0^{1/2} - \frac{\phi_1}{\sqrt{2\gamma_1}}\left|\varepsilon_{\lambda_m}\right| - \frac{\phi_2}{\sqrt{2\gamma_2}}\left|\varepsilon_{4_1}\right| \\ &\quad + \frac{1}{\gamma_1}\varepsilon_{2_m}\dot{\lambda}_m + \frac{1}{\gamma_2}\varepsilon_{u_1}\dot{u}_1 + \frac{\phi_1}{\sqrt{2\gamma_1}}\left|\varepsilon_{n_m}\right| + \frac{\phi_2}{\sqrt{2\gamma_2}}\left|\varepsilon_{u_1}\right| \\ &\le -\eta_0\sqrt{V(\zeta_1,\zeta_2,\lambda_m,u_1)} + \frac{1}{\gamma_1}\varepsilon_{\lambda_m}\dot{\lambda}_m \\ &\quad + \frac{1}{\gamma_2}\varepsilon_{u_1}\dot{u}_1 + \frac{\phi_1}{\sqrt{2\gamma_1}}\left|\varepsilon_{\lambda_m}\right| + \frac{\phi_2}{\sqrt{2\gamma_2}}\left|\varepsilon_{u_1}\right| \\ &\le -\eta_0\sqrt{V(\zeta_1,\zeta_2,\lambda_m,u_1)}.\end{aligned} \tag{27}$$

The proof of Theorem 1 is completed. □

Remark 1. It is worth pointing out that the proposed scheme is concluded as follows. Firstly, we introduce the model of surface-mounted PMSM, and the model uncertainties are analyzed. Secondly, the proposed ASMC controller design is proposed. Under the developed controller, the stability of the closed-loop system is guaranteed. Finally, the simulation and experimental results are given to confirm the feasibility of the proposed control strategy.

4. Simulation and Experimental Results

4.1. Simulation Results. In order to validate the effectiveness of the proposed scheme, a group of comparative simulations of speed loop controllers is performed in Matlab-Simulink 2013b environments by, respectively, using PI, STW, and ASTW algorithms. The simulation and experiment parameters of PMSM are listed in Table 1.

The parameters of current loop PI controller are consistent. The proportional gain is $k_p = 10$, and the integral gain is $k_i = 0.1$. The system reference speed is given as 600 rpm. The load torque $T_l = 1.65$ N is suddenly added to the PMSM system at 0.1 s and abruptly removed from the system at 0.2 s. The parameters of the proposed speed controller are $\phi = 1, \gamma = 2, \mu = 0.001, \varepsilon = 250, \eta = 10000$, and $\lambda_M = 5$.

The speed waveforms of the three methods from 0 to 600 rpm are shown in Figure 1. It can be observed from Figure 1 that the PI has a very short rise time but a very large overshoot compared with the other two controllers. The rise time and adjusting time of ASTW are a little shorter compared with the STW method. Simulation results of anti-load disturbance of the three controllers are shown in Figure 2. When the same load torque is suddenly added or removed from the system at the same time, the fluctuation of speed of the system under the ASTW method is the smallest, and the recovering time against disturbance is the shortest. Additionally, the response of motor q axial current, load torque, and phase current in the presence of a sudden disturbance load is, respectively, shown in Figures 3 and 4. One can see that the starting current of motor under ASTW is the smallest. Meanwhile, the chattering has been attenuated for the ASTW algorithm. A comparison of performance indices on the three methods is shown in Table 2. Moreover, the comparisons of the d-axis current responses and the T_L under the three controllers are, respectively, shown in Figures 5 and 6.

Table 1: Main parameters of PMSM.

Quantity	Symbol	Value and unit
Stator flux linkage	φ_f	0.1068 wb
Stator resistance	R	0.925 Ω
Moment of inertia	J	0.1068 kg/m^2
Torque constant	K_t	0.641 Nm/A
Number of pole pairs	P_n	4

4.2. Experimental Results. The core equipment of PMSM servo system mainly consists of the PMSM control board, permanent magnet synchronous motor drive board, orthogonal encoder, signal acquisition device, magnetic powder brake, permanent magnet synchronous motor, and so on. The control board of the experimental platform uses DSP TMS320F28335 as the main control chip, and the experimental program is written in a mixture of C language and assembly language. The permanent magnet synchronous motor of the experimental platform is driven by IPM three-phase voltage source inverter. The IPM module of the experimental platform adopts PS21865-AP chip produced by Mitsubishi Corporation of Japan. The collection of experimental data can be completed by using oscilloscope.

Similarly, the current values of different algorithms are the same in order to guarantee the fairness of the experiment, i.e., the proportional gains are $k_p = 0.2$ and the integral gains are $k_p = 0.04$. The experimental parameters of the proposed speed controller are $\phi = 1, \gamma = 0.1, \mu = 0.05, \varepsilon = 5, \eta = 500$, and $\lambda_M = 0.1$.

Figure 7 shows the speed waveform diagram at startup phase under different algorithms. It reveals that the overshoot time, adjusting time, and the rise time in ASTW are all shortest compared with the other algorithms. Figure 8 shows the experimental results of PI, STW, and ASTW with load torque disturbance at 600 rpm. It shows that the maximum speed drop of ASTW, which is almost 10 rpm, is the smallest. Meanwhile, the speed of ASTW can return to reference in the shortest time. In Figures 9–11, each image contains three subimages. The three subimages are PI, STW, and ASTW from top to bottom, respectively. Figure 9 is the response of q-axis current in the startup phase and with load, and Figure 10 is the response of d-axis current in the startup phase and with load. Figure 11 is comparison of the phase current

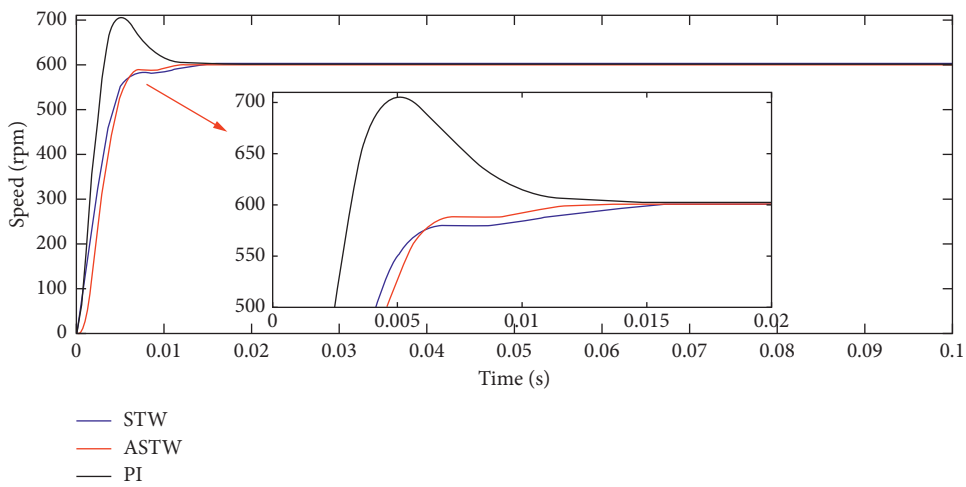

Figure 1: Comparison of the speed responses without load.

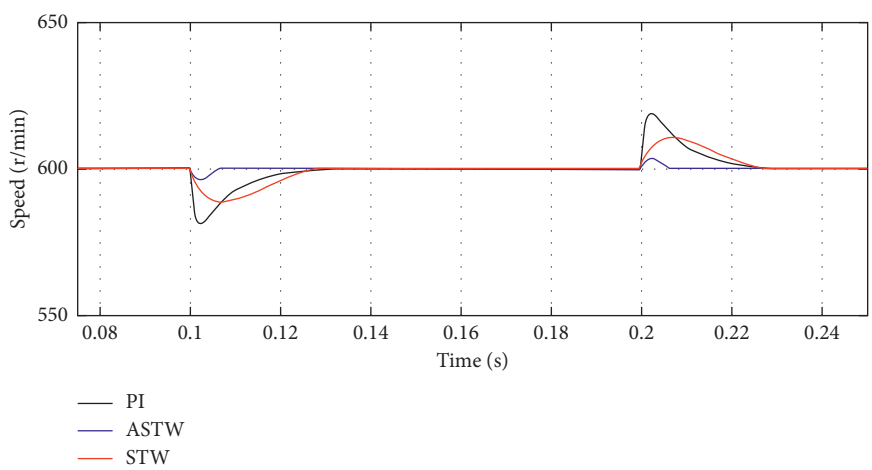

Figure 2: Comparison of the speed responses with load.

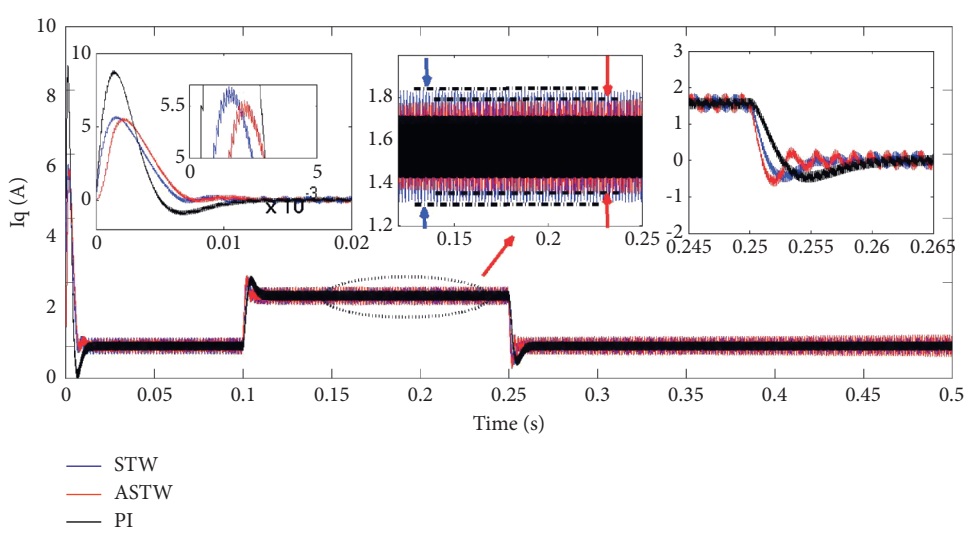

Figure 3: Comparison of the q-axis current responses.

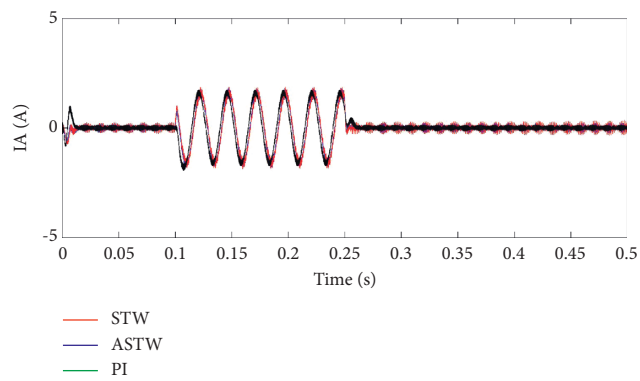

Figure 4: Comparison of the IA responses.

Table 2: Comparison of performance indices in PMSM simulation.

Symbol	PI	STW	ASTW
Rise time (t_r)	0.0025 s	0.015 s	0.01 s
Adjusting time (t_s)	0.0125 s	0 s	0 s
Drop	30r	20r	5r

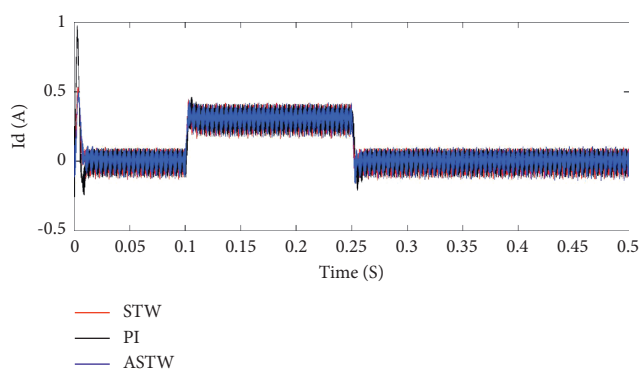

Figure 5: Comparison of the d-axis current responses.

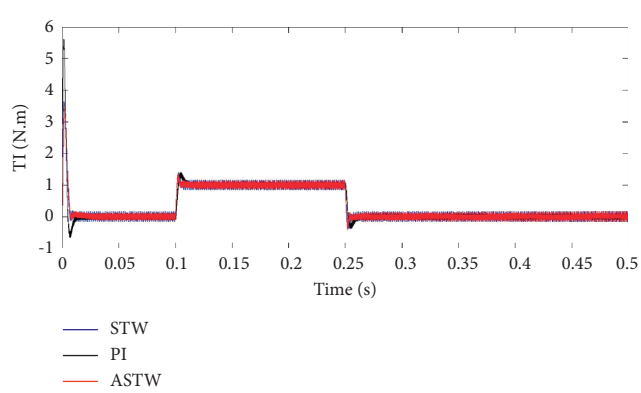

Figure 6: Comparison of the Tl.

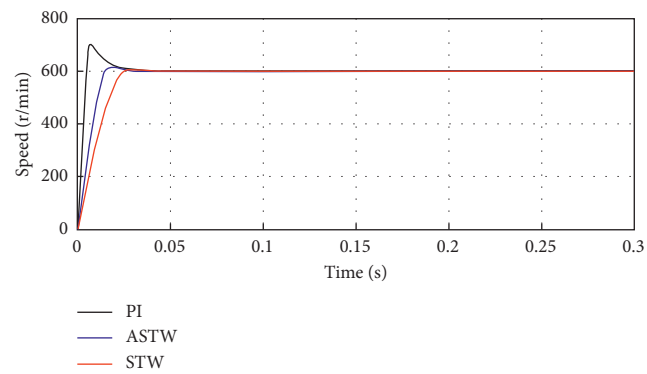

Figure 7: Comparative experimental diagram of PMSM motor speed in starting stage under PI, STW, and ASTW.

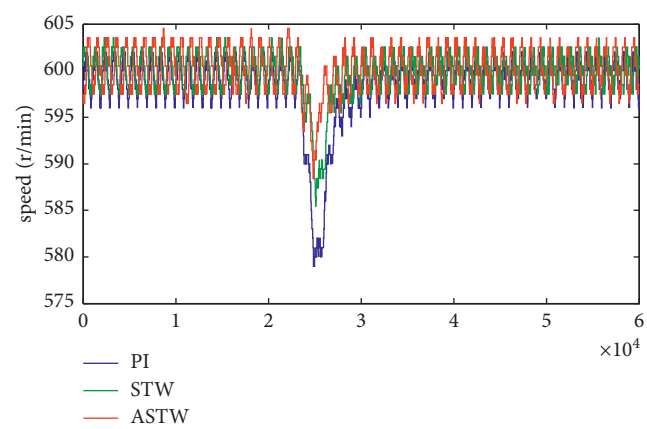

Figure 8: Comparative experimental diagram of PMSM motor speed in loading stage under PI, STW, and ASTW.

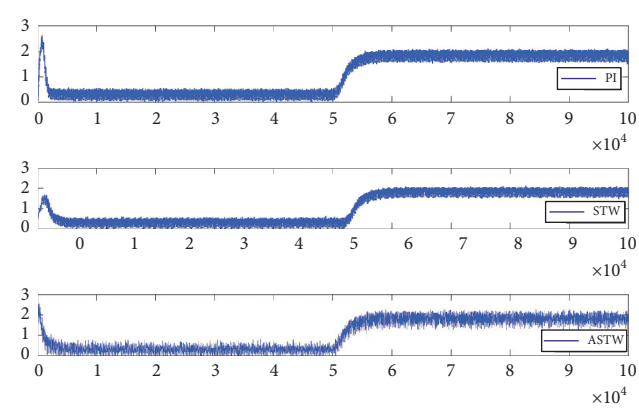

Figure 9: Comparative experimental diagram of i_q.

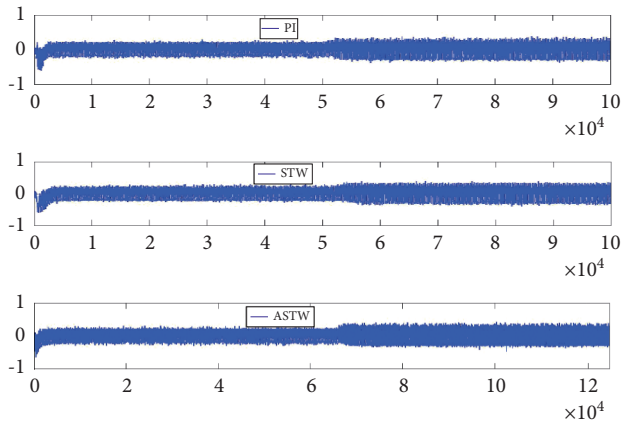

Figure 10: Comparative experimental diagram of i_d.

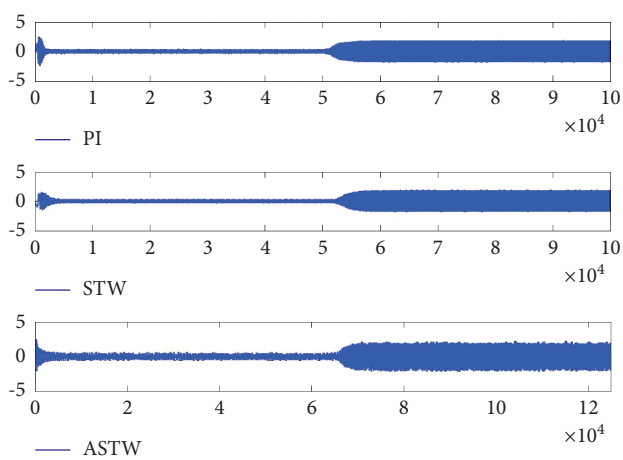

Figure 11: Comparative experimental diagram of i_a.

Table 3: Comparison of performance indices in PMSM experiment.

Symbol	PI	STW	ASTW
Rise time (t_r)	0.097 s	0.143 s	0.014 s
Adjusting time (t_s)	0.114 s	0.029 s	0 s
Drop	$20r$	$14r$	$9r$

responses in the startup phase and with load, respectively. A comparison of performance indices on the three methods is shown in Table 3.

5. Conclusions

This paper has developed a novel speed loop controller for the PMSM system. By combining the super-twisting algorithm with the adaptive law, the proposed speed controller has excellent robustness because it does not depend on the information of the lumped disturbance. It has also been proved that the signal of the lumped disturbance is bounded, and the speed error of the closed-loop system converges to zero at the mathematical level. Both simulation and experiment results are given to clearly confirm that the proposed speed regulator gives very remarkable speed-control performance without the information on the lumped disturbance.

Data Availability

No data were used to support this study.

Conflicts of Interest

The authors declare that they have no conflicts of interest.

Acknowledgments

This study was supported by the Guiding Funds for Industrial Development of Suqian City under grant no. S201920.

References

[1] B. Xu, L. Zhang, and W. Ji, "Improved non-singular fast terminal sliding mode control with disturbance observer for PMSM drives," *IEEE Transactions on Transportation Electrification*, p. 1, 2021.

[2] S. Li and Z. Liu, "Adaptive speed control for permanent-magnet synchronous motor system with variations of load inertia," *IEEE Transactions on Industrial Electronics*, vol. 56, no. 8, pp. 3050–3059, 2009.

[3] Q. Hou and S. Ding, "GPIO based super-twisting sliding mode control for PMSM," *IEEE Transactions on Circuits and Systems II: Express Briefs*, vol. 68, no. 2, pp. 747–751, 2021.

[4] X. Li, J. Shen, H. Akca, and R. Rakkiyappan, "LMI-based stability for singularly perturbed nonlinear impulsive differential systems with delays of small parameter," *Applied Mathematics and Computation*, vol. 250, pp. 798–804, 2015.

[5] Q. Hou, S. Ding, and X. Yu, "Composite super-twisting sliding mode control design for PMSM speed regulation problem based on a novel disturbance observer," *IEEE Transactions on Energy Conversion*, vol. 99, p. 1, 2020.

[6] S. Tong and H. X. Li, "Fuzzy adaptive sliding-mode control for MIMO nonlinear systems," *IEEE Transactions on Fuzzy Systems*, vol. 11, no. 3, pp. 354–360, 2003.

[7] L. Fang, S. Ding, J. H. Park, and L. Ma, "Adaptive fuzzy output-feedback control design for a class of p-norm stochastic nonlinear systems with output constraints," *IEEE Transactions on Circuits and Systems I: Regular Papers*, vol. 68, no. 6, pp. 2626–2638, 2021.

[8] S. Ding, W. X. Zheng, J. Sun, and J. Wang, "Second-order sliding-mode controller design and its implementation for buck converters," *IEEE Transactions on Industrial Informatics*, vol. 14, no. 5, pp. 1990–2000, 2018.

[9] L. Liu, W. X. Zheng, and S. Ding, "An adaptive SOSM controller design by using a sliding-mode-based filter and its application to buck converter," *IEEE Transactions on Circuits and Systems I: Regular Papers*, vol. 67, no. 7, pp. 2409–2418, 2020.

[10] Y. Luo, Y. Chen, H.-S. Ahn, and Y. Pi, "Fractional order robust control for cogging effect compensation in PMSM position servo systems: stability analysis and experiments," *Control Engineering Practice*, vol. 18, no. 9, pp. 1022–1036, 2010.

[11] X. Li, D. O'Regan, and H. Akca, "Global exponential stabilization of impulsive neural networks with unbounded continuously distributed delays," *IMA Journal of Applied Mathematics*, vol. 80, no. 1, pp. 85–99, 2015.

[12] N. Jin, X. Wang, and X. Wu, "Current sliding mode control with a load sliding mode observer for permanent magnet synchronous machines," *Journal of Power Electronics*, vol. 14, no. 1, pp. 105–114, 2014.

[13] D. Yang, X. Li, and J. Qiu, "Output tracking control of delayed switched systems via state-dependent switching and dynamic output feedback," *Nonlinear Analysis: Hybrid Systems*, vol. 32, pp. 294–305, 2019.

[14] S. Li, M. Zhou, and X. Yu, "Design and implementation of terminal sliding mode control method for PMSM speed regulation system," *IEEE Transactions on Industrial Informatics*, vol. 9, no. 4, pp. 1879–1891, 2013.

[15] D. Yang, X. Li, J. Shen, and Z. Zhou, "State-dependent switching control of delayed switched systems with stable and unstable modes," *Mathematical Methods in the Applied Sciences*, vol. 41, no. 16, pp. 6968–6983, 2018.

[16] K. Mei and S. Ding, "HOSM controller design with asymmetric output constraints," *Science China Information Sciences*, vol. 65, Article ID 189202, 2022.

[17] J. Yuan, S. Ding, and K. Mei, "Fixed-time SOSM controller design with output constraint," *Nonlinear Dynamics*, vol. 102, no. 3, pp. 1567–1583, 2020.

[18] S. Ding, B. Zhang, K. Mei, and J. H. Park, "Adaptive fuzzy SOSM controller design with output constraints," *IEEE Transactions on Fuzzy Systems*, p. 1, 2021.

[19] J. Hu, G. Sui, X. Lv, and X. Li, "Fixed-time control of delayed neural networks with impulsive perturbations," *Nonlinear Analysis: Modelling and Control*, vol. 23, no. 6, pp. 904–920, 2018.

[20] Y. Feng, X. Yu, and F. Han, "High-order terminal sliding-mode observer for parameter estimation of a permanent-magnet synchronous motor," *IEEE Transactions on Industrial Electronics*, vol. 60, no. 10, pp. 4272–4280, 2013.

[21] K. Mei and S. Ding, "Second-order sliding mode controller design subject to an upper-triangular structure," *IEEE Transactions on Systems, Man, and Cybernetics: Systems*, vol. 51, no. 1, pp. 497–507, 2021.

[22] Y. Shtessel, M. Taleb, and F. Plestan, "A novel adaptive-gain supertwisting sliding mode controller: methodology and application," *Automatica*, vol. 48, no. 5, pp. 759–769, 2012.

[23] E. Cruz-Zavala and J. A. Moreno, "Homogeneous high order sliding mode design: a Lyapunov approach," *Automatica*, vol. 80, pp. 232–238, 2017.

[24] V. Utkin, "Discussion aspects of high-order sliding mode control," *IEEE Transactions on Automatic Control*, vol. 61, no. 3, pp. 829–833, 2016.

[25] L. Feng, M. Deng, S. Xu, and D. Huang, "Speed regulation for PMSM drives based on a novel sliding mode controller," *IEEE Access*, vol. 8, pp. 63577–63584, 2020.

[26] H.-W. Chai, "Sliding mode control of PMSM based on robust differentiator," in *Proceedings of the 2010 Second International Conference on Computational Intelligence and Natural Computing*, pp. 37–40, Wuhan, China, September 2010.

[27] J. Ma, G. G. Zhu, and H. Schock, "Adaptive control of a pneumatic valve actuator for an internal combustion engine," *IEEE Transactions on Control Systems Technology*, vol. 19, no. 4, pp. 730–743, 2011.

[28] H. Lee and V. I. Utkin, "Chattering suppression methods in sliding mode control systems," *Annual Reviews in Control*, vol. 31, no. 2, pp. 179–188, 2007.

[29] A. C. Huang and Y. H. Chen, "Adaptive multiple-surface sliding control for nonautonomous systems with mismatched uncertainties," *Automatica*, vol. 40, no. 1, pp. 1939–1945, 2004.

[30] Y. Zuo, X. Zhu, L. Quan, C. Zhang, Y. Du, and Z. Xiang, "Active disturbance rejection controller for speed control of electrical drives using phase-locking loop observer," *IEEE Transactions on Industrial Electronics*, vol. 66, no. 3, pp. 1748–1759, 2018.

Hindawi
Complexity
Volume 2021, Article ID 9042402, 7 pages
https://doi.org/10.1155/2021/9042402

Research Article

Some Fixed-Point Theorems on Generalized Cyclic Mappings in *B*-Metric-Like Spaces

Shengquan Weng [1] **and Quanxin Zhu** [2]

[1] *Faculty of Physics and Mathematics, Yibin University, Yibin 644000, China*
[2] *School of Mathematics and Statistics, Hunan Normal University, Changsha 410081, China*

Correspondence should be addressed to Quanxin Zhu; zqx22@hunnu.edu.cn

Received 20 June 2021; Accepted 6 August 2021; Published 30 August 2021

Academic Editor: Xiaodi Li

In this paper, it is concerned with the cyclic mapping in b-metric-like spaces. The definition of W-type cyclic mappings is proposed, and then, the existence-uniqueness of the fixed points of these cyclic mappings and the corresponding fixed point theorems are studied. In b-metric-like spaces, the promotion of the concept of cyclic mapping is an interesting topic; then, it is worthy to continue to this part of the promotion. On this basis, the concept of φ-type cyclic mapping is proposed in this article, and the existence-uniqueness of fixed-point problems and the corresponding fixed-point theorem are considered and studied. The results of this paper further generalize and extend some previous results.

1. Introduction

The problem of solving the equation is involved in many research areas of mathematics; in addition, there is more than just one way to solve the equation. The fixed-point theory is a kind of general theory which is closely related to solving equations. Algebraic equations, functional equations, differential equations, and so on have various forms. These different kinds of equations, although they have different forms, can often be rewritten in terms of $f(x) = x$. So, x here is a point in some appropriate space X, and f is a mapping or movement from X to X, moving every point x to the point $f(x)$. The solution of equation $f(x) = x$ is exactly the point that is left in place under the action of f, so it is called the fixed point. So, the problem of solving the equation becomes a geometric problem of finding a fixed point.

It is a very interesting work and a hot topic to find out whether fixed points of many mappings exist and are unique. There are a lot of papers on this aspect. Mathematical researchers study the fixed-point problems in a metric space, which generally involve two aspects; on the one hand, it was to the definition of a metric space, that is, the three basic properties of metric space in the definition have been widely discussed, then all kinds of generalized metric spaces are obtained, and in the generalized metric spaces, the classic Banach mapping contraction principle is frequently extended [1]. On the other hand, based on the study of related problems of generalized metric space, the extension of the original some mappings, and the proposal of some new mappings, through the hard work of many mathematical researchers, many conclusions have been obtained. Next, we will properly elaborate on these two aspects.

The concept of a metric space is introduced as follows.

Definition 1. Let X be a nonempty set and $d: X \times X \longrightarrow [0, \infty)$ be a function such that, for all $x, y \in X$, the following three conditions hold true:

(i) $d(x, y) \geq 0, d(x, y) = 0 \Leftrightarrow x = y$
(ii) $d(x, y) = d(y, x)$
(iii) $d(x, y) \leq d(x, z) + d(z, y)$

Then, the pair (X, d) is called a metric space.

In fact, letting $d(x, y) = |x - y|$, it is easy to know that it is a metric.

Next, let us see how each of the three properties of metric spaces has been investigated.

In 2012, Amini-Harandi [2] considered the first property of metric space and made appropriate modifications, and thus they proposed the definition of metric-like space.

Definition 2. Let X be a nonempty set and $\varphi\colon X \times X \longrightarrow R_+$ be a function such that, for all $x, y, z \in X$, the following three conditions hold true:

(i) $\varphi(x, y) = 0 \Rightarrow x = y$

(ii) $\varphi(x, y) = \varphi(y, x)$

(iii) $\varphi(x, y) \leq \varphi(x, z) + \varphi(z, y)$

Then, the pair (X, φ) is called a metric-like space.

In 1993, Czerwik [3] considered the third property of metric space and thus proposed the definition of b-metric space.

Definition 3. A mapping $D\colon X \times X \longrightarrow [0, \infty)$, where X is a nonempty set, is said to be a b-metric on X if, for any $x, y, z \in X$ and $K \geq 1$, the following three conditions hold true:

(1) $D(x, y) = 0 \Leftrightarrow x = y$

(2) $D(x, y) = D(y, x)$

(3) $D(x, z) \leq K(D(x, y) + D(y, z))$

The pair (X, D) is then called a b-metric-like space.

In 2013, Alghamdi et al. [4] considered the first and third properties of metric space and thus proposed the definition of b-metric-like space.

Definition 4. Letting a b-metric-like on a nonempty set X be a function $D\colon X \times X \longrightarrow [0, +\infty)$ such that, for all $x, y, z \in X$ and a constant $K \geq 1$, the following three conditions hold true:

(**D**1) if $D(x, y) = 0 \Rightarrow x = y$

(**D**2) $D(x, y) = D(y, x)$

(**D**3) $D(x, y) \leq K(D(x, z) + D(z, y))$

The pair (X, D) is called a b-metric-like space.

It is important to note that the symbols d, D, φ, r in Definitions 1 to 4 all represent a measure symbol. In essence, the meaning is the same. In fact, there are many generalizations of the definition of metric space, such as Definitions 5–9.

Definition 5 (see [5]). A mapping $p\colon X \times X \longrightarrow R_+$, where X is a nonempty set, is said to be a partial metric on X if, for any $x, y, z \in X$, the following four conditions hold true:

(**P**1) $x = y$ if and only if $p(x, x) = p(y, y) = p(x, y)$

(**P**2) $p(x, x) \leq p(x, y)$

(**P**3) $p(x, y) = p(y, x)$

(**P**4) $p(x, z) \leq p(x, y) + p(y, z) - p(y, y)$

The pair (X, p) is then called a partial metric space.

In 2017, Kamran et al. [6] obtained some fixed-point theorems in a generalized b-metric space.

Definition 6. Consider the set $F \neq \varnothing$ and a function $\hbar\colon F \times F \longrightarrow [1, \infty)$. Suppose that a function $\zeta\colon F \times F \longrightarrow R^+$ satisfies the following conditions, for all $g, h, w \in F$:

(1) $\zeta(g, h) = 0 \Leftrightarrow g = h$

(2) $\zeta(g, h) = \zeta(h, g)$

(3) $\zeta(g, h) \leq \hbar(g, h)[D(g, w) + D(w, h)]$

The pair (F, ζ) is called an extended b-metric space.

Some results for b-metric space and extended b-metric space are in [7–14]. The definition of controlled metric-type space [15] is presented as follows.

Definition 7. Given a nonempty set F and a function $\varpi\colon F^2 \to [1, \infty)$. Suppose that a function $\rho\colon F^2 \to [0, \infty)$ satisfies the following conditions, for all $g, h, w \in F$:

(ρ1) $\rho(g, h) = 0 \Leftrightarrow g = h$

(ρ2) $\rho(g, h) = \zeta(h, g)$

(ρ3) $\rho(g, h) \leq \varpi(g, w)\rho(g, w) + \varpi(w, h)\rho(w, h)$

The pair (F, ρ) is called a controlled metric-type space.

In fact, the definition of a generalization of controlled metric-type spaces to double controlled metric-type spaces is given as follows.

Definition 8 (see [16]). Consider a set $F \neq \varnothing$ and noncomparable functions $\hbar, \varepsilon\colon F \times F \longrightarrow [1, \infty)$. Suppose that a function $\zeta\colon F \times F \longrightarrow [0, \infty)$ satisfies the following conditions for all $g, h, w \in F$:

(1) $\zeta(g, h) = 0$ if only and if $g = h$

(2) $\zeta(g, h) = \zeta(h, g)$

(3) $\zeta(g, h) \leq \varpi(g, w)\zeta(g, w) + \varepsilon(w, h)\zeta(w, h)$

The pair (F, ζ) is called a double controlled metric-type space.

Next, the generalization of the double controlled metric-type space [17] is given as follows.

Definition 9. Consider a set $F \neq \varnothing$ and noncomparable functions $\hbar, \varepsilon\colon F \times F \longrightarrow [1, \infty)$. Suppose that a function $\zeta\colon F \times F \longrightarrow [0, \infty)$ satisfies the following conditions for all $g, h, w \in F$:

(1) $\zeta(g, h) = 0 \Rightarrow g = h$

(2) $\zeta(g, h) = \zeta(h, g)$

(3) $\zeta(g, h) \leq \varpi(g, w)\zeta(g, w) + \varepsilon(w, h)\zeta(w, h)$

The pair (F, ζ) is called a double controlled metric-like space.

We have explored the development of generalized metric spaces above; for these generalized metric spaces, many mappings in metric spaces and generalization of generalized metric spaces have produced many results. Next, we will focus on the generalization of related mappings in b-metric-like spaces. However, we are going to start with a classic result from metric space. In a metric space, Banach contractions' principle is a classical result in fixed-point theory. Here, we state the concept of contractive mapping as follows.

Definition 10. Let X be a metric space and $T\colon X \longrightarrow X$ be a mapping. If there exists a constant $\alpha \in (0,1)$ such that, for all $x, y \in X$, the following condition is satisfied,

$$d(Tx, Ty) \leq \alpha\, d(x, y), \tag{1}$$

then the mapping T is called a contractive mapping.

It is natural that Banach contractions principle [1] is extended in kinds of metric space, for example, partial metric space, b-metric space, and b-metric-like space.

In 2017, Lei and Wu [18] proposed the concept of the LW-type cyclic mapping in a complete b-metric-like space and obtained the corresponding fixed-point theorem as follows.

Definition 11. Let G_1, G_2 be nonempty closed sets in (X, r). If (B, S) is a pair semicyclic mapping in $G_1 \times G_2$ and there exists some nonnegative real constants γ, δ, t such that, for all $x \in G_1$, $y \in G_2$ satisfy the following condition,

$$\gamma r(x, Bx) + \delta r(y, Sy) + t r(Bx, Sy) \leq r(x, y), \tag{2}$$

then (B, S) is called as a LW-type cyclic mapping.

Theorem 1. *Let (X, r) be a complete b-metric-like space, and (B, S) be a LW-type cyclic mapping in (X, r). Suppose that G_1, G_2 are nonempty closed sets in (X, r) and $G_1 \cap G_2 \neq \varnothing$, if $\gamma + \delta + t > s$, $t > 1$. Then, there exists a unique $z^* \in G_1 \cap G_2$ such that $Bz^* = z^* = Sz^*$, that is, B and S have a unique common fixed point.*

In 2018, Weng et al. [19] proposed the concept of LW-type Lipschitz cyclic mapping in a complete b-metric-like space as follows.

Definition 12. Let G_1, G_2 be nonempty closed sets in (X, r). If (B, S) is a pair semicyclic mapping in $G_1 \times G_2$ and there exists some nonnegative real constants γ, δ, t, L and $L < \gamma + \delta + t$ such that, for all $x \in G_1$, $y \in G_2$ satisfy the following condition,

$$\gamma r(x, Bx) + \delta r(y, Sy) + t r(Bx, Sy) \leq L r(x, y), \tag{3}$$

then (B, S) is called a LW-type Lipschitz cyclic mapping.

Here, the definition of a pair semicyclic mapping and the definition of a complete b-metric-like space are given in Section 2. Next, we give the fixed-point theorem for LW-type Lipschitz cyclic mapping as follows.

Theorem 2. *Let (X, r) be a complete b-metric-like space, and (B, S) be a LW-type Lipschitz cyclic mapping in (X, r). Suppose that G_1, G_2 are nonempty closed sets in (X, r) and $G_1 \cap G_2 \neq \varnothing$ if $L \leq t$, $L = \max\{\gamma, \delta\}$, $\gamma \neq \delta$, and $s \in [1, ((L+t)/|\gamma - \delta|))$. Then, there exists a unique $x^* \in G_1 \cap G_2$ such that $Bx^* = x^* = Sx^*$, that is, B and S have a unique common fixed point.*

In fact, based on Definition 12 and Theorem 2, in 2019, S. Weng [20] proposed the concept of an extended mapping for the above cyclic mapping and named it as a general LW-type cyclic mapping.

Definition 13. Let G_1, G_2 be nonempty closed sets in (X, r). If (B, S) is a pair semicyclic mapping in $G_1 \times G_2$ and there exists some nonnegative functions β, δ, t such that, for all $x \in G_1$, $y \in G_2$ satisfy the following condition,

$$\begin{aligned} &\beta(r(x, y)) r(x, Bx) + \delta(r(x, y)) r(y, Sy) \\ &\quad + t(r(x, y)) r(Bx, Sy) \leq r(x, y), \end{aligned} \tag{4}$$

where $\beta, \delta\colon [0, +\infty) \longrightarrow [0, +\infty)$, $t\colon [0, +\infty) \longrightarrow [1, +\infty)$, then (B, S) is called as a general LW-type cyclic mapping.

At the same time, a fixed-point theorem for a general LW-type cyclic mapping was obtained as follows.

Theorem 3. *Suppose that (X, r) is a complete b-metric-like space. Let (B, S) be a general LW-type cyclic mapping and G_1,G_2 be nonempty closed sets in (X, r) and $G_1 \cap G_2 \neq \varnothing$. Consider there exists λ such that the following conditions are satisfied:*

(1) $\max\{((1 - \beta(z))/(\delta(z) + t(z))), ((1 - \delta(z))/(\beta(z) + t(z))), z \in [0, +\infty)\}) \leq \lambda < 1$

(2) $\lambda s < 1$

Then, there exists a unique $x^* \in G_1 \cap G_2$ such that $Bx^* = x^* = Sx^*$, that is, B and S have a unique common fixed point.

In 2020, Weng et al. [21] proposed the concept of a general LW-type Lipschitz cyclic mapping and obtained some fixed-point theorems as follows.

Definition 14. Let G_1, G_2 be nonempty closed sets in (X, r). If (B, S) is a pair semicyclic mapping in $G_1 \times G_2$ and there exists some nonnegative functions β, δ, t and nonnegative real number L such that, for all $x \in G_1$, $y \in G_2$ satisfy the following condition,

$$\begin{aligned} &\beta(r(x, y)) r(x, Bx) + \delta(r(x, y)) r(y, Sy) + t(r(x, y)) \\ &\quad r(Bx, Sy) \leq L r(x, y), \end{aligned} \tag{5}$$

where $\beta, \delta\colon [0, +\infty) \longrightarrow [0, +\infty)$, $t\colon [0, +\infty) \longrightarrow [1, +\infty)$, then (B, S) is called as a general LW-type Lipschitz cyclic mapping.

Theorem 4. *Suppose that (X, r) is a complete b-metric-like space. Let (B, S) be a general LW-type cyclic mapping and*

G_1, G_2 be nonempty closed sets in (X, r) and $G_1 \cap G_2 \neq \varnothing$. Consider there exists some λ such that the following conditions are satisfied:

(1) $\max\{((L-\beta(z))/(\delta(z)+t(z))), ((L-\delta(z))/(\beta(z)+t(z))), z \in [0,+\infty\}) \leq \lambda < 1$

(2) $\lambda s < 1$

(3) $L \in [1, t(z)]$

Then, there exists a unique $x^* \in G_1 \cap G_2$ such that $Bx^* = x^* = Sx^*$, that is, B and S have a unique common fixed point.

In 2021, Weng and Liang [22] proposed the concept of W-type cyclic mapping in b-metric-like spaces and obtained a fixed-point theorem as follows.

Definition 15. Let G_1, G_2 be nonempty closed sets in (X, r). If (B, S) is a pair semicyclic mapping in $G_1 \times G_2$ and there exists some nonnegative numbers γ, δ, t, L and $L < \gamma + \delta$ such that, for all $x \in G_1$, $y \in G_2$ satisfy the following condition,

$$r(Bx, Sy) \leq L[r(x, y) - M(x, y)], \tag{6}$$

where $M(x, y) = \{\gamma r(x, Bx), \delta r(y, Sy)\}$, then (B, S) is called a W-type cyclic mapping.

Theorem 5. *Suppose that (X, r) is a complete b-metric-like space. Let (B, S) be a W-type cyclic mapping and G_1, G_2 be nonempty closed sets in (X, r) and $G_1 \cap G_2 \neq \varnothing$. If the following conditions are satisfied:*

(1) $\delta + \gamma = 1$, $\delta, \gamma \in (0, 1)$

(2) $sp < 1$, $p = \max\{(L/(1+L\delta)), L\delta, L\gamma, (L/(1+L\gamma))\}$

Then, there exists a unique $x^* \in G_1 \cap G_2$ such that $Bx^* = x^* = Sx^*$, that is, B and S have a unique common fixed point.

Our work in b-metric-like space is continuous and is a series of work. It is interesting to generalize the results of cyclic mappings in b-metric-like spaces. Let $L = 1$; it is easy to know that a LW-type Lipschitz cyclic mapping is a LW-type cyclic mapping, a general LW-type Lipschitz cyclic mapping is a general LW-type cyclic mapping, and so on. Recently, we have reviewed the previous research work, and we will propose the concept of φ-type cyclic mapping in this paper and study the existence and uniqueness of its fixed point.

2. Preliminaries

In this part, some necessary definitions that will be used in Section 3 are given.

Definition 16 (see [4]). Let (X, r) be a b-metric-like space, and let $\{x_n\}$ be a sequence of points of X. A point $x \in X$ is said to be the limit of the sequence $\{x_n\}$ if $\lim_{n\longrightarrow\infty} r(x, x_n) = r(x, x)$, and we say that the sequence $\{x_n\}$ is convergent to x and denotes it by $x_n \longrightarrow x$ as $n \longrightarrow \infty$.

Definition 17 (see [4]). Let (X, r) be a b-metric-like space.

(i) A sequence $\{x_n\}$ is called Cauchy if and only if $\lim_{n\longrightarrow\infty} r(x_n, x_m)$ exists and is finite.

(ii) A b-metric-like space (X, r) is said to be complete if and only if every Cauchy sequence $\{x_n\}$ in X converges to $x \in X$ so that

$$\lim_{m,n\longrightarrow\infty} r(x_n, x_m) = r(x, x) = \lim_{n\longrightarrow\infty} r(x_n, x). \tag{7}$$

Definition 18 (see [4]). Let G_1, G_2 be nonempty sets of metric space; if $B(G_1) \subset G_2$ and $S(G_2) \subset G_1$, then the mapping (B, S): $G_1 \times G_2 \longrightarrow G_2 \times G_1$ is called as a pair semicyclic mapping, where B is said to be a lower semicyclic mapping and S is said to be a upper semicyclic mapping. If $B = S$, then B is said to be a cyclic mapping.

Definition 19 (see [12]). If $\prec$ is partially ordered in b-metric-like spaces (X, r), then $(X, r, \prec)$ is a partially ordered b-metric-like space.

3. Main Results

Now, we give the results for φ-type cyclic mapping proposed by us in this section.

Definition 20. Let G_1, G_2 be nonempty closed sets in (X, r). If (B, S) is a pair semicyclic mapping in $G_1 \times G_2$ and there exists some nonnegative real constants β, δ, t, and a nonnegative bounded function $\varphi(z)$ such that, for all $x \in G_1$, $y \in G_2$ satisfy the following condition,

$$\beta r(x, Bx) + \delta r(y, Sy) + t r(Bx, Sy) \leq \varphi(r(x, y)) r(x, y), \tag{8}$$

then (B, S) is called as a φ-type cyclic mapping.

Theorem 6. *Suppose that (X, r) is a complete b-metric-like space. Let (B, S) be a φ-type cyclic mapping and G_1, G_2 be nonempty closed sets in (X, r), and $G_1 \cap G_2 \neq \varnothing$, $h = \max\{\gamma, \delta\}$, and $P = \max\{(1/(\gamma+t)), (1/(\delta+t))\}$. Consider the following conditions are satisfied:*

(1) $\varphi(z)$: $[0, \infty) \longrightarrow [h, (1/sP)]$

(2) $hsP < 1$

Then, there exists a $z^* \in G_1 \cap G_2$ such that $Bz^* = z^* = Sz^*$, that is, B and S have the common fixed point.

Proof. The sequence $\{z_n\}$ is defined as follows:

$$\begin{aligned} z_0 \in G_1, z_1 = Bz_0, z_2 = Sz_1, z_3 = Bz_2, z_4 = Sz_3, \ldots, z_{2n+1} \\ = Bz_{2n}, z_{2n+2} = Sz_{2n+1}, \ldots, n \geq 0. \end{aligned} \tag{9}$$

Step 1 : prove that the sequence $\{z_n\}$ is a Cauchy sequence. Because (B, S) is a φ-type cyclic mapping, thus, we have

$$\gamma r(z_0, Bz_0) + \delta r(z_1, Sz_1) + tr(Bz_0, Sz_1) \leq \varphi(r(z_0, z_1))r(z_0, z_1), \tag{10}$$

that is,

$$\gamma r(z_0, z_1) + \delta r(z_1, z_2) + tr(z_1, z_2) \leq \varphi(r(z_0, z_1))r(z_0, z_1). \tag{11}$$

Because of $h = \max\{\gamma, \delta\}, \varphi(x) \geq h$, then we have

$$r(z_1, z_2) \leq \frac{\varphi(r(z_0, z_1)) - \gamma}{\delta + t} r(z_0, z_1) \leq \frac{1}{\delta + t} \varphi(r(z_0, z_1))r(z_0, z_1). \tag{12}$$

Continue with the above steps; then, we obtain

$$\gamma r(z_2, Bz_2) + \delta r(z_1, Sz_1) + tr(Bz_2, Sz_1) \leq \varphi(r(z_2, z_1))r(z_2, z_1), \tag{13}$$

that is,

$$\gamma r(z_2, z_3) + \delta r(z_1, z_2) + tr(z_3, z_2) \leq \varphi(r(z_2, z_1))r(z_2, z_1). \tag{14}$$

Because of $h = \max\{\gamma, \delta\}, \varphi(x) \geq h$ and (12) and (13), then we have

$$r(z_2, z_3) \leq \frac{\varphi(r(z_2, z_1)) - \delta}{\gamma + t} r(z_1, z_2) \leq \frac{1}{\gamma + t} \varphi(r(z_2, z_1)) \frac{1}{\delta + t} \varphi(r(z_0, z_1))r(z_0, z_1). \tag{15}$$

Let $Q = r(z_0, z_1)$; because of $P = \max\{(1/(\gamma + t)), (1/(\delta + t))\}$, from the definition of the φ-type cyclic mapping, it shows that $\varphi(x)$ is bounded, and $\varphi(x) \leq M = (1/sp)$; then, according to conditions (1) and (2), it implies that

$$r(z_2, z_3) \leq PMr(z_1, z_2) \leq P^2 M^2 Q. \tag{16}$$

Continue the above steps; then, we have

$$r(z_n, z_{n+1}) \leq P^n M^n Q. \tag{17}$$

Let $m > n$, $\forall m, n \in N$; this shows

$$\begin{aligned}
r(z_n, z_m) &\leq s(r(z_n, z_{n+1}) + r(z_{z+1}, z_m)) \\
&\leq sr(z_n, z_{n+1}) + s^2 r(z_{n+1}, z_{n+2}) + \cdots + s^{m-n} r(z_{m-1}, z_m) \\
&\leq s(PM)^n r(z_0, z_1) + s^2 (PM)^{n+1} r(z_0, z_1) + \cdots \\
&\quad + s^{m-n} (PM)^{m-1} r(z_0, z_1) \\
&\leq \left[s(PM)^n + s^2 (PM)^{n+1} + \cdots + s^{m-n} (PM)^{m-1}\right] Q \\
&= \frac{1 - (sPM)^{m-n}}{1 - sPM} sP^n Q \\
&\leq \frac{1}{1 - sPM} (PM)^{n-1} Q.
\end{aligned} \tag{18}$$

Since $P = \max\{(1/(\gamma+t)), (1/(\delta+t))\}$, $s \geq 1, M = (1/sP), 0 \leq PM = (1/s) \leq 1$, from (18), and $n \longrightarrow \infty$, we get that

$$\lim_{n\longrightarrow\infty} r(z_m, z_n) = 0. \tag{19}$$

This implies from (19) that the sequence $\{z_n\}$ is a Cauchy sequence.

Step 2 : ecause (X, r) is a complete b-metric-like space, $G_1 \cap G_2 \neq \varnothing$, then there exists a point $z \in X$ such that

$$z_n \longrightarrow z \ (n \longrightarrow \infty). \tag{20}$$

Therefore,

$$\begin{aligned} z_{2n} &\longrightarrow z, \\ z_{2n+1} &\longrightarrow z \ (n \longrightarrow \infty). \end{aligned} \tag{21}$$

Because $\{z_{2n}\} \subset G_1$, $\{z_{2n+1}\} \subset G_2$, and G_1, G_2 is closed, then

$$z \in G_1 \cap G_2. \tag{22}$$

Step 3 : prove that z is a fixed point of the mapping B and S, that is, $Bz = z = Sz$. Because (B, S) is a φ-type cyclic mapping, then we get that

$$\gamma r(z, Bz) + \delta r(z, Sz) + tr(Bz, Sz) \leq \varphi(r(z, z)) r(z, z). \tag{23}$$

Because $r(z, z) = \lim_{n,m\longrightarrow\infty} r(z_n, z_m)$, then, by (23), we have

$$\begin{aligned} r(z, Bz) &= 0, \\ r(z, Sz) &= 0. \end{aligned} \tag{24}$$

It implies that

$$Bz = z = Sz. \tag{25}$$

This completes the proof. □

Remark 1. With regard to the nonnegative bounded function in Definition 20, we give a concrete example here and give a concrete expression of the nonnegative bounded function. The nonnegative bounded function is defined as

$$\varphi(x) = h\frac{x}{1+x} + \left(\frac{1}{sP} - h\right)\frac{1}{1+x}. \tag{26}$$

It is definitely a nonnegative bounded function that conforms to the definition of $\varphi(x)$, that is, $\varphi(x)$: $[0, +\infty) \longrightarrow [h, (1/sP)]$.

Corollary 1. *Suppose that (X, r) is a complete partially ordered b-metric-like space. Let (B, S) be a φ-type cyclic mapping and G_1, G_2 be nonempty closed sets in (X, r), and $G_1 \cap G_2 \neq \varnothing$, $h = \max\{\gamma, \delta\}$, and $P = \max\{(1/(\gamma+t)), (1/(\delta+t))\}$. Consider the following conditions are satisfied:*

(1) $\varphi(x)$: $[0, \infty) \longrightarrow [h, (1/sP)]$

(2) $hsP < 1$

Then, there exists a $z^* \in G_1 \cap G_2$ such that $Bz^* = z^* = Sz^*$, that is, B and S have the common fixed point.

4. Conclusion

B-metric-like space is a kind of generalized metric space. The existence-uniqueness problem of fixed points in generalized metric spaces is an important problem in the field of fixed point theory. In this paper, we study the generalization of LW-type Lipschitz cyclic mapping. By using the definition of φ-type mapping, we establish the existence-uniqueness of its fixed point and a fixed-point existence theorem of φ-type mapping. In a word, the category of fixed point theory is very broad. The development of the theory of fixed points in generalized metric space is very significant. At the same time, it is beneficial to promote the study of stability of stochastic systems in [23–30] by applying our theory.

Data Availability

No data were used to support the study.

Conflicts of Interest

The authors declare that they have no conflicts of interest.

Authors' Contributions

All authors contributed equally.

Acknowledgments

This work was jointly supported by the National Natural Science Foundation of China (61773217), the Qi Hang Project of Yibin University (2021QH07), and the Scientific Research Fund of Yibin University (2021YY03).

References

[1] S. Banach, "Sur les opérations dans les ensembles abstraits et leur application aux équations intégrales," *Fundamenta Mathematicae*, vol. 3, no. 1, pp. 133–181, 1922.

[2] A. Amini Harandi, "Metric-like spaces, partial metric spaces and fixed points," *Journal of Fixed Point Theory and Application*, vol. 2012, Article ID 204, 2012.

[3] S. Czerwik, "Contraction mappings in b-metric spaces," *Acta Mathematica et Informatica Universitatis Ostraviensis*, vol. 1, no. 1, pp. 5–11, 1993.

[4] M. Alghamdi, N. Hussain, and P. Salimi, "Fixed point and coupled fixed point theorems on b-metric-like spaces," *Journal of Inequalities and Applications*, vol. 2013, no. 1, p. 402, 2013.

[5] S. G. Matthews, "Partial metric topology," *Annals of the New York Academy of Sciences* in *Proceedings of the 8th Summer Conference on General Topology and Applications*, vol. 728,

pp. 183–197, Annals of the New York Academy of Sciences, New York, NY, USA, November 1994.

[6] T. Kamran, M. Samreen, and Q. UlAin, "A generalization of b-metric space and some fixed point theorems," *Mathematics*, vol. 5, Article ID 19, 2017.

[7] W. Shatanawi, K. Abodayeh, and A. Mukhemer, "Some fixed point theorems in extended b-metric spaces," *UPB Science Bulletin, Series A, Applied Mathematical Physics*, vol. 80, no. 4, pp. 71–78, 2018.

[8] H. Afshari, M. Atapour, and H. Aydi, "Generalized $\alpha - \psi-$ Geraghty multivalued mappings on b-metric spaces endowed with agraph," *TWMS Journal of Applied and Engineering Mathematics*, vol. 7, no. 2, pp. 248–260, 2017.

[9] N. Alharbi, H. Aydi, A. Felhi, C. Ozel, and S. Sahmim, "Contractive mappings on rectangular b-$\alpha-$metric spaces and an application to integral equations," *Journal of Mathematical and Analysis*, vol. 9, no. 3, pp. 47–60, 2018.

[10] H. Aydi, R. Bankovic, I. Mitrovic, and M. Nazam, "Nemytzki-Edelstein-Meir-Keelertype results in b-metric spaces," *Discrete Dynamics in Nature and Society*, vol. 2018, Article ID 4745764, 7 pages, 2018.

[11] H. Qawaqneh, M. S. M. Noorani, W. Shatanawi, H. Aydi, and H. Alsamir, "Fixed point results for multi-valued contractions in b-metric spaces and an application," *Mathematics*, vol. 7, no. 2, Article ID 132, 2019.

[12] H. Aydi, A. Felhi, and S. Sahmim, "On common fixed points for (α, ψ)-contractions and generalized cyclic contractions in b-metric-like spaces and consequences," *The Journal of Nonlinear Science and Applications*, vol. 9, no. 5, pp. 2492–2510, 2016.

[13] H. Nashine and Z. Kadelburg, "Existence of solutions of cantilever beam problem via (α-β-FG)-contractions in b-metric-like spaces," *Filomat*, vol. 31, no. 11, pp. 3057–3074, 2017.

[14] Q. Kiran, N. Alamgir, N. Mlaiki, and H. Aydi, "On some new fixed point results in complete extended b-metric spaces," *Mathematics*, vol. 7, no. 5, Article ID 476, 2019.

[15] N. Mlaiki, H. Aydi, N. Souayah, and T. Abdeljawad, "Controlled metric type spaces and the related contraction principle," *Mathematics*, vol. 6, no. 10, Article ID 194, 2018.

[16] T. Abdeljawad, N. Mlaiki, H. Aydi, and N. Souayah, "Double controlled metric type spaces and some fixed point results," *Mathematics*, vol. 6, no. 12, p. 320, Article ID 320, 2018.

[17] N. Mlaiki, "Double controlled metric-like spaces," *Journal of Inequalities and Applications*, vol. 2020, no. 1, 2020.

[18] M. Lei and D. Wu, "Fixed point theorems concerning new type cyclic maps in complete B-metric-like spaces," *Journal of Chengdu University of Information Technology*, vol. 32, no. 1, pp. 82–85, 2017.

[19] S. Weng, Y. Zhang, and D. Wu, "Fixed point theorems of LW− type lipschitz cyclic mappings in complete B-Metric-Like spaces," *International Journal of Research in Industrial Engineering*, vol. 7, no. 2, pp. 136–146, 2018.

[20] S. Weng, "Some fixed point results involving a general LW− type cyclic mappings in complete B-Metric-Like spaces," *International Journal of Research in Industrial Engineering*, vol. 8, no. 3, pp. 262–273, 2019.

[21] S. Weng, X. Liu, and Z. Chao, "Some fixed point theorems for cyclic mapping in a complete B-Metric-Like space," *Results in Nonlinear Analysis*, vol. 3, no. 4, pp. 206–212, 2020.

[22] S. Weng and L. Liang, "Fixed point theorem for cyclic mapping in complete B-Metric-Like spaces," *Journal of Yinbin University*, vol. 21, no. 6, pp. 77–80, 2021.

[23] W. Cao and Q. Zhu, "Razumikhin-type theorem for pth exponential stability of impulsive stochastic functional differential equations based on vector Lyapunov function," *Nonlinear Analysis: Hybrid Systems*, vol. 39, Article ID 100983, 2021.

[24] W. Ma, X. Luo, and Q. Zhu, "Practical exponential stability of stochastic age-dependent capital system with Levy noise," *Systems & Control Letters*, vol. 144, Article ID 104759, 2020.

[25] R. Song, B. Wang, and Q. Zhu, "Delay-dependent stability of nonlinear hybrid neutral stochastic differential equations with multiple delays," *International Journal of Robust and Nonlinear Control*, vol. 31, no. 1, pp. 250–267, 2021.

[26] M. Zhang and Q. Zhu, "Stability analysis for switched stochastic delayed systems under asynchronous switching: a relaxed switching signal," *International Journal of Robust and Nonlinear Control*, vol. 30, no. 18, pp. 8278–8298, 2020.

[27] Y. Zhao and Q. Zhu, "Stabilization by delay feedback control for highly nonlinear switched stochastic systems with time delays," *International Journal of Robust and Nonlinear Control*, vol. 31, no. 8, pp. 3070–3089, 2021.

[28] D. Peng, X. Li, R. Rakkiyappan, and Y. Ding, "Stabilization of stochastic delayed systems: event-triggered impulsive control," *Applied Mathematics and Computation*, vol. 401, Article ID 126054, 2021.

[29] L. Peng, X. Li, and J. Cao, "Input-to-state stability of nonlinear switched systems via lyapunov method involving indefinite derivative," *Complexity*, vol. 2018, Article ID 8701219, 8 pages, 2018.

[30] X. Li, D. O'Regan, and H. Akca, "Global exponential stabilization of impulsive neural networks with unbounded continuously distributed delays," *IMA Journal of Applied Mathematics*, vol. 80, no. 1, pp. 85–99, 2015.

Hindawi
Complexity
Volume 2021, Article ID 7029058, 12 pages
https://doi.org/10.1155/2021/7029058

Research Article

Adaptive Differentiator-Based Predefined-Time Control for Nonlinear Systems Subject to Pure-Feedback Form and Unknown Disturbance

Man Yang,[1] **Qiang Zhang**,[1] **Ke Xu**,[1] **and Ming Chen**[2]

[1]*School of Mathematical Sciences, Bohai University, Jinzhou 121000, Liaoning, China*
[2]*School of Electronic and Information Engineering, University of Science and Technology Liaoning, Anshan 114000, Liaoning, China*

Correspondence should be addressed to Man Yang; yangman@qymail.bhu.edu.cn

Received 20 May 2021; Accepted 15 July 2021; Published 28 July 2021

Academic Editor: Xiaodi Li

In this article, by utilizing the predefined-time stability theory, the predefined-time output tracking control problem for perturbed uncertain nonlinear systems with pure-feedback structure is addressed. The nonaffine structure of the original system is simplified as an affine form via the property of the mean value theorem. Furthermore, the design difficulty from the uncertain nonlinear function is overcome by the excellent approximation performance of RBF neural networks (NNs). An adaptive predefined-time controller is designed by introducing the finite-time differentiator which is used to decrease the computational complexity problem appeared in the traditional backstepping control. It is proved that the proposed control method guarantees all signals in the closed-loop system remain bound and the tracking error converges to zero within the predefined time. Based on the controller designed in this paper, the expected results can be obtained in predefined time, which can be illustrated by the simulation results.

1. Introduction

Nonlinear control systems with uncertain parameters are widely existed in practical applications, which can be dealt with effectively by the adaptive backstepping control [1]. The idea of backstepping is to construct the Lyapunov function step by step according to the system, and the corresponding virtual controller is deduced to obtain the control law in the final step [2]. The main advantage of the adaptive backstepping method is that the considered control systems do not require the matching conditions. The research on backstepping-based adaptive control for nonlinear systems in strict-feedback form attracted increasing attention in the control field and many interesting results have been published in [3–7], such as the results on SISO nonlinear systems [3–5] and the results on MIMO nonlinear systems [6, 7]. In addition, by combining neural network (NN) [8, 9] with adaptive backstepping design method, many control methods were proposed for nonlinear systems [10–12].

Many models of real systems are pure-feedback systems such as robots [13], spacecrafts [14], and engineering machinery [15]. In order to deal with the stability problem of pure-feedback system, many effective control schemes have been proposed. For example, the authors in [16] simplify the nonlinear pure-feedback system using the implicit function theorem, and then an improved controller was obtained. Using the small-gain theorem, an ISS-modular approach for nonlinear systems with pure-feedback structure was created in [17] and an improved controller with a novel weight estimator was constructed to solve the problems in controlling the nonaffine pure-feedback system. In addition, in [18], based on the mean value theorem, the problem that arises from the structure of nonlinear pure-feedback system is settled by an adaptive neural control.

All of the abovementioned control methods achieve the control objectives when time goes to infinity. It is obvious that, in the system for practical application, we would like the system to be stable in finite time. Therefore, it is very

meaningful to study the finite-time control (FTC) method. The related theory of finite-time stability can be found in literature studies [19, 20], which is put forward by P. Dorato and L. Weiss et al. Since then, the design of finite-time controller has attracted the attention of many researchers, and a lot of relevant results have been presented. In [21], the stability of strict-feedback nonlinear systems with time delay and quantization was investigated for the first time by combining finite-time theory, neural networks, and adaptive control methods, and an improved barrier Lyapunov function (BLF) was constructed. Mehdi Golestani et al. [22] designed a finite-time robust controller using the fast terminal sliding mode approach, in which a bipolar sigmoid function is proposed to alleviate chattering phenomenon. In [23], a finite-time global stabilizer was designed for uncertain nonlinear systems, which guarantees global finite-time stabilization of Hölder continuous nonlinear systems. Based on the properties of fuzzy logic system, an effective adaptive fault-tolerant control method was received in [24], which effectively addressed the stability problem of the system with actuator faults. More recently, the authors in [25] introduced an improved finite-time controller to deal with the problems of nonlinear systems with unknown hysteresis. In all of the FTC results presented above, the convergence time is related to the initial value of the system states, which is going to be long when the initial states are far away from the equilibrium $x = 0$. So, in order to let the convergence time in finite-time control be independent of the initial value of the system states, the concept of fixed-time control was proposed.

Fixed-time stability was proposed by Polyakov, and then he systematically elaborated the difference between finite-time stability and fixed-time stability in [26]. According to fixed-time stability theory, the settling time to stabilize nonlinear system is a constant, which has no relation with the initial states. Furthermore, the fixed-time controller can effectively improve the transient performance of the control system, and many improved fixed-time controllers have been proposed. For example, two novel fixed-time controllers were applied to the nonlinear systems in [27, 28], which take advantage of the approximate performance of fuzzy logic system and the backstepping method. Besides, fixed-time stability of delayed static neural networks was concerned in [29]. In [30], a fixed-time adaptive event-triggered tracking controller of uncertain nonlinear systems was proposed. In addition, by combining the characteristics of the barrier Lyapunov function with the backstepping technique, a new controller was introduced in [31] for the nonlinear system with multi-input and multioutput uncertainties, and the convergence time of this control strategy is a fixed constant. In spite of having the meaningful advantage over finite-time stability, fixed-time stability theory cannot give an exact expression of the convergence time according to the design parameters. Thus, in order to overcome this shortcoming, the predefined-time stability theorem was derived by Sánchez-Torres et al. in [32], which can give the expression of the convergence time function according to the design controller parameters. The predefined-time theory has been applied to various types of systems by plenty of researchers, and a large number of meaningful research results have emerged subsequently. Recently, the advantages of predefined-time theory were applied to second-order multi-intelligent systems [33] and nonlinear mechanical systems [34]. In [35], according to the characteristic of predefined-time stability theory, an improved predefined-time adaptive control structure was proposed to deal with the system with dead zone. Furthermore, in [36], based on sliding mode control technology, a predefined-time controller was designed for second-order nonlinear systems. Although many improved predefined-time controllers have been presented, it is difficult to design a predefined-time controller for the nonlinear pure-feedback system due to the nonaffine structure; therefore, we need to design a predefined-time control scheme for the nonlinear pure-feedback system with unknown disturbance.

Inspired by the aforementioned discussions, an advanced adaptive predefined-time control scheme was constructed for pure-feedback nonlinear system with unknown disturbances, and the expected performance was achieved within a predefined time. Based on the above discussions, the innovations of this article are listed as follows:

(i) The theory of predefined time was firstly applied to n-order nonlinear pure-feedback system. Then, an NN-based adaptive predefined-time controller was firstly used for nonlinear systems in pure-feedback form with unknown disturbance, too.

(ii) Based on the mean value theorem, the simplified system structure is obtained, which can reduce the complexity of the controller design. Furthermore, the derivatives of the virtual controllers are estimated by finite-time differentiators in this work, which avoids the issue of explosion of complexity.

The rest of this article is organized as follows. In Section 2, the nonlinear pure-feedback system is simplified by mean value theorem, and the relevant preliminary knowledge is presented. The design process of the controller is elaborately described in Section 3 and the stability analysis of the system is elaborately described in Section 4. In Section 5, the effectiveness of the designed controller is illustrated by the simulation results. Finally, Section 6 summarizes this article.

2. System Formulation and Preliminaries

2.1. System Formulation. A nonlinear pure-feedback system with unknown disturbance is considered as follows:

$$\begin{cases} \dot{x}_i(t) = f_i(\overline{x}_i, x_{i+1}), \quad 1 \le i \le n-1, \\ \dot{x}_n(t) = f_n(\overline{x}_n, u) + d(t), \\ y(t) = x_1(t), \end{cases} \tag{1}$$

in which $\overline{x}_i(t) = [x_1(t), \ldots, x_i(t)]^T \in R^i, i = 1, \ldots, n$ is the vector of the states; $y(t) \in R$ represents the system output; $u \in R$ denotes the input signal; $d(t)$ is an unknown bounded disturbance and satisfies $|d(t)| \le \overline{d}$ with $\overline{d}$ being a constant; and $f_i(\cdot), i = 1, \ldots, n$ represents unknown smooth functions.

The nonaffine structure of the original system (1) can be simplified by the property of the mean value theorem [18]. Alternative expressions for the unknown smooth functions $f_i(\cdot), i = 1, \ldots, n$ in system (1) are shown as follows:

$$f_i(\overline{x}_i, x_{i+1}) = f_i\left(\overline{x}_i, x_{i+1}^0\right) + \left.\frac{\partial f_i(\overline{x}_i, x_{i+1})}{\partial x_{i+1}}\right|_{x_{i+1}=x_{\mu_i}} \times\left(x_{i+1} - x_{i+1}^0\right), \quad 1 \le i \le n-1, \tag{2}$$

$$f_n(\overline{x}_n, u) = f_n\left(\overline{x}_n, u^0\right) + \left.\frac{\partial f_n(\overline{x}_n, u)}{\partial u}\right|_{u=x_{\mu_n}} \times\left(u - u^0\right), \tag{3}$$

where $x_{\mu_i} = \mu_i x_{i+1} + (1-\mu_i)x_{i+1}^0$, with $0 < \mu_i < 1$, $i = 1, \ldots, n-1$, and $x_{\mu_n} = \mu_n u + (1-\mu_n)u^0$, with $0 < \mu_n < 1$.

Define $h_i(\overline{x}_i, x_{\mu_i}) = (\partial f_i(\overline{x}_i, x_{i+1})/(\partial x_{i+1}))|_{x_{i+1}=x_{\mu_i}}$ and $h_n(\overline{x}_n, x_{\mu_n}) = (\partial f_n(\overline{x}_n, u))/(\partial u)|_{u=x_{\mu_n}}$, which are unknown nonlinear functions. After that, substituting (2) and (3) into system (1) and choosing $x_{i+1}^0 = 0$, $u^0 = 0$, one has

$$\begin{cases} \dot{x}_i(t) = f_i(\overline{x}_i) + h_i\left(\overline{x}_i, x_{\mu_i}\right)x_{i+1}, \\ \dot{x}_n(t) = f_n(\overline{x}_n) + h_n\left(\overline{x}_n, x_{\mu_n}\right)u + d(t), \\ y(t) = x_1(t). \end{cases} \tag{4}$$

The aim of this paper is to design a predefined-time adaptive controller for system (1), which can ensure all signals in the closed-loop system are bounded, while the tracking error converges to zero within a predefined time. The following assumptions and lemmas are provided to ease the controller design.

Assumption 1 [37]: the function $h_i(\overline{x}_i, x_{\mu_i})$ satisfies $0 < \underline{h}_i \le h_i(\cdot) \le \overline{h}_i < \infty$, for $i = 1, \ldots, n$, where $\underline{h}_i$ and $\overline{h}_i$ are unknown constants.

Assumption 2 [35]: the trajectory signal y_r is a continuous and bounded function. Usually, the time derivatives of y_r is also continuous and bounded function. One can find constants A_1, A_2 such that $|y_r| \le A_1, |\dot{y}_r| \le A_2$, but A_1 and A_2 are unknown.

2.2. On Predefined-Time Stability. Consider the following system:

$$\begin{aligned} \dot{x} &= h(x, \rho), \\ x_0 &= x(0), \end{aligned} \tag{5}$$

where $x \in R^n$ and $\rho \in R^b$ denote the state and the parameter of system (5), respectively; h: $R^n \longrightarrow R^n$ stands for nonlinear function and $h(0, \rho) = 0$; $x_0 = x(0) \in D$ represents initial state of system (5) and suppose that the equilibrium of system (5) is the origin $x = 0$.

Definition 1 (see [38]). The origin is a fixed-time stable equilibrium of system (5), if it is finite-time stable and $T(x_0)$ is bounded on R^n, i.e., $\exists T_{\max} > 0, \forall x_0 \in R^n, T(x_0) \le T_{\max}$.

Definition 2 (predefined-time stability [32, 39]). If the constant $T_{\max}$ given in Definition 1 is a function of the system parameter ρ, i.e., $T_{\max} = T_{\max}(\rho)$, the origin of system (5) is weak predefined-time stable. Furthermore, if the time $T_{\max}$ is also a minimum setting time bound, the origin of system (5) is strong predefined-time stable.

Definition 3 (see [40]).

$$\operatorname{sig}(x)^\rho = \left[|x_1|^\rho \operatorname{sign}(x_1), \ldots, |x_n|^\rho \operatorname{sign}(x_n)\right]^T, \tag{6}$$

for $x = [x_1, x_2, \ldots, x_n]^T \in R^n$, where $\rho > 0$ and $\operatorname{sign}(\cdot)$ denotes the standard signum function.

2.3. Mathematical Lemmas

Lemma 1 (see [32, 41]). *If there exists a continuous radially unbounded function $V: R^n \longrightarrow R_+ \cup \{0\}$, such that $V(x) = 0$ for $x \in G$ and any solution $x(t)$ satisfies*

$$\dot{V} \le \frac{-\beta}{\rho T}\exp\left(\frac{1}{\beta}(2V)^{(\rho/2)}\right)(2V)^{1-(\rho/2)}, \tag{7}$$

for $0 < \beta$ and $0 < \rho < 2$, the set G is globally predefined-time attractive for system (5); then $T_{\max} = T$.

Proof. By solving the above differential inequality, the following inequality can be obtained:

$$V(x) \le \frac{1}{2}\left[\beta \ln\left(\frac{T}{t + T\exp\left(-(1/\beta)(2V_0)^{(\rho/2)}\right)}\right)\right]^{-(\rho/2)}, \tag{8}$$

where $V_0 = V(x_0)$. It is a fact that $V(x) = 0$ if $T/(t + T\exp(-(1/\beta)(2V_0)^{(\rho/2)})) = 1$, and thus, the convergence time function is

$$T(x_0) = T\left(1 - \exp\left(-\frac{1}{\beta}(2V_0)^{(\rho/2)}\right)\right). \tag{9}$$

Then, $T_{\max} = T$ since $1 - \exp(-(1/\beta)(2V_0)^{(\rho/2)}) \le 1$. □

Lemma 2 (see [3]). *Let $x_q = [x_1, x_2, \ldots, x_q]^T$ and $S(\overline{x}_q) = [s_1(\overline{x}_q), \ldots, s_l(\overline{x}_q)]^T$ is the basis function vector. Then, for any positive integer $m \le q$, we have*

$$\left\|S\left(\overline{x}_q\right)\right\|^2 \le \left\|s\left(\overline{x}_m\right)\right\|^2. \tag{10}$$

Lemma 3 (see [35]). *Suppose two similarly ordered sequences $a = (a_1, \ldots, a_n)$ and $b = (b_1, \ldots, b_n)$ satisfy*

$a_1 \le \cdots \le a_n, b_1 \le \cdots \le b_n$ or $a_1 \ge \cdots \ge a_n, b_1 \ge \cdots \ge b_n$, then we have

$$\sum_{i=1}^{n} a_i b_i \ge \frac{1}{n} \sum_{i=1}^{n} a_i \sum_{i=1}^{n} b_i. \tag{11}$$

Lemma 4 (see [42]). *For $X = [x_1, \ldots, x_l]^T$, $Y = [y_1, \ldots, y_l]^T$, one has*

$$\begin{aligned} &\left|x_1 y_1 + x_2 y_2 + \cdots + x_l y_l\right| \\ &\le \sqrt{x_1^2 + x_2^2 + \cdots + x_l^2}\sqrt{y_1^2 + y_2^2 + \cdots + y_l^2} \\ &\le \|X\|\|Y\|. \end{aligned} \tag{12}$$

Lemma 5 (see [35]). *For positive real sequence $a = (a_1, \ldots, a_n)$, the following inequality holds:*

$$\left(\prod_{i=1}^{n} a_i\right)^{(1/n)} \le \frac{1}{n} \sum_{i=1}^{n} a_i. \tag{13}$$

Lemma 6 (see [35]). *Suppose $\kappa_i \in R$ and $0 < l \le 1$, then*

$$\sum_{i=1}^{m} \left|\kappa_i\right|^l \ge \left(\sum_{i=1}^{m} \left|\kappa_i\right|\right)^l. \tag{14}$$

The universal approximation performance of radial basis function neural networks (RBF NN) can be utilized to estimate the unknown function $f(\xi)$, and the approximation function is given as follows:

$$f(\xi) = W^T \Phi(\xi) + \delta(\xi), \quad \delta(\xi) < \varepsilon, \tag{15}$$

where $\xi \in \Omega_\xi \subset R^m$ is the input vector and $W = [w_1, w_1, \ldots, w_n]$ represents the weight vector; $\delta(\xi)$ is an approximation error and $\varepsilon > 0$ expresses the accuracy level; and $\Phi(\xi) = [\varphi_1(\xi), \varphi_2(\xi), \ldots, \varphi_n(\xi)]$ denotes the basis function vector with the NN node number $n > 1$. In addition, $\varphi_i(\xi)$ is the Gaussian function which is written as follows:

$$\varphi_i(\xi) = \exp\left(-\frac{(\xi - \zeta_i)^T (\xi - \zeta_i)}{\eta_i^T \eta_i}\right), \quad i = 1, 2, \ldots, n, \tag{16}$$

where $\zeta_i = [\zeta_{i1}, \zeta_{i1}, \ldots, \zeta_{im}]$ is the center of the receptive field and $\eta_i = [\eta_{i1}, \eta_{i1}, \ldots, \eta_{im}]$ denotes the width of the Gaussian function.

Lemma 7 (see [37]). *A continuous function $f(\xi)$ on a compact set $\Omega_\xi \subset R^m$ can be approximated by RBF NN (15) if the node number n is sufficiently large, and*

$$f(\xi) = W^{*T} \Phi(\xi) + \delta(\xi), \quad \delta(\xi) < \varepsilon, \tag{17}$$

where W^* is the ideal weight vector and defined by

$$W^* = \arg\min_{W \in R^m} \left\{ \sup_{\xi \in \Omega_\xi} \left| f(\xi) - W^T \varphi(\xi) \right| \right\}. \tag{18}$$

3. Controller Design

In this section, an adaptive predefined-time tracking controller will be designed for system (4) via backstepping technique. In the design process, we will use the following coordinate transformation:

$$\begin{aligned} z_1 &= y - y_r, \\ z_i &= x_i - \alpha_{i-1}, \quad i = 2, \ldots, n, \end{aligned} \tag{19}$$

where $\alpha_{(i-1)}, i = 2, \ldots, n$ is the virtual control signal for the $(i-1)$th subsystem, y_r represents the trajectory function, and z_1 denotes the tracking error. Then the main design procedure of this paper is given as follows.

Remark 1. In the process of controller design, define $f_i = f_i(\overline{x}_i), i = 1, \ldots, n, h_i = h_i(\overline{x}_i, x_{\mu_i}), i = 1, \ldots, n-1$, and $h_n = h_n(\overline{x}_n, x_{\mu_n})$.

Step 1. A Lyapunov function is constructed as $V_1 = (1/2)z_1^2$. Then, based on systems (4) and (19), we can get

$$\begin{aligned} \dot{z}_1 &= \dot{y} - \dot{y}_r = \dot{x}_1 - \dot{y}_r = f_1 + h_1 x_2 - \dot{y}_r \\ &= f_1 + h_1(z_2 + \alpha_1) - \dot{y}_r, \end{aligned} \tag{20}$$

where $x_2 = z_2 + \alpha_1$.

Differentiating V_1 results in

$$\begin{aligned} \dot{V}_1 &= z_1 \dot{z}_1 \\ &= z_1(f_1 + h_1(z_2 + \alpha_1) - \dot{y}_r) \\ &= z_1(f_1 - \dot{y}_r) + z_1 h_1 z_2 + z_1 h_1 \alpha_1. \end{aligned} \tag{21}$$

The universal approximation performance of RBF NN can be utilized to estimate the unknown function f_1, and the approximation function is given as follows:

$$f_1 = \widehat{W}_1^T \Phi_1(\overline{x}_1) + \delta_1(\overline{x}_1). \tag{22}$$

Then, according to Lemmas 2 and 4, we can obtain

$$\begin{aligned} f_1 - \dot{y}_r &= \widehat{W}_1^T \Phi_1(\overline{x}_1) + \delta_1(\overline{x}_1) - \dot{y}_r \\ &\le \widehat{W}_1^T \Phi_1(\overline{x}_1) + \delta_{M1} + A_1 \\ &\le \|\overline{W}_1\|\|\overline{\Phi}_1\| \le \sqrt{q+2}\|\overline{W}_1\| \\ &\le \frac{1}{2}\left(q + 2 + \|\overline{W}_1\|^2\right), \end{aligned} \tag{23}$$

where $\widehat{W}_1 \in R^q$ is the RBF NN weight vector, $\Phi_1(\overline{x}_1) = [\Phi_{11}(\overline{x}_1), \ldots, \Phi_{1q}(\overline{x}_1)]^T$ denotes the basis function vector, $\delta_1(\overline{x})$ is the approximation error and satisfies $\delta_1(\overline{x}_1) \le \delta_{M1}$ with δ_{M1} being a constant, and $\overline{W}_1 = [\widehat{W}_1, \delta_{M1}, A_1]$, $\overline{\Phi}_1 = [\Phi_1(\overline{x}_1), 1, 1]^T$.

Let $\theta_1 = \|\overline{W}_1\|^2$ and $\widetilde{\theta}_1 = \theta_1 - \widehat{\theta}_1$, where $\widehat{\theta}_1$ is the estimation of θ_1. Subsequently, using Young's inequality, the following inequality can be obtained:

$$z_1(f_1 - \dot{y}_r) \le \frac{1}{2}(q + 2 + \theta_1)|z_1|. \tag{24}$$

Substituting (24) into (21), we have

$$\begin{aligned}\dot{V}_1 &\le \frac{1}{2}\left(q+2+\widehat{\theta}_1+\widetilde{\theta}_1\right)|z_1| + z_1h_1z_2 + z_1h_1\alpha_1 \\ &\le \frac{1}{2}\left(q+2+\widehat{\theta}_1\right)|z_1| + \frac{1}{2}\widetilde{\theta}_1|z_1| + z_1h_1z_2 + z_1h_1\alpha_1.\end{aligned} \tag{25}$$

The unknown parameter $\widetilde{\theta}_1$ can be solved by defining a Lyapunov function W_1 as follows:

$$W_1 = V_1 + \frac{1}{2}\widetilde{\theta}_1^2. \tag{26}$$

Differentiating W_1 results in

$$\begin{aligned}\dot{W}_1 &= \dot{V}_1 - \widetilde{\theta}_1\dot{\widehat{\theta}}_1 \\ &\le \frac{1}{2}\left(q+2+\widehat{\theta}_1\right)|z_1| + \frac{1}{2}|z_1|\widetilde{\theta}_1 + z_1h_1z_2 + z_1h_1\alpha_1 - \widetilde{\theta}_1\dot{\widehat{\theta}}_1 \\ &\le \frac{1}{2}\left(q+2+\widehat{\theta}_1\right)|z_1| + z_1h_1z_2 + z_1h_1\alpha_1 + \widetilde{\theta}_1\left(\frac{1}{2}|z_1| - \dot{\widehat{\theta}}_1\right).\end{aligned} \tag{27}$$

Now, we design the feasible virtual control α_1 as

$$\alpha_1 = \frac{-1}{\underline{h}_1}\left(\frac{n}{\rho T}\operatorname{sig}(z_1)^{1-\rho}\exp\left(|z_1|^{\rho}\right) + \frac{1}{2}\left(\widehat{\theta}_1+q+2\right)\operatorname{sign}(z_1) + \lambda_1\operatorname{sign}(z_1)\right), \tag{28}$$

where T is the predefined time, q is the hidden neuron number, n is the NN node number, λ_1 is a positive tuning parameter which will be given later, and ρ is the design parameter which satisfies $0<\rho<2$.

Remark 2. By selecting the value of the designed parameter λ_1 in the virtual controller α_1, we can make sure that $(1/2)\widetilde{\theta}_1 - \lambda_1$ is a negative number.

The adaptive law for the parameter $\widehat{\theta}_1$ is designed as follows:

$$\begin{aligned}\dot{\widehat{\theta}}_1 &= \frac{1}{2}|z_1|, \\ \dot{\widehat{\theta}}_1(0) &> 0.\end{aligned} \tag{29}$$

Then, we have

$$\dot{W}_1 \le \frac{-n}{\rho T}|z_1|^{2-\rho}\exp\left(|z_1|^{\rho}\right) + z_1h_1z_2 - \lambda_1|z_1|. \tag{30}$$

Step 2. In order to overcome the obstacle of finding the first-order derivative of the virtual controller, an effective approximation tool called finite-time differentiator is brought out with the following structure:

$$\begin{cases}\dot{\sigma}_{11} = \sigma_{12} - k_1\operatorname{sig}(\sigma_{11}-\alpha_1)^{(1/2)}, \\ \dot{\sigma}_{12} = -k_2\operatorname{sign}(\sigma_{11}-\alpha_1),\end{cases} \tag{31}$$

where σ_{11} and σ_{12} represent the states of differentiator and k_1 and k_2 are differentiator parameters. According to [10, 43], the boundedness of $\sigma_{11}(0)-\alpha_1(0)$ and $\sigma_{12}(0)-\dot{\alpha}_1(0)$ ensure that the finite-time differentiator can estimate the first-order derivative of the virtual controller with arbitrary accuracy. Thus, another alternative form of the first-order derivative of the virtual controller is $\dot{\alpha}_1(t) = \sigma_{12}(t) + \varepsilon_1$, where ε_1 denotes the bounded estimation error, and a constant $\varepsilon_{M1}>0$ can be found such that ε_1 satisfies the inequality $|\varepsilon_1| \le \varepsilon_{M1}$.

The dynamic of tracking error $z_2 = x_2 - \alpha_1$ satisfies

$$\dot{z}_2 = f_2 + h_2(z_3+\alpha_2) - \dot{\alpha}_1, \tag{32}$$

where $z_3 = x_3 - \alpha_2$.

Design the Lyapunov function as

$$V_2 = V_1 + \frac{1}{2}z_2^2. \tag{33}$$

Differentiating V_2 results in

$$\begin{aligned}\dot{V}_2 &= \dot{V}_1 + z_2(f_2 - \dot{\alpha}_1) + z_2h_2z_3 + z_2h_2\alpha_2 \\ &= \dot{V}_1 + z_2(f_2 - \dot{\alpha}_1 + \sigma_{12}) - z_2\sigma_{12} + z_2h_2z_3 + z_2h_2\alpha_2 \\ &= \dot{V}_1 + z_2(f_2 + \varepsilon_1) - z_2\sigma_{12} + z_2h_2z_3 + z_2h_2\alpha_2,\end{aligned} \tag{34}$$

where $\varepsilon_1 = \sigma_{12} - \dot{\alpha}_1$. The universal approximation performance of RBF NN can be utilized to estimate the unknown function f_2, and the approximation function is given as follows:

$$f_2 = \widehat{W}_2^T\Phi_2(\overline{x}_2) + \delta_2(\overline{x}_2). \tag{35}$$

Then, according to Lemmas 2 and 4, we can obtain

$$\begin{aligned}f_2 + \varepsilon_1 &= \widehat{W}_2^T\Phi_2(\overline{x}_2) + \delta_2(\overline{x}_2) + \varepsilon_1 \\ &\le \left(\widehat{W}_2^T\Phi_2(\overline{x}_2) + \delta_{M2}(\overline{x}_2) + \varepsilon_{M1}\right) \\ &\le \|\overline{W}_2\|\|\overline{\Phi}_2\| \le \sqrt{q+2}\|\overline{W}_2\| \\ &\le \frac{1}{2}\left(q+2+\|\overline{W}_2\|^2\right) \\ &\le \frac{1}{2}(q+2+\theta_2),\end{aligned} \tag{36}$$

where $\widehat{W}_2 \in R^q$ is the RBF NN weight vector, $\Phi_2(\overline{x}_2) = [\Phi_{21}(\overline{x}_2), \ldots, \Phi_{2q}(\overline{x}_2)]^T$ denotes the basis function vector, and $\delta_2(\overline{x})$ is the approximation error and satisfies $\delta_2(\overline{x}_2) \le \delta_{M2}$ with δ_{M2} being a constant; besides, we define $\overline{W}_2 = [\widehat{W}_2, \delta_{M2}, \varepsilon_{M1}]^T$, $\overline{\Phi}_2 = [\Phi_2(\overline{x}_2), 1, 1]^T$, and let $\theta_2 = \|\overline{W}_2\|^2$, $\widetilde{\theta}_2 = \theta_2 - \widehat{\theta}_2$, where $\widehat{\theta}_2$ is the estimation of θ_2.

Substituting (36) into (34) and using Young's inequality give

$$\begin{aligned}\dot{V}_2 &\le \dot{V}_1 + \frac{1}{2}|z_2|(q+2+\theta_2) - z_2\sigma_{12} + z_2h_2z_3 + z_2h_2\alpha_2\\ &\le \dot{V}_1 + \frac{1}{2}|z_2|\left(q+2+\widehat{\theta}_2\right) + \frac{1}{2}|z_2|\widetilde{\theta}_2 - z_2\sigma_{12} + z_2h_2z_3 + z_2h_2\alpha_2.\end{aligned} \tag{37}$$

The unknown parameter $\widetilde{\theta}_2$ can be solved by defining a Lyapunov function W_2 as follows:

$$W_2 = V_2 + \frac{1}{2}\widetilde{\theta}_2^2. \tag{38}$$

Then, differentiating W_2 results in

$$\begin{aligned}\dot{W}_2 &= \dot{V}_2 - \widetilde{\theta}_2\dot{\widehat{\theta}}_2\\ &\le \dot{V}_1 + \frac{1}{2}\left(q+2+\widehat{\theta}_2\right)|z_2| + \frac{1}{2}|z_2|\widetilde{\theta}_2 - z_2\sigma_{12} + z_2h_2z_3 + z_2h_2\alpha_2 - \widetilde{\theta}_2\dot{\widehat{\theta}}_2\\ &\le \dot{V}_1 + \frac{1}{2}\left(q+2+\widehat{\theta}_2\right)|z_2| - z_2\sigma_{12} + z_2h_2z_3 + z_2h_2\alpha_2 + \widetilde{\theta}_2\left(\frac{1}{2}|z_2| - \dot{\widehat{\theta}}_2\right).\end{aligned} \tag{39}$$

We design the feasible virtual control α_2 as

$$\begin{aligned}\alpha_2 = -\frac{1}{\underline{h}_2}\Bigg(&\frac{n}{\rho T}\mathrm{sig}(z_2)^{1-\rho}\exp\left(|z_2|^{\rho}\right) + \frac{1}{2}\left(\widehat{\theta}_2 + q + 2\right)\mathrm{sign}(z_2)\\ &+ |\sigma_{12}|\mathrm{sign}(z_2) + \lambda_2\mathrm{sign}(z_2) + |z_1|\overline{h}_1\mathrm{sign}(z_2)\Bigg),\end{aligned} \tag{40}$$

where T is the predefined time, q is the hidden neuron number, λ_2 is a positive tuning parameter which will be given later, and the parameter ρ satisfies $0 < \rho < 2$.

The adaptive law for the parameter $\widehat{\theta}_2$ is designed as follows:

$$\begin{aligned}\dot{\widehat{\theta}}_2 &= \frac{1}{2}|z_2|,\\ \dot{\widehat{\theta}}_2(0) &> 0.\end{aligned} \tag{41}$$

Then we can rewrite (37) in the following form:

$$\dot{V}_2 \le \sum_{i=1}^{2}\left(\frac{-n}{\rho T}|z_i|^{2-\rho}\exp\left(|z_i|^{\rho}\right) + \left(\frac{1}{2}\widetilde{\theta}_i - \lambda_i\right)|z_i|\right) + z_2h_2z_3, \tag{42}$$

and we can get

$$\dot{W}_2 \le \sum_{i=1}^{2}\left(\frac{-n}{\rho T}|z_i|^{2-\rho}\exp\left(|z_i|^{\rho}\right) - \lambda_i|z_i|\right) + z_2h_2z_3. \tag{43}$$

Step i. $(3 \le i \le n-1)$. In order to overcome the obstacle of finding the first-order derivative of the virtual controller α_{i-1}, an effective approximation tool called finite-time differentiator is brought out with the following structure:

$$\begin{aligned}\dot{\sigma}_{(i-1)1} &= \sigma_{(i-1)2} - k_1\mathrm{sig}\left(\sigma_{(i-1)1} - \alpha_{i-1}\right)^{(1/2)},\\ \dot{\sigma}_{(i-1)2} &= -k_2\mathrm{sign}\left(\sigma_{(i-1)1} - \alpha_{i-1}\right),\end{aligned} \tag{44}$$

where $\sigma_{(i-1)1}$ and $\sigma_{(i-1)2}$ represent the states of differentiator and k_1 and k_2 denote differentiator parameters. Differentiator (44) can produce an approximate function of $\dot{\alpha}_{i-1}$ with any precision only if the initial deviations $\sigma_{(i-1)1}(0) - \alpha_{i-1}(0)$ and $\sigma_{(i-1)2}(0) - \dot{\alpha}_{i-1}(0)$ are bounded. Thus, another alternative form of the first-order derivative of the virtual controller is $\dot{\alpha}_{i-1}(t) = \sigma_{(i-1)2}(t) + \varepsilon_{i-1}$, where ε_{i-1} denotes the bounded estimation error, and we can find a positive constant $\varepsilon_{M(i-1)}$ such that the inequality $|\varepsilon_{i-1}| \le \varepsilon_{M(i-1)}$ holds.

The dynamic of tracking error $z_i = x_i - \alpha_{i-1}$ satisfies

$$\dot{z}_i = f_i + h_i(z_{i+1} + \alpha_i) - \dot{\alpha}_{i-1}. \tag{45}$$

The universal approximation performance of RBF NN can be utilized to estimate the unknown function f_i, and the approximation function is given as follows:

$$f_i = \widehat{W}_i^T\Phi_i(\overline{x}_i) + \delta_i(\overline{x}_i), \tag{46}$$

where $\widehat{W}_i \in R^q$ is the RBF NN weight vector, $\Phi_i(\overline{x}) = [\Phi_{i1}(\overline{x}), \ldots, \Phi_{iq}(\overline{x})]^T$ denotes the basis function vector, and $\delta_i(\overline{x})$ is the approximation error and satisfies $\delta_i(\overline{x}) \le \delta_{Mi}$ with δ_{Mi} being a constant.

We design the feasible virtual control α_i as

$$\begin{aligned}\alpha_i = -\frac{1}{\underline{h}_i}\Bigg(&\frac{n}{\rho T}\mathrm{sig}(z_i)^{1-\rho}\exp\left(|z_i|^{\rho}\right)\\ &+ \frac{1}{2}\left(\widehat{\theta}_i + q + 2\right)\mathrm{sign}(z_i) + |\sigma_{(i-1)2}|\mathrm{sign}(z_i)\\ &+ \lambda_i\mathrm{sign}(z_i) + |z_{i-1}|\overline{h}_{i-1}\mathrm{sign}(z_i)\Bigg),\end{aligned} \tag{47}$$

where T is the predefined time, q is the hidden neuron number, λ_i is a positive tuning parameter which will be designed later, and the parameter ρ satisfies $0 < \rho < 2$.

The dynamic adaptive law for the unknown parameter is

$$\dot{\hat{\theta}}_i = \frac{1}{2}|z_i|, \qquad \dot{\hat{\theta}}_i(0) > 0. \tag{48}$$

The Lyapunov function is structured as follows:

$$V_i = V_{i-1} + \frac{1}{2}z_i^2. \tag{49}$$

The time derivative of V_i is obtained as follows:

$$\begin{aligned}\dot{V}_i &= \dot{V}_{i-1} + z_i\left(f_i + h_i x_{i+1} + \sigma_{(i-1)2} - \dot{\alpha}_{i-1}\right) - z_i\sigma_{(i-1)2}\\ &= \dot{V}_{i-1} + z_i\left(f_i + \sigma_{(i-1)2} - \dot{\alpha}_{i-1}\right) - z_i\sigma_{(i-1)2} + z_i h_i x_{i+1}\\ &\le \dot{V}_{i-1} + z_i\left(f_i + \varepsilon_{M(i-1)}\right) - z_i\sigma_{(i-1)2} + z_i h_i\left(z_{i+1} + \alpha_i\right)\\ &\le \dot{V}_{i-1} + z_i\left(\hat{W}_i^T\Phi_i(\overline{x}_i) + \delta_i(\overline{x}_i) + \varepsilon_{M(i-1)}\right) - z_i\sigma_{(i-1)2} + z_i h_i\left(z_{i+1} + \alpha_i\right),\end{aligned} \tag{50}$$

where $x_{i+1} = z_{i+1} + \alpha_i$.

Then, according to Lemmas 2 and 4 and (46), we can have

$$\begin{aligned}f_i + \varepsilon_{M(i-1)} &= \hat{W}_i^T\Phi_i(\overline{x}_i) + \delta_i(\overline{x}_i) + \varepsilon_{M(i-1)}\\ &\le \left(\hat{W}_i^T\Phi_i(\overline{x}_i) + \delta_{Mi}(\overline{x}_i) + \varepsilon_{M(i-1)}\right)\\ &\le \|\overline{W}_i\|\|\overline{\Phi}_i\| \le \sqrt{q+2}\|\overline{W}_i\|\\ &\le \frac{1}{2}\left(q + 2 + \|\overline{W}_i\|^2\right),\end{aligned} \tag{51}$$

where $\overline{W}_i = [\hat{W}_i, \delta_{Mi}, \varepsilon_{Mi}]^T$ and $\overline{\Phi}_i = [\Phi_i(x_i), 1, 1]^T$.

Employing Young's inequality leads to the following inequality:

$$z_i\left(f_i + \varepsilon_{M(i-1)}\right) \le \frac{1}{2}(q + 2 + \theta_i)|z_i|, \tag{52}$$

where $\theta_i = \|\overline{W}_i\|^2$, $\tilde{\theta}_i = \theta_i - \hat{\theta}_i$, and $\hat{\theta}_i$ is the estimation of θ_i.

Substituting (47) and (51) into (50), we have

$$\begin{aligned}\dot{V}_i &\le \sum_{j=1}^{i}\left(\frac{-n}{\rho T}|z_j|^{2-\rho}\exp\left(|z_j|^{\rho}\right) + \left(\frac{1}{2}\tilde{\theta}_j - \lambda_j\right)|z_j|\right) + z_i h_i z_{i+1},\\ \dot{W}_i &\le \sum_{j=1}^{i}\left(\frac{-n}{\rho T}|z_j|^{2-\rho}\exp\left(|z_j|^{\rho}\right) - \lambda_j|z_j|\right) + z_i h_i z_{i+1}.\end{aligned} \tag{53}$$

Step n. Similar to Step i, we construct the following differentiator to estimate $\dot{\alpha}_{n-1}$:

$$\begin{cases}\dot{\sigma}_{(n-1)1} = \sigma_{(n-1)2} - k_1\mathrm{sig}\left(\sigma_{(n-1)1} - \alpha_{(n-1)}\right)^{(1/2)},\\ \dot{\sigma}_{(n-1)2} = -k_2\mathrm{sign}\left(\sigma_{(n-1)1} - \alpha_{n-1}\right),\end{cases} \tag{54}$$

where $\sigma_{(n-1)1}$ and $\sigma_{(n-1)2}$ represent the states of differentiator and k_1 and k_2 denote the differentiator parameters. Similar to the reason of Step i, another alternative form of the first-order derivative of the virtual controller α_{n-1} is $\dot{\alpha}_{n-1}(t) = \sigma_{(n-1)2}(t) + \varepsilon_{n-1}$, where ε_{n-1} denotes the bounded estimation error, and a positive constant $\varepsilon_{M(n-1)}$ satisfying $|\varepsilon_{n-1}| \le \varepsilon_{M(n-1)}$ can be found.

The dynamic of z_n satisfies

$$\begin{aligned}\dot{z}_n &= \dot{x}_n - \dot{\alpha}_{n-1}\\ &= f_n + h_n u + d(t) - \dot{\alpha}_{n-1}.\end{aligned} \tag{55}$$

The real control input is chosen as follows:

$$\begin{aligned}u = -\frac{1}{\underline{h}_n}\Bigg(&\frac{n}{\rho T}\mathrm{sig}(z_n)^{1-\rho}\exp\left(|z_n|^{\rho}\right)\\ &+ \frac{1}{2}\left(\hat{\theta}_n + q + 3\right)\mathrm{sign}(z_n) + |\sigma_{(n-1)2}|\mathrm{sign}(z_n)\\ &+ \lambda_n\mathrm{sign}(z_n) + |z_{n-1}|\overline{h}_{n-1}\mathrm{sign}(z_n)\Bigg),\end{aligned} \tag{56}$$

where T is the predefined time, q is the hidden neuron number, λ_n is a positive tuning parameter which will be given later, and the parameter ρ satisfies $0 < \rho < 2$.

The dynamic of the adaptive parameters is

$$\dot{\hat{\theta}}_n = \frac{1}{2}|z_n|, \qquad \dot{\hat{\theta}}_i(0) > 0. \tag{57}$$

The Lyapunov function is structured as follows:

$$V_n = V_{n-1} + \frac{1}{2}z_n^2. \tag{58}$$

Differentiating V_n leads to

$$\begin{aligned}\dot{V}_n &= z_n \cdot \dot{z}_n + \dot{V}_{n-1} = z_n\left(f_n + h_n u - \dot{\alpha}_{n-1} + d(t)\right) + \dot{V}_{n-1} \\ &= \dot{V}_{n-1} + z_n\left(f_n - \dot{\alpha}_{n-1} + d(t) + \sigma_{(n-1)2}\right) - z_n\sigma_{(n-1)2} + z_n h_n u.\end{aligned} \tag{59}$$

The universal approximation performance of RBF NN can be utilized to estimate the unknown function f_n, and the approximation function is given as follows:

$$f_n = \widehat{W}_n^T \Phi_n(\overline{x}) + \delta_n(\overline{x}), \tag{60}$$

where $\widehat{W}_n \in R^q$ is the RBF NN weight vector, $\Phi_n(\overline{x}) = [\Phi_{n1}(\overline{x}), \ldots, \Phi_{nq}(\overline{x})]^T$ denotes the basis function vector, and $\delta_n(\overline{x})$ is the approximation error and satisfies $\delta_n(\overline{x}) \le \delta_{Mn}$ with δ_{Mn} being a constant.

Let $\overline{W}_n = [\widehat{W}_n, \delta_{Mn}, \varepsilon_{Mn}, \overline{d}]^T, \overline{\Phi}_n = [\Phi_n(\overline{x}), 1, 1, 1]^T$, and RBF NN is introduced to approximate the unknown nonlinear function f_n. Then, using Lemmas 2 and 4, we get

$$\begin{aligned}&f_n + \sigma_{(n-1)2} - \dot{\alpha}_{n-1} + d(t) \\ &= \widehat{W}_n^T \Phi_n(\overline{x}) + \delta_n(\overline{x}) + \sigma_{(n-1)2} - \dot{\alpha}_{n-1} + d(t) \\ &\le \widehat{W}_n^T \Phi_n(\overline{x}) + \delta_{Mn} + \varepsilon_{Mn} + \overline{d} \\ &\le \|\overline{W}_n\|\|\overline{\Phi}_n\| \le \frac{1}{2}\sqrt{q+3}\|\overline{W}_n\|.\end{aligned} \tag{61}$$

Utilizing Young's inequality, we get

$$z_n\left(f_n(\overline{x}) + \sigma_{(n-1)2} - \dot{\alpha}_{n-1} + d(t)\right) \le \frac{1}{2}(q + 3 + \theta_n)|z_n|, \tag{62}$$

where $\theta_n = \|\overline{W}_n\|^2$, $\widetilde{\theta}_n = \theta_n - \widehat{\theta}_n$, and $\widehat{\theta}_n$ is the estimation of θ_n.

Substituting (56) and (62) into (59), we have

$$\begin{aligned}\dot{V}_n &\le \dot{V}_{n-1} + z_n\left(f_n - \dot{\alpha}_{n-1} + d(t) + \sigma_{(n-1)2}\right) - z_n\sigma_{(n-1)2} + z_n h_n u \\ &\le \dot{V}_{n-1} + \frac{1}{2}(q + 3 + \theta_n)|z_n| - z_n\sigma_{(n-1)2} + z_n h_n u \\ &\le \sum_{i=1}^{n}\left(-\frac{n}{\rho T}|z_i|^{2-\rho}\exp\left(|z_i|^{\rho}\right) + \frac{1}{2}\sum_{i=1}^{n}\widetilde{\theta}_i|z_i| - \sum_{i=1}^{n}\lambda_i|z_i|\right).\end{aligned} \tag{63}$$

The unknown parameter $\widetilde{\theta}_n$ can be solved by designing a Lyapunov function as follows:

$$W_n = V_n + \frac{1}{2}\sum_{i=1}^{n}\widetilde{\theta}_i^2. \tag{64}$$

Differentiating W_n results in

$$\begin{aligned}\dot{W}_n &= \dot{V}_n - \sum_{i=1}^{n}\widetilde{\theta}_i\dot{\widehat{\theta}}_i \\ &\le \sum_{i=1}^{n}\left(-\frac{n}{\rho T}|z_i|^{2-\rho}\exp\left(|z_i|^{\rho}\right) + \frac{1}{2}\sum_{i=1}^{n}\widetilde{\theta}_i|z_i| - \sum_{i=1}^{n}\lambda_i|z_i|\right) - \sum_{i=1}^{n}\widetilde{\theta}_i\dot{\widehat{\theta}}_i \\ &= \sum_{i=1}^{n}\left(-\frac{n}{\rho T}|z_i|^{2-\rho}\exp\left(|z_i|^{\rho}\right) - \sum_{i=1}^{n}\lambda_i|z_i|\right) < 0.\end{aligned} \tag{65}$$

4. Stability Analysis

The main result of this research is analysed in this section.

Theorem 1. *Take into account the closed system consisting of system (1), control laws (28), (40), (47), and (56), and the adaptive laws (29), (41), (48), and (57). If there is a tuning parameter λ_i such that $(1/2)\widetilde{\theta}_i \le \lambda_i$, then based on assumptions 1 and 2, we can guarantee that all the closed-loop signals are bounded and the tracking error converges to zero within the predefined time T.*

Proof

(1) According to (64) and (65), we can know that z_i, $\widetilde{\theta}_i$ are bounded. The boundedness of $\widehat{\theta}_i$ can be deduced from the fact that θ_i is a constant and $\widetilde{\theta}_i$ is bounded. Depend on the boundedness property of y_r, we can know that the system state x_1 is bounded. By utilizing the boundedness of z_1 and constants q, $\underline{h}_1$, n, ρ, T, and λ_1, the boundedness property of α_1 is known. In addition, we already know that z_2 is bounded, then we can obtain that x_2 is bounded. Since $(\partial\alpha_1/\partial z_1)$ and $(\partial\alpha_1/\partial\widetilde{\theta}_1)$ are continuous functions with bounded arguments and ε_1 is bounded, $\dot{\alpha}_1$ and σ_{12} are bounded. Considering that z_2 and $\widetilde{\theta}_2$ are bounded and $\underline{h}_2$, q, $\overline{h}_1$, n, ρ, T, and λ_2 are constants, we have α_2 is bounded. Because α_2 and z_3 are bounded, we have x_3 is bounded. Likewise, we can obtain that x_i, α_i, and σ_{i2} are bounded. Accordingly, we can obtain the boundedness property of all closed-loop signals.

(2) Because of the boundedness property of all the closed-loop signals, we can find a constant λ_i such that $(1/2)\widetilde{\theta}_i \le \lambda_i$. Then we have

$$\begin{aligned}\dot{V}_n &\le \sum_{i=1}^{n}\left(-\frac{n}{\rho T}|z_i|^{2-\rho}\exp\left(|z_i|^{\rho}\right)\right) \\ &= -\frac{n}{\rho T}\sum_{i=1}^{n}\left(\left(z_i^2\right)^{1-(\rho/2)}\exp\left(\left(z_i^2\right)^{(\rho/2)}\right)\right).\end{aligned} \tag{66}$$

According to Lemma 3, we have

$$-\frac{n}{\rho T}\sum_{i=1}^{n}\left(\left(z_i^2\right)^{1-(\rho/2)}\exp\left(\left(z_i^2\right)^{(\rho/2)}\right)\right)$$
$$\leq -\frac{n}{\rho T}\cdot\frac{1}{n}\sum_{i=1}^{n}\left(z_i^2\right)^{1-(\rho/2)}\left(\sum_{i=1}^{n}\exp\left(\left(z_i^2\right)^{(\rho/2)}\right)\right). \tag{67}$$

From Lemma 5, we can derive

$$\frac{1}{n}\sum_{i=1}^{n}\exp\left(\left(z_i^2\right)^{(\rho/2)}\right)\geq\left(\prod_{i=1}^{n}\exp\left(\left(z_i^2\right)^{(\rho/2)}\right)\right)^{(1/n)}$$
$$=\exp\left(\frac{1}{n}\sum_{i=1}^{n}\left(z_i^2\right)^{(\rho/2)}\right). \tag{68}$$

Therefore, based on (67) and (68), one has

$$\dot{V}_n\leq -\frac{n}{\rho T}\sum_{i=1}^{n}\left(z_i^2\right)^{1-(\rho/2)}\left(\prod_{i=1}^{n}\exp\left(\left(z_i^2\right)^{(\rho/2)}\right)\right)^{(1/n)}$$
$$\leq -\frac{n}{\rho T}\sum_{i=1}^{n}\left(z_i^2\right)^{1-(\rho/2)}\exp\left(\frac{1}{n}\sum_{i=1}^{n}\left(z_i^2\right)^{(\rho/2)}\right). \tag{69}$$

Then, from Lemma 6, we obtain

$$\dot{V}_n\leq -\frac{n}{\rho T}\left(\sum_{i=1}^{n}z_i^2\right)^{1-(\rho/2)}\exp\left(\frac{1}{n}\left(\sum_{i=1}^{n}z_i^2\right)^{(\rho/2)}\right). \tag{70}$$

Since $0<(\rho/2)<1$, according to Lemma 1, we can estimate the stabilization time as

$$t=T\left(1-\exp\left(-\frac{1}{\beta}(2V_0)^{(\rho/2)}\right)\right)\leq T. \tag{71}$$

Therefore, the tracking error z_1 will converge to zero within predefined time T. □

5. Simulation Example

The superior performance of the predefined-time controller can be illustrated by the simulation in this section. An uncertain second-order nonlinear system with pure-feedback form is considered as follows:

$$\begin{cases}\dot{x}_1=0.5\cos(x_1)+6x_2+0.05\sin(x_2),\\ \dot{x}_2=\cos\left(x_2^2\right)+12u+0.5\sin u+0.1\sin(t),\\ y=x_1,\end{cases} \tag{72}$$

where $f_1(\overline{x}_1,x_2)=0.5\cos(x_1)+6x_2+0.05\sin(x_2)$, $f_2(\overline{x}_2,u)=\cos(x_2^2)+12u+0.5\sin u$, and $d(t)=0.1\sin(t)$. In the simulation, it is desired that all signals in the closed-loop system are bounded under the proposed control approach, and the system output $y=x_1$ can follow the reference trajectory $y_r=0.4(\sin(t))+\sin(0.5t)$.

According to the predefined-time control strategy that has been designed, the virtual controller and actual controller are designed as follows:

$$\alpha_1=-\frac{1}{\underline{h}_1}\left(\frac{n}{\rho T}\mathrm{sig}(z_1)^{1-\rho}\exp\left(|z_1|^{\rho}\right)+\left(\frac{1}{2}\widehat{\theta}_1+q+2\right)\mathrm{sign}(z_1)+\lambda_1\mathrm{sign}(z_1)\right),$$
$$u=-\frac{1}{\underline{h}_2}\left(\frac{n}{\rho T}\mathrm{sig}(z_2)^{1-\rho}\exp\left(|z_2|^{\rho}\right)+\left(\frac{1}{2}\widehat{\theta}_2+q+3\right)\mathrm{sign}(z_2)\right.$$
$$\left.+|\sigma_{12}|\mathrm{sign}(z_2)+\lambda_2\mathrm{sign}(z_2)+z_1\overline{h}_1\mathrm{sign}(z_2)\right). \tag{73}$$

And the adaptive laws are constructed with the following forms:

$$\dot{\widehat{\theta}}_1=\frac{1}{2}|z_1|,$$
$$\dot{\widehat{\theta}}_2=\frac{1}{2}|z_2|. \tag{74}$$

In the simulation, the initial values are assigned as $[x_1(0),x_2(0),\widehat{\theta}_1(0),\widehat{\theta}_2(0),\sigma 11(0),\sigma 12(0)]=[0.5,0.5,0.05,0.05,0.05,0.05]^T$, where $\sigma_{11}(0)$ and $\sigma_{12}(0)$ represent initial values of the states in finite-time differentiator. Consequently, the design parameters for the virtual controller and actual controller are selected as $\underline{h}_1=5$, $\overline{h}_1=10$, $\underline{h}_2=5$, $q=10$, $n=3$, $\rho=0.3$, $T=0.8$, $\lambda_1=10.2$, $\lambda_2=10.2$, and the differentiator parameters for the finite-time differentiator are assigned as $k_1=2$ and $k_2=2.2$.

The results of the simulation can be seen directly in Figures 1 to 3. Figure 1 gives the system's output y and reference signal y_r, through which we know that the output y can realize the tracking performance. It can be observed obviously in Figure 1 that y can track the trajectory of the reference signal y_r in a predefined time $T=0.8$. From Figure 2, it is obvious that the tracking error z_1 rapidly approaches 0. Obviously, the boundedness of states $x_1(t)$ and $x_2(t)$ can be observed in Figures 1 and 3. The

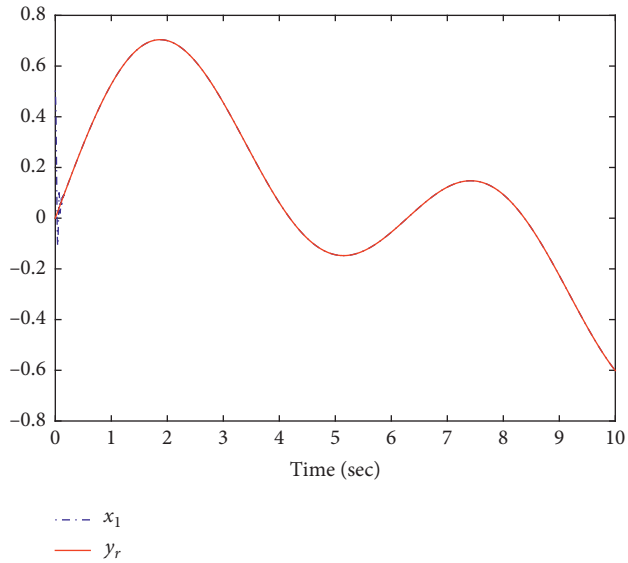

Figure 1: System output y and reference signal y_r.

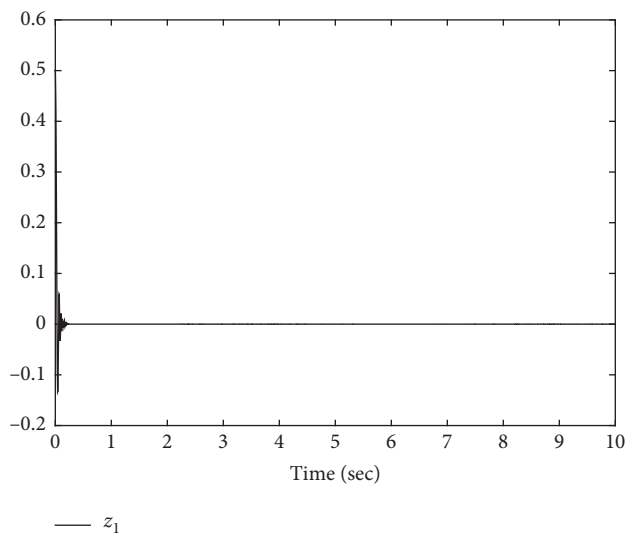

Figure 2: The tracking error z_1.

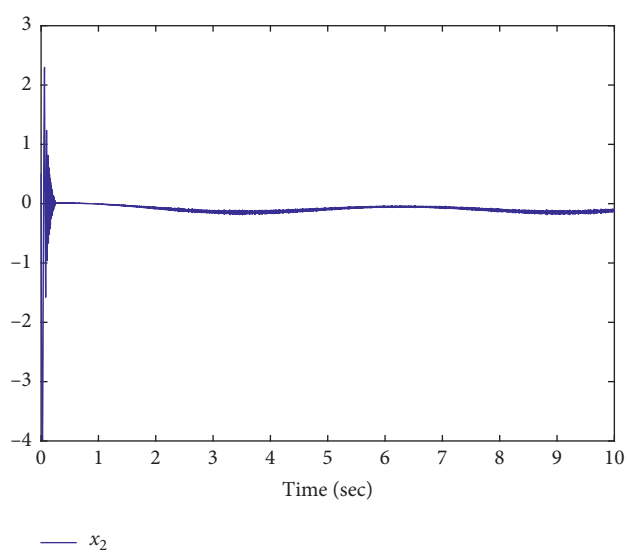

Figure 3: System state x_2.

predefined-time controller in this article is effective, which has been illustrated by the simulation in this paper.

6. Conclusions

Based on the predefined-time stability theory combined with RBF NN and finite-time differentiator, the adaptive predefined-time controller is designed in this paper for the nonlinear pure-feedback systems with unknown disturbance; simultaneously, it needs to construct the Lyapunov function using the backstepping method. The mean value theorem is used to address the nonaffine problem of the pure-feedback systems, and RBF NN is applied to deal with the unknown nonlinear functions such that the virtual control inputs can be obtained, whose derivatives are further estimated by the finite-time differentiators such that the problem of explosion of complexity can be avoided. The boundedness of all the signals in the closed-loop system can be obtained, and the tracking error can approach zero in a setting time. In the actual situation, the upper bound of the setting time can be arbitrarily designed. Thereby, the adaptive predefined-time controller in this article can be applied to many practical nonlinear pure-feedback systems. However, there are fewer adjustable parameters for the adaptive law $\widehat{\theta}_i$, which affects the tracking performance of the proposed predefined-time controller. Thereby, we will continue to study how to design an improved adaptive law $\widehat{\theta}_i$ to improve the performance of the proposed predefined-time controller.

Data Availability

The data used to support the findings of this study are available from the corresponding author upon request.

Conflicts of Interest

The authors declare that they have no conflicts of interest.

Acknowledgments

This work was supported in part by the National Natural Science Foundation of China under Grant 61773072 and in part by the Education Department of Liaoning Province under the general project research under Grant no. LJ2020001.

References

[1] M. Krstic, I. Kanelakopoulos, and P. V. Kokotovic, *Nonlinear and Adaptive Control Design*, Wiley, New York, NY, USA, 1995.

[2] I. Kanellakopoulos, P. V. Kokotovic, and A. S. Morse, "Systematic design of adaptive controllers for feedback linearizable systems," *IEEE Transactions on Automatic Control*, vol. 36, no. 11, pp. 1241–1253, 1991.

[3] Y. Sun, B. Chen, C. Lin, H. Wang, and S. Zhou, "Adaptive neural control for a class of stochastic nonlinear systems by backstepping approach," *Information Sciences*, vol. 369, pp. 748–764, 2016.

[4] D. Yang, X. Li, and J. Qiu, "Output tracking control of delayed switched systems via state-dependent switching and dynamic output feedback," *Nonlinear Analysis: Hybrid Systems*, vol. 32, pp. 294–305, 2019.

[5] S. S. Ge and C. Cong Wang, "Direct adaptive NN control of a class of nonlinear systems," *IEEE Transactions on Neural Networks*, vol. 13, no. 1, pp. 214–221, 2002.

[6] S. S. Ge, G. Y. Li, J. Zhang, and T. H. Lee, "Direct adaptive control for a class of MIMO nonlinear systems using neural networks," *IEEE Transactions on Automatic Control*, vol. 49, no. 11, pp. 2001–2006, 2004.

[7] Y. C. Yeong-Chan Chang, "An adaptive H/sup ∞/tracking control for a class of nonlinear multiple-input multiple-output (MIMO) systems," *IEEE Transactions on Automatic Control*, vol. 46, no. 9, pp. 1432–1437, 2001.

[8] M. M. Polycarpou, "Stable adaptive neural control scheme for nonlinear systems," *IEEE Transactions on Automatic Control*, vol. 41, no. 3, pp. 447–451, 1996.

[9] X. Li, D. O'Regan, and H. Akca, "Global exponential stabilization of impulsive neural networks with unbounded continuously distributed delays," *IMA Journal of Applied Mathematics*, vol. 80, no. 1, pp. 85–99, 2015.

[10] M. Chen and S. S. Ge, "Adaptive neural output feedback control of uncertain nonlinear systems with unknown hysteresis using disturbance observer," *IEEE Transactions on Industrial Electronics*, vol. 62, no. 12, pp. 7706–7716, 2015.

[11] H. Wang, P. Shi, H. Li, and Q. Zhou, "Adaptive neural tracking control for a class of nonlinear systems with dynamic uncertainties," *IEEE Transactions on Cybernetics*, vol. 47, no. 10, pp. 3075–3087, 2017.

[12] X. Zhao, X. Wang, S. Zhang, and G. Zong, "Adaptive neural backstepping control design for A class of nonsmooth nonlinear systems," *IEEE Transactions on Systems, Man, and Cybernetics: Systems*, vol. 49, no. 9, pp. 1820–1831, 2019.

[13] J. Na, M. N. Mahyuddin, G. Herrmann, X. Ren, and P. Barber, "Robust adaptive finite-time parameter estimation and control for robotic systems," *International Journal of Robust and Nonlinear Control*, vol. 25, no. 16, pp. 3045–3071, 2015.

[14] H. Du, W. Zhu, G. Wen, and D. Wu, "Finite-time formation control for a group of quadrotor aircraft," *Aerospace Science and Technology*, vol. 69, pp. 609–616, 2017.

[15] W. He, S. Zhang, and S. S. Ge, "Adaptive control of a flexible crane system with the boundary output constraint," *IEEE Transactions on Industrial Electronics*, vol. 61, no. 8, pp. 4126–4133, 2014.

[16] S. S. Ge and C. Wang, "Adaptive NN control of uncertain nonlinear pure-feedback systems," *Automatica*, vol. 38, no. 4, pp. 671–682, 2002.

[17] C. Wang, D. J. Hill, S. S. Ge, and G. Chen, "An ISS-modular approach for adaptive neural control of pure-feedback systems," *Automatica*, vol. 42, no. 5, pp. 723–731, 2006.

[18] B. Ren, S. S. Ge, C. Y. Su, and T. H. Lee, "Adaptive neural control for a class of uncertain nonlinear systems in pure-feedback form with hysteresis input," *IEEE Transactions on Systems, Man, and Cybernetics, Part B (Cybernetics)*, vol. 39, no. 2, pp. 431–443, 2009.

[19] P. Dorato, *Short Time Stability in Linear Time-Varying Systems*, Polytechnic Institute of Brooklyn, Microwave Research Institute, New York, NY, USA, 1961.

[20] L. Weiss and E. Infante, "Finite time stability under perturbing forces and on product spaces," *IEEE Transactions on Automatic Control*, vol. 12, no. 1, pp. 54–59, 1967.

[21] Y. Liu, X. Liu, Y. Jing, X. Chen, and J. Qiu, "Direct adaptive preassigned finite-time control with time-delay and quantized

input using neural network," *IEEE Transactions on Neural Networks and Learning Systems*, vol. 31, no. 4, pp. 1222–1231, 2020.

[22] M. Golestani, S. Mobayen, and F. Tchier, "Adaptive finite-time tracking control of uncertain non-linear n -order systems with unmatched uncertainties," *IET Control Theory & Applications*, vol. 10, no. 14, pp. 1675–1683, 2016.

[23] X. Huang, W. Lin, and B. Yang, "Global finite-time stabilization of a class of uncertain nonlinear systems," *Automatica*, vol. 41, no. 5, pp. 881–888, 2005.

[24] H. Wang, P. X. Liu, X. Zhao, and X. Liu, "Adaptive fuzzy finite-time control of nonlinear systems with actuator faults," *IEEE Transactions on Cybernetics*, vol. 50, no. 5, pp. 1786–1797, 2020.

[25] W. Lv, F. Wang, and Y. Li, "Finite-time adaptive fuzzy output-feedback control of MIMO nonlinear systems with hysteresis," *Neurocomputing*, vol. 296, pp. 74–81, 2018.

[26] A. Polyakov, D. Efimov, and W. Perruquetti, "Finite-time and fixed-time stabilization: implicit Lyapunov function approach," *Automatica*, vol. 51, pp. 332–340, 2015.

[27] M. Chen, H. Wang, and X. Liu, "Adaptive fuzzy practical fixed-time tracking control of nonlinear systems," *IEEE Transactions on Fuzzy Systems*, vol. 29, no. 3, pp. 664–673, 2021.

[28] H. Wang, K. Xu, and J. Qiu, "Event-triggered adaptive fuzzy fixed-time tracking control for a class of nonstrict-feedback nonlinear systems," *IEEE Transactions on Circuits and Systems I: Regular Papers*, vol. 68, no. 7, pp. 3058–3068, 2021.

[29] J. Hu, G. Sui, X. Lv, and X. Li, "Fixed-time control of delayed neural networks with impulsive perturbations," *Nonlinear Analysis: Modelling and Control*, vol. 23, no. 6, pp. 904–920, 2018.

[30] S. Ling, H. Wang, and P. X. Liu, "Fixed-time adaptive event-triggered tracking control of uncertain nonlinear systems," *Nonlinear Dynamics*, vol. 100, no. 4, pp. 3381–3397, 2020.

[31] X. Jin, "Adaptive fixed-time control for MIMO nonlinear systems with asymmetric output constraints using universal barrier functions," *IEEE Transactions on Automatic Control*, vol. 64, no. 7, pp. 3046–3053, 2019.

[32] J. D. Sánchez-Torres, D. Gómez-Gutiérrez, and E. López, "A class of predefined-time stable dynamical systems," *IMA Journal of Mathematical Control and Information*, vol. 35, pp. i1–i29, 2018.

[33] J. K. Ni, L. Liu, Y. Tang, and C. X. Liu, "Predefined-time consensus tracking of second-order multiagent systems," *IEEE Transactions on Systems, Man, and Cybernetics: Systems*, vol. 51, no. 4, pp. 2550–2560, 2019.

[34] J. D. Snchez-Torres, D. Gmez-Gutirrez, and A. G. Loukianov, "Predefined-time backstepping control for tracking aclass of mechanical systems," in *20th IFAC World Congress*, vol. 50, no. 1, pp. 1680–1685, Toulouse, France, July 2017.

[35] J. Ni and P. Shi, "Global predefined time and accuracy adaptive neural network control for uncertain strict-feedback systems with output constraint and dead zone," *IEEE Transactions on Systems, Man, and Cybernetics: Systems*, vol. 80, pp. 1–16, 2020.

[36] A. Ferrara and G. P. Incremona, "Predefined-time output stabilization with second order sliding mode generation," *IEEE Transactions on Automatic Control*, vol. 66, no. 3, pp. 1445–1451, 2021.

[37] H. Wang, S. Liu, and W. Bai, "Adaptive neural tracking control for non-affine nonlinear systems with finite-time output constraint," *Neurocomputing*, vol. 397, no. 15, pp. 60–69, 2020.

[38] X. F. Zhang, G. Feng, and Y. H. Sun, "Finite-time stabilization by state feedback control for a class of time-varying nonlinear systems," *Automatica*, vol. 48, no. 14, pp. 499–504, 2012.

[39] E. Jimenez-Rodriguez, J. D. Snchez-Torres, and A. G. Loukianov, "On optimal predefined-time stabilization," *International Journal of Robust and Nonlinear Control*, vol. 27, no. 17, pp. 3620–3642, 2017.

[40] J. Bao, H. Wang, and P. X. Liu, "Finite-time synchronization control for bilateral teleoperation systems with asymmetric time-varying delay and input dead zone," *IEEE/ASME Transactions on Mechatronics*, vol. 255, 2018.

[41] X. Li, J. Shen, and R. Rakkiyappan, "Persistent impulsive effects on stability of functional differential equations with finite or infinite delay," *Applied Mathematics and Computation*, vol. 329, pp. 14–22, 2018.

[42] G. Hardy and J. Littlewood, *Inequalities*, Cambridge University Press, London, UK, 1988.

[43] A. Levant, "Robust exact differentiation via sliding mode technique," *Automatica*, vol. 34, no. 3, pp. 379–384, 1998.

Hindawi
Complexity
Volume 2021, Article ID 3462317, 11 pages
https://doi.org/10.1155/2021/3462317

Research Article

Convergence Theorems for m-Coordinatewise Negatively Associated Random Vectors in Hilbert Spaces

Lyurong Shi

Department of Foundational Teaching, Wuhu Institute of Technology, Wuhu 241003, China

Correspondence should be addressed to Lyurong Shi; slr@whit.edu.cn

Received 7 May 2021; Revised 2 June 2021; Accepted 14 June 2021; Published 20 July 2021

Academic Editor: Xiaodi Li

In this study, some new results on convergence properties for m-coordinatewise negatively associated random vectors in Hilbert space are investigated. The weak law of large numbers, strong law of large numbers, complete convergence, and complete moment convergence for linear process of H-valued m-coordinatewise negatively associated random vectors with random coefficients are established. These results improve and generalise some corresponding ones in the literature.

1. Introduction

The random variables $X_1, X_2, \ldots, X_n$ are said to be negatively associated (NA, in short) if, for every pair of disjoint subsets A and B of $\{1, 2, \ldots, n\}$ and any real coordinatewise nondecreasing (or nonincreasing) functions f_1 on $\mathbb{R}^{|A|}$ and f_2 on $\mathbb{R}^{|B|}$,

$$Cov\left(f_1\left(X_i, i \in A\right), f_2\left(X_j, j \in B\right)\right) \leq 0, \tag{1}$$

whenever the covariance above exists, where $|A|$ and $|B|$ denote the cardinalities of A and B, respectively. A sequence $\{X_i, i \geq 1\}$ of random variables is NA if every finite subcollection is NA.

The concept of NA random variables can be seen in Joag-Dev and Proschan [1], which also illustrated that many well-known multivariate distributions, such as multinomial, convolution of unlike multinomial, multivariate hypergeometric, permutation distribution, negatively correlated normal distribution, and joint distribution of ranks, all satisfy the NA property.

Because of its wide applications, the concept of NA random variables was extended to many different directions. For example, Chandra and Ghosal [2] extended NA to asymptotically almost negative association (AANA); Hu et al. [3] extended the concept of NA random variables to m-NA random variables; Zhang and Wang [4] generalised it to a more broad case, i.e., asymptotically negative association (ANA); Zhang [5] extended it to $\mathbb{R}^d$-valued random vectors; Ko et al. [6] introduced the concept of NA random vectors taking values in real separable Hilbert spaces.

Since the concept of NA random vectors was introduced, some related works were established. For the details, we refer to Miao [7], for the Hajeck-Renyi inequality, Thanh [8], for the almost sure convergence, and Hien and Thanh [9], for weak laws of large numbers, among others. For more recent studies, we refer to Hu et al. [10], Li et al. [11], Yang et al. [12], Yang et al. [13], Fang et al. [14, 15], Mei et al. [16], and Yuan et al. [17].

Let H be a real separable Hilbert space with the norm $\|\cdot\|$ generated by an inner product $\langle\cdot,\cdot\rangle$. Denote $X^{(j)} = \langle X, e_j\rangle$, where $\{e^{(j)}, j \in \mathscr{B}\}$ is an orthonormal basis in H, X is also a random vector taking values in H, and $\mathscr{B}$ is a subset of $\{1, 2, \ldots\}$.

Huan et al. [18] first introduced the concept of coordinatewise negatively associated (CNA) random vectors in Hilbert spaces. Huan et al. [18] exemplified that a sequence of NA random vectors is also CNA in Hilbert spaces while the reverse is not true in general. There are also some interesting results concerning the CNA random vectors in

Hilbert spaces, most of which mainly extended the following Baum–Katz type convergence theorem from independent and identically distributed (i.i.d.) random variables in classical probability space to CNA random vectors in Hilbert space.

Baum–Katz theorem (see [19]): let $p > 1, \alpha > (1/2)$ and $\alpha p > 1$. Let $\{X_n, n \geq 1\}$ be a sequence of i.i.d. random variables with zero mean. Then, the following statements are equivalent:

(i) $E|X_1|^p < \infty$

(ii) $\sum_{n=1}^{\infty} n^{\alpha p-2} P(|\sum_{k=1}^{n} X_k| > \varepsilon n^{\alpha}) < \infty$

(iii) $\sum_{n=1}^{\infty} n^{\alpha p-2} P(\sup_{k\geq n} k^{-\alpha} |\sum_{i=1}^{k} X_i| > \varepsilon n^{\alpha}) < \infty$

Huan et al. [18] proved the sufficient conditions of the Baum–Katz type complete convergence with $1 \leq p < 2$ and $\alpha p > 1$, which partially extends Theorem A to CNA random vectors in Hilbert space. Huan [20] considered the case $\alpha p = 1$ with $1 < p < 2$. Ko [21] extended the result of Huan et al. [18] to the complete moment convergence, where, however, the case $p = 1$ is wrongly proved as pointed out by Huang and Wu [22]. Ko [23] also established the complete moment convergence with $\alpha p = 1$ and $1 \leq p < 2$. However, there are still some mistakes for $\alpha = p = 1$. To be specific, it shows in equation (2.9) of [23] that $\int_1^u y^{(1/(\alpha-2))} \log y dy \leq C u^{(1/(\alpha-1))} \log u$, where we know it is wrong when $\alpha = 1$; furthermore, the formula $\sum_{n=1}^{m} (\log n/n^{\alpha}) \leq C(\log m/n^{\alpha-1})$ in equation (2.11) of [23] is yet invalid for $\alpha = 1$. One goal of this work is to further investigate the Baum–Katz type convergence theorem such as complete convergence and complete moment convergence under a much broad dependence assumption and obtain some new results including the interesting case $\alpha = p = 1$. Moreover, to the best of my knowledge, there was no paper investigating the limit properties of random vectors with random coefficients in Hilbert spaces. Therefore, the work will mainly focus on this topic to obtain some results which were not established before.

In this paper, some new results on the weak law of large numbers, strong law of large numbers, complete convergence, and complete moment convergence for linear process of H-valued m-coordinatewise negatively associated (m-CNA, in short) random vectors with random coefficients are established successfully. The results improve and generalise the corresponding ones of Hien and Thanh [9], Huan et al. [18], Huan [20], Ko [21], and Ko [23].

In what follows, let C denote a generic positive constant whose value may vary in different lines. $x_+ = \max\{x, 0\}$ and $I(A)$ implies the indicator function of the set A. $\mathbb{Z} = \{\ldots, -2, -1, 0, 1, 2, \ldots\}$ represents the set of integers.

The paper is organized as follows. Section 2 gives some preliminary definitions and lemmas. Section 3 presents the main results and their proofs. Section 4 contains the conclusion of the paper.

2. Preliminaries

In this section, we will present some concepts and important lemmas as below.

Definition 1 (see [18]). A sequence $\{X_i, i \geq 1\}$ of random vectors taking values in H is said to be CNA if, for each $j \in \mathscr{B}$, the sequence $\{X_i^{(j)}, i \geq 1\}$ of random variables is NA, where $X_i^{(j)} = \langle X_i, e_j \rangle$. Inspired by Hu et al. [3] and Huan et al. [18], we introduce the concept of m-CNA random vectors in Hilbert space as follows.

Definition 2. Let $m \geq 1$ be a given integer. A sequence $\{X_n, n \geq 1\}$ of random variables is said to be m-CNA if, for any $n \geq 2$ and any $(i_1, i_2, \ldots, i_n)$ such that $|i_j - i_k| \geq m$ for all $1 \leq k \neq j \leq n$, we have that $(X_{i_1}, X_{i_2}, \ldots, X_{i_n})$ are CNA. Obviously, if $m = 1$, then m-CNA random vectors is CNA. Hence, the concept of m-CNA random vectors is a natural extension of that of CNA random vectors. We also present an example of m-CNA random vectors which are not CNA, as follows.

Example 1. Let $\{\xi_i, i \geq 1\}$ be a sequence of independent random vectors, where ξ_i follows the standard multivariate normal distribution for each $i \geq 1$. Take $X_i = \xi_i + \theta_1 \xi_{i+1} - \theta_2 \xi_{i+2}$ for each $i \geq 1$, where $0 < \theta_1, \theta_2 < 1$. Then, it is easy to check that, for any $j \in \mathscr{B}$ and $i \geq 1$, $\mathrm{Cov}(X_i^{(j)}, X_{i+1}^{(j)}) = \theta_1(1 - \theta_2) > 0$ but $\mathrm{Cov}(X_i^{(j)}, X_{i+2}^{(j)}) = -\theta_2 < 0$ and $\mathrm{Cov}(X_i^{(j)}, X_{i+l}^{(j)}) = 0$ for $l \geq 3$. That is to say, $\{X_i, i \geq 1\}$ is a sequence of m-CNA random vectors with $m = 2$. We also introduce the following concept of the linear process of random vectors in Hilbert spaces with random coefficients.

Definition 3. Assume that $\{X_i, -\infty < i < \infty\}$ is a sequence of H-valued random vectors and $\{A_i, -\infty < i < \infty\}$ is a sequence of random variables. The sequence $\{Y_t, t \geq 1\}$ of random vectors is said to be linear process with random coefficients if

$$Y_t = \sum_{i=-\infty}^{\infty} A_i X_{t-i}. \tag{2}$$

The following concept is often used in the literature while dealing with the convergence theorems of random vectors in Hilbert spaces.

Definition 4. A sequence $\{X_n, n \geq 1\}$ is said to be coordinatewise weakly upper bounded by X if there exists a positive constant C such that $\sup_{n\geq 1} n^{-1} \sum_{i=1}^{n} P(|X_i^{(j)}| > x) \leq C P(|X_i^{(j)}| > x)$, for all $j \in \mathscr{B}$ and $x \geq 0$.

Lemma 1. *Let $\{X_i, -\infty < i < \infty\}$ be a sequence of m-CNA random vectors. If $\{f_i(\cdot), -\infty < i < \infty\}$ is a sequence of coordinatewise nondecreasing (or nonincreasing) continuous real functions, then $\{\sum_{j\in\mathscr{B}} f_i(X_i^{(j)}) e_j, -\infty < i < \infty\}$ is still a sequence of m-CNA random vectors.*

Proof. It follows from Definitions 1 and 2 that, for any $n \geq 2$ and any $(i_1, i_2, \ldots, i_n)$ taking values in $\mathbb{Z}$ such that $|i_j - i_k| \geq m$ for all $1 \leq k \neq j \leq n$, $\{X_{i1}^{(j)}, X_{i2}^{(j)}, \ldots, X_{in}^{(j)}\}$ is a sequence of NA random variables for each $j \in \mathscr{B}$. By Lemma 2.1 of [24], one can see that $\{f_{i1}(X_{i1}^{(j)}), f_{i2}(X_{i2}^{(j)}), \ldots, f_{in}(X_{in}^{(j)})\}$ is still a sequence of

NA random variables for each $j \in \mathscr{B}$. Hence, by Definitions 1 and 2 again, it follows that $f_{i_1}(X_{i_1}), f_{i_2}(X_{i_2}), \ldots, f_{i_n}(X_{i_n})$ are CNA, i.e., $\left\{\sum_{j\in\mathscr{B}} f_i(X_i^{(j)}),\ -\infty < i < \infty\right\}$ is m-CNA. □

Lemma 2 (see [18]). *Let $\{X_n, n \geq 1\}$ be a sequence of H-valued CNA random vectors with zero mean and $E\|X_n\|^2 < \infty$, for all $n \geq 1$. Then,*

$$E \max_{1\leq k\leq n} \left\| \sum_{i=1}^{k} X_i \right\|^2 \leq 2 \sum_{i=1}^{n} E\|X_i\|^2. \tag{3}$$

Lemma 3. *Let $\{X_n, n \geq 1\}$ be a sequence of H-valued m-CNA random vectors with zero mean and $E\|X_n\|^2 < \infty$ for all $n \geq 1$. Then,*

$$E \max_{1\leq k\leq n} \left\| \sum_{i=1}^{k} X_i \right\|^2 \leq 2m \sum_{i=1}^{n} E\|X_i\|^2. \tag{4}$$

Proof. Notice that

$$\max_{1\leq k\leq n} \left\| \sum_{i=1}^{k} X_i \right\| \leq \sum_{l=0}^{m-1} \max_{k\geq 1, mk\leq n} \left\| \sum_{i=1}^{k} X_{mi+l} \right\|, \tag{5}$$

where we can define without loss of generality that $X_0 = 0$. From Definition 1, we see that $\{X_{mi+l}, i \geq 0\}$ is CNA for each $(l = 1, 2, \ldots, m)$. Hence, by c_r inequality and Lemma 2, we have

$$\begin{aligned} E \max_{1\leq k\leq n} \left\| \sum_{i=1}^{k} X_i \right\|^2 &\leq m \sum_{l=0}^{m-1} E \max_{k\geq 1, mk\leq n} \left\| \sum_{i=1}^{k} X_{mi+l} \right\|^2 \\ &\leq 2m \sum_{l=0}^{m-1} \sum_{i\geq 0, mi\leq n} E\|X_{mi+l}\|^2 \\ &\leq 2m \sum_{i=0}^{n} E\|X_i\|^2. \end{aligned} \tag{6}$$

□

Lemma 4. *Let $\{X_i, -\infty < i < \infty\}$ be a sequence of H-valued m-CNA random vectors with zero mean and $E\|X_i\|^2 < \infty$ for all $-\infty < i < \infty$. If $\{A_i, -\infty < i < \infty\}$ is a sequence of random variables independent of $\{X_i, -\infty < i < \infty\}$ and $E(\sum_{i=-\infty}^{\infty} A_i)^2 < \infty$, then*

$$E \max_{1\leq k\leq n} \left\| \sum_{l=-\infty}^{\infty} \sum_{i=1-l}^{k-l} A_i X_l \right\|^2 \leq C \sup_{-\infty<i<\infty} \sum_{l=1-i}^{n-i} E\|X_l\|^2. \tag{7}$$

Proof. It follows by Hölder inequality and Lemma 3 that

$$\begin{aligned} E \max_{1\leq k\leq n} \left\| \sum_{l=-\infty}^{\infty} \sum_{i=1-l}^{k-l} A_i X_l \right\|^2 &= E \max_{1\leq k\leq n} \left\| \sum_{i=-\infty}^{\infty} A_i \sum_{l=1-i}^{k-i} X_l \right\|^2 \\ &\leq E\left[\sum_{i=-\infty}^{\infty} |A_i| \max_{1\leq k\leq n} \left\| \sum_{l=1-i}^{k-i} X_l \right\| \right]^2 \\ &= E\left[\sum_{i=-\infty}^{\infty} |A_i|^{(1/2)} \cdot |A_i|^{(1/2)} \max_{1\leq k\leq n} \left\| \sum_{l=1-i}^{k-i} X_l \right\| \right]^2 \\ &\leq E\left[\left(\sum_{i=-\infty}^{\infty} |A_i| \right)^{(1/2)} \left(\sum_{i=-\infty}^{\infty} |A_i| \max_{1\leq k\leq n} \left\| \sum_{l=1-i}^{k-i} X_l \right\|^2 \right)^{(1/2)} \right]^2 \\ &= \sum_{s=1}^{\infty} E\left[\left(\sum_{i=-\infty}^{\infty} |A_i| \right) \left(\sum_{i=-\infty}^{\infty} |A_i| \max_{1\leq k\leq n} \left\| \sum_{l=1-i}^{k-i} X_l \right\|^2 \right) I\left(s-1 \leq \sum_{i=-\infty}^{\infty} |A_i| < s \right) \right] \\ &\leq \sum_{s=1}^{\infty} sE\left[\sum_{i=-\infty}^{\infty} |A_i| I\left(s-1 \leq \sum_{i=-\infty}^{\infty} |A_i| < s \right) \right] E \max_{1\leq k\leq n} \left\| \sum_{l=1-i}^{k-i} X_l \right\|^2 \\ &\leq 2m \sup_{-\infty<i<\infty} \sum_{l=1-i}^{n-i} E\|X_l\|^2 \left[1 + 2\sum_{s=2}^{\infty} E\left(\sum_{i=-\infty}^{\infty} |A_i| \right)^2 I\left(s-1 \leq \sum_{i=-\infty}^{\infty} |A_i| < s \right) \right] \\ &\leq C \sup_{-\infty<i<\infty} \sum_{l=1-i}^{n-i} E\|X_l\|^2. \end{aligned} \tag{8}$$

The proof is therefore complete. □

Lemma 5 (see [25]). *Let $\{X_n, n \geq 1\}$ be a sequence of random variables satisfying $n^{-1}\sum_{i=1}^{n} P(|Z_i| > x) \leq CP(|Z| > x)$ for a random variable Z and any $x \geq 0$. Then, for any $a > 0$ and $b > 0$, there exist some positive constants c_1 and c_2 such that*

$$\begin{aligned} n^{-1}\sum_{i=1}^{n} E|Z_i|^a I\left(|Z_i| > b\right) &\leq c_1 E|Z|^a I(|Z| > b), \\ n^{-1}\sum_{i=1}^{n} E|X_i|^a I\left(|Z_i| \leq b\right) &\leq c_2\left[E|Z|^a I(|Z| \leq b) + b^a P(|Z| > b)\right]. \end{aligned} \tag{9}$$

Following the method of Lemma 2.3 in [26], we can obtain the following inequality in Hilbert spaces.

Lemma 6. *Let $\{Y_i, 1 \leq i \leq n\}$ and $\{Z_i, 1 \leq i \leq n\}$ be two sequences of random vectors. Then, for any $q > 1$, $\varepsilon > 0$, and $a > 0$, the following inequality holds:*

$$E\left(\max_{1\leq k\leq n}\left\|\sum_{i=1}^{k}(Y_i + Z_i)\right\| - \varepsilon a\right)^{+} \leq \left(\frac{1}{\varepsilon^q} + \frac{1}{q-1}\right)a^{1-q}E\left(\max_{1\leq k\leq n}\left\|\sum_{i=1}^{k} Y_i\right\|^q\right) + E\max_{1\leq k\leq n}\left\|\sum_{i=1}^{k} Z_i\right\|. \tag{10}$$

3. Main Results and Their Proofs

In this section, we will present our main results. The first one is the weak law of large numbers for linear process $\{Y_t, t \geq 1\}$ of m-CNA random vectors in Hilbert spaces with random coefficients.

Theorem 1. *Let $\{X_i, -\infty < i < \infty\}$ be a sequence of zero mean H-valued m-CNA random vectors coordinatewise weakly upper bounded by a random vector X. Suppose that $\{A_i, -\infty < i < \infty\}$ is a sequence of random variables independent of $\{X_i, -\infty < i < \infty\}$ and $E(\sum_{i=-\infty}^{\infty} A_i)^2 < \infty$. Assume further $\sum_{j\in\mathscr{B}} E|X^{(j)}|I(|X^{(j)}| > n) \longrightarrow 0$ as $n \longrightarrow \infty$ if the cardinality $|\mathscr{B}| < \infty$ or $\sum_{j\in\mathscr{B}} E|X^{(j)}| < \infty$ if $|\mathscr{B}| = \infty$. Then,*

$$\frac{1}{n}\sum_{t=1}^{n} Y_t \xrightarrow{P} 0, \quad \text{as } n \longrightarrow \infty. \tag{11}$$

Proof. For each $-\infty < i < \infty$ and $j \in \mathscr{B}$, denote

$$\begin{aligned} X_{ni}^{(j)} &= -nI\left(X_i^{(j)} < -n\right) + X_i^{(j)} I\left(\left|X_i^{(j)}\right| \leq n\right) + nI\left(X_i^{(j)} > n\right); \\ Z_{ni}^{(j)} &= X_i^{(j)} - X_{ni}^{(j)} = \left(X_i^{(j)} + n\right)I\left(X_i^{(j)} < -n\right) + \left(X_i^{(j)} - n\right)I\left(X_i^{(j)} > n\right), \\ X_{ni} &= \sum_{j\in\mathscr{B}} X_{ni}^{(j)} e_j, \\ Z_{ni} &= \sum_{j\in\mathscr{B}} Z_{ni}^{(j)} e_j. \end{aligned} \tag{12}$$

Note that

$$\begin{aligned} \sum_{t=1}^{n} Y_t &= \sum_{t=1}^{n}\sum_{i=-\infty}^{\infty} A_i X_{t-i} = \sum_{l=-\infty}^{\infty}\sum_{i=1-l}^{n-l} A_i X_l \\ &= \sum_{l=-\infty}^{\infty}\sum_{i=1-l}^{n-l} A_i\left(X_{nl} - EX_{nl}\right) + \sum_{l=-\infty}^{\infty}\sum_{i=1-l}^{n-l} A_i\left(Z_{nl} - EZ_{nl}\right) \\ &= \sum_{l=-\infty}^{\infty}\sum_{i=1-l}^{n-l} A_i\left(X_{nl} - EX_{nl}\right) + \sum_{t=1}^{n}\sum_{i=-\infty}^{\infty} A_i\left(Z_{n,t-i} - EZ_{n,t-i}\right). \end{aligned} \tag{13}$$

It is sufficient to prove that, for any $\varepsilon > 0$,

$$P\left(\left\|\sum_{l=-\infty}^{\infty}\sum_{i=1-l}^{n-l} A_i\left(X_{nl} - EX_{nl}\right)\right\| > n\varepsilon\right) \longrightarrow 0, \tag{14}$$

$$P\left(\left\|\sum_{t=1}^{n}\sum_{i=-\infty}^{\infty} A_i\left(Z_{n,t-i} - EZ_{n,t-i}\right)\right\| > n\varepsilon\right) \longrightarrow 0. \tag{15}$$

It follows from Lemma 1 that $\{X_{ni},\ -\infty < i \le \infty\}$ is still a sequence of m-CNA random vectors. Furthermore, it is easy to check that, as $n \longrightarrow \infty$,

$$\begin{aligned} n^{-1}\sum_{j\in\mathscr{B}}\int_0^1 xP\left(\left|X^{(j)}\right| > x\right)\mathrm{d}x &\le n^{-1}\sum_{j\in\mathscr{B}} E\left|X^{(j)}\right| \longrightarrow 0, \quad \text{if } |\mathscr{B}| = \infty, \\ n^{-1}\sum_{j\in\mathscr{B}}\int_0^1 xP\left(\left|X^{(j)}\right| > x\right)\mathrm{d}x &\le n^{-1}|\mathscr{B}| \longrightarrow 0, \quad \text{if } |\mathscr{B}| < \infty. \end{aligned} \tag{16}$$

Hence, we obtain by Chebyshev inequality, $E(\sum_{i=-\infty}^{\infty} A_i)^2 < \infty$, Lemmas 4 and 5, and integration by parts that

$$\begin{aligned} P\left(\left\|\sum_{l=-\infty}^{\infty}\sum_{i=1-l}^{n-l} A_i\left(X_{nl} - EX_{nl}\right)\right\| > n\varepsilon\right) &\le Cn^{-2}E\left\|\sum_{l=-\infty}^{\infty}\sum_{i=1-l}^{n-l} A_i\left(X_{nl} - EX_{nl}\right)\right\|^2 \\ &\le Cn^{-2}\sup_{-\infty<i<\infty}\sum_{l=1-i}^{n-i} E\left\|\left(X_{nl} - EX_{nl}\right)\right\|^2 \\ &\le Cn^{-2}\sup_{-\infty<i<\infty}\sum_{l=1-i}^{n-i}\left\{\sum_{j\in\mathscr{B}}\left[E\left|X_l^{(j)}\right|^2 I\left(\left|X_l^{(j)}\right| \le n\right) + n^2P\left(\left|X_l^{(j)}\right| > n\right)\right]\right\} \\ &\le Cn^{-1}\sum_{j\in\mathscr{B}}\left[E\left|X^{(j)}\right|^2 I\left(\left|X^{(j)}\right| \le n\right) + n^2P\left(\left|X^{(j)}\right| > n\right)\right] \\ &= Cn^{-1}\sum_{j\in\mathscr{B}}\int_0^n x\left(P\left|X^{(j)}\right| > x\right)dx \\ &= Cn^{-1}\sum_{j\in\mathscr{B}}\sum_{k=0}^{n-1}\int_k^{k+1} x\left(P\left|X^{(j)}\right| > x\right)dx \\ &\le Cn^{-1}\sum_{j\in\mathscr{B}}\int_0^1 xP\left(\left|X^{(j)}\right| > x\right)dx + Cn^{-1}\sum_{j\in\mathscr{B}}\sum_{k=1}^{n}\left[(k+1)^2 - k^2\right]P\left(\left|X^{(j)}\right| > k\right) \\ &\le Cn^{-1}\sum_{j\in\mathscr{B}}\int_0^1 xP\left(\left|X^{(j)}\right| > x\right)dx + Cn^{-1}\sum_{k=1}^{n}\left(\sum_{j\in\mathscr{B}} kP\left(\left|X^{(j)}\right| > k\right)\right) \\ &\le Cn^{-1}\sum_{j\in\mathscr{B}}\int_0^1 xP\left(\left|X^{(j)}\right| > x\right)dx + Cn^{-1}\sum_{k=1}^{n}\left(\sum_{j\in\mathscr{B}} E\left|X^{(j)}\right| I\left(\left|X^{(j)}\right| > k\right)\right), \end{aligned} \tag{17}$$

which converges to 0 as $n \longrightarrow \infty$, and thus, equation (14) holds true. On the contrary, we have, by Markov inequality, Lemma 5, and Jensen inequality, that

$$
\begin{aligned}
P\left(\left\|\sum_{t=1}^{n}\sum_{i=-\infty}^{\infty}A_i\left(Z_{n,t-i}-EZ_{n,t-i}\right)\right\|>n\varepsilon\right) &\le Cn^{-1}E\left\|\sum_{t=1}^{n}\sum_{i=-\infty}^{\infty}A_i\left(Z_{n,t-i}-EZ_{n,t-i}\right)\right\|,\\
&\le Cn^{-1}\sum_{t=1}^{n}\sum_{i=-\infty}^{\infty}E\left|A_i\right|E\left\|Z_{n,t-i}-EZ_{n,t-i}\right\|\\
&\le CE\left(\sum_{i=-\infty}^{\infty}\left|A_i\right|\right)\sum_{j\in\mathscr{B}}n^{-1}\sum_{t=1}^{n}E\left|X_{t-i}^{(j)}\right|I\left(\left|X_{t-i}^{(j)}\right|>n\right)\\
&\le C\left[E\left(\sum_{i=-\infty}^{\infty}\left|A_i\right|\right)^2\right]^{(1/2)}\sum_{j\in\mathscr{B}}E\left|X^{(j)}\right|I\left(\left|X^{(j)}\right|>n\right),
\end{aligned}
\tag{18}
$$

which obtains equation (15) as $n \longrightarrow \infty$ by the assumption of Theorem 1, and the proof is thus complete. □

Remark 1. Hien and Thanh [9] obtained the weak law of large numbers for NA random vectors under the moment condition $\sum_{j\in\mathscr{B}}E|X^{(j)}|<\infty$. Contrasting to Corollary 2.5 of Hien and Thanh [9], Theorem 1 not only extends the assumption of NA random vectors to linear process of m-CNA random vectors with random coefficients but also improves the moment condition when $|\mathscr{B}|<\infty$.

Theorem 2. *Let $1<p<2$ and $\alpha p\ge 1$. Let $\{X_i,\ -\infty<i<\infty\}$ be a sequence of zero mean H-valued m-CNA random vectors coordinatewise weakly upper bounded by a random vector X with $\sum_{j\in\mathscr{B}}E|X^{(j)}|^p<\infty$. Suppose that $\{A_i,\ -\infty<i<\infty\}$ is a sequence of random variables independent of $\{X_i,\ -\infty<i<\infty\}$ and $E(\sum_{i=-\infty}^{\infty}A_i)^2<\infty$. Then, for any $\varepsilon>0$,*

$$
\sum_{n=1}^{\infty}n^{\alpha p-\alpha-2}E\left(\max_{1\le k\le n}\left\|\sum_{t=1}^{k}Y_t\right\|-\varepsilon n^{\alpha}\right)_+<\infty,
\tag{19}
$$

and thus,

$$
\sum_{n=1}^{\infty}n^{\alpha p-2}P\left(\max_{1\le k\le n}\left\|\sum_{t=1}^{k}Y_t\right\|>\varepsilon n^{\alpha}\right)<\infty.
\tag{20}
$$

Proof. Define for each $-\infty<i<\infty$ and $j\in\mathscr{B}$ that

$$
\begin{aligned}
W_{ni}^{(j)} &= -nI\left(X_i^{(j)}<-n^{\alpha}\right)+X_i^{(j)}I\left(\left|X_i^{(j)}\right|\le n^{\alpha}\right)+nI\left(X_i^{(j)}>n^{\alpha}\right),\\
T_{ni}^{(j)} &= X_i^{(j)}-W_{ni}^{(j)}=\left(X_i^{(j)}+n^{\alpha}\right)I\left(X_i^{(j)}<-n^{\alpha}\right)+\left(X_i^{(j)}-n^{\alpha}\right)I\left(X_i^{(j)}>n^{\alpha}\right),\\
W_{ni} &= \sum_{j\in\mathscr{B}}W_{ni}^{(j)}e_j,\\
T_{ni} &= \sum_{j\in\mathscr{B}}T_{ni}^{(j)}e_j.
\end{aligned}
\tag{21}
$$

Similar to the argument of equation (13), we have that, for each $1\le k\le n$,

$$
\sum_{t=1}^{k}Y_t=\sum_{l=-\infty}^{\infty}\sum_{i=1-l}^{k-l}A_iX_l=\sum_{l=-\infty}^{\infty}\sum_{i=1-l}^{k-l}A_i\left(W_{nl}-EW_{nl}\right)+\sum_{t=1}^{k}\sum_{i=-\infty}^{\infty}A_i\left(T_{n,t-i}-ET_{n,t-i}\right).
\tag{22}
$$

On the one hand, noting that $\{W_{ni},\ -\infty<i\le\infty\}$ is still a sequence of m-CNA random vectors by Lemma 1, we obtain by Lemmas 4 and 5 that

$$
\begin{aligned}
&\sum_{n=1}^{\infty} n^{\alpha p-2\alpha-2} E \max_{1\le k\le n}\left\|\sum_{l=-\infty}^{\infty}\sum_{i=1-l}^{k-l} A_i\left(W_{nl}-EW_{nl}\right)\right\|^2 \\
&\le C\sum_{n=1}^{\infty} n^{\alpha p-2\alpha-2}\sup_{-\infty<i<\infty}\sum_{l=1-i}^{n-i}\left\{\sum_{j\in\mathscr{B}}\left[E\left|X_l^{(j)}\right|^2 I\left(\left|X_l^{(j)}\right|\le n^{\alpha}\right)+n^{2\alpha}P\left(\left|X_l^{(j)}\right|>n^{\alpha}\right)\right]\right\} \\
&\le C\sum_{j\in\mathscr{B}}\sum_{n=1}^{\infty} n^{\alpha p-2\alpha-1}E\left|X^{(j)}\right|^2 I\left(\left|X^{(j)}\right|\le n^{\alpha}\right)+C\sum_{j\in\mathscr{B}}\sum_{n=1}^{\infty} n^{\alpha p-1}P\left(\left|X^{(j)}\right|>n^{\alpha}\right) \\
&\le C\sum_{j\in\mathscr{B}}\sum_{n=1}^{\infty} n^{\alpha p-2\alpha-1}\sum_{l=1}^{n} E\left|X^{(j)}\right|^2 I\left((l-1)^{\alpha}<\left|X^{(j)}\right|\le l^{\alpha}\right)+C\sum_{j\in\mathscr{B}} E\left|X^{(j)}\right|^p \\
&\le C\sum_{j\in\mathscr{B}}\sum_{l=1}^{\infty} l^{\alpha p-2\alpha}E\left|X^{(j)}\right|^2 I\left((l-1)^{\alpha}<\left|X^{(j)}\right|\le l^{\alpha}\right)+C\sum_{j\in\mathscr{B}} E\left|X^{(j)}\right|^p \\
&\le C\sum_{j\in\mathscr{B}} E\left|X^{(j)}\right|^p<\infty.
\end{aligned}
\tag{23}
$$

On the other hand, it follows from Lemma 5 and Jensen inequality that

$$
\begin{aligned}
&\sum_{n=1}^{\infty} n^{\alpha p-\alpha-2} E \max_{1\le k\le n}\left\|\sum_{t=1}^{k}\sum_{i=-\infty}^{\infty} A_i\left(T_{n,t-i}-ET_{n,t-i}\right)\right\| \\
&\le C\sum_{n=1}^{\infty} n^{\alpha p-\alpha-2}\sum_{t=1}^{n}\sum_{i=-\infty}^{\infty} E\left|A_i\right|E\left\|T_{n,t-i}-ET_{n,t-i}\right\| \\
&\le C\sum_{n=1}^{\infty} n^{\alpha p-\alpha-1}E\left(\sum_{i=-\infty}^{\infty}\left|A_i\right|\right)\sum_{j\in\mathscr{B}} n^{-1}\sum_{t=1}^{n} E\left|X_{t-i}^{(j)}\right| I\left(\left|X_{t-i}^{(j)}\right|>n^{\alpha}\right) \\
&\le C\sum_{j\in\mathscr{B}}\sum_{n=1}^{\infty} n^{\alpha p-\alpha-1}\left[E\left(\sum_{i=-\infty}^{\infty}\left|A_i\right|\right)^2\right]^{(1/2)} E\left|X^{(j)}\right| I\left(\left|X^{(j)}\right|>n^{\alpha}\right) \\
&\le C\sum_{j\in\mathscr{B}}\sum_{l=1}^{\infty} E\left|X^{(j)}\right| I\left(l^{\alpha}<\left|X^{(j)}\right|\le (l+1)^{\alpha}\right)\sum_{n=1}^{l} n^{\alpha p-\alpha-1} \\
&\le C\sum_{j\in\mathscr{B}}\sum_{l=1}^{\infty} l^{\alpha p-\alpha}E\left|X^{(j)}\right| I\left(l^{\alpha}<\left|X^{(j)}\right|\le (l+1)^{\alpha}\right) \\
&\le C\sum_{j\in\mathscr{B}} E\left|X^{(j)}\right|^p<\infty.
\end{aligned}
\tag{24}
$$

Hence, it follows from Lemma 6 (with $q=2$) and equations (22)–(24) that

$$\begin{aligned}
&\sum_{n=1}^{\infty} n^{\alpha p-\alpha-2} E\left(\max_{1\le k\le n}\left\|\sum_{t=1}^{k} Y_t\right\| - \varepsilon n^{\alpha}\right)_+ \\
&\le C\sum_{n=1}^{\infty} n^{\alpha p-2\alpha-2} E\max_{1\le k\le n}\left\|\sum_{l=-\infty}^{\infty}\sum_{i=1-l}^{k-l} A_i\left(W_{nl}-EW_{nl}\right)\right\|^2 + \sum_{n=1}^{\infty} n^{\alpha p-\alpha-2} E\max_{1\le k\le n}\left\|\sum_{t=1}^{k}\sum_{i=-\infty}^{\infty} A_i\left(T_{n,t-i}-ET_{n,t-i}\right)\right\| \\
&\le C\sum_{j\in\mathscr{B}} E\left\|X^{(j)}\right\|^p < \infty,
\end{aligned} \tag{25}$$

which obtains equation (19). Now, we prove equation (20). It follows from equation (19) that

$$\begin{aligned}
\infty &> \sum_{n=1}^{\infty} n^{\alpha p-\alpha-2} E\left(\max_{1\le k\le n}\left\|\sum_{t=1}^{k} Y_t\right\| - \varepsilon n^{\alpha}\right)_+, \\
&\ge \sum_{n=1}^{\infty} n^{\alpha p-\alpha-2}\int_0^{\varepsilon n^{\alpha}} P\left(\max_{1\le k\le n}\left\|\sum_{t=1}^{k} Y_t\right\| - \varepsilon n^{\alpha} > s\right) \mathrm{d}s \\
&\ge \varepsilon\sum_{n=1}^{\infty} n^{\alpha p-2} P\left(\max_{1\le k\le n}\left\|\sum_{t=1}^{k} Y_t\right\| > 2\varepsilon n^{\alpha}\right),
\end{aligned} \tag{26}$$

which combining with the arbitrariness of ε gets equation (20). The proof is complete. □

Remark 2. Huan et al. [18] and Huan [20] established equation (20) for CNA random vectors, respectively, for $1 \le p < 2$, $\alpha p > 1$, and $1 < p < 2$, $\alpha p = 1$. Although Ko [21] extended the result of Huan et al. [18] to complete moment convergence, it only holds for $1 < p < 2$, $\alpha p > 1$, as illustrated in Section 1. Hence, Theorem 2 improves and extends the results of Huan et al. [18], Huan [20], and Ko [21] from CNA random vectors to linear process of m-CNA random vectors with random coefficients. By Theorem 2, we can easily get the following conclusion.

Corollary 1. *Under the conditions of Theorem 2, if $\alpha p > 1$, we have that, for any $\varepsilon > 0$,*

$$\sum_{n=1}^{\infty} n^{\alpha p-2} E\left(\sup_{k\ge n} k^{-\alpha}\left\|\sum_{t=1}^{k} Y_t\right\| - \varepsilon\right)_+ < \infty, \tag{27}$$

and thus,

$$\sum_{n=1}^{\infty} n^{\alpha p-2} P\left(\sup_{k\ge n} k^{-\alpha}\left\|\sum_{t=1}^{k} Y_t\right\| > \varepsilon\right) < \infty. \tag{28}$$

Proof. It follows from Theorem 2 that

$$\begin{aligned}
\sum_{n=1}^{\infty} n^{\alpha p-2} E\left(\sup_{k\ge n} k^{-\alpha}\left\|\sum_{t=1}^{k} Y_t\right\| - \varepsilon\right)_+ &= \sum_{l=1}^{\infty}\sum_{2^{l-1}\le n<2^l} n^{\alpha p-2} E\left(\sup_{k\ge n} k^{-\alpha}\left\|\sum_{t=1}^{k} Y_t\right\| - \varepsilon\right)_+, \\
&\le C\sum_{l=1}^{\infty} 2^{l(\alpha p-1)} E\left(\sup_{k\ge 2^{l-1}} k^{-\alpha}\left\|\sum_{t=1}^{k} Y_t\right\| - \varepsilon\right)_+ \\
&\le C\sum_{s=1}^{\infty} E\left(\max_{2^{s-1}\le k<2^s} k^{-\alpha}\left\|\sum_{t=1}^{k} Y_t\right\| - \varepsilon\right)_+ \sum_{l=1}^{s} 2^{l(\alpha p-1)} \\
&\le C\sum_{s=1}^{\infty} 2^{s(\alpha p-1)} E\left(\max_{2^{s-1}\le k<2^s} 2^{-\alpha(s-1)}\left\|\sum_{t=1}^{k} Y_t\right\| - \varepsilon\right)_+ \\
&\le C\sum_{s=1}^{\infty} 2^{s(\alpha p-\alpha-1)} E\left(\max_{1\le k<2^s}\left\|\sum_{t=1}^{k} Y_t\right\| - \varepsilon 2^{-\alpha}2^{\alpha s}\right)_+ \\
&\le C\sum_{s=0}^{\infty}\sum_{2^s\le n<2^{s+1}} n^{\alpha p-\alpha-2} E\left(\max_{1\le k<2^s}\left\|\sum_{t=1}^{k} Y_t\right\| - \varepsilon 2^{-\alpha}2^{\alpha s}\right)_+ \\
&\le C\sum_{n=1}^{\infty} n^{\alpha p-\alpha-2} E\left(\max_{1\le k\le n}\left\|\sum_{t=1}^{k} Y_t\right\| - \varepsilon 2^{-2\alpha} n^{\alpha}\right)_+ < \infty.
\end{aligned} \tag{29}$$

Furthermore, similar to the proof of equation (20), we have that

$$\begin{aligned}\infty &> \sum_{n=1}^{\infty} n^{\alpha p-2} E\left(\sup_{k\geq n} k^{-\alpha}\left\|\sum_{t=1}^{k} Y_t\right\| - \varepsilon\right)_+ \\ &\geq \sum_{n=1}^{\infty}\sum_{n=1}^{\infty} n^{\alpha p-2}\int_0^{\varepsilon} P\left(\sup_{k\geq n} k^{-\alpha}\left\|\sum_{t=1}^{k} Y_t\right\| - \varepsilon > s\right) \mathrm{d}s \\ &\geq \varepsilon \sum_{n=1}^{\infty} n^{\alpha p-2} P\left(\sup_{k\geq n} k^{-\alpha}\left\|\sum_{t=1}^{k} Y_t\right\| > 2\varepsilon\right).\end{aligned} \tag{30}$$

The proof is complete.

For $p = 1$, we can obtain the following result. □

Theorem 3. *Let $\alpha \geq 1$. Let $\{X_i, -\infty < i < \infty\}$ be a sequence of zero mean H-valued m-CNA random vectors coordinatewise weakly upper bounded by a random vector X with $\sum_{j\in\mathscr{B}} E|X^{(j)}| ln^{\delta+1}(1 + |X^{(j)}|) < \infty$ for some $\delta \geq 0$. Suppose that $\{A_i, -\infty < i < \infty\}$ is a sequence of random variables independent of $\{X_i, -\infty < i < \infty\}$ and $E(\sum_{i=-\infty}^{\infty} A_i)^2 < \infty$. Then, for any $\varepsilon > 0$,*

$$\sum_{n=1}^{\infty} n^{-2}\ln^{\delta} nE\left(\max_{1\leq k\leq n}\left\|\sum_{t=1}^{k} Y_t\right\| - \varepsilon n^{\alpha}\right)_+ < \infty, \tag{31}$$

and thus,

$$\sum_{n=1}^{\infty} n^{\alpha-2}\ln^{\delta} nP\left(\max_{1\leq k\leq n}\left\|\sum_{t=1}^{k} Y_t\right\| > \varepsilon n^{\alpha}\right) < \infty. \tag{32}$$

Proof. We still use the notations and method in the proof of Theorem 2. Similar to the argument of equation (23), we have

$$\begin{aligned}&\sum_{n=1}^{\infty} n^{-\alpha-2}\ln^{\delta} nE\max_{1\leq k\leq n}\left\|\sum_{l=-\infty}^{\infty}\sum_{i=1-l}^{k-l} A_i\left(W_{nl} - EW_{nl}\right)\right\|^2 \\ &\leq C\sum_{j\in\mathscr{B}}\sum_{n=1}^{\infty} n^{-\alpha-1}\ln^{\delta} nE\left|X^{(j)}\right|^2 I\left(\left|X^{(j)}\right| \leq n^{\alpha}\right) + C\sum_{j\in\mathscr{B}}\sum_{n=1}^{\infty} n^{\alpha-1}\ln^{\delta} nP\left(\left|X^{(j)}\right| > n^{\alpha}\right) \\ &\leq C\sum_{j\in\mathscr{B}}\sum_{l=1}^{\infty} l^{-\alpha}\ln^{\delta} lE\left|X^{(j)}\right|^2 I\left((l-1)^{\alpha} < \left|X^{(j)}\right| \leq l^{\alpha}\right) + C\sum_{j\in\mathscr{B}}\sum_{l=1}^{\infty} l^{\alpha}\ln^{\delta} lP\left(l^{\alpha} < \left|X^{(j)}\right| \leq (l+1)^{\alpha}\right) \\ &\leq C\sum_{j\in\mathscr{B}}\sum_{l=1}^{\infty} E\left|X^{(j)}\right|^2\cdot\left|X^{(j)}\right|^{-1}\left(\ln\left(1 + \left|X^{(j)}\right|\right)^{(1/\alpha)}\right)^{\delta} I\left((l-1)^{\alpha} < \left|X^{(j)}\right| \leq l^{\alpha}\right) \\ &+ C\sum_{j\in\mathscr{B}}\sum_{l=1}^{\infty} E\left|X^{(j)}\right|\left(\ln\left(1 + \left|X^{(j)}\right|\right)^{(1/\alpha)}\right)^{\delta} I\left((l-1)^{\alpha} < \left|X^{(j)}\right| \leq l^{\alpha}\right) \\ &\leq C\sum_{j\in\mathscr{B}}\sum_{l=1}^{\infty} E\left|X^{(j)}\right|\ln^{\delta}\left(1 + \left|X^{(j)}\right|\right) I\left((l-1)^{\alpha} < \left|X^{(j)}\right| \leq l^{\alpha}\right) \\ &\leq C\sum_{j\in\mathscr{B}} E\left|X^{(j)}\right|\ln^{\delta}\left(1 + \left|X^{(j)}\right|\right) < \infty.\end{aligned} \tag{33}$$

Furthermore, similar to the argument of equation (24), we have

$$\begin{aligned}&\sum_{n=1}^{\infty} n^{-2}\ln^{\delta} nE\max_{1\leq k\leq n}\left\|\sum_{t=1}^{k}\sum_{i=-\infty}^{\infty} A_i\left(T_{n,t-i} - ET_{n,t-i}\right)\right\| \\ &\leq C\sum_{j\in\mathscr{B}}\sum_{l=1}^{\infty} E\left|X^{(j)}\right| I\left(l^{\alpha} < \left|X^{(j)}\right| \leq (l+1)^{\alpha}\right)\sum_{n=1}^{l} n^{-1}\ln^{\delta} n \\ &\leq C\sum_{j\in\mathscr{B}}\sum_{l=1}^{\infty}\ln^{\delta+1} lE\left|X^{(j)}\right| I\left(l^{\alpha} < \left|X^{(j)}\right| \leq (l+1)^{\alpha}\right) \\ &\leq C\sum_{j\in\mathscr{B}}\sum_{l=1}^{\infty} E\left|X^{(j)}\right|\ln^{\delta+1}\left(1 + \left|X^{(j)}\right|\right) I\left(l^{\alpha} < \left|X^{(j)}\right| \leq (l+1)^{\alpha}\right) \\ &\leq C\sum_{j\in\mathscr{B}} E\left|X^{(j)}\right|\ln^{\delta+1}\left(1 + \left|X^{(j)}\right|\right) I\left(\left|X^{(j)}\right| > 1\right) \\ &\leq C\sum_{j\in\mathscr{B}} E\left|X^{(j)}\right|\ln^{\delta+1}\left(1 + \left|X^{(j)}\right|\right) < \infty.\end{aligned} \tag{34}$$

Hence, by Lemma 1 and equations (22), (33), and (34), we can obtain equation (31). Following the proof of equation (20), we can also get equation (32) by equation (31). The proof is complete. □

Remark 3. Ko [23] proved the complete moment convergence for coordinatewise asymptotically almost negatively associated (CAANA) random vectors with $\alpha p = 1$ and $(1/2) < \alpha \leq 1$. However, as stated in Section 1, the meaningful case $\alpha = 1$ is wrongly proved. Note that Theorem 3 also works if $\alpha = p = 1$. Thus, Theorem 3 fills the vacancy and extends it to some more general settings. By Theorems 2 and 3, one can obtain the following strong law of large numbers for linear process of m-CNA random vectors with random coefficients.

Corollary 2. *Let $1 \leq p < 2$. Let $\{X_i, -\infty < i < \infty\}$ be a sequence of zero mean H-valued m-CNA random vectors*

coordinatewise weakly upper bounded by a random vector X with $\sum_{j\in\mathscr{B}} E|X^{(j)}|^p < \infty$ *if* $p > 1$ *or* $\sum_{j\in\mathscr{B}} E|X^{(j)}|ln(1+|X^{(j)}|) < \infty$ *if* $p = 1$. *Suppose that* $\{A_i, -\infty < i < \infty\}$ *is a sequence of random variables independent of* $\{X_i, -\infty < i < \infty\}$ *and* $E(\sum_{i=-\infty}^{\infty} A_i)^2 < \infty$. *Then, with probability 1,*

$$n^{(-1/p)}\left\|\sum_{t=1}^{k} Y_t\right\| \longrightarrow 0, \quad \text{as } n \longrightarrow \infty. \tag{35}$$

Proof. Let $\alpha = (1/p)$. It follows from equations (20) and (32) (with $\delta = 0$) that

$$\begin{aligned}\infty &> \sum_{n=1}^{\infty} n^{-1} P\left(\max_{1\le k\le n}\left\|\sum_{t=1}^{k} Y_t\right\| > \varepsilon n^{(1/p)}\right)\\ &= \sum_{l=0}^{\infty}\sum_{2^l\le n<2^{l+1}} n^{-1} P\left(\max_{1\le k\le n}\left\|\sum_{t=1}^{k} Y_t\right\| > \varepsilon n^{(1/p)}\right)\\ &\ge \frac{1}{2}\sum_{l=1}^{\infty} P\left(\max_{1\le k\le 2^l}\left\|\sum_{t=1}^{k} Y_t\right\| > 2^{(2/p)}\varepsilon\left(2^{l-1}\right)^{(1/p)}\right).\end{aligned} \tag{36}$$

By Borel–Cantelli lemma, the formula above implies that, as $l \longrightarrow \infty$, with probability 1,

$$\frac{1}{\left(2^{l-1}\right)^{(1/p)}}\max_{1\le k\le 2^l}\left\|\sum_{t=1}^{k} Y_t\right\| \longrightarrow 0. \tag{37}$$

Meanwhile, for any fixed n, there exists positive integer l such that $2^{l-1} \le n < 2^l$. Hence, with probability 1, one has

$$n^{-(1/p)}\left\|\sum_{t=1}^{k} Y_t\right\| \le \frac{1}{\left(2^{l-1}\right)^{(1/p)}}\max_{1\le k\le 2^l}\left\|\sum_{t=1}^{k} Y_t\right\| \longrightarrow 0. \tag{38}$$

□

4. Conclusion

In this study, the concept of m-CNA random vectors is introduced as a natural extension of CNA random vectors. The weak law of large numbers, complete convergence, and complete moment convergence for linear process of H-valued m-CNA random vectors with random coefficients are established. As a corollary of the complete convergence, the strong law of large numbers is also obtained. These results improve and generalise the corresponding ones of recent works such as Hien and Thanh [9], Huan et al. [18], Huan [20], Ko [21], and Ko [23].

However, there are still two open problems should be conquered. In specific, the Baum–Katz type theorem is only extended under the restriction $1 \le p < 2$; the first problem is that whether it is possible to release to $p \ge 2$? Another problem is whether the moment condition $\sum_{j\in\mathscr{B}} E|X^{(j)}|\ln(1+|X^{(j)}|) < \infty$ for the strong law of large numbers with $p = 1$ can be weakened to $\sum_{j\in\mathscr{B}} E|X^{(j)}| < \infty$?.

Data Availability

No data were used to support the findings of the study.

Conflicts of Interest

The author declares no conflicts of interest.

Acknowledgments

This work was supported by the Key Research Projects of Natural Science in Colleges and Universities of Anhui (KJ2020A0908) and the Key Research Projects of Natural Science of Wuhu Institute of Technology (Wzyzrzd202006).

References

[1] K. Joag-Dev and F. Proschan, "Negative association of random variables with applications," *The Annals of Statistics*, vol. 11, no. 1, pp. 286–295, 1983.

[2] T. K. Chandra and S. Ghosal, "Extensions of the strong law of large numbers of Marcinkiewicz and Zygmund for dependent variables," *Acta Mathematica Hungarica*, vol. 71, no. 4, pp. 327–336, 1996.

[3] T. C. Hu, C. Y. Chiang, and R. L. Taylor, "On complete convergence for arrays of rowwise m-negatively associated random variables," *Nonlinear Analysis: Theory, Methods and Applications*, vol. 71, no. 12, pp. 1075–1081, 2009.

[4] L. X. Zhang and X. Y. Wang, "Convergence rates in the strong laws of asymptotically negatively associated random fields," *Applied Mathematics-A Journal of China Universities, Series B*, vol. 14, no. 4, pp. 406–416, 1999.

[5] L. X. Zhang, "Strassen's law of the iterated logarithm for negatively associated random vectors," *Stochastic Processes and Their Applications*, vol. 95, no. 2, pp. 311–328, 2001.

[6] M. H. Ko, T. S. Kim, and K. H. Han, "A note on the almost sure convergence for dependent random variables in a Hilbert space," *Journal of Theoretical Probability*, vol. 22, pp. 506–513, 2009.

[7] Y. Miao, "Hajeck-renyi inequality for dependent random variables in Hilbert space and applications," *Revista De La Unión Matemática Argentina*, vol. 53, no. 1, pp. 101–112, 2012.

[8] L. V. Thanh, "On the almost sure convergence for dependent random vectors in Hilbert spaces," *Acta Mathematica Hungarica*, vol. 139, no. 3, pp. 276–285, 2013.

[9] N. T. T. Hien and L. V. Thanh, "On the weak laws of large numbers for sums of negatively associated random vectors in Hilbert spaces," *Statistics and Probability Letters*, vol. 107, pp. 236–245, 2015.

[10] J. T. Hu, G. X. Sui, X. X. Lv, and X. D. Li, "Fixed-time control of delayed neural networks with impulsive perturbations," *Nonlinear Analysis: Modelling and Control*, vol. 23, no. 6, pp. 904–920, 2018.

[11] X. D. Li, J. H. Shen, and R. Rakkiyappan, "Persistent impulsive effects on stability of functional differential equations with finite or infinite delay," *Applied Mathematics and Computation*, vol. 329, pp. 14–22, 2018.

[12] D. Yang, X. D. Li, J. H. Shen, and Z. J. Zhou, "State-dependent switching control of delayed switched systems with stable and unstable modes," *Mathematical Methods in the Applied Sciences*, vol. 41, no. 16, pp. 6968–6983, 2018.

[13] D. Yang, X. D. Li, and J. L. Qiu, "Output tracking control of delayed switched systems via state-dependent switching and dynamic output feedback," *Nonlinear Analysis: Hybrid Systems*, vol. 32, pp. 294–305, 2019.

[14] L. D. Fang, S. H. Ding, H. P. Ju, and L. Ma, "Adaptive fuzzy control for nontriangular stochastic high-order nonlinear

systems subject to asymmetric output constraints," *IEEE Transactions on Cybernetic*, 2020.

[15] L. D. Fang, S. H. Ding, H. P. Ju, and L. Ma, "Adaptive fuzzy control for stochastic high-order nonlinear systems with output constraints," *IEEE Transactions on Fuzzy Systems*, 2020.

[16] K. Q. Mei, L. Ma, Q. X. He, and S. H. Ding, "Finite-time controller design of multiple integrator nonlinear systems with input saturation," *Applied Mathematics and Computation*, vol. 372, Article ID 124986, 2020.

[17] J. H. Yuan, S. H. Ding, and K. Q. Mei, "Fixed-time SOSM controller design with output constraint," *Nonlinear Dynamics*, vol. 102, no. 3, pp. 1567–1583, 2020.

[18] N. V. Huan, N. V. Quang, and N. T. Thuan, "Baum-Katz type theorems for coordinatewise negatively associated random vectors in Hilbert spaces," *Acta Mathematica Hungarica*, vol. 144, no. 1, pp. 132–149, 2014.

[19] L. E. Baum and M. Katz, "Convergence rates in the law of large numbers," *Transactions of the American Mathematical Society*, vol. 120, pp. 108–123, 1965.

[20] N. V. Huan, "On complete convergence for sequences of random vectors in Hilbert spaces," *Acta Mathematica Hungarica*, vol. 147, no. 1, pp. 205–219, 2014.

[21] M. H. Ko, "The complete moment convergence for CNA random vectors in Hilbert spaces," *Journal of Inequalities and Applications*, vol. 2017, p. 290, 2017.

[22] X. Huang and Y. F. Wu, "Strong convergence theorems for coordinatewise negatively associated random vectors in Hilbert space," *Journal of Inequalities and Applications*, vol. 2018, p. 86, 2018.

[23] M. H. Ko, "On complete moment convergence for CAANA random vectors in Hilbert spaces," *Statistics and Probability Letters*, vol. 138, pp. 104–110, 2018.

[24] A. Shen, Y. Zhang, B. Xiao, and A. Volodin, "Moment inequalities for m-negatively associated random variables and their applications," *Statistical Papers*, vol. 58, no. 3, pp. 911–928, 2017.

[25] A. Kuczmaszewska, "On complete convergence in Marcinkiewicz-Zygmund type SLLN for negatively associated random variables," *Acta Mathematica Hungarica*, vol. 128, pp. 116–130, 2010.

[26] S. H. Sung, "Moment inequalities and complete moment convergence," *Journal of Inequalities and Applications*, vol. 2009, Article ID 271265, 2009.

Hindawi
Complexity
Volume 2021, Article ID 6295003, 12 pages
https://doi.org/10.1155/2021/6295003

Research Article

Evaluation of College Students' Emergency Response Capability Based on Questionnaire-TOPSIS Innovative Algorithm

Yanyan Liu,[1] **Wei Zhou**,[2] **and Yang Song**[2]

[1]*College of Environmental Science & Engineering, Qingdao University, Qingdao 266071, China*
[2]*Department of Student Affairs, Qingdao University, Qingdao 266071, China*

Correspondence should be addressed to Yanyan Liu; lyyfighting@126.com and Wei Zhou; jeoway@163.com

Received 11 May 2021; Accepted 24 June 2021; Published 6 July 2021

Academic Editor: Xiaodi Li

With the development of our society, the diversity of the university environment has been increased. The complexity of the diversified university environment also greatly increases the frequency of campus crisis incidents. Therefore, how to evaluate the emergency response ability of college students and how to take effective response measures have become problems that need urgent attentions. In this study, the evaluation of college students' emergency response capability based on the questionnaire-TOPSIS innovative algorithm is conducted. Firstly, the questionnaire method is used to analyze the current situation of college students' ability of emergency response, and then a comprehensive evaluation is made using the TOPSIS innovative algorithm. The results of the ranking of emergency response ability are as follows: excellent > good > undergraduate > graduate > inferior. Secondly, the reasons for the lack of ability of emergency response to students based on the evaluation results are studied intensively. Finally, the development countermeasures for college students' emergency response ability training are put forward.

1. Introduction

What is the campus crisis? The general understanding of the term "crisis" is danger, which makes our physical and psychological health or surrounding environment suffer devastating damage. However, we often ignore its deep meaning, where danger and opportunity coexist. In this way, the understanding of "crisis" is as follows: the combination of factors leads to the occurrence of certain events and situations, these events are harmful to the existence of individuals or groups, and people cannot use conventional methods and ways to solve them in a short period of time. To a certain extent, crisis puts people in a state of high pressure disintegration, and it drives people to make choices and take action to solve crisis in a state of near-collapse. It is the test of comprehensive ability and comprehensive quality of decision-maker, manager, and the parties [1]. As a kind of crisis, campus crisis has the universal definition of crisis, but it also has its special connotation. It is defined as some events that happen suddenly, which will seriously damage the personal and property safety of students and teachers, and these events occur during normal teaching time, teaching order, and the condition of the school managers, teachers, and students without any precautions [2, 3].

It has the characteristics of the special regional property, the directivity of the subject, and social concern. At the same time, the university campus crisis is different from the crisis of primary and junior high school campuses. Its dissemination and diffusion are faster and stronger, and it is similar to social security incidents and rule of law incidents.

Campus crises generally include the following types: natural disasters (floods, fires, wind storms, earthquakes, and so on), public safety (accidental injuries to public facilities, collapses of buildings, accidental injuries of sports equipment and experimental items, and so on), teacher-student conflicts (correctional conflicts, corporal punishment, and so on), campus violence (bullying, verbal abuse, and physical repression), campus crime (intimidation and extortion, fights, thefts, sexual harassment, sexual crimes, and so on), campus self-harm (self-harm and suicide), cyber-social networking crises (campus online loan, fraud of online part-time job, online appointments to fight, and so on),

occasional accident disasters (crowded stampede and traffic accident disaster), and various crises from external interference (demonstrations and gangster loan intervention) [4–6].

The risk of these campus crises always exists, such as campus violence against freshmen by four senior members of the judo department at Tenri University in Japan in May 2013, a stabbing incident at the University of Texas, USA, in May 2017, the shocking Collin Wiant incident at Ohio University in November 2018, and a student of Jinan University committed suicide in the dormitory on March 6, 2021. These individual crisis events have a high incidence in campus crisis events. Meanwhile, group crisis events also occur from time to time, such as violent protests at the University of California, Berkeley, United States, in February 2017. Henan University of Technology had a food poisoning incident with nearly 100 students in September 2020. And these group crisis events are more reflective of the inadequacy of administrators.

Therefore, in the face of many campus crises, in addition to avoiding the occurrence of crisis events from the root causes, carrying out a scientific evaluation of the emergency response ability of contemporary college students and putting forward effective emergency response measures have become an urgent work in today's colleges and universities.

2. Evaluation of the Emergency Response Capacity of College Students' Current Situation

2.1. Evaluation Methodology. Questionnaire Method. First, data are collected through the questionnaire method. The questionnaire consists of 20 selection questions and 2 short descriptions, which are divided into four aspects: knowledge of handling representative emergencies, access to emergency knowledge, attention to emergency knowledge, and learning desire. The questionnaire method is a statistical-based approach to processing data and obtaining laws; however, it cannot eliminate the effects of different measures; it cannot evaluate the event as a whole and draw conclusions.

TOPSIS Method. TOPSIS method is a kind of close-up ideal solution of the multiobjective decision analysis of limited scheme, also known as the distance method of good and bad solution. It is a comprehensive method of evaluating distance and does not require or limit the sample size of the evaluation object, the number of indicators, and the distribution of data. It can eliminate the impact of different evaluation indicators through the same trend and normalization treatment [7–10]. The TOPSIS method determines the optimal scheme and the worst scheme in the evaluation object by standardizing the raw data matrix. Based on the determined optimal scheme and the worst scheme, the distances between the evaluation object and the optimal scheme as well as the object and the worst scheme are calculated, respectively. These distances are used to determine how close different evaluation objects are to the optimal solution [11–15]. At the same time, all evaluation objects can be sorted according to the size of the proximity between each evaluation object and the optimal scheme, so that the evaluation object can be evaluated comprehensively [16, 17].

This study combines the two methods effectively. The questionnaire method is used to analyze the current situation of college students' ability of emergency response, which objectively reflects the value of various indicators in this research and makes an evaluation of the results. On this basis, we make a comprehensive evaluation of the current situation of emergency response ability of graduate and undergraduate students based on the TOPSIS method. The effective combination of questionnaire and the innovative algorithm of TOPSIS can make the evaluation method more scientific and the evaluation results closer to reality. This combination can provide a more valuable reference for taking targeted measures.

2.2. Analysis of the Individual Index of Emergency Response Ability of College Students Based on Questionnaire Method. In order to understand the current situation of the emergency response ability of college students, we randomly select undergraduates and graduate students for all grades in different majors to investigate, respectively. The number of graduate students is 1000, and the number of undergraduates is 3000. The survey is conducted in the form of a questionnaire. The questionnaire consists of 20 selection questions and 2 short descriptions, which are divided into four aspects: knowledge of handling representative emergencies, access to emergency knowledge, attention to emergency knowledge, and learning desire. The results of the survey are shown in Figure 1.

As shown in Figure 1, for the overall student group's understanding of the identification of basic risk factors, accident emergency management, disaster escape techniques, and the other related knowledge, the pass rate is only 47%. Most of the students for emergency knowledge are in a state of half-understanding. This fully reflects the current situation that most of the students in contemporary colleges and universities are short of the emergency knowledge. Some college students lack initiative and enthusiasm for the emergency drills organized by the school and various emergencies of the popular knowledge lecture. The emergency knowledge education work of most colleges and universities stays on the surface. The various reasons lead to the low pass rate. Graduate students have a lower pass rate than undergraduates, which may be due to the high pressure of postgraduate studies. They do not have enough time for emergency knowledge intake. This also reflects that highly educated personnel emergency knowledge is seriously inadequate, and this is a group that is easily ignored and risky.

According to Figure 2, 57% of students do not go through the professional study of emergency knowledge, which is closely related to the lack of attention given to emergency education by schools and families. Only 5% of students can be carried out in practice, which reflects the problem that even if we have mastered some theoretical knowledge, it has not been put into practice. At present, the

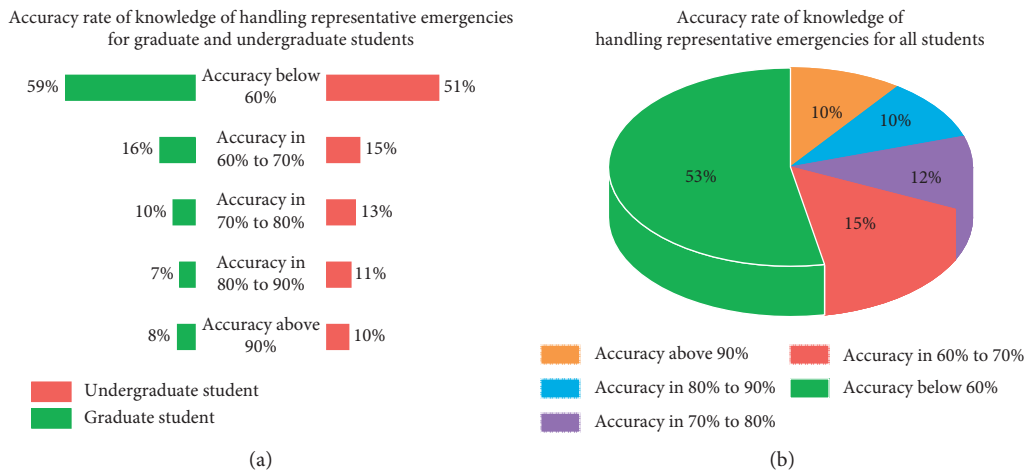

Figure 1: Accuracy rate of knowledge of handling representative emergencies.

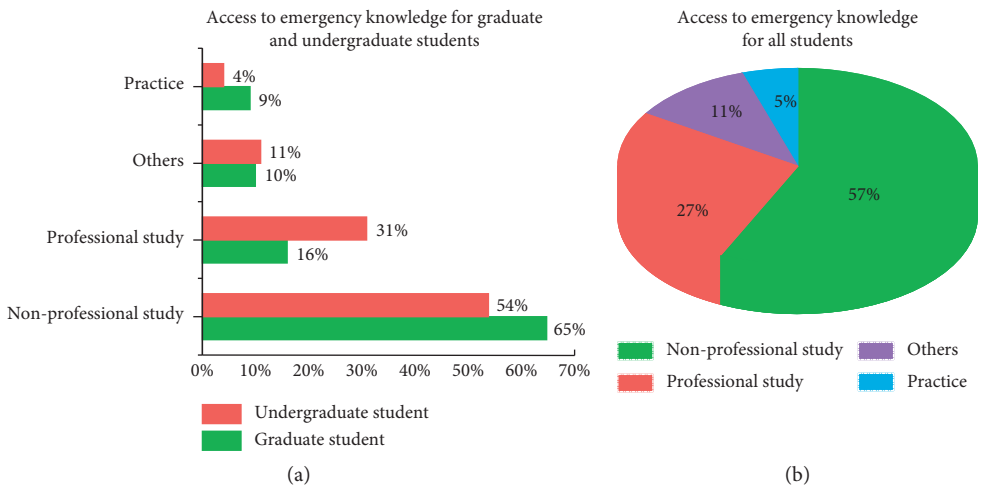

Figure 2: Access to emergency knowledge.

formalization of the emergency drill in schools and the low subjective willingness of students to participate in the emergency drill will lead to the phenomenon of "armchair strategy."

According to Figures 3 and 4, the survey found that 91% of people showed concern about handling methods of the basic response to emergency situations and 66% of students are willing to consciously receive emergency education. This shows that college students are easy to accept and spread new things. It means that improving the knowledge of a college student's campus crisis with emergency education is effective. By comparing the attention of the graduate student group's concern with the undergraduate group's concern for emergency knowledge and the data of whether the graduate student group is willing to receive emergency education, it can be seen that the graduate student group is more concerned about the emergency knowledge and the willingness to accept emergency education is better. This indicates that the graduate group has a strong sense of concern and acceptance desire for emergency education.

In general, the analysis of the individual index of college students' emergency ability based on questionnaire method shows the following. (1) Students' storage of emergency theoretical knowledge is insufficient, and the level of emergency ability is low. (2) Students are unable to combine the small amount of theoretical knowledge they have with actual operation to reach the level of proficient application. The above problems can lead to the occurrence of a crisis. Even if students have certain emergency capacity, the impact of the burning mentality will lead to the loss of reason. This makes it difficult for students to calm response and correct solution to the crisis. In general, the overall emergency response capacity is seriously lacking, which is similar to previous studies. At the same time, we can see that the performance levels of the graduate student group and undergraduate group are different in the four aspects of the questionnaire. Its awareness and ability to deal with crisis events are uneven. A single index analysis can reflect the relative high and low value of the indicators in this study but cannot comprehensively evaluate the emergency ability of

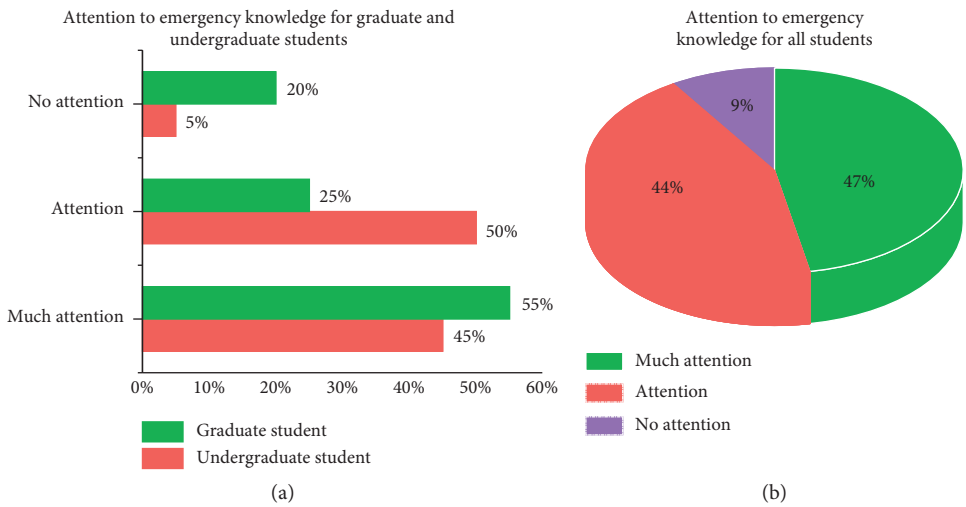

Figure 3: Attention to emergency knowledge.

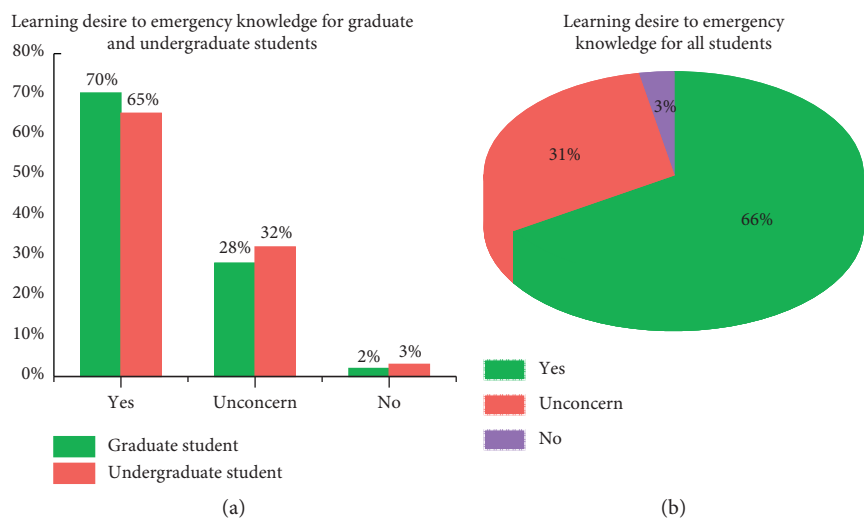

Figure 4: Learning desire to emergency knowledge.

college students and scientific judgment of the different levels of college students' emergency ability.

2.3. Comprehensive Evaluation of the Emergency Ability of College Students Based on TOPSIS. Based on the results of the single index analysis of the abovementioned survey statistical methods, this study uses the TOPSIS method to carry out the comprehensive evaluation of the emergency response capacity of college students.

2.3.1. TOPSIS Method Principle. The development of evaluation models offers the possibility to solve a number of scientific problems [18–26]. Chen et al. [27] first proposed the TOPSIS model, and they evaluated the advantages and disadvantages of the decision-making unit by establishing positive and negative ideal solutions and using the parameters of each decision unit in the actual problem and the relative distance of the two solutions. The best solution was to minimize the distance between positive and ideal solution and to maximize the distance between the maximization and negative ideal solution. Kacprzak [28] used sequential preference techniques to sort the ideal solution based on ordered fuzzy numbers and sort and evaluate the alternatives for group decisions. Zhang et al. [29] solved the multicriterion decision-making problem in fuzzy-covering approximate space by the TOPSIS method, i.e., selecting the most suitable material in a variety of bionanomaterials with similar properties. Wu et al. [30] proposed a new method of rock mass classification based on MCS and TOPSIS. Oenuet Soner [31] proposed waste management sites using fuzzy TOPSIS (by combining sequential preference techniques with the desired solution) and AHP (hierarchical analysis) techniques. A new group multicriteria language decision for group multicriteria language decision-making was proposed by Ou et al. [32], which was inspired by the preference level between the TOPSIS method and the two hesitant fuzzy language term sets (HFLTSs). Shi [33] and others used the

TOPSIS method to evaluate the quality of care in the operating room. Li and Lei [34] made a comprehensive evaluation of the low-carbon economic development of China's subprovinces based on the TOPSIS model combined with the entropy method. In this study, the TOPSIS method is used to evaluate the emergency response capacity of college students, and the specific calculation method is as follows [34, 35]:

(1) Assimilation for indicator value is as follows:

$$x_{ij}' = \begin{cases} x_{ij}, & \text{high} - \text{class excellent indicator}, \\ \dfrac{1}{x_{ij}}, & \text{low} - \text{class excellent indicator}, \\ \dfrac{M}{\left[M + \left|x_{ij} - M\right|\right]}, & \text{medium} - \text{class excellent indicator}, \end{cases} \quad i = 1, 2, \ldots, n;\ j = 1, 2, 3, \ldots, m, \tag{1}$$

where x_{ij} denotes indicator value of j indicator for i type student. M is the ideal value of indicator.

(2) Data normalization is as follows:

$$Z_{ij} = \begin{cases} \dfrac{x_{ij}}{\sqrt{\sum_{i=1}^{n}\left(x_{ij}\right)^2}}, & (\text{original high} - \text{class excellent indicator}), \\ \dfrac{x_{ij}'}{\sqrt{\sum_{i=1}^{n}\left(x_{ij}'\right)^2}}, & (\text{original low or medium} - \text{class excellent indicator}). \end{cases} \tag{2}$$

(3) Determination for the best and the worst scheme is as follows:

$$\begin{aligned} Z^+ &= \left(X_1, X_2, X_3, \ldots\right), \\ Z^- &= \left(Y_1, Y_2, Y_3, \ldots\right). \end{aligned} \tag{3}$$

(4) Euclidean distance between indicator and best/worst scheme is as follows:

$$\begin{aligned} D_i^+ &= \sqrt{\left(Z_{ij} - Z_j^+\right)^2}, \\ D_i^- &= \sqrt{\left(Z_{ij} - {}^{j}_{Z}\right)^2}. \end{aligned} \tag{4}$$

(5) Approaching degree of evaluation object to the best scheme is as follows:

$$C_i = \frac{D_i^-}{D_i^+ + D_i^-}, \quad 0 \le C_i \le 1. \tag{5}$$

(6) The closer that C_i is to 1, the better the object is.

2.3.2. TOPSIS Method Evaluation Results. Based on the emergency situation and TOPSIS model method, the emergency response capacity of graduate students and undergraduates is evaluated. Four indexes such as the correct rate of emergency response, the way to obtain emergency knowledge, the attention to emergency knowledge, and the desire to learn were investigated. High-quality detailed indicators include the correct rate is more than 90%, teaching in classroom, practical operation, very concerned, and willing percent in graduate and undergraduate students, respectively. Neutral detailed indicators include the percentage of graduate and undergraduate students which is 90% to 60% of the correct rate, and the other way and general attention are in the proportion of graduate and undergraduate students, respectively. Low-quality detailed indicators include the percentage of graduate and undergraduate students below 60% of the correct rate, no professional study, no concern, no want, and no willing, respectively. The original indicator value matrix is shown in Table 1. The homogenized naturalized matrix is treated as shown in Table 2. The best and worst vectors calculated are shown in Table 3.

According to the formula, the Euclidean distance and C value of each evaluation index and the optimal and inferior vector are calculated and sorted, as shown in Table 4.

As shown in Table 4, the results for the ranking of emergency response capacity comprehensive evaluation are as follows: excellent > good > undergraduates > graduate students > inferior. Undergraduates have better emergency response capacity than graduate students. On the whole,

Table 1: Evaluation of students' emergency ability initial index value.

Index	Accuracy rate of emergency incident handling knowledge					Access to emergency knowledge				Focus on emergency knowledge			Learning aspirations		
Indicators	Over 90% (%)	90%~80% (%)	80%~70% (%)	70%~60% (%)	Below 60% (%)	Class study (%)	Actual operating (%)	Other ways (%)	No professional study (%)	Very concerned (%)	General concerns (%)	Indifference (%)	Willing (%)	Unwilling (%)	Indifference (%)
Graduate	8	7	10	16	59	16	9	10	65	55	25	20	70	2	28
Undergraduate	10	11	13	15	51	31	4	11	54	45	50	5	65	3	32
Excellent	70	10	5	3	2	46	46	5	3	80	15	5	90	5	5
Good	60	11	8	3	8	37	37	10	16	70	17	13	80	10	10
Inferior	30	12	10	3	45	20	20	11	49	30	20	50	40	30	30

Table 2: Normalized results of the same trending process.

Index	Accuracy rate of emergency incident handling knowledge					Access to emergency knowledge				Focus on emergency knowledge			Learning aspirations		
Indicators	Over 90% (%)	90%~80% (%)	80%~70% (%)	70%~60% (%)	Below 60% (%)	Class study (%)	Actual operating (%)	Other ways (%)	No professional study (%)	Very concerned (%)	General concerns (%)	Indifference (%)	Willing (%)	Unwilling (%)	Indifference (%)
Graduate	0.0719	0.3571	0.4481	0.1069	0.0328	0.2240	0.1426	0.4940	0.0452	0.4188	0.3861	0.1678	0.4407	0.7788	0.1546
Undergraduate	0.0899	0.4869	0.3447	0.1141	0.0380	0.4340	0.0634	0.4491	0.0544	0.3426	0.1931	0.6711	0.4093	0.5192	0.1353
Excellent	0.7195	0.4463	0.4073	0.5703	0.9680	0.6440	0.7290	0.3294	0.9786	0.6091	0.5081	0.6711	0.5667	0.3115	0.8658
Good	0.6295	0.4869	0.5601	0.5703	0.2420	0.5180	0.5863	0.4940	0.1835	0.5330	0.5679	0.2581	0.5037	0.1558	0.4329
Inferior	0.2698	0.4463	0.4481	0.5703	0.0430	0.2800	0.3169	0.4491	0.0599	0.2284	0.4827	0.0671	0.2519	0.0519	0.1443

Table 3: The best and worst vectors calculated based on the emergency situation and the TOPSIS model method.

Name of vectors	Concrete vector
The best vectors calculated	$Z_j^+ = (0.7195, 0.4869, 0.5601, 0.5703, 0.9680, 0.6440, 0.7290, 0.4940, 0.9786, 0.6091, 0.5679, 0.6711, 0.5667, 0.7788, 0.8658)$
The worst vectors calculated	$Z_j^- = (0.0719, 0.3571, 0.3447, 0.1069, 00328, 0.2240, 0.0634, 0.3294, 0.0452, 0.2284, 0.3861, 0.0671, 0.2519, 0.0519, 0.1353)$

Table 4: C value of students' emergency ability and the result of ranking emergency ability.

Type of student	D^+	D^-	C	Sort results
Graduate	1.9426	0.8092	0.2941	4
Undergraduate	1.9226	0.8566	0.3082	3
Excellent	0.5235	2.0290	0.7949	1
Good	1.3998	1.1451	0.4500	2
Inferior	1.9711	0.6454	0.2467	5

graduate students and undergraduates have inferior emergency response capacity, both between good and inferior. Therefore, an in-depth analysis of the reasons for the lack of emergency response capacity and putting forward reasonable countermeasures become an urgent problem to be solved.

3. Reason Analysis of Lack of Students' Emergency Response Ability

Combining the realistic performance of college students in the campus crisis and evaluation results above, all the results reflect the serious lack of emergency ability of college students. There are three main reasons for this phenomenon.

3.1. Impact of Social Environment and Thought. The advent of information age, while promoting social progress, has brought advanced Internet information technology, so that contemporary students have more access to the dissemination of information. This makes the students' leisure life more colorful, broadens the knowledge level and the circle of friends, increases the insight, and broadens the horizon. However, everything has two sides; with the rapid iterative update of information, a large number of redundant information impact on the students' thinking so that their ability to identify has been reduced. At this time, some bad ideas take the opportunity to confuse their cognition, subtly change their thoughts and ideas, and thus lose themselves. Especially for junior undergraduates, because of their strong curiosity and no complicated academic burden, they are vulnerable to the influence of bad ideas and easy to set up the wrong moral values and ideas.

3.2. Backwardness of the Management Concept and System of Colleges and Universities. For students, the environment is wrapped in layers. Its level from outside is social-campus-family-self. And this environment leads to the lack of emergency capacity of students. In addition to social impact, the second reason should be attributed to the school. It is understood that as of August 2017, only 150 of China's 2,879 colleges and universities have opened safety engineering programs. And there are only a few colleges and universities that offer public safety emergency courses such as escape and self-rescue and emergency rescue overview [36]. The lack of safety education in colleges and universities is a major reason for the lack of students' emergency knowledge. Most of the ways for students to obtain emergency knowledge come from teaching in classroom and family education. However, there are few systematic education systems and prevention systems for campus crisis in colleges and universities. Failure to take effective measures to prevent and block the occurrence of crises from the root causes has led to frequent campus crises events. In addition, colleges and universities have not perfected the corresponding emergency response system so that the crisis cannot be quickly contained. And it is difficult to obtain timely redress in the aftermath of a crisis. It cannot be stopped in time, resulting in the crisis causing adverse effects and sequelae. The occurrence of a campus crisis has caused some impact and change on the concept and thought of college teachers and students, and to a certain extent, it affects the stability and atmosphere of the campus environment.

3.3. Lack of Awareness among College Students. For both undergraduate and graduate students, they have been educated for more than a decade before entering the university campus. The educational experience has made them form an independent thought, ideas, and unique character. However, these thought and ideas have the nature of "ivory tower," which has a certain degree of immaturity and simplicity relative to the complex social environment. Like the "barrel principle," this immaturity would immediately playout when an emergency is encountered as a shortboard effect. This can lead to a situation where the student's mentality and reason suffered shock, collapse, and a tragic event caused by confused thinking or impulsivity. In addition, even if the students still have rational existence, they are mostly teenagers who grow up in care, lack of experience, and ability to be independent. Moreover, students lack practical operation in ordinary times, so they can only passively accept the damage caused by the crisis.

4. College Students' Emergency Capacity Training Countermeasures

4.1. Improve Corresponding Rules and Regulations and Promote the Construction of a Safety Education System. First of all, if the corresponding rules and regulations are not formulated, there will be no rules to follow. The rules and regulations protect teachers and students before a crisis

occurs. It regulates the behavior of teachers and students on campus to prevent the occurrence of crises and isolate the incentives that cause them. The rules and regulations are "guide signs" to guide the right direction in the chaos when a crisis occurs. It ensures that the most basic remedial measures are carried out in an orderly manner and to avoid greater harm caused by the chaos and disorder of the scene. Schools should formulate corresponding campus regulations and emergency plans to provide scientific, correct, and powerful theoretical basis and methods for responding to campus crisis events [37]. Through daily compliance and learning, students form daily habits and clear cognition so as to reduce the occurrence of crisis events and improve students' ability to respond to crisis events.

Universities should establish a systematic and safe campus education system. Teachers infiltrate crisis education in daily classroom teaching and convey concepts such as personal safety, traffic safety, and social safety to students. In this way, students are guided to gradually form their own unique sense of sensitivity, perceive from different angles and details, and discover potential crisis information in the campus environment. It is necessary to learn to further identify the importance and credibility of information and master the focus of information. The student's crisis early warning ability should be cultivated. For example, the campus loan incidents have a serious impact. For students who intend to participate in campus loans, most of them participate because of unexpected events in their lives and urgent need for money. They often have many abnormal behaviors in their daily lives. If the students around them can find these details and signals in time, understand their psychological thoughts, convey the harm of the relevant events, and temporarily stabilize their emotions through communication, more time to report to the counselor would be gained and problem can be solved. If students have certain early warning capabilities, they can perceive the advent of a crisis and respond in a timely manner based on the signs that appear. Schools can prepare corresponding campus safety manuals based on school conditions, which can be used as written textbooks for safety education and used in safety education classroom teaching [38, 39]. The manual should guide students to identify the content and nature of crises, familiarize themselves with the basic measures and methods of crisis handling, strengthen students' ability to develop basic rapid response, prevention, and early warning capabilities, and master certain risk control skills to achieve the basis of grasping crisis-related theoretical knowledge. It allows students to make scientific and decisive decisions based on crisis information and play an effective role in intervention. Of course, it is still difficult to solve the crisis by relying on the ability of the student group alone. Through daily safety education, the connection between the school and the students can be established so as to achieve the goal of communication and order and establish a complete campus crisis management system. After a campus emergency, under the complete information management system, students can obey the school's unified deployment and the school's official information release. And students can achieve correct information, abandon false information, cooperate with the school to control the development of the situation, and do their best to cooperate with the school to deal with campus safety incidents.

4.2. Implement Simulations to Examine Students' Emergency Response Capabilities. The previous survey results also reflect a phenomenon as follows: even if students have a certain theoretical foundation, they cannot apply this knowledge to practice, which is basically a matter of fact. Therefore, while the school promotes safety education into the classroom, it should also conduct regular practical exercises for students to achieve the dual purpose of reviewing theoretical knowledge and testing emergency response capabilities.

The school can formulate corresponding simulation training in combination with the safety manual prepared. It can also formulate various campus emergencies that may occur in combination with the actual school situation and regularly lead students to train in different real scenarios in groups, as a form of reviewing safety education. After the drill, a group summary will be conducted, and the teachers and students will understand the specific situation and the safety education required at each stage through the summary. Through simulation training, students who combine theory with practice can skillfully use various processing methods, and their psychological endurance has been improved to a certain extent. Finally, theoretical knowledge, actual combat exercises, and psychological ability are perfected.

Daily training ensures that students are proficient in the application of theoretical knowledge. However, campus safety incidents are uncertain and always dynamic. Although corresponding emergency plans have been formulated, they must be applied and changed flexibly in the actual process. This requires students to break the formulation of fixed theories on the basis of mastering the basic processing methods and completes the process of "decomposing old theories-assembling new theories" in conjunction with specific events. The handling of crisis events is targeted and planned. Students can adjust and respond calmly at any time according to the complete emergency plan established by themselves and finally reach the level of strategic planning.

4.3. Innovative Ways to Guide Psychological Counseling and Adjust Students' Recovery Ability. The entire process of "preliminary brewing-intense occurrence-calming down" of emergencies swept across the entire campus like a typhoon, causing varying degrees of a psychological and physical shock to students. Symptoms such as anxiety and panic may occur. Although daily safety education includes psychological construction, it is all preconstruction before the crisis. There are certain individual differences between different students. This difference includes both the appearance of different preconstruction effects and the postcrisis psychological changes. The daily psychological quality education of the school is designed according to the commonality of students, but the personality part of each person is not involved. And the traditional classroom education model

cannot realize the systematic psychological guidance of each student. So, this requires the school to establish a cloud database based on the school's situation with the help of the Internet platform while carrying out the traditional classroom psychological quality education and mental health education. Under the guidance of professional psychologists, we summarize and sort out existing psychological counseling methods and establish multiple sets of psychological adjustment models. And it is updated and maintained constantly according to the occurrence of subsequent crisis events. Each student has his own independent account and conducts regular psychological questions and answers. He can open his heart to the maximum and accept the most systematic psychological guidance in a relatively hidden environment whether in daily campus life or when suffering a major psychological impact. Under the premise of ensuring the privacy of students, professional teachers analyze the background data, conduct face-to-face conversations with individual serious students, and follow up on the students' psychological conditions in time. This psychological guidance system that combines the traditional classroom model and the innovative network model can realize the school's comprehensive psychological quality education for students to the greatest extent. It can also seamlessly connect the psychological construction of students before and after the crisis, improve students' psychological endurance and self-healing ability, guide students to sum up, and increase the experience of self. To a certain extent, it can also ensure that students' psychology is always in a healthy state so as to avoid some campus safety incidents caused by individual students' psychological problems.

4.4. Accurately Implement Policies Based on the Characteristics of Students and Focus on Targeting. Based on the characteristics of undergraduates and graduate students, the cultivation of their emergency response capabilities should be guided by the circumstances and be implemented precisely. Graduate students have high academic qualifications, and their educational experience makes them pay more attention to emergency knowledge and they are willing to receive emergency education. However, their education stage has caused them not have enough time to learn and understand seriously and carefully the knowledge about campus crisis events. Based on the current situation of graduate students, it is necessary to explore efficient and effective ways for the graduate students to acquire knowledge and capabilities about campus crises. The role of mass media and the Internet in popularizing emergency knowledge can be utilized to enable graduate students to quickly improve themselves processing power in crisis events.

Undergraduates' attention to emergency knowledge and willingness to receive emergency education are not as high as those of graduate students, which may be related to the current emergency education mode. It is because of the lack of education on emergency disaster prevention and first aid skills in colleges and universities. In response to this, student crisis education should be included in the normal education plan of school education. Student crisis education becomes a required course for students in universities and colleges, making it linked to student credits, and passing this method forces college students to learn emergency knowledge. And, this further arouses students' disgust; this is mainly because emergency education in most colleges and universities is mostly traditional classroom theory teaching, which is less attractive to students. Firstly, in order to arouse students' interest, the mode of emergency education can be changed to a practical form so that students can personally operate emergency facilities to master their use. By enhancing students' hands-on ability and strengthening their psychological quality, they can achieve better "achievements" in the "actual combat" of the campus crisis. Schools should improve students' interest and enthusiasm by optimizing the classroom form of crisis education. Secondly, teachers should improve their personal charm. Teachers should continuously improve their knowledge while spreading knowledge to students. Through ordinary observation, we can find that teachers who are witty, humorous, and knowledgeable are more likely to be welcomed by students so as to get a better classroom experience, and students will be more serious.

5. Conclusions

In summary, this research gained insight into the evaluation of college students' emergency response capability based on the questionnaire-TOPSIS innovative algorithm. Firstly, the questionnaire method was used to analyze the current situation of college students' ability of emergency response, and then a comprehensive evaluation was made using the TOPSIS innovative algorithm. The results of the investigation and statistical analysis show that students have a relatively scarce store of emergency response theory knowledge and a low level of emergency response capability. Students are unable to combine the small amount of theoretical knowledge they have with actual operation to reach the level of proficient application. Even though college students have a certain emergency response ability, the impact of anxious mentality will cause a loss of calmly respond and correctly resolve the crisis. The TOPSIS comprehensive evaluation results are excellent > good > undergraduate > graduate > inferior. The emergency response ability of undergraduates is better than that of graduate students, but in general, the emergency response ability of graduates and undergraduates is inferior, and both are between good and inferior. Therefore, an in-depth analysis of the reasons for the lack of emergency response capabilities and reasonable countermeasures has become problems that need to be resolved.

This study focused on the influence of educational background on students' emergency response ability. In contrast, emergency response ability is influenced by numerous factors, such as students' own gender, age, personality, physical condition, school, and social environment. Blair et al. [40] studied the safety beliefs and behaviors of Midwestern college students in the United States and found that female students had stronger safety beliefs and behaviors than male students of the same age. And, Liu et al.

[41] studied the level of emergency knowledge of college students and found that there were significant differences in college students' emergency abilities with respect to age. In addition, family education also has an important influence on students' emergency response ability. Scientific and reasonable family education is the key of students' healthy growth and the formation of a sound personality. The influence of these influencing factors on emergency response ability is obvious but not studied in this study, and further research can be conducted on the influence of various influencing factors on students' emergency response ability.

College students' emergency response capabilities should be further improved for the campus crisis which is widespread nowadays. Under the traditional Chinese education model, students' educational experience before entering university is passive. To a certain extent, their minds are not yet matured. It is unrealistic to rely on their own strength to improve their emergency response capabilities. This requires colleges and universities to follow the half-open mode of education and establish a "precrisis knowledge education and psychological construction-systematic guidance, stable mentality maintainability during the crisis, and postcrisis psychological counseling and summary error correction" chain-style campus security incident handling system in view of the three states of campus safety incidents (before, during, and after). Through "system construction + simulation + psychological counseling + precise policy implementation," the students' ability of comprehensive emergency response will gradually improve, the incidence of campus safety incidents will gradually decrease, and the loss of campus after the crisis will gradually reduce.

Data Availability

The data used to support this study are included within the manuscript.

Conflicts of Interest

The authors declare that they have no conflicts of interest.

References

[1] M. Jian, *Innovative Strategies Crisis Management for Universities: Realistic Choice of the Stability of the Higher Institutions*, China Procuratorial Press, Beijing, China, 2007.

[2] J. Mastrodicasa, "Technology use in campus crisis," *New Directions for Student Services*, vol. 2008, no. 124, pp. 37–53, 2010.

[3] M. Shaw, "Teaching campus crisis management through case studies: moving between theory and practice," *Journal of Student Affairs Research and Practice*, vol. 55, no. 1, pp. 1–14, 2018.

[4] J. L. Christina, "College of the overwhelmed: the campus mental health crisis and what to do about it," *Journal of the American Academy of Child & Adolescent Psychiatry*, vol. 44, no. 12, pp. 1317-1318, 2005.

[5] M. Kennedy, *Crisis on Campus*, Vol. 79, MIT Press, Cambridge, MA, USA, 2007.

[6] R. Eaker and J. Viars, "Campus crisis response at Viberg college," *Journal of Cases in Educational Leadership*, vol. 17, no. 4, pp. 86–95, 2014.

[7] H. Deng, C.-H. Yeh, and R. J. Willis, "Inter-company comparison using modified TOPSIS with objective weights," *Computers & Operations Research*, vol. 27, no. 10, pp. 963–973, 2000.

[8] J. Cheng, W. Zhang, H. Yang, X. Su, T. Ma, and X. Chen, "A seed-expanding method based on TOPSIS for community detection in complex networks," *Complexity*, vol. 2020, Article ID 9017239, 14 pages, 2020.

[9] M. S. Yang, Z. Hussain, and M. Ali, "Belief and plausibility measures on intuitionistic fuzzy sets with construction of belief-plausibility TOPSIS," *Complexity*, vol. 2020, Article ID 7849686, 12 pages, 2020.

[10] W. Zhang, X. Zhang, F. Liu, Y. Huang, and Y. Xie, "Evaluation of the urban low-carbon sustainable development capability based on the TOPSIS-BP neural network and grey relational analysis," *Complexity*, vol. 2020, Article ID 6616988, 16 pages, 2020.

[11] Y.-J. Lai, T.-Y. Liu, and C.-L. Hwang, "TOPSIS for MODM," *European Journal of Operational Research*, vol. 76, no. 3, pp. 486–500, 1994.

[12] M. Behzadian, S. Khanmohammadi Otaghsara, and J. Ignatius, "A state-of the-art survey of TOPSIS applications," *Expert Systems with Applications*, vol. 39, no. 17, pp. 13051–13069, 2012.

[13] D. L. Olson, "Comparison of weights in TOPSIS models," *Mathematical & Computer Modelling*, vol. 40, no. 7-8, pp. 721–727, 2004.

[14] X. B. Liu, Y. J. Zhang, and W. K. Cui, "Development assessment of higher education system based on TOPSIS-entropy, hopfield neural network, and cobweb model," *Complexity*, vol. 2021, Article ID 5520030, 11 pages, 2021.

[15] M. Lin, C. Huang, and Z. Xu, "TOPSIS method based on correlation coefficient and entropy measure for linguistic pythagorean fuzzy sets and its application to multiple attribute decision making," *Complexity*, vol. 2019, Article ID 6967390, 16 pages, 2019.

[16] C. Mao, "Research on university campus crisis and countermeasures," *Technology and Economic Guide*, vol. 35, 2016.

[17] H. S. Shih, H. J. Shyur, and E. S. Lee, "An extension of TOPSIS for group decision making," *Mathematical & Computer Modelling*, vol. 45, no. 7-8, pp. 801–813, 2007.

[18] X. Liu and H. Yu, "Continuous adaptive integral-type sliding mode control based on disturbance observer for PMSM drives," *Nonlinear Dynamics*, vol. 104, no. 2, pp. 1429–1441, 2021.

[19] J. Yu, P. Shi, J. Liu, and C. Lin, "Neuroadaptive finite-time control for nonlinear MIMO systems with input constraint," *IEEE Transactions on Cybernetics*, vol. 99, pp. 1–8, 2020.

[20] X. Li, X. Yang, and T. Huang, "Persistence of delayed cooperative models: impulsive control method," *Applied Mathematics and Computation*, vol. 342, pp. 130–146, 2019.

[21] C. Fu, Q.-G. Wang, J. Yu, and C. Lin, "Neural network-based finite-time command filtering control for switched nonlinear systems with backlash-like hysteresis," *IEEE Transactions on Neural Networks and Learning Systems*, vol. 99, pp. 1–6, 2020.

[22] H. Zhang, J. Yu, Y. Ma, Z. Pan, and J. Zhao, "Image restoration based on stochastic resonance in a parallel array of fitzhugh-nagumo neuron," *Complexity*, vol. 2020, Article ID 8843950, 9 pages, 2020.

[23] J. Hu, G. Sui, X. Lv, and X. Li, "Fixed-time control of delayed neural networks with impulsive perturbations," *Nonlinear Analysis: Modelling and Control*, vol. 23, no. 6, pp. 904–920, 2018.

[24] J. Zhao, Y. Ma, and Z. Pan, "Research on image signal identification based on adaptive array stochastic resonance," *Journal of Systems Science and Complexity*, vol. 2021, no. 10, 2021.
[25] J. P. Yu, P. Shi, and X. K. Chen, *Finite-Time Command Filtered Adaptive Control for Nonlinear Systems via Immersion and Invariance*, Science China Information Sciences, Beijing, China, 2021.
[26] T. Xu, H. Yu, and J. Yu, "Finite-time control for a coupled four-tank liquid level system based on the port-controlled Hamiltonian method," *Complexity*, vol. 2020, Article ID 5320756, 14 pages, 2020.
[27] Y. Chen, J. Liu, and Q. An, "Analysis and research on car sales service satisfaction based on statistics and AHP," *China Collective Economy*, vol. 21, pp. 75–77, 2009.
[28] D. Kacprzak, "An extended TOPSIS method based on ordered fuzzy numbers for group decision making," *Artificial Intelligence Review*, vol. 53, no. 3, pp. 2099–2129, 2020.
[29] K. Zhang, J. Zhan, and Y. Yao, "TOPSIS method based on a fuzzy covering approximation space: an application to biological nano-materials selection," *Information Sciences*, vol. 502, pp. 297–329, 2019.
[30] L. Z. Wu, S. H. Li, and M. Zhang, "A new method for classifying rock mass quality based on MCS and TOPSIS," *Environmental Earth Sciences*, vol. 78, no. 6, 2019.
[31] S. Oenuet and S. Soner, "Transshipment site selection using the AHP and TOPSIS approaches under fuzzy environment," *Waste Management*, vol. 28, no. 9, pp. 1552–1559, 2008.
[32] Y. Ou, L. Yi, B. Zou, and Z. Pei, "The linguistic intuitionistic fuzzy set TOPSIS method for linguistic multi-criteria decision makings," *International Journal of Computational Intelligence Systems*, vol. 11, no. 1, p. 120, 2018.
[33] S. Shi, "Comprehensive evaluation of nursing quality in operating rooms of tertiary grade A hospitals based on TOPSIS method," *Chinese Nursing Research*, vol. 11, 2019.
[34] S. Li and M. Lei, "TOPSIS based assessment of low carbon economy development and spatial econometric analysis," *Chinese Journal of Management Science*, vol. S1, 2014.
[35] X. Ao, P. Fu, and Q. Liu, "Comprehensive evaluation using DTOPSiS method and grey correlation method analysis and research on alfalfa introduction test," *Prataculture & Animal Husbandry*, vol. 5, pp. 7–10, 2010.
[36] P. Guo, "Research on crisis education and emergency ability training for college students in China," *Research in Teaching*, vol. 36, no. 3, pp. 19–21, 2013.
[37] L. Wang, L. Li, and J. Zeng, "Study and practice on the promotion of emergency prevention and protection capability for college students," *Journal of Catastrophology*, vol. 33, no. 2, pp. 172–176, 2018.
[38] W. W. Shelley, J. T. Pickett, and C. Mancini, "Race, bullying, and public perceptions of school and university safety," *Journal of Interpersonal Violence*, vol. 36, no. 1-2, pp. NP824–NP849, 2017.
[39] A. L. Etopio, P. Devereux, and M. Crowder, "Perceived campus safety as a mediator of the link between gender and mental health in a national U.S. college sample," *Women & Health*, vol. 59, no. 7, pp. 703–717, 2018.
[40] E. H. Blair, D.-C. Seo, M. R. Torabi, and M. A. Kaldahl, "Safety beliefs and safe behavior among midwestern college students," *Journal of Safety Research*, vol. 35, no. 2, pp. 131–140, 2004.
[41] Y. Liu, Y. H. Hao, and H. Sun, "Emergency manage knowledge among college students and associated factors in Heilongjiang province," *Chinese Journal of School Health*, vol. 36, no. 3, pp. 330–332, 2015.

Hindawi
Complexity
Volume 2021, Article ID 9442358, 9 pages
https://doi.org/10.1155/2021/9442358

Research Article

Structural Controllability of Boolean Control Networks under Partial Information

Qinyao Pan,[1] **Jie Zhong**,[1] **Shalin Tong**,[1] **Bowen Li**,[2,3] **and Xiaoxu Liu**[4]

[1]*College of Mathematics and Computer Science, Zhejiang Normal University, Jinhua 321004, China*
[2]*School of Computer Science, Nanjing University of Posts and Telecommunications, Nanjing 210096, China*
[3]*School of Information Science and Engineering, Southeast University, Nanjing 210096, China*
[4]*Sino-German College of Intelligent Manufacturing, Shenzhen Technology University, Shenzhen 518000, China*

Correspondence should be addressed to Bowen Li; qfhxjy@126.com

Received 23 April 2021; Accepted 20 June 2021; Published 30 June 2021

Academic Editor: Xiaodi Li

It is worth noting that both nodes' coupling connections and logical updating functions play a vital role in state evolutions of Boolean networks (BNs). In this paper, a new concept named structural controllability (SC) about Boolean control networks (BCNs) with known partial information on nodes' connections is studied. Then, by referring to semi-tensor product (STP) techniques, several types of SC are presented according to different issues of Boolean functions. Thereafter, several necessary and sufficient conditions are derived for SC of BCNs. Finally, a biological model of the lactose operon in *Escherichia coli* is simulated to show the effectiveness of the main theoretical results.

1. Introduction

Boolean networks (BNs) are known as discrete-time logical dynamics, firstly proposed in [1], where nodes evolute the corresponding states according to several Boolean functions. In a BN, every gene can be chosen from a set with logical variables 1 and 0. Therefore, a BN is illustrated according to certain Boolean functions $(g_1, \ldots, g_n)$: $\{1,0\}^{n^2} \longrightarrow \{1,0\}^n$. A digraph (named as network structure digraph) with nodes $\{a_1, \ldots, a_n\}$ can well show the connections among every node (named as network structure), where there exists a directed edge from node a_i to node a_j if g_j depends on a_i, i.e., if there is a sequence of variables $\tilde{a} \in \{1,0\}^{n-1}$ satisfying $g_j(\tilde{a}, a_i) \neq g_j(\tilde{a}, a_i)$, where $\tilde{a} = (a_1, \ldots, a_{i-1}, a_{i+1}, \ldots, a_n)$. Recently, many important properties of BNs have been issued [2–18], and so on.

Recently, great attention has been paid to BN owing to a new concept called semi-tensor product (STP) of matrices [19]. STP is firstly proposed by Cheng and his collaborators [19], which is a generalization of conventional matrix product. STP can be used as an efficient tool to convert BNs into corresponding algebraic representations. Then, many fundamental results about BNs have been issued [20–22]. Please refer to [23, 24] for more applications of STP.

It is worth noting that stability and controllability are of importance in different research fields, such as impulsive differential systems [25, 26], functional differential equations [27], switched systems, and Boolean networks [28–30]. If we take external control inputs into consideration, BNs will be Boolean control networks (BCNs) established by Akutsu [28] for the first time. Note that it has been increasingly challenging for researches concerning BNs and BCNs [29, 30]. Recently, the problem of controllability has been studied rapidly; some fundamental results have been established. To list a few, one of the main results on controllability has been issued [31], based on an input-state incidence matrix, where controllability is illustrated by the positiveness of a controllability matrix. Moreover, by Perron–Frobenius theory, controllability has been studied in [20]. In the past few years, another important issue (called pinning control method) gets great attention with less control cost and lower computational complexity [32–34].

It is noted that both nodes' coupling connections and logical updating functions play a vital role in state evolutions of BNs. During the past few decades, a relationship between nodes' connection and some concepts of BNs, such as stability and oscillatority, has been issued in [35–39]. Note that in real-world, not all the messages about nodes coupling and the updating Boolean functions are available, that is, only part of the nodes' connections are available. For instance, a new research concept named structural controllability (SC) concerning BCNs is well addressed in [40], whose full messages of nodes' connections are available while Boolean functions are unavailable. Therefore, it is important to analyze dynamical properties with only part of the messages on nodes' connections, i.e., all the messages of BNs are unavailable.

Therefore, based on the above analysis, some contributions of this paper are given: (i) SC of BCNs with partial information of nodes' connections available has been firstly issued, where partial nodes' connections are available; (ii) four cases of SC are defined owing to different types of network structure and logical functions. Then, several types of SC matrices are constructed using STP and Hadamard product, and some criteria are issued; (iii) SC of BCNs with partial information of nodes' connections available is a simple extension of general controllability of BCNs with full information of both network structure and logical functions.

The rest of the paper is organized as follows: in Section 2, some preliminaries are given. In Section 3, the main results of SC are given, and some criteria are obtained. In Section 4, to explain the main results, one biological model is provided. In Section 5, a brief conclusion is established.

Compared with the conference version of this paper [41], in this paper, much more detailed descriptions of the theoretical results about SC have been established. In [41], only two cases of SC are considered. However, in the revision, totally four cases of SC are discussed, and several necessary and sufficient conditions are derived for SC of BCNs, which is a generalization of the theoretical results in [41]. In addition, in this paper, some comments and detailed comparisons with the existing references have been presented, as well as a new figure has been added to better illustrate the implication relationships between four different types of SC.

Here, some notations are given: $\mathbb{N}^+$ denotes the set consisting of positive integers. $[s\colon t] = \{s, s+1, \ldots, t\}$, where $s < t$ and $s, t \in \mathbb{N}^+$. δ_n^m is the m-th column of the identity matrix I_n. $\Delta_n = \{\delta_n^m | 1 \le m \le n\}$. $\mathrm{Col}_k(B)$ $(\mathrm{Col}(B))$ denotes the m-th column (columns) of matrix B. $\mathfrak{R}_{q\times r}$ $(\mathfrak{L}_{q\times r})$ denotes the set of $q \times r$ real matrices (logical matrices). $\mathfrak{B}_{u\times v}$ is the set consisting of $u \times v$ Boolean matrices. $M = [\delta_n^{j_1}, \ldots, \delta_n^{j_p}] := \delta_n[j_1, \ldots, j_p]$ is a logical matrix. Boolean addition is defined as $u +_{\mathscr{B}} v := u \vee v$, where $u, v \in \mathfrak{D}$. $(A +_{\mathscr{B}} B)_{ij} = a_{ij} +_{\mathscr{B}} b_{ij}$, where $A = [a_{ij}] \in \mathfrak{B}_{n\times s}$, $B = [b_{ij}] \in \mathfrak{B}_{n\times s}$. $\mathrm{Blk}_i(A)$ represents the i-th block of matrix A. A Boolean matrix satisfies all the entries belonging to $\mathfrak{D} = \{0, 1\}$. $W_{[m,n]} = [I_n \otimes \delta_m^1, I_n \otimes \delta_m^2, \ldots, I_n \otimes \delta_m^m]$. "$\otimes$" denotes the known Kronecker product, "$*$" denotes the known Khatri–Rao product, "$\circ$" denotes the known Hadamard product, and "$\ltimes$" denotes STP of two given matrices.

2. Preliminaries

Firstly, here, some basic illustrations on STP and BCNs are introduced.

Definition 1. The STP of two given matrices $C \in \mathfrak{R}^{m\times n}$ and $D \in \mathfrak{R}^{p\times q}$ is defined as $C \ltimes D = (C \otimes I_{(s/n)})(D \otimes I_{(s/p)})$, where s is the least common multiple of n and p.

Define the bijective relationship "$\sim$" between $\mathfrak{D} := \{1, 0\}$ and Δ_2 as $\gamma \sim \delta_2^{2-\gamma}$, which naturally extends to $(\gamma_1, \ldots, \gamma_n) \sim \ltimes_{i=1}^n \delta_2^{2-\gamma_i}$ between $\mathfrak{D}^n$ and Δ_{2^ν}. Equivalently, Boolean functions can be transferred into an algebraic representation.

Lemma 1. *Given a logical function* $\mathbf{g}\colon \mathfrak{D}^n \longrightarrow \mathfrak{D}$, *its multilinear form is given as* $\mathbf{g}(x_1, \ldots, x_\nu) \sim M_{\mathbf{g}} \sim \ltimes_{i=1}^n x_i$, *where* $M_{\mathbf{g}} \in \mathfrak{L}_{2\times 2^\nu}$ *is the structure matrix, uniquely determined by* $\mathbf{g}$.

Some well-known structure matrices of binary operators are presented based on Lemma 1, such as negation "" $(M_n = \delta_2[\,1\ \ 2\,])$, conjunction "$\wedge$" $(M_c = \delta_2[\,1\ \ 2\ \ 2\ \ 2\,])$, disjunction "$\vee$" $(M_d = \delta_2[\,1\ \ 1\ \ 1\ \ 2\,])$, conditional "$\longrightarrow$" $(M_i = \delta_2[\,1\ \ 2\ \ 1\ \ 1\,])$, and biconditional "$\leftrightarrow$" $(M_e = \delta_2[\,1\ \ 2\ \ 2\ \ 1\,])$.

Normally, a BCN consisting of ν nodes and κ external inputs can be described:

$$x_i(\tau+1) = \mathbf{g}_i\left(\left[x_k(\tau)\right]_{k\in\Theta_i}, \left[\overline{x}_k(\tau)\right]_{k\in\overline{\Theta}_i}, \left[\vartheta_k(\tau)\right]_{k\in\Xi_i}, \left[\overline{\vartheta}_k(\tau)\right]_{k\in\overline{\Xi}_i}\right), \quad i \in [1\colon \nu], \tag{1}$$

where the negation of x is denoted by $\overline{x}$, i.e., $\overline{x} = x$. Here, $x_1, \ldots, x_\nu \in \mathfrak{D}$ express the states, $\vartheta_i \in \mathfrak{D}$ expresses the control input, and $\Theta_i \subseteq [1\colon \nu]$ and $\Xi_i \subseteq [1\colon \kappa]$ are the index sets of the in-neighbors of i-th node. For each $i \in [1\colon \nu]$, we call sets Θ_i, Ξ_i as the activating coupling node sets of the i-th node. In addition, for each $i \in [1\colon \nu]$, $\overline{\Theta}_i \subseteq [1\colon \nu] \backslash \Theta_i$ and $\overline{\Xi}_i \subseteq [1\colon \kappa] \backslash \Xi_i$ are the index sets of coupling nodes of i-th node, and we call sets $\overline{\Theta}_i, \overline{\Xi}_i$ as the inhibiting couplings node sets of the i-th node. $\mathbf{g}_i\colon \mathfrak{D}^{|\Theta_i|+|\overline{\Theta}_i|+|\Xi_i|+|\overline{\Xi}_i|} \longrightarrow \mathfrak{D}$, $i \in [1\colon \nu]$, are Boolean functions, which only consist of "$\wedge$" and "$\vee$." Therefore, the logical dynamics of (1) is only connected by logical operators "$\wedge$," "$\vee$," and "." Thus, given a BCN (1), one can always obtain its corresponding algebraic representation using Lemma 1.

2.1. Problem Formulation. It is noted that dynamical evolutions of BN (1) are determined by the Boolean functions $\mathbf{g}_1, \ldots, \mathbf{g}_\nu$, as well as its coupling sets Θ_i, $\overline{\Theta}_i$, Ξ_i, and $\overline{\Xi}_i$, $i \in [1\colon \nu]$. In practical biological applications, due to experimental impacts and other reasons, we might only know the in-neighbors of some nodes, but cannot acquire the coupling relationship for each node. Therefore, assume that only partial information of (1) is known in this paper. Here, we assume that the sets $\Theta_i, \overline{\Theta}_i, \Xi_i$, and $\overline{\Xi}_i$, $i \in \{i_1, \ldots, i_\mu\} \subseteq [1\colon \nu]$, are given beforehand, while binary operators among different nodes in Θ_i, $\overline{\Theta}_i$, Ξ_i, and $\overline{\Xi}_i$, $i \in \{i_1, \ldots, i_\mu\} \subseteq [1\colon \nu]$, are unavailable, which implies that for nodes $x_{i_1}, \ldots, x_{i_\mu}$, the corresponding activating coupling nodes, and inhibiting coupling nodes are given, whereas binary operators among nodes are unavailable.

For simple illustrations, suppose only activating coupling nodes and inhibiting coupling nodes for nodes $x_1, \ldots, x_\mu$, are given, which is as follows:

$$\begin{cases} x_i(\tau+1) = \mathbf{g}_i\left(\left[x_k(\tau)\right]_{k\in\Theta_i}, \left[\overline{x}_k(\tau)\right]_{k\in\overline{\Theta}_i}, \left[\vartheta_k(\tau)\right]_{k\in\Xi_i}, \left[\overline{\vartheta}_k(\tau)\right]_{k\in\overline{\Xi}_i}\right), & i \in [1\colon \mu], \\ x_j(\tau+1) = \mathbf{g}_j\left(\left[x_k(\tau)\right]_{k\in\Theta_j}, \left[\overline{x}_k(\tau)\right]_{k\in\overline{\Theta}_j}, \left[\vartheta_k(\tau)\right]_{k\in\Xi_j}, \left[\overline{\vartheta}_k(\tau)\right]_{k\in\overline{\Xi}_j}\right), & j \in [\mu+1\colon \nu], \end{cases} \tag{2}$$

where $\Theta_i, \overline{\Theta}_i, \Xi_i$, and $\overline{\Xi}_i$, $i \in [1\colon \mu]$, are known and $\Theta_j, \overline{\Theta}_j, \Xi_j$, and $\overline{\Xi}_j$, $j \in [\mu+1\colon \nu]$, are unknown. The binary operators among all the nodes are unknown, which implies that the logical operators between nodes in $\Theta_i, \overline{\Theta}_i, \Xi_i$, and $\overline{\Xi}_i$, $i \in [1\colon \nu]$, are unknown.

Based on Lemma 1, one has equivalent algebraic form of logical dynamics of (2). Given sets $\Theta_i, \overline{\Theta}_i, \Xi_i$, and $\overline{\Xi}_i$, $i \in [1\colon \mu]$, we make the following ordering assumptions to simplify calculation:

$$\begin{aligned} \Theta_i &= \left\{a_1^i, \ldots, a_{|\Theta_i|}^i\right\}, \quad a_1^i < \cdots < a_{|\Theta_i|}^i \in [1\colon \nu], \\ \overline{\Theta}_i &= \left\{b_1^i, \ldots, b_{|\overline{\Theta}_i|}^i\right\}, \quad b_1^i < \cdots < b_{|\overline{\Theta}_i|}^i \in [1\colon \nu], \\ \Xi_i &= \left\{c_1^i, \ldots, c_{|\Xi_i|}^i\right\}, \quad c_1^i < \cdots < c_{|\Xi_i|}^i \in [1\colon \kappa], \\ \overline{\Xi}_i &= \left\{d_1^i, \ldots, d_{|\overline{\Xi}_i|}^i\right\}, \quad d_1^i < \cdots < d_{|\overline{\Xi}_i|}^i \in [1\colon \kappa]. \end{aligned} \tag{3}$$

Then, under assumption (3), one has that

$$\begin{aligned} x_i(\tau+1) = {} & \left[x_{a_1^i}(\tau)\right]\sigma_1^i\left[x_{a_2^i}(\tau)\right]\sigma_2^i, \ldots, \sigma_{|\Theta_i|-1}^i\left[x_{a_{|\Theta_i|}^i}(\tau)\right]\sigma_{|\Theta_i|}^i\left[\overline{x}_{b_1^i}(\tau)\right]\sigma_{|\Theta_i|+1}^i \\ & \cdot\left[\overline{x}_{b_2^i}(\tau)\right]\sigma_{|\Theta_i|+2}^i, \ldots, \sigma_{|\Theta_i|+|\overline{\Theta}_i|-1}^i\left[\overline{x}_{b_{|\overline{\Theta}_i|}^i}(\tau)\right]\sigma_{|\Theta_i|+|\overline{\Theta}_i|}^i\left[\vartheta_{c_1^i}(\tau)\right] \\ & \widehat{\sigma}_1^i\left[\vartheta_{c_2^i}(\tau)\right]\widehat{\sigma}_2^i, \ldots < \widehat{\sigma}_{|\Xi_i|-1}^i\left[\vartheta_{c_{|\Xi_i|}^i}(\tau)\right]\widehat{\sigma}_{|\Xi_i|}^i\left[\overline{\vartheta}_{d_1^i}(\tau)\right]\widehat{\sigma}_{|\Xi_i|+1}^i\left[\overline{\vartheta}_{d_2^i}(\tau)\right]\widehat{\sigma}_{|\Xi_i|+2}^i, \ldots, \widehat{\sigma}_{|\Xi_i|+|\overline{\Xi}_i|-1}^i\left[\overline{\vartheta}_{d_{|\overline{\Xi}_i|}^i}(\tau)\right], \quad i \in [1\colon \mu], \end{aligned} \tag{4}$$

where binary operators $\sigma_j^i \in \{\vee, \wedge\}$, $j \in [1\colon |\Theta_i| + |\overline{\Theta}_i|]$, $i \in [1\colon \nu]$, $\widehat{\sigma}_j^i \in \{\vee, \wedge\}$, $j \in [1\colon |\Xi_i| + |\overline{\Xi}_i| - 1]$, and $i \in [1\colon \nu]$. Here, operators σ_j^i, $j \in [1\colon |\Theta_i| + |\overline{\Theta}_i|]$, $\widehat{\sigma}_j^i$, and $j \in [1\colon |\Xi_i| + |\overline{\Xi}_i| - 1]$ are binary operators connecting the in-neighbor sets $\Theta_i, \overline{\Theta}_i, \Xi_i$, and $\overline{\Xi}_i$, $i \in [1\colon \nu]$.

Given binary operators $\sigma_j \in \{\vee, \wedge\}$, $j \in [1\colon |\Theta_i| + |\overline{\Theta}_i|]$, and $\widehat{\sigma}_j \in \{\vee, \wedge\}$, $j \in [1\colon |\Xi_i| + |\overline{\Xi}_i| - 1]$, one has that

$$\begin{aligned} x_i(\tau+1) = {} & \mathbf{O}_i \ltimes_{j=1}^{|\Theta_i|} x_{a_{i,j}}(\tau) \not\ltimes_{j=1}^{|\overline{\Theta}_i|}\left(M_n \not\ltimes x_{b_{i,j}}(\tau)\right) \\ & \ltimes_{j=1}^{|\Xi_i|} \vartheta_{c_{i,j}}(\tau) \ltimes_{j=1}^{|\overline{\Xi}_i|}\left(M_n \ltimes \vartheta_{d_{i,j}}(\tau)\right), \end{aligned} \tag{5}$$

where matrix $\mathbf{O}_i$ is uniquely calculated according to binary operators $\sigma_j \in \{\vee, \wedge\}$, $j \in [1\colon |\Theta_i| + |\overline{\Theta}_i|]$, and $\widehat{\sigma}_j \in \{\vee, \wedge\}$, $j \in [1\colon |\Xi_i| + |\overline{\Xi}_i| - 1]$. Thus, there totally exist $2^{|\Theta_i|+|\overline{\Theta}_i|+|\Xi_i|+|\overline{\Xi}_i|-1}$ different kinds of structure matrices for matrices $\mathbf{O}_i$, $i \in [1\colon \mu]$. Given each $i \in [1\colon \mu]$, illustrate all the $2^{|\Theta_i|+|\overline{\Theta}_i|+|\Xi_i|+|\overline{\Xi}_i|-1}$ kinds of matrices $\mathbf{O}_i$ in (5) by set Γ_i.

Denoting $x(\tau) = \ltimes_{i=1}^{\nu} x_i(\tau)$ and $\vartheta(\tau) = \ltimes_{i=1}^{\kappa} \vartheta_i(\tau)$, one can further calculate a unique matrix $\mathbf{T}_i \in \mathfrak{L}_{2\times 2^{\nu+\kappa}}$, $i \in [1\colon \mu]$, based on Lemma 1, satisfying

$$\begin{aligned} & \ltimes_{j=1}^{|\Theta_i|} x_{a_{i,j}}(\tau) \ltimes_{j=1}^{|\overline{\Theta}_i|}\left(M_n \ltimes x_{b_{i,j}}(\tau)\right) \ltimes_{j=1}^{|\Xi_i|} \vartheta_{c_{i,j}}(\tau) \ltimes_{j=1}^{|\overline{\Xi}_i|}\left(M_n \ltimes \vartheta_{d_{i,j}}(\tau)\right) \\ & = \mathbf{T}_i \vartheta(\tau) x(\tau). \end{aligned} \tag{6}$$

Thus, for $x_1, \ldots, x_\mu$, the following equation is obtained:

$$x_i(\tau+1) = \mathbf{O}_i \mathbf{T}_i \vartheta(\tau) x(\tau). \tag{7}$$

Let $\mathbf{x}_1(\tau) = \ltimes_{i=1}^{\mu} x_i(\tau) \in \Delta_{2^\mu}$; it leads to a simplification illustration of (4) for nodes $x_1, \ldots, x_\mu$, using Khatri–Rao product,

$$\mathbf{x}_1(\tau+1) = F_1 \vartheta(\tau) x(\tau), \tag{8}$$

where $F_1 \in \Lambda_1$: $\triangleq \{*_{i=1}^{\mu}(\mathbf{O}_i \ltimes \mathbf{T}_i)$: $\mathbf{O}_i \in \Gamma_i, i \in [1: \mu]\}$. Then, one has $|\Lambda_1| = 2^{\sum_{i=1}^{\mu}(|\Theta_i|+|\overline{\Theta}_i|+|\Xi_i|+|\overline{\Xi}_i|)-\mu}$. Denoting $r = |\Lambda_1|$, assume that $\Lambda_1 = \{F_1^1, F_1^2, \ldots, F_1^r\}$, where matrices $F_1^1, F_1^2, \ldots, F_1^r \in \mathfrak{L}_{2^\mu \times 2^{\nu+\kappa}}$.

Then, let $\mathbf{x}_2(\tau) = \ltimes_{i=\mu+1}^{\nu} x_i(\tau) \in \Delta_{2^{\nu-\mu}}$; one can obtain algebraic form for the last $\nu - \mu$ nodes:

$$\mathbf{x}_2(\tau+1) = F_2 \vartheta(\tau) x(\tau), \tag{9}$$

where $F_2 \in \mathfrak{L}_{2^{\nu-\mu} \times 2^{\nu+\kappa}}$ expresses the structure matrix determined by in-neighbor sets $\Theta_i, \overline{\Theta}_i, \Xi_i$, and $\overline{\Xi}_i$, $i \in [\mu+1: \nu]$, and its binary operators. Therefore, it leads to totally $s = 2^{(\nu-\mu)(2^{\nu+\kappa})}$ cases for matrix F_2. Denote the set of all the $2^{(\nu-\mu)(2^{\nu+\kappa})}$ different kinds of F_2 by Λ_2, that is, $F_2 \in \Lambda_2 \triangleq \{F_2^1, F_2^2, \ldots, F_2^s\}$, where $F_2^1, F_2^2, \ldots, F_2^s \in \mathfrak{L}_{2^{\nu-\mu} \times 2^{\nu+\kappa}}$. Therefore, considering (2), one has that

$$\begin{cases} \mathbf{x}_1(\tau+1) = F_1 \vartheta(\tau) x(\tau), \\ \mathbf{x}_2(\tau+1) = F_2 \vartheta(\tau) x(\tau), \end{cases} \tag{10}$$

where $F_1 \in \Lambda_1 = \{F_1^1, F_1^2, \ldots, F_1^r\}$ and $F_2 \in \Lambda_2 = \{F_2^1, F_2^2, \ldots, F_2^s\}$. Multiplying (10) yields an algebraic form of (2),

$$x(\tau+1) = F_1 \vartheta(\tau) x(\tau) F_2 \vartheta(\tau) x(\tau) \coloneqq L \vartheta(\tau) x(\tau), \tag{11}$$

where matrix L is called the state transition matrix of system (2) choosing from a set $\Omega \triangleq \{F_1 * F_2, F_1 \in \Lambda_1, F_2 \in \Lambda_2\}$. In addition, one can calculate that $|\Omega| = rs$ and represent all of the state transition matrices by $\Omega \triangleq \{L_1, L_2, \ldots, L_{rs}\}$, where $L_1, L_2, \ldots, L_{rs} \in \mathfrak{L}_{2^\nu \times 2^{\nu+\kappa}}$. This implies that each matrix L_i, $i \in [1: rs]$, is one possible state transition matrix for system (2), where only the corresponding in-neighbor sets $\Theta_i, \overline{\Theta}_i, \Xi_i$, and $\overline{\Xi}_i$, $i \in [1: \mu]$, for those first μ nodes, are known.

3. Main Results

In this section, several types of controllability of (2) are presented, where only the corresponding in-neighbors of nodes $x_1, \ldots, x_\mu$, are known.

3.1. First Class of Structural Controllability. At the beginning, only the corresponding in-neighbor sets $\Theta_i, \overline{\Theta}_i, \Xi_i$, and $\overline{\Xi}_i$ for $x_1, \ldots, x_\mu$, are supposed to be known, the corresponding Boolean functions $\mathbf{g}_i$, $i \in [1: \mu]$, and both the in-neighbor sets $\Theta_j, \overline{\Theta}_j, \Xi_j$, and $\overline{\Xi}_j$ and the Boolean functions $\mathbf{g}_j$, $j \in [\mu+1: \nu]$, are unknown. Under these assumptions, reachability and controllability for (2) are firstly defined as follows.

Firstly, consider the first class structural reachability (FCSR) between two given states x_0 and x_d under any Boolean functions $\mathbf{g}_i$, $i \in [1: \nu]$.

Definition 2. Consider system (2) and the neighbor sets $\Theta_i, \overline{\Theta}_i, \Xi_i$, and $\overline{\Xi}_i$ for $x_1, \ldots, x_\mu$, are available. The destination state $x_d \in \Delta_{2^\nu}$ achieves FCSR from the initial state $x_0 \in \Delta_{2^\nu}$, if x_0 can be steered to x_d for arbitrary Boolean functions $\mathbf{g}_1, \ldots, \mathbf{g}_\nu$. In addition, (2) achieves first class structural controllability (FCSC) if for any initial state x_0 and destination state x_d, x_d achieves FCSR from x_0.

By considering $\Xi = \{L_1, L_2, \ldots, L_{rs}\}$, divide $L_1, \ldots, L_{rs}$, as follows: $L_i = [\mathrm{Blk}_1(L_i), \mathrm{Blk}_2(L_i), \ldots, \mathrm{Blk}_{2^\kappa}(L_i)]$, and denote

$$\mathrm{C}_i = \sum_{l=1}^{2^\nu} \mathrm{B}(M_i)^{(l)}, \quad \in \mathfrak{L}_{2^\nu \times 2^\nu}, i \in [1: rs], \tag{12}$$

where $M_i = L_i \ltimes 1_{2^\kappa} \in \mathfrak{L}_{2^\nu \times 2^\nu}$, and matrix C_i, $i \in [1: rs]$, is the controllability matrix when state transition matrix of system (2) is L_i. Then, introduce the following Boolean matrix in order to issue FCSC,

$$S_1 = \mathrm{C}_1 \circ \mathrm{C}_2 \circ \cdots \circ \mathrm{C}_{rs} \in \mathfrak{L}_{2^\nu \times 2^\nu}, \tag{13}$$

where "$\circ$" represents the well-known Hadamard matrix product. Here, name S_1 as FCSC matrix of (2) with partial in-neighbor sets $\Theta_i, \overline{\Theta}_i, \Xi_i$, and $\overline{\Xi}_i$ for nodes x_i available, $i \in [1: \mu]$.

By referring to matrix S_1 established in (13), the following criteria for FCSC are established.

Theorem 1. *Consider system (2) with available sets $\Theta_i, \overline{\Theta}_i, \Xi_i$, and $\overline{\Xi}_i$ for nodes $x_1, \ldots, x_\mu$, then state $x_d = \delta_{2^\nu}^{\pi} \in \Delta_{2^\nu}$ ($\pi \in [1: 2^\nu]$) achieves FCSR from state $x_0 = \delta_{2^\nu}^{\eta} \in \Delta_{2^\nu}$ ($\eta \in [1: 2^\nu]$) if and only if the following condition $[S_1]_{\pi,\eta} = 1$ holds.*

Proof. According to the definition of Hadamard product "$\circ$," one can easily obtain that $[S_1]_{\pi,\eta} = 1$ if and only if for each $i \in [1: rs]$, $[\mathrm{C}_i]_{\pi,\eta} = 1$. For system $x(\tau+1) = L_i \vartheta(\tau) x(\tau)$, $i \in [1: rs]$, according to [31], one has that $x_d = \delta_{2^\nu}^{\pi}$ is reachable from $x_0 = \delta_{2^\nu}^{\eta}$ if and only if $[\mathrm{C}_i]_{\pi,\eta} = 1$. Thus, by Definition 2, $x_d = \delta_{2^\nu}^{\pi}$ achieves FCSC from $x_0 = \delta_{2^\nu}^{\eta}$ if and only if condition $[S_1]_{\pi,\eta} = 1$ holds.

Then, FCSC for (2) with available partial in-neighbor sets $\Theta_i, \overline{\Theta}_i, \Xi_i$, and $\overline{\Xi}_i$, $i \in [1: \mu]$, is established. □

Theorem 2. *Given system (2) with available neighbor sets $\Theta_i, \overline{\Theta}_i, \Xi_i$, and $\overline{\Xi}_i$ for nodes $x_1, \ldots, x_\mu$, (2) achieves FCSC if and only if condition $S_1 = 1_{2^\nu \times 2^\nu}$ holds.*

Proof. From Theorem 1, for any initial state x_0 and destination state $x_d \in \Delta_{2^\nu}$, x_d achieves FCSR from x_0 if and only if $S_1 = 1_{2^\nu \times 2^\nu}$. Thus, according to Definition 2, system (2) achieves FCSC. □

3.2. Second Class of Structural Controllability. Based on Definition 2, FCSR is introduced on reachability between the initial state x_0 and destination state x_d for any Boolean functions $\mathbf{g}_1, \ldots, \mathbf{g}_\nu$. Hence, assume that state x_0 can be steered to state x_d under certain possible Boolean mappings $\mathbf{g}_i$, $i \in [1: \nu]$, then the following second class of structural controllability is established.

Definition 3. Given system (2) and the neighbor sets $\Theta_i, \overline{\Theta}_i, \Xi_i$, and $\overline{\Xi}_i$, for nodes $x_1, \ldots, x_\mu$, are available, the destination state $x_d \in \Delta_{2^\nu}$ achieves second class structural reachability (SCSR) from the initial state $x_0 \in \Delta_{2^\nu}$, if there is certain Boolean functions $\mathbf{g}_1, \ldots, \mathbf{g}_\nu$ satisfying that x_d can be reachable from x_0. In addition, (2) achieves SCSC if for any $x_0, x_d \in \Delta_{2^\nu}$, x_d achieves second class structural controllability (SCSR) from x_0.

By referring to established matrices C_i in (12), $i \in [1\colon rs]$, define

$$S_2 = \sum_{i=1}^{rs} {}_{\mathrm{B}}\mathrm{C}_i, \quad \in \mathfrak{L}_{2^\nu \times 2^\nu}. \tag{14}$$

We name S_2 as the SCSC matrix of (2) with available sets $\Theta_i, \overline{\Theta}_i, \Xi_i$, and $\overline{\Xi}_i$ for nodes x_i, $i \in [1\colon \mu]$. According to S_2 defined in (14), the following necessary and sufficient criteria are derived.

Theorem 3. *Consider system (2) with available neighbor sets $\Theta_i, \overline{\Theta}_i, \Xi_i$, and $\overline{\Xi}_i$ for nodes $x_1, \ldots, x_\mu$, then state $x_d = \delta_{2^\nu}^\pi \in \Delta_{2^\nu}$ achieves SCSR from state $x_0 = \delta_{2^\nu}^\eta \in \Delta_{2^\nu}$ if and only if condition $[S_2]_{\pi,\eta} = 1$ holds.*

Proof. $[S_2]_{\pi,\eta} = 1$ if and only if there is a sequence of Boolean matrices C_k, $k \in [1\colon rs]$, such that $[\mathrm{C}_k]_{\pi,\eta} = 1$. For system $x(\tau+1) = L_k \vartheta(\tau) x(\tau)$, according to [31], one has that $x_d = \delta_{2^\nu}^\pi$ can be reachable from $x_0 = \delta_{2^\nu}^\eta$ if and only if $[\mathrm{C}_k]_{\pi,\eta} = 1$. Thus, by Definition 3, $x_d = \delta_{2^\nu}^\pi$ achieves SCSR from $x_0 = \delta_{2^\nu}^\eta$ if and only if condition $[S_2]_{\pi,\eta} = 1$ holds. □

Theorem 4. *Considering system (2), the neighbor sets $\Theta_i, \overline{\Theta}_i, \Xi_i$, and $\overline{\Xi}_i$ for nodes x_i, $i \in [1\colon \mu]$, are available, then (2) achieves SCSC if and only if condition $S_2 = 1_{2^\nu \times 2^\nu}$ holds.*

Proof. From Theorem 3, for any two states $x_0, x_d \in \Delta_{2^\nu}$, state x_d achieves SCSR from state x_0 if and only if condition $S_2 = 1_{2^\nu \times 2^\nu}$ holds. Thus, according to Definition 3, system (2) achieves SCSC.

In the above, controllability of (2) with known in-neighbor sets $\Theta_i, \overline{\Theta}_i, \Xi_i$, and $\overline{\Xi}_i$ for nodes $x_1, \ldots, x_\mu$, under the situations of the arbitrariness and existence of logical functions $\mathbf{g}_1, \ldots, \mathbf{g}_\nu$, has been established, which are shown in Theorems 1 and 3. In the following, controllability of (2) under the situation of arbitrary logical functions $\mathbf{g}_i$, $i \in [1\colon \mu]$, and certain possible logical functions $\mathbf{g}_j$, $j \in [\mu+1\colon \nu]$, will be studied. □

3.3. Third Class of Structural Controllability. In the following sequel, we consider the reachability between two given states x_0 and x_d under any Boolean functions $\mathbf{g}_i$, $i \in [1\colon \mu]$, and certain possible logical functions $\mathbf{g}_i$, $i \in [\mu+1\colon \nu]$.

Definition 4. Considering system (2) and the neighbor sets $\Theta_i, \overline{\Theta}_i, \Xi_i$, and $\overline{\Xi}_i$, for nodes $x_1, \ldots, x_\mu$, are available, the destination state $x_d \in \Delta_{2^\nu}$ achieves third class structural reachability (TCSR) from the initial state $x_0 \in \Delta_{2^\nu}$, if for any Boolean functions $\mathbf{g}_i, i \in [1\colon \mu]$, there are certain Boolean mappings $\mathbf{g}_j, j \in [\mu+1\colon \nu]$ satisfying that x_d can be reachable from x_0. In addition, (2) achieves third class structural controllability (TCSC), if for any $x_0, x_d \in \Delta_{2^\nu}$, x_d achieves TCSR from x_0.

For convenience, denote the set of L in (11) by $\Xi = \{F_1 * F_2, F_1 \in \Lambda_1, F_2 \in \Lambda_2\} \triangleq \{L^{1,1}, L^{1,2}, \ldots, L^{1,s}, L^{2,1}, L^{2,2}, \ldots, L^{2,s}, \ldots, L^{r,1}, L^{r,2}, \ldots, L^{r,s}\}$, where $L^{i,j} = F_1^i * F_2^j$, $i \in [1\colon r]$, $j \in [1\colon s]$. Divide $L^{i,j}$ into 2^κ equal blocks as $L^{i,j} = [\mathrm{Blk}_1 L^{i,j}, \mathrm{Blk}_2 L^{i,j}, \ldots, \mathrm{Blk}_{2^\kappa} L^{i,j}]$, and denote

$$\mathrm{C}^{i,j} = \sum_{l=1}^{2^\nu} {}_{\mathrm{B}}\left(M^{i,j}\right)^{(l)}, \quad \in \mathfrak{L}_{2^\nu \times 2^\nu}, i \in [1\colon r], \ j \in [1\colon s], \tag{15}$$

where $M^{i,j} = L^{i,j} < i \operatorname{mes} 1_{2^\kappa} \in \mathfrak{L}_{2^\nu \times 2^\nu}$, and matrix $\mathrm{C}^{i,j}$ is the corresponding controllability matrix when state transition matrix of system (2) is $L^{i,j}$. In addition, introduce the following Boolean matrix in order to issue TCSC,

$$S_3 = T^1 \circ T^2 \circ \cdots \circ T^r, \quad \in \mathfrak{L}_{2^\nu \times 2^\nu}, \tag{16}$$

where $T^i = \sum_{j=1}^{s} {}_{\mathrm{B}}\mathrm{C}^{i,j}$, $\in \mathfrak{L}_{2^\nu \times 2^\nu}$, $i \in [1\colon r]$. We name S_3 as TCSC matrix of (2) with available sets $\Theta_i, \overline{\Theta}_i, \Xi_i$, and $\overline{\Xi}_i$ for $x_1, \ldots, x_\mu$.

By referring to matrix S_3 defined in (16), the following criteria for TCSC are established.

Theorem 5. *Given system (2), for $i \in [1\colon \mu]$, the neighbor sets $\Theta_i, \overline{\Theta}_i, \Xi_i$, and $\overline{\Xi}_i$ for nodes x_i are available, then state $x_d = \delta_{2^\nu}^\pi \in \Delta_{2^\nu}$ achieves LCSR from state $x_0 = \delta_{2^\nu}^\eta \in \Delta_{2^\nu}$ if and only if condition $[S_3]_{\pi,\eta} = 1$ holds.*

Proof. $[S_3]_{\pi,\eta} = 1$ if and only if $[T^i]_{\pi,\eta} = 1, i \in [1\colon r]$, and there is a sequence of Boolean matrices $\mathrm{C}^{i,k}, k \in [1\colon s]$, such that $[\mathrm{C}^{i,k}]_{\pi,\eta} = 1$ for every $[T^i]$. For system $x(\tau+1) = L^{i,k} \vartheta(\tau) x(\tau)$, according to [31], one has that $x_d = \delta_{2^\nu}^\pi$ is reachable from $x_0 = \delta_{2^\nu}^\eta$ if and only if $[\mathrm{C}^{i,k}]_{\pi,\eta} = 1$. Thus, by Definition 4, state $x_d = \delta_{2^\nu}^\pi$ achieves TCSR from state $x_0 = \delta_{2^\nu}^\eta$ if and only if condition $[S_3]_{\pi,\eta} = 1$ holds. □

Theorem 6. *Given system (2), the neighbor sets $\Theta_i, \overline{\Theta}_i, \Xi_i$, and $\overline{\Xi}_i$ for nodes x_i, $i \in [1\colon \mu]$, are available, then (2) achieves TCSC if and only if condition $S_3 = 1_{2^\nu \times 2^\nu}$ holds.*

Proof. From Theorem 5, for any two states $x_0, x_d \in \Delta_{2^\nu}$, state x_d achieves TCSR from state x_0 if and only if condition $S_3 = 1_{2^\nu \times 2^\nu}$ holds. Thus, according to Definition 4, system (2) achieves TCSC. □

Remark 1. More strictly, if for $\mathbf{g}_j$, $j \in [\mu+1\colon \nu]$, logical functions are the same, then for any functions $\mathbf{g}_i, i \in [1\colon \mu]$, we define the TCSC matrix as $S_3 = \sum_{j=1}^{s} {}_{\mathrm{B}}\widetilde{T}^j$, $\in \mathfrak{L}_{2^\nu \times 2^\nu}$, where $\widetilde{T}^j = \mathrm{C}^{1,j} \circ \mathrm{C}^{2,j} \circ \cdots \circ \mathrm{C}^{r,j} \in \mathfrak{L}_{2^\nu \times 2^\nu}$, $j \in [1\colon s]$.

3.4. Last Class of Structural Controllability. Based on Definition 4, TCSR is introduced on reachability between the initial state x_0 and destination state x_d for any Boolean

functions $\mathbf{g}_i, i \in [1: \mu]$ and certain Boolean functions $\mathbf{g}_i$, $i \in [\mu + 1: \nu]$. Thus, if destination state x_d is reachable from the initial state x_0 under certain Boolean functions $\mathbf{g}_i$, $i \in [1: \mu]$ and any Boolean functions $\mathbf{g}_i, i \in [\mu + 1: \nu]$, the following last class of structural controllability is established.

Definition 5. Considering system (2), for $i \in [1: \mu]$, the neighbor sets $\Theta_i, \overline{\Theta}_i, \Xi_i$, and $\overline{\Xi}_i$ for nodes x_i are available. The destination state $x_d \in \Delta_{2^\nu}$ achieves last class structural reachability (LCSR) from initial state $x_0 \in \Delta_{2^\nu}$, if there is certain Boolean functions $\mathbf{g}_1, \ldots, \mathbf{g}_p$ satisfying that x_d can be reachable from x_0 for any Boolean functions $\mathbf{g}_i, i \in [\mu + 1: \nu]$. Moreover, (2) achieves last class structural controllability (LCSC) if for any $x_0, x_d \in \Delta_{2^\nu}$, state x_d achieves LCSR from state x_0.

By referring to matrix $C^{i,j}$ established in (15), $i \in [1: r], j \in [1: s]$, define

$$S_4 = \sum_{i=1}^{r} {}_{\mathrm{B}}\widehat{T}^i \in \mathfrak{L}_{2^\nu \times 2^\nu}, \tag{17}$$

where $\widehat{T}^i = C^{i,1} \circ C^{i,2} \circ \cdots \circ C^{i,s}, i \in [1: r]$. We call S_4 as LCSC matrix of (2) with available sets $\Theta_i, \overline{\Theta}_i, \Xi_i$, and $\overline{\Xi}_i$ for nodes $x_1, \ldots, x_\mu$.

By referring to matrix S_4 defined in (17), the following criteria for LCSC are obtained.

Theorem 7. *Given system (2), for $i \in [1: \mu]$, the neighbor sets $\Theta_i, \overline{\Theta}_i, \Xi_i$, and $\overline{\Xi}_i$ for nodes x_i are available, then the destination state $x_d = \delta_{2^\nu}^{\pi} \in \Delta_{2^\nu}$ achieves LCSR from the initial state $x_0 = \delta_{2^\nu}^{\eta} \in \Delta_{2^\nu}$ if and only if condition $[S_4]_{\pi,\eta} = 1$ holds.*

Proof. $[S_4]_{\pi,\eta} = 1$ if and only if there exists a sequence of matrices $\widehat{T}^k, k \in [1: r]$, such that $[\widehat{T}^k]_{\pi,\eta} = 1$, and for every matrix $C^{k,j}, j \in [1: s]$, $[C^{k,j}]_{\pi,\eta} = 1$. For system $x(\tau + 1) = L^{k,j}\vartheta(\tau)x(\tau)$, according to [31], one has that $x_d = \delta_{2^\nu}^{\pi}$ is reachable from $x_0 = \delta_{2^\nu}^{\eta}$ if and only if $[C^{k,j}]_{\pi,\eta} = 1$. Thus, by Definition 5, $x_d = \delta_{2^\nu}^{\pi}$ achieves LCSR from $x_0 = \delta_{2^\nu}^{\eta}$ if and only if condition $[S_4]_{\pi,\eta} = 1$ holds. □

Theorem 8. *Given system (2), for $i \in [1: \mu]$, the neighbor sets $\Theta_i, \overline{\Theta}_i, \Xi_i$, and $\overline{\Xi}_i$ for nodes x_i are available, then (2) achieves LCSC if and only if condition $S_4 = 1_{2^\nu \times 2^\nu}$ holds.*

Proof. From Theorem 7, for any initial state x_0 and destination state $x_d \in \Delta_{2^\nu}$, state x_d achieves LCSR from state x_0 if and only if condition $S_4 = 1_{2^\nu \times 2^\nu}$ holds. Thus, according to Definition 5, system (2) achieves LCSC. □

Remark 2. In this paper, four types of SC of BCNs with partial information available have been studied, where one only knows part of messages on nodes' connections. Among the abovementioned four different kinds of structural controllability, the relationships are shown as follows: FCSC implies TCSC and LCSC; the third and the last class of SC both imply SCSC. In addition, FCSC is the most conservative definition and all other types of SC can be implied by FCSC, and the diagram describing the detailed relationships among different kinds of SC is shown as Figure 1.

Remark 3. By comparing with the recent theoretical results [39, 40], the established theoretical results in this paper are more general. If $p = n$, that is, one knows all the in-neighbors of (2), then the results in [40] can be directly obtained from FCSC in this paper. Moreover, if $p = n$, FCSC in this paper implies common controllability [39], which means that system (2) is always controllable no matter which functions are chosen. Thus, the study of these four cases of SC of BCNs with partial information available is a simple extension of common controllability, which provides a new insight for further studying and reducing the high computational complexity of BCNs.

4. Simulations

Here, simulations on a Boolean model of the lactose operon in *Escherichia coli* are given to illustrate the obtained results.

Example 1. Firstly, a lactose operon model in *Escherichia coli* modeled by a BCN is considered [42]:

$$\begin{aligned} w_1(\tau + 1) &= (\xi_2(\tau) \vee w_3(\tau)) \wedge \overline{\xi}_1(\tau), \\ w_2(\tau + 1) &= w_1(\tau), \\ w_3(\tau + 1) &= [(\xi_2(\tau) \wedge w_2(\tau)) \vee (\overline{w}_2(\tau) \wedge w_3(\tau))] \wedge \overline{\xi}_1(\tau), \end{aligned} \tag{18}$$

where $w_1 \in \mathfrak{D}$ denotes the biological structure of mRNA, $w_2 \in \mathfrak{D}$ denotes the biological structure of lacZ polypeptide, $w_3 \in \mathfrak{D}$ denotes the intracellular lactose, $\xi_1 \in \mathfrak{D}$ denotes the external glucose, and $\xi_2 \in \mathfrak{D}$ denotes the external lactose.

Using STP tool, the corresponding algebraic form of system (18) is given as follows: $w(\tau + 1) = Lu(\tau)w(\tau)$, where $L = \delta_8[6, 6, 6, 6, 8, 8, 8, 8, 6, 6, 6, 6, 8, 8, 8, 8, 1, 1, 1, 2, 3, 3, 3, 4, 2, 6, 1, 6, 4, 8, 3, 8]$. Then, split matrix L into four blocks and obtain its controllability matrix $C = \sum_{l=1}^{8} {}_{\mathrm{B}}(M)^{(l)} \in \mathfrak{B}_{8\times 8}$, where $M = L \ltimes 1_4 \in \mathfrak{B}_{8\times 8}$. After a straightforward calculation, one has that $C = [\delta_8^1 + \delta_8^2 + \delta_8^3 + \delta_8^4 + \delta_8^6 + \delta_8^8, \delta_8^1 + \delta_8^2 + \delta_8^3 + \delta_8^4 + \delta_8^6 + \delta_8^8, \ldots, \delta_8^1 + \delta_8^2 + \delta_8^3 + \delta_8^4 + \delta_8^6 + \delta_8^8] \in \mathfrak{B}_{8\times 8}$. By referring to [31], one can conclude that system (18) is not controllable.

Suppose that only in-neighbors for nodes w_1 and w_2 are given, but the detailed logical functions are unknown. Thus, the following system is considered:

$$\begin{aligned} w_1(\tau + 1) &= f_1\left(w_3(\tau), \xi_2(\tau), \overline{\xi}_1(\tau)\right), \\ w_2(\tau + 1) &= f_2(w_1(\tau)), \\ w_3(\tau + 1) &= f_3\left(\left[w_j(\tau)\right]_{j\in\Theta_3}, \left[\overline{w}_j(\tau)\right]_{j\in\overline{\Theta}_3}, \left[\xi_j(\tau)\right]_{j\in\Xi_3}, \left[\overline{\xi}(\tau)\right]_{j\in\overline{\Xi}_3}\right), \end{aligned} \tag{19}$$

where Θ_3 and Ξ_3 ($\overline{\Theta}_3$ and $\overline{\Xi}_3$) express the unavailable sets of the activating indegrees (inhibiting indegrees) of node w_3.

Based on equations (5)–(9), a simple equivalent algebraic illustration of (19) can be derived:

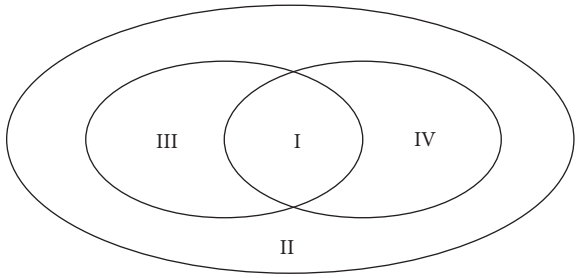

Figure 1: The implication relationships among different types of SC (I, II, III, and IV represent abbreviations of FCSC, SCSC, TCSC, and LCSC).

$$\begin{aligned} \mathbf{x}_1(\tau+1) &= F_1\xi(\tau)w(\tau), \\ \mathbf{w}_2(\tau+1) &= F_2\xi(\tau)w(\tau), \end{aligned} \tag{20}$$

where $\mathbf{w}_1 = w_1w_2$, $\mathbf{w}_2 = w_3$, $\xi = \xi_1\xi_2$, $F_1 \in \Lambda_1 = \{F_1^1, F_1^2, F_1^3, F_1^4\}$, matrix $F_2 \in \Lambda_2 = \{F_2^1, \ldots, F_2^{2^{32}}\}$, and the cardinality of $|\Lambda_2|$ is 2^{32}. Here, $F_1^1 = \delta_4[3,3,3,3,4,4,4,4,4,3,3,3,3,4,4,4,4,1,3,1,3,2,4,2,4,3,3,3,3,4,4,4,4]$, $F_1^2 = \delta_4[3,3,3,3,4,4,4,4,3,3,3,3,4,4,4,4,1,1,1,1,2,2,2,2,1,3,1,3,2,4,2,4]$, $F_1^3 = \delta_4[1,3,1,3,2,4,2,4,3,3,3,3,4,4,4,4,1,1,1,1,2,2,2,2,1,1,1,1,2,2,2,2]$, and $F_1^4 = \delta_4[1,1,1,1,2,2,2,2,1,3,1,3,2,4,2,4,1,1,1,1,2,2,2,2,1,1,1,1,2,2,2,2]$. Thus, one can obtain its equivalent augmented system of (19): $w(\tau+1) = L\xi(\tau)w(\tau)$, where matrix $L \in \Omega = \{F_1 * F_2, F_1 \in \Lambda_1, F_2 \in \Lambda_2\} = \{L_1, L_2, \ldots, L_{2^{34}}\}$. Due to the high computational complexity of the set Ξ, the detailed information for matrices $L_1, L_2, \ldots, L_{2^{34}}$ is omitted.

A straightforward computation shows that $S_1 \neq 1_{8\times8}, S_2 = 1_{8\times8}, S_3 = 1_{8\times8}, S_4 \neq 1_{8\times8}$. By referring to Theorems 1, 3, 5, and 7, system (19) achieves SCSC and TCSC, while it cannot achieve FCSC or LCSC.

When $F_2 = \delta_2[2,2,2,2,2,1,2,2,1,1,1,2,1,2,1,1,2,1,1,2,1,2,2,2,2,2,1,1,1,2,2,2]$, if $F_1 = F_1^1$, then $L = \delta_8[6,6,6,6,8,7,8,8,5,5,5,6,7,8,7,7,2,5,1,6,3,8,4,8,6,6,5,5,7,8,8,8]$, $C = 1_{8\times8}$; if $F_1 = F_1^2$, then $L = \delta_8[6,6,6,6,8,7,8,8,5,5,5,6,7,8,7,7,2,1,1,2,3,4,4,4,2,6,1,5,3,8,4,8]$, $C = 1_{8\times8}$; if $F_1 = F_1^3$, then $L = \delta_8[2,6,2,6,4,7,4,8,5,5,5,6,7,8,7,7,2,1,1,2,3,4,4,4,2,2,1,1,3,4,4,4]$, $C = 1_{8\times8}$; if $F_1 = F_1^4$, then $L = \delta_8[2,2,2,2,4,3,4,4,1,5,1,6,3,8,3,7,2,1,1,2,3,4,4,4,2,2,1,1,3,4,4,4]$, $C = 1_{8\times8}$. Thus, $S_2 = S_3 = 1_{8\times8}$. By referring to Theorems 3 and 5, system (19) achieves SCSC and TCSC. This implies that, for any $w_0, w_d \in \Delta_{2^\nu}$, and any logical functions f_1, f_2, there is a logical functions f_3 satisfying that state x_d can be reached from initial state w_0. According to Definitions 3 and 4, one can conclude that system (19) achieves SCSC and TCSC, respectively.

When $F_2 = \delta_2[2,2,2,2,2,2,2,2,2,2,2,2,2,2,2,2,1,\underline{1},1,2,1,1,1,2,2,2,1,2,2,2,1,2]$, that is, $w_3(\tau+1) = \overline{\xi}_1(\tau)\wedge[(w_2(\tau)\wedge\xi_2(\tau))\vee(w_3(\tau)\wedge\overline{w}_2(\tau))]$, if $F_1 = F_1^1$, then $L = \delta_8[6,6,6,6,8,8,8,8,6,6,6,6,8,8,8,8,1,5,1,6,3,7,3,8,6,6,5,6,8,8,7,8]$, $C \neq 1_{8\times8}$; if $F_1 = F_1^2$, then $L = \delta_8[6,6,6,6,8,8,8,8,6,6,6,6,8,8,8,8,1,1,1,2,3,3,3,4,2,6,1,6,4,8,3,8]$, $C \neq 1_{8\times8}$; if $F_1 = F_1^3$, then $L = \delta_8[2,6,2,6,4,8,4,8,6,6,6,6,8,8,8,8,1,1,1,2,3,3,3,4,2,2,1,2,4,4,3,4]$, $C \neq 1_{8\times8}$; if $F_1 = F_1^4$, then $L = \delta_8[2,2,2,2,4,4,4,4,2,6,2,6,4,8,4,8,1,1,1,2,3,3,3,4,2,2,1,2,4,4,3,4]$, $C \neq 1_{8\times8}$. Thus, $S_4 \neq 1_{8\times8}$. According to Theorem 7, system (19) cannot achieve LCSC. In this case, there exists a logical function f_3, such that system (19) is not controllable for any logical functions f_1, f_2. By Definition 5, system (19) cannot achieve LCSC.

5. Conclusion

In this paper, SC of BCNs has been systematically addressed, where only partial information of nodes' connections is available. By referring to its equivalent algebraic representation of BCNs, four kinds of SC have been established, based on different issues of nodes' connections. Then, certain criteria for different types of SC have been proposed, by defining its corresponding SC matrix. Finally, a Boolean model of the lactose operon in *Escherichia coli* has been simulated to show the effectiveness of the main theoretical results. One interesting research issue for future works includes SC of probabilistic BCNs with time-variant information of nodes' connections.

Data Availability

No data were used to support this study.

Disclosure

This paper was presented in part at the 11th International Conference on Information Science and Technology (ICIST), Chengdu, China, May 21–23, 2021.

Conflicts of Interest

The authors declare that they have no conflicts of interest.

Acknowledgments

This work was jointly supported by the National Natural Science Foundation of China (61903339), the National Training Programs of Innovation and Entrepreneurship (202010345009), the Guangdong Basic and Applied Basic Research Foundation (2019A1515110234), and the Shenzhen Science and Technology Program (RCBS20200714114921371).

References

[1] S. Kauffman, C. Peterson, B. Samuelsson, and C. Troein, "Random Boolean network models and the yeast transcriptional network," *Proceedings of the National Academy of Sciences*, vol. 100, no. 25, pp. 14796–14799, 2003.

[2] Z. Zhang, T. Leifeld, and P. Zhang, "Reduced-order observer design for Boolean control networks," *IEEE Transactions on Automatic Control*, vol. 65, no. 1, pp. 434–441, 2020.

[3] J. Zhong, Z. Yu, Y. Li, and J. Lu, "State estimation for probabilistic Boolean networks via outputs observation," *IEEE Transactions on Neural Networks and Learning Systems*, pp. 1–13, 2021.

[4] J. Zhong, B. Li, Y. Liu, J. Lu, and W. Gui, "Steady-state design of large-dimensional Boolean networks," *IEEE Transactions on Neural Networks and Learning Systems*, vol. 32, no. 3, pp. 1149–1161, 2021.

[5] M. Meng, J. Lam, J. Feng, and K. Cheung, "Stability and guaranteed cost analysis of time-triggered Boolean networks," *IEEE Transactions on Neural Networks and Learning Systems*, vol. 29, no. 8, pp. 3893–3899, 2018.

[6] S. Zhu, J. Lu, and Y. Liu, "Asymptotical stability of probabilistic Boolean networks with state delays," *IEEE Transactions on Automatic Control*, vol. 65, no. 4, pp. 1779–1784, 2020.

[7] Y. Wu, Y. Guo, and M. Toyoda, "Policy iteration approach to the infinite horizon average optimal control of probabilistic Boolean networks," *IEEE Transactions on Neural Networks and Learning Systems*, pp. 1–15, 2020.

[8] R. Liu, J. Lu, W. X. Zheng, and J. Kurths, "Output feedback control for set stabilization of Boolean control networks," *IEEE Transactions on Neural Networks and Learning Systems*, vol. 31, no. 6, pp. 2129–2139, 2020.

[9] Y. Liu, L. Sun, J. Lu, and J. Liang, "Feedback controller design for the synchronization of Boolean control networks," *IEEE Transactions on Neural Networks and Learning Systems*, vol. 27, no. 9, pp. 1991–1996, 2016.

[10] G. Zhao, Y. Wang, and H. Li, "A matrix approach to the modeling and analysis of networked evolutionary games with time delays," *IEEE/CAA Journal of Automatica Sinica*, vol. 5, no. 4, pp. 818–826, 2018.

[11] F. Li and Y. Tang, "Pinning controllability for a Boolean network with arbitrary disturbance inputs," *IEEE Transactions on Cybernetics*, vol. 51, no. 6, pp. 3338–3347, 2021.

[12] M. Xu, Y. Liu, J. Lou, Z.-G. Wu, and J. Zhong, "Set stabilization of probabilistic Boolean control networks: a sampled-data control approach," *IEEE Transactions on Cybernetics*, vol. 50, no. 8, pp. 3816–3823, 2020.

[13] H. Chen and J. Liang, "Local synchronization of interconnected Boolean networks with stochastic disturbances," *IEEE Transactions on Neural Networks and Learning Systems*, vol. 31, no. 2, pp. 452–463, 2020.

[14] J. Zhong, Y. Liu, J. Lu, and W. Gui, "Pinning control for stabilization of Boolean networks under knock-out perturbation," *IEEE Transactions on Automatic Control*, p. 1, 2021.

[15] L. Lin, J. Zhong, S. Zhu, and J. Lu, "Sampled-data general partial synchronization of Boolean control networks," *Journal of the Franklin Institute*, 2020.

[16] S. Zhu, J. Lu, Y. Lou, and Y. Liu, "Induced-equations-based stability analysis and stabilization of Markovian jump Boolean networks," *IEEE Transactions on Automatic Control*, p. 1, 2020.

[17] S. Zhu, J. Lu, L. Lin, and Y. Liu, "Minimum-time and minimum-triggering control for the observability of stochastic Boolean networks," *IEEE Transactions on Automatic Control*, p. 1, 2021.

[18] L. Sun, W.-k. Ching, and J. Lu, "Stabilization of aperiodic sampled-data Boolean control networks: a delay approach," *IEEE Transactions on Automatic Control*, p. 1, 2021.

[19] D. Cheng, H. Qi, and Z. Li, "Analysis and control of Boolean networks: a semi-tensor product approach," in *Proceedings of the 2009 7th Asian Control Conference*, Hong Kong, China, August 2009.

[20] D. Laschov and M. Margaliot, "Controllability of Boolean control networks via the Perron-Frobenius theory," *Automatica*, vol. 48, no. 6, pp. 1218–1223, 2012.

[21] J. Zhong, B.-w. Li, Y. Liu, and W.-h. Gui, "Output feedback stabilizer design of Boolean networks based on network structure," *Frontiers of Information Technology & Electronic Engineering*, vol. 21, no. 2, pp. 247–259, 2019.

[22] H. Li, S. Wang, X. Li, and G. Zhao, "Perturbation analysis for controllability of logical control networks," *SIAM Journal on Control and Optimization*, vol. 58, no. 6, pp. 3632–3657, 2020.

[23] J. Lu, H. Li, Y. Liu, and F. Li, "Survey on semi-tensor product method with its applications in logical networks and other finite-valued systems," *IET Control Theory & Applications*, vol. 11, no. 13, pp. 2040–2047, 2017.

[24] Y. Wu and T. Shen, "Policy iteration approach to control residual gas fraction in IC engines under the framework of stochastic logical dynamics," *IEEE Transactions on Control Systems Technology*, vol. 25, no. 3, pp. 1100–1107, 2017.

[25] X. Li, X. Yang, and T. Huang, "Persistence of delayed cooperative models: impulsive control method," *Applied Mathematics and Computation*, vol. 342, pp. 130–146, 2019.

[26] X. Li, J. Shen, H. Akca, and R. Rakkiyappan, "LMI-based stability for singularly perturbed nonlinear impulsive differential systems with delays of small parameter," *Applied Mathematics and Computation*, vol. 250, pp. 798–804, 2015.

[27] X. Li, J. Shen, and R. Rakkiyappan, "Persistent impulsive effects on stability of functional differential equations with finite or infinite delay," *Applied Mathematics and Computation*, vol. 329, pp. 14–22, 2018.

[28] T. Akutsu, M. Hayashida, W.-K. Ching, and M. K. Ng, "Control of Boolean networks: hardness results and algorithms for tree structured networks," *Journal of Theoretical Biology*, vol. 244, no. 4, pp. 670–679, 2007.

[29] D. Cheng, H. Qi, Z. Li, and J. B. Liu, "Stability and stabilization of Boolean networks," *International Journal of Robust and Nonlinear Control*, vol. 21, no. 2, pp. 134–156, 2011.

[30] E. Fornasini and M. E. Valcher, "On the periodic trajectories of Boolean control networks," *Automatica*, vol. 49, no. 5, pp. 1506–1509, 2013.

[31] Y. Zhao, H. Qi, and D. Cheng, "Input-state incidence matrix of Boolean control networks and its applications," *Systems & Control Letters*, vol. 59, no. 12, pp. 767–774, 2010.

[32] F. Li, "Pinning control design for the stabilization of Boolean networks," *IEEE Transactions on Neural Networks and Learning Systems*, vol. 27, no. 7, pp. 1585–1590, 2015.

[33] J. Lu, J. Zhong, C. Huang, and J. Cao, "On pinning controllability of Boolean control networks," *IEEE Transactions on Automatic Control*, vol. 61, no. 6, pp. 1658–1663, 2016.

[34] F. Li, "Robust stabilization for a logical system," *IEEE Transactions on Control Systems Technology*, vol. 25, no. 6, pp. 2176–2184, 2017.

[35] E. Sontag, A. Veliz-Cuba, R. Laubenbacher, and A. S. Jarrah, "The effect of negative feedback loops on the dynamics of Boolean networks," *Biophysical Journal*, vol. 95, no. 2, pp. 518–526, 2008.

[36] C. Campbell and R. Albert, "Stabilization of perturbed Boolean network attractors through compensatory interactions," *BMC Systems Biology*, vol. 8, no. 1, p. 53, 2014.

[37] E. Weiss, M. Margaliot, and G. Even, "Minimal controllability of conjunctive Boolean networks is NP-complete," *Automatica*, vol. 92, pp. 56–62, 2018.

[38] S.-i. Azuma, T. Yoshida, and T. Sugie, "Structural oscillatority analysis of Boolean networks," *IEEE Transactions on Control of Network Systems*, vol. 6, no. 2, pp. 464–473, 2019.

[39] Z. Gao, X. Chen, and T. Basar, "Controllability of conjunctive Boolean networks with application to gene regulation," *IEEE Transactions on Control of Network Systems*, vol. 5, no. 2, pp. 770–781, 2018.

[40] S. Liang, H. Li, and S. Wang, "Structural controllability of Boolean control networks with an unknown function structure," *Science China Information Sciences*, vol. 63, no. 11, Article ID 219203, 2020.

[41] S. Tong, J. Zhong, and B. Li, "Structural controllability of Boolean control networks with known nodes coupling relationships," in *Proceedings of the 2021 11th International Conference on Information Science and Technology*, pp. 370–374, Chengdu, China, May 2021.

[42] R. Robeva and T. Hodge, *Mathematical Concepts and Methods in Modern Biology: Using Modern Discrete Models*, Academic Press, Cambridge, MA, USA, 2003.

Hindawi
Complexity
Volume 2021, Article ID 9940257, 13 pages
https://doi.org/10.1155/2021/9940257

Research Article

Adaptive Fuzzy Consensus Tracking Control for Nonlinear Multiagent Systems with Time-Varying Delays and Constraints

Jie Lan[1,2] and Tongyu Xu[1]

[1]*College of Information and Electrical Engineering, Shenyang Agricultural University, Shenyang 110000, Liaoning, China*
[2]*College of Science, Liaoning University of Technology, Jinzhou 121001, Liaoning, China*

Correspondence should be addressed to Tongyu Xu; xutongyu@syau.edu.cn

Received 31 March 2021; Revised 25 April 2021; Accepted 9 June 2021; Published 29 June 2021

Academic Editor: Xiaodi Li

This paper proposes an adaptive fuzzy distributed consensus tracking control scheme for a class of uncertain nonlinear dynamic multiagent systems (MASs) with state time-varying delays and state time-varying constraints. The existing controllers with Lyapunov–Krasovskii functions (LKFs) were not suitable to address time-varying delays and time-varying constraints in nonlinear MASs simultaneously. State constraints further increase the difficulty of controller design and stability analysis, especially for nonstrict feedback systems. Fuzzy logic systems (FLSs) tackle the approximation of unknown dynamics functions and parameters. Especially when the distributed consensus tracking error is infinitely close to the origin, although there is no singular value, it would lead to the rapid growth of control rate or uncontrollability. Constructing appropriate piecewise functions can effectively avoid the above occurrence and accelerate convergence. Based on Lyapunov stability theory and algebraic graph theory, the constructed tracking control can ensure states within defined time-varying constraint bounds and eliminate the influence of time delays. All signals in closed-loop systems can be guaranteed semiglobally uniformly ultimately bounded (SUUB). Finally, the validity of the theoretical method is verified by the simulation.

1. Introduction

Over the past few decades, inspired by flocking behavior in nature, related research on multiagent systems (MASs) had developed rapidly due to potential military and civilian applications. The literature involved many aspects such as satellites, flights, distributed computing, robotics, power systems, surveillance and reconnaissance systems, multi-missile coordinated attacks, and intelligent transportation systems in [1–7]. In [8], based on the urgent needs of intelligent agriculture, the bioinspired coordination protocol was employed to achieve refinement in agricultural management. Consensus control is the most fundamental and most valuable core research of multiagent. The research directions include consensus control [9, 10], tracking control [11], aggregation control [12], formation control [13], and synchronous control [1, 14].

The consensus framework is proposed by Olfatil-Saber and Murray in [14, 15]. Previous literature mainly focused on linear MASs and acquired large numbers of breakthrough achievements. Communication security, information samples, edge maps, and other related methods have also made some achievements in [16–18]. In practical mechanical systems, the problems of inherent nonlinearity and uncertainty would be further enhanced on account of the complex cooperative tasks, the limitation or lack of system dynamic cognition, and so forth. Several remarkable consensus control approaches of linear MASs would not directly be employed to nonlinear MASs. It is indispensable to apply adaptive technology and intelligent control methods to solve uncertain nonlinear distributed MASs.

Adaptive technology had become an effective method to address various nonlinear systems in the literature [19–21]. The neural networks (NNs) [19, 20] were related to the event trigger. The fuzzy logic systems (FLSs) [21–23] solved the finite time of stochastic nonlinear systems in [21]. Distributed nonlinear MASs among the literature [24–27] had been proved distinguished approximation ability to solve the

unknown dynamics. The consensus control was discussed in [9], and consensus tracking control protocols were studied in [24–26]. The multileader consensus control method was researched in [27]. However, the above methods have not involved the problem of state time delays.

The differences in controller performance are often accompanied by state time delays which would reduce the speed of convergence, affect system performance, and lead to instability or ineffectiveness. Meanwhile, once time delays exceed the threshold, they would affect the whole systems. Therefore, time delays would be an important consideration. Some achievements had been made for time delays in uncertain nonlinear systems in [28–31]. Particularly, [30, 31] solved the time delayed switched systems. In [32, 33], LKFs were employed to eliminate time delays in cooperative tracking control with visual leader and leader-following, respectively. Nevertheless, it is obvious that the above omitted the constraints. In particular, it is unavoidable to consider the physical limits and safety performance of each agent, the mutual internal collision avoidance, and other operation restrictions. If ignoring constraints, system performance would be damaged or reduced and even would cause fatal accidents. From a practical point of view, the theoretical study of constraints becomes crucially important in MASs.

In the design of constrained controllers, reliable methods needed to be applied. The Barrier Lyapunov functions have been preferred as the primary candidate functions for designing controllers with constraints. The study in [34] presented the method to indirectly address the constraint by constructing barrier functions. Many BLFs, integral BLF (IBLF), and ABLF based adaptive approximate controllers were designed for different categories of the nonlinear systems in [34–41], and nonlinear MASs in [27, 42]. Integral barrier Lyapunov functions have been employed in [39–41]. The study in [27] proposed an adaptive fuzzy containment control based on the distributed observer and distributed sliding mode estimators with state constraints via multiple BLFs. Note that the above constraint strategies are indirect methods, which are applicable to the case that the feasibility of virtual controllers needs to be satisfied and the constraint boundaries are not infinitesimal. The nonlinear coordinate transformation function was used to construct the constraint completely dependent on states in [43] and [44], and the complicated feasibility analysis was reduced. The authors of [45, 46] proposed the control strategies to solve both the state constraints and state time-varying delays. Therefore, direct constraints on output or states are worth further investigation of the constrained cooperative control.

Motivated by the above analysis, this paper schedules a novel adaptive fuzzy distributed cooperative tracking control approach for a class of uncertain nonlinear MASs with state time-varying delays and constraints. The main contributions of the paper are as follows:

(1) Contrasting with the existing literature on time delays in [32, 33], time delays in the case of time variation are further investigated. The most important one is to overcome the failure of the decomposition theorem in nonstrict feedback. Meanwhile, state time-varying constraints are introduced into distributed time delayed MASs since the state time-varying delays and constraints further increase the difficulty of controller design, which is an enormous challenge.

(2) Distinguished from BLFs, the constraints construct by a nonlinear coordinate transformation in [43] that directly constrain on states, which are applicable to avoid complex feasibility analysis of virtual controllers. The constructed appropriate piecewise functions can effectively avoid the rapid growth and uncontrollability of the control rate and accelerate the convergence when the synchronization error is infinitely close to the origin.

The proposed strategy is aimed at the study of the time-varying state of the agents, which has great realistic significance and further enriches the exploration of the uncertain nonlinear MASs.

The organization of the article is as follows: the presentation and problem of the systems are described in Section 2; the adaptive fuzzy distributed cooperative control design is provided in Section 3; simulation is given in Section 4; and the conclusion is given in Section 5.

2. Systems Presentation and Problem Description

2.1. Systems Description and Problem Presentation. Consider a class of uncertain nonlinear distributed consensus systems with time-varying delay and the ith dynamic is described as

$$\dot{x}_i(t) = f_i(x_i(t)) + \rho_i(x_i(t-\tau_i(t))) + u_i(t), \tag{1}$$

where $x_i(t) = [x_{i1}, x_{i2}, \ldots, x_{im}]^T \in R^m$ represents the state vector of ith agent, $i = 1, 2, \ldots, n$, and n is the number of agents; $f_i(x_i)$ and $\rho_i(x_i(t-\tau_i(t)))$: $R^m \longrightarrow R^m$ are unknown nonlinear continuous vector functions; $\tau_i(t)$ represents the uncertain time-varying delay; and $u_i(t) \in R^m$ is the control input vector.

Assumption 1. $\forall t \geq 0$, the ith unknown smooth nonlinear time delayed function $\rho_i(x_i(t-\tau_i(t)))$, satisfies

$$\left\|\rho_i(x_i(t-\tau_i(t)))\right\| \leq q_i(x_i(t-\tau_i(t))), \tag{2}$$

where $q_i(x_i(t-\tau_i(t)))$ is the known positive smooth function.

Remark 1. The unknown time-varying delays function $\rho(x_i(t-\tau_i(t)))$ contains the time-varying delayed state. The separation technique is used to decompose the unknown with all the time-varying delays into positive continuous functions in order to compensate for the time delays by LKFs in [45].

Assumption 2. The unknown time-varying $\tau_i(t)$ should satisfy the following: (1) the $\dot{\tau}_i(t)$ is bounded by a known constant $\tau_{d\max}$ and $\dot{\tau}_i(t) \leq \tau_{d\max} \leq 1$ and (2) the continuous

$\tau_i(t)$ should be uniformly bounded by a known constant $\tau_{\max}$ and $\tau_i(t) \le \tau_{\max}$ in [33, 45, 46].

The desired reference leader signal is described by the following dynamic function:

$$\dot{x}_l(t) = g_l(t), \tag{3}$$

where $x_l(t) \in R^m$ is the state of reference leader and $g_l(t) \in R^m$ is a bounded smooth vector function.

The time-varying state constraint is considered, and the constraint boundary of ith agent meets requirements as follows:

$$-k_{c_j}(t) < x_{ij}(t) < k_{c_j}(t), \tag{4}$$

where x_{ij} represents the jth state of the ith agent; $j = 1, 2, \ldots, m$; $k_{c_j}(t)$ is a user-defined time-varying bound function in j^{th} state; and $k_c(t) \in R^m$. The initial value should satisfy $-k_{c_j}(0) < x_{ij}(0) < k_{c_j}(0)$.

The requirement of (4) can be satisfied by choosing a nonlinear coordinate transformation as follows:

$$s_{ij}(t) = \frac{x_{ij}(t)}{\left(k_{c_j}(t) + x_{ij}(t)\right)\left(k_{c_j}(t) - x_{ij}(t)\right)}, \tag{5}$$

where $s_{ij}(t)$ is a constructed state transition that converts the original $x_{ij}(t)$ bounded within $(-k_{c_j}(t), k_{c_j}(t))$ into a nonconstrained state, $s_i(t) = [s_{i1}, s_{i2}, \ldots, s_{im}]^T \in R^m$.

Then, (5) satisfies

$$\begin{cases} \lim\limits_{x_i(t) \longrightarrow -k_c(t)} s_i(t) = -\infty, \\ \lim\limits_{x_i(t) \longrightarrow k_c(t)} s_i(t) = +\infty. \end{cases} \tag{6}$$

Take the derivative of $s_{ij}(t)$ as follows:

$$\dot{s}_{ij}(t) = \frac{\partial s_{ij}(t)}{\partial x_{ij}(t)} \dot{x}_{ij}(t) + \frac{\partial s_{ij}(t)}{\partial k_{c_j}(t)} \dot{k}_{c_j}(t), \tag{7}$$

where $\partial s_{ij}(t)/\partial x_{ij}(t) = k_{c_j}^2(t) + x_{ij}^2(t)/(k_{c_j}^2(t) - x_{ij}^2(t))^2$ and $\partial s_{ij}(t)/\partial k_{c_j}(t) = -2x_{ij}(t)k_{c_j}(t)/(k_{c_j}^2(t) - x_{ij}^2(t))^2$.

The state of the leader in (3) can be transformed by the same form of (5); it can be expressed as

$$\alpha_{lj}(t) = \frac{x_{lj}(t)}{\left(k_{c_j}(t) + x_{lj}(t)\right)\left(k_{c_j}(t) - x_{lj}(t)\right)}, \tag{8}$$

where $\alpha_{lj}(t)$ is a state transition to transform the constrained $x_{lj}(t)$ within $(-k_{c_j}(t), k_{c_j}(t))$ into an unconstrained state, $\alpha_i(t) = [\alpha_{i1}, \alpha_{i2}, \ldots, \alpha_{im}]^T \in R^m$. Then, (8) satisfies

$$\begin{cases} \lim\limits_{x_l(t) \longrightarrow -k_c(t)} \alpha_l(t) = -\infty, \\ \lim\limits_{x_l(t) \longrightarrow k_c(t)} \alpha_l(t) = +\infty. \end{cases} \tag{9}$$

Take the derivative of (8) as follows:

$$\dot{\alpha}_{lj}(t) = \frac{\partial \alpha_{lj}(t)}{\partial x_{lj}(t)} \dot{x}_{lj}(t) + \frac{\partial \alpha_{lj}(t)}{\partial k_{c_j}(t)} \dot{k}_{c_j}(t), \tag{10}$$

where $\partial \alpha_{lj}(t)/\partial x_{lj}(t) = k_{c_j}^2(t) + x_{lj}^2(t)/(k_{c_j}^2(t) - x_{lj}^2(t))^2$ and $\partial \alpha_{lj}(t)/\partial k_{c_j}(t) = -2x_{lj}(t)k_{c_j}(t)/(k_{c_j}^2(t) - x_{lj}^2(t))^2$.

Remark 2. The states x_i and x_l are converted into s_i and α_l, respectively; $\partial s_{ij}(t)/\partial x_{ij}(t) > 0$ and $\partial \alpha_{lj}(t)/\partial x_{lj}(t) > 0$ are invertible functions; and $s_{ij}(t)$ and $\alpha_{lj}(t)$ are monotonically increasing. Just proving $s_{ij}(t)$ and $\alpha_{lj}(t)$ are bounded, by criteria of monotone bounded, the original states x_i and x_l would converge and satisfy the constraint region.

Assumption 3. The time-varying bound vector functions $k_c(t)$ and $\dot{k}_c(t)$ satisfy the following: $\forall t \ge 0$; there exist positive constant vectors $K_c \in R^m$ and $K_c^1 \in R^m$ that satisfy $|k_{c_j}(t)| \le K_{c_j}$ and its time derivative $\dot{k}_{c_j}(t)$ satisfies $|\dot{k}_{c_j}(t)| \le K_{c_j}^1$.

Remark 3. In numbers of practical cooperative control of multiagent systems, inevitably, constraints need to be addressed due to physical limitations or performance. If the constraints were ignored, the systems may be degraded or damaged by interagent influences, and even fatal accidents would occur. State constraints are more effective in solving states of transient or steady real systems than only with output constraints. The control process is time-varying, so it is significant to study the time-varying full state constraints.

Remark 4. The constraints based on BLFs (or IBLFs) require additional complex stability analysis to ensure the feasibility conditions of virtual controllers. The state-dependent transition method in [43, 44] which can circumvent the above problems, flexibly solve initial conditions, and reduce the difficulty of stability analysis.

Remark 5. The nonlinear coordinate transformation function is constructed and purely dependent on the constraint states. Introducing a new coordinate transformation for the backstepping design of MASs, it directly responses to state constraints and completely avoids the harsh feasibility conditions. This will get rid of the tedious feasibility verification. Let the designer have more freedom and be humanized to choose the designed parameters in implementations. Apply a wider range of initial conditions.

This paper only shows the feasibility and effectiveness of constructing state time-varying constraints to distributed nonlinear and uncertain time-varying delayed MASs. The asymmetric forms would be further discussed in other papers.

2.1.1. Control Objective. Devise an adaptive fuzzy decentralized tracking controller u_i that, for the dynamic of agents described in (1) and (3), can guarantee the following:

(i) All followers converge to the desired small neighborhood around the origin by tracking the leader. (ii) The full states would not violate the time-varying constraint boundaries in (5) and (8). (iii) All the signals in the closed-loop systems are SUUB.

The following assumptions and lemmas should be satisfied in order to establish a cooperative control objective.

2.2. Algebraic Graph Theory and Notations. An undirected connected topology expresses as $G = (V, E, A)$, where

$V = \{v_1, v_2, \ldots, v_n\}$ denotes a set of nodes and v_i is i^{th} node. $E \subseteq V \times V$ denotes the set of edges, $\wp_{ij} = (v_i, v_j) \in E$ refers to the edge from node i to node j, and $\wp_{ij} = \wp_{ji}$. $A = [a_{ij}] \in R^{n\times n}$ is a weighted adjacency matrix that a weight corresponds to the edge, and when $\wp_{ij} \in R^{n\times n}$, $a_{ij} = 1$. Otherwise, $a_{ij} = 0$. In particular, define $a_{ii} = 0$.

The graph Laplacian matrix L is given in the following definition:

$$L = D - A, \tag{11}$$

where $L = [l_{ij}] \subset R^{n\times n}$; $D = \text{diag}\{d_1, d_2, \ldots, d_n\} \in R^{n\times n}$ defines an in-degree matrix; $d_i = \sum_{j\in N_i} a_{ij}$ represents the in-degree of node i; $N_i = \{j\colon (j, i) \in E\}$; L is an irreducible matrix; and $[1, 1, \ldots, 1]^T \in R^n$ is a right eigenvector with the eigenvalue zero.

Lemma 1. *The graph Laplacian matrix L is a semidefinite symmetric matrix; all eigenvalues are nonnegative real; and its n real eigenvalues can be listed in ascending order as follows:*

$$0 = \lambda_1 < \lambda_2 \le \lambda_3 \le \ldots \le \lambda_n \le C, \tag{12}$$

where $C = 2(\max_{1\le i\le n} d_i)$ is algebraic connectivity and it is used to analyze the rate of consensus convergence.

Lemma 2. *$\forall t > 0$, the continuous function $V(t)$ satisfies $V(t) > 0$, and $V(0)$ is bounded. If it can prove the inequality $\dot{V}(t) \le -\ell V(t) + \hbar$ where $\ell > 0$, $\hbar > 0$, then*

$$\dot{V}(t) \le V(0)e^{-\ell t} + \frac{\hbar}{\ell}\left(1 - e^{-\ell t}\right). \tag{13}$$

Assumption 4. In the graph topology G, for the leader, there is at least one directed path from the root node to follower nodes.

2.3. Distributed Controller. The proposed distributed control algorithm can make arbitrary i^{th} agent feedback to itself and communicate with neighbor agents via adjacent matrix. Since fixed topology graphs are the basis for different types of switching connection topology and are widely applied such as [27, 28], this paper is based on the fixed topological form.

The synchronization error $e_i(t) \in R^m$ consists of the ith local consensus error and the tracking error among the leader and followers, and that can be defined as follows:

$$e_i(t) = \sum_{j=1}^{N_i} a_{ij}\left(s_i(t) - s_j(t)\right) + b_i\left(s_i(t) - \alpha_l(t)\right), \tag{14}$$

where a_{ij} represents the element in adjacency matrix A. b_i is the communication weight when only i^{th} agent exchanges information with leader $b_i > 0$; otherwise $b_i = 0$, and $B = \text{diag}\{b_1, b_2, \ldots, b_n\}$ is the communication weight matrix and satisfies $b_1 + b_2 + \cdots + b_n > 0$:

Let

$$\widetilde{L} = L + B, \tag{15}$$

where $\widetilde{L}$ is a symmetrical positive definite matrix and its real eigenvalues $\widetilde{\lambda}_1, \widetilde{\lambda}_2, \ldots, \widetilde{\lambda}_n$ satisfy Lemma 1.

Based on the matrix theory and graph theory, it can be readily concluded that zero is an m−multiplicity eigenvalue of $\widetilde{L} \otimes I_m$; $\otimes$ and I_m, respectively, stand for the Kronecker product and identity matrix of dimension $m \times m$. Let $\varphi_{11}, \varphi_{12}, \ldots, \varphi_{1m}, \ldots, \varphi_{2m}, \ldots, \varphi_{nm}$ be the eigenvectors and $\widetilde{\lambda}_2, \ldots, \widetilde{\lambda}_n$ eigenvalues of $\widetilde{L} \otimes I_m$ such there can be a set of orthogonal bases of R^{nm}. The definition is given by graph theory:

$$\widetilde{L} \otimes I_m = P\Lambda P^T, \tag{16}$$

where $P^T P = \text{PP}^T = I_{nm}$, I_{nm} denoting identity matrix of dimension $nm \times nm$ and $P = [\varphi_{11}, \varphi_{12}, \ldots \varphi_{\text{nm}}] \in R^{nm\times nm}$.

Define the tracking error vector as the following form:

$$\varsigma_i(t) = s_i(t) - \alpha_l(t), \tag{17}$$

where $\varsigma_i(t) = [\varsigma_{i1}(t), \varsigma_{i2}(t), \ldots, \varsigma_{im}(t)]^T \in R^m$ represents the tracking error between the ith follower agent and the leader agent. Then, (14) can be rewritten as

$$e_i(t) = \sum_{j=1}^{N_i} a_{ij}\left(\varsigma_i(t) - \varsigma_j(t)\right) + b_i\varsigma_i(t), \tag{18}$$

where $e_i(t) = [e_{i1}(t), e_{i2}(t), \ldots, e_{im}(t)]^T$.

The unknown functions and variables in multiagent systems can be approximated by FLSs as follows:

$$F_{ij}\left(X_{ij}\right) = \omega_{ij}^T \Psi_{ij}\left(X_{ij}\right) + \varepsilon_{ij}, \tag{19}$$

where $\omega_{ij} \in R^{l_j}$ is the optimal fuzzy weight vector, l_j denotes the number of fuzzy rules, $\Psi_{ij}(X_{ij})$ is the fuzzy basis vector function, ε_{ij} shows estimation error satisfied $\|\varepsilon_{ij}\| \le \overline{\varepsilon}_{ij}$, and $\overline{\varepsilon}_{ij}$ is an arbitrary indeterminate positive constant.

3. Adaptive Fuzzy Distributed Cooperative Control Design

In this section, an adaptive fuzzy distributed cooperative control algorithm will be designed for (1) and (3). Define the following candidate function:

$$V_\omega = \frac{1}{2}\varsigma(t)^T Q\varsigma(t) + \frac{1}{2}\sum_{i=1}^{n} tr\left[\widetilde{\omega}_i^T \Gamma_i^{-1} \widetilde{\omega}_i\right], \tag{20}$$

where $\varsigma(t) = (\varsigma_1^T(t), \varsigma_2^T(t), \ldots, \varsigma_n^T(t))^T \in R^{\text{nm}}$ is the consensus error vector that $\varsigma_i(t)$ has defined in (17), then $\varsigma(t) = (\widetilde{L} \otimes I_m)e(t)$, $Q = P\widehat{\Lambda}^{-1}P^T$, $\widetilde{\omega}_{ij} = \omega_{ij} - \widehat{\omega}_{ij}$, $\widehat{\omega}_{ij}$ is the estimate of adaptive laws, and ω_{ij} and $\widehat{\omega}_{ij}$ will be given later.

The inequality can be described as follows:

$$\frac{\lambda_{\min}(Q)}{2} \le \frac{1}{2}\varsigma(t)^T Q\varsigma(t) \le \frac{\lambda_{\max}(Q)}{2}, \tag{21}$$

where $\lambda_{\min}(Q)$ and $\lambda_{\max}(Q)$ are the smallest and largest eigenvalues of Q, respectively. From (16), it yields

$$\frac{1}{2}\left(\varsigma(t)^T Q\varsigma(t)\right) = \frac{1}{2}\, e^T(t)\left(\tilde{L}\otimes I_m\right)^T P\hat{\Lambda}^{-1}P^T\left(\tilde{L}\otimes I_m\right)e(t) = \frac{1}{2}\, e^T(t)P\Lambda P^T P\hat{\Lambda}^{-1}P^T P\Lambda P^T e(t)$$
$$= \frac{1}{2}\, e^T(t)\left(\tilde{L}\otimes I_m\right)e(t) = \frac{1}{2}\varsigma(t)^T e(t) = \frac{1}{2}\sum_{i=1}^{n}\varsigma_i^T(t)e_i(t), \tag{22}$$

where $\Lambda = \mathrm{diag}\left\{0I_m, \tilde{\lambda}_2 I_m, \ldots, \tilde{\lambda}_n I_m\right\}$.

Redefine the Lyapunov candidate function as follows:

$$V_\omega = \frac{1}{2}\sum_{i=1}^{n}\varsigma_i^T(t)e_i(t) + \frac{1}{2}\sum_{i=1}^{n} tr\left[\tilde{\omega}_i^T\Gamma_i^{-1}\tilde{\omega}_i\right]. \tag{23}$$

Take the derivative of (23). Then, $\dot{V}_\omega$ can yield

$$\dot{V}_\omega = \frac{1}{2}\dot{\varsigma}(t)^T Q\varsigma(t) + \frac{1}{2}\varsigma(t)^T Q\dot{\varsigma}(t) + \frac{1}{2}\sum_{i=1}^{n} tr\left[\dot{\tilde{\omega}}_i^T\Gamma_i^{-1}\tilde{\omega}_i\right] + \frac{1}{2}\sum_{i=1}^{n} tr\left[\tilde{\omega}_i^T\Gamma_i^{-1}\dot{\tilde{\omega}}_i\right] = \sum_{i=1}^{n} e_i^T(t)\dot{\varsigma}_i(t) - \sum_{i=1}^{n} tr\left[\tilde{\omega}_i^T\Gamma_i^{-1}\dot{\hat{\omega}}_i\right]. \tag{24}$$

$\dot{V}_\omega$ can be written as follows:

$$\dot{V}_\omega = \sum_{j=1}^{m}\dot{V}_{\omega j} = \sum_{j=1}^{m}\sum_{i=1}^{n}\left[e_{ij}^T(t)\dot{\varsigma}_{ij}(t) - \tilde{\omega}_{ij}^T\Gamma_{ij}^{-1}\dot{\hat{\omega}}_{ij}\right]. \tag{25}$$

The derivative of $\varsigma_{ij}(t)$ in the form of (17) can be described as

$$\dot{\varsigma}_{ij}(t) = \frac{\partial s_{ij}(t)}{\partial x_{ij}(t)}\dot{x}_{ij}(t) - \frac{\partial \alpha_{lj}(t)}{\partial x_{lj}(t)}\dot{x}_{lj}(t) + \left(\frac{\partial s_{ij}(t)}{\partial k_{c_j}(t)} - \frac{\partial \alpha_{lj}(t)}{\partial k_{c_j}(t)}\right)\dot{k}_{c_j}(t). \tag{26}$$

Combining systems (1), (3), and (26) into $\dot{V}_{\omega j}$ yields

$$\dot{V}_{\omega j} \le \sum_{i=1}^{n} e_{ij}^T(t)\left\{\frac{\partial s_{ij}(t)}{\partial x_{ij}(t)}\left[u_{ij}(t) + \rho_{ij}\left(x_{ij}(t-\tau_i(t))\right) + f_{ij}\left(x_{ij}(t)\right)\right] + K_{ij}(t) - \frac{\partial \alpha_{lj}(t)}{\partial x_{lj}(t)}g_{lj}(t)\right\} - \sum_{i=1}^{n}\left(\tilde{\omega}_{ij}^T\Gamma_{ij}^{-1}\dot{\hat{\omega}}_{ij}\right), \tag{27}$$

where $K_{ij}(t)$ is i^{th} time-varying gain described as follows:

$$K_{ij}(t) = \sup\sqrt{\left(\frac{\partial s_{ij}(t)}{\partial k_{c_j}(t)}\dot{k}_{c_j}(t)\right)^2 + \left(\frac{\partial \alpha_{l_j}(t)}{\partial k_{c_j}(t)}\dot{k}_{c_j}(t)\right)^2 + \beta_{ij}}. \tag{28}$$

β_{ij} is a positive parameter to be given.

Using Young's inequality and Assumption 1, in order to separate e_{ij} and uncertainties $\rho_{ij}(x_{ij}(t-\tau_i(t)))$, the inequality gets

$$e_{ij}^T(t)\frac{\partial s_{ij}(t)}{\partial x_{ij}(t)}\rho_{ij}\left(x_{ij}(t-\tau_i(t))\right) \le \frac{1}{2\sqrt{\nu}}\left\|e_{ij}(t)\right\|^2 M_{ij}^2 + \frac{1}{2}\nu q_{ij}^2\left(x_{ij}(t-\tau_i(t))\right), \tag{29}$$

where $\nu = 1 - \tau_{d\max}$ has been illustrated in Remark 4 and $M_{ij} = \|\partial s_{ij}(t)/\partial x_{ij}(t)\|$.

The unknown smooth function $F_{ij}(X_{ij})$ is approximated by FLSs to tackle the unknown dynamics functions and parameters. $F_{ij}(X_{ij})$ is denoted as

$$F_{ij}\left(X_{ij}\right) = f_{ij}\left(x_{ij}(t)\right) + \frac{1}{2}\frac{1}{\sqrt{\nu}}e_{ij}(t)\frac{\partial s_{ij}(t)}{\partial x_{ij}(t)}, \tag{30}$$

where $X_{i1} = [x_{i1}, x_{i2}, k_{c_1}, e_{i1}]^T$, $X_{i2} = [x_{i1}, x_{i2}, k_{c_2}, e_{i2}]^T$, and $\|e_{ij}(t)\|^2 M_{ij}^2$ takes the norm of $e_{ij}(t)\partial s_{ij}(t)/\partial x_{ij}(t)$ in (29).

Equation (30) can be estimated by (19) as follows:

$$F_{ij}\left(X_{ij}\right) = \omega_{ij}^T\Psi_{ij}\left(X_{ij}\right) + \varepsilon_{ij}. \tag{31}$$

Combining (28), (29), and (30) by FLSs, then (27) can yield

$$\dot{V}_{\omega j} \le \sum_{i=1}^{n} e_{ij}^{T}(t)\left[\frac{\partial s_{ij}(t)}{\partial x_{ij}(t)}\left(u_{ij}(t)+\omega_{ij}^{T}\Psi_{ij}\left(X_{ij}\right)+\varepsilon_{ij}\right)+U_{ij}(t)\right]+\frac{1}{2}\sum_{i=1}^{n} \nu q_{ij}^{2}\left(x_{ij}\left(t-\tau_{i}(t)\right)\right)-\sum_{i=1}^{n}\left(\tilde{\omega}_{ij}^{T}\Gamma_{ij}^{-1}\dot{\hat{\omega}}_{ij}\right), \tag{32}$$

where $U_{ij}(t) = K_{ij}(t) - \partial\alpha_{lj}(t)/\partial x_{lj}(t) g_{lj}(t)$.

By using Young's inequality, we obtain the following:

$$\sum_{i=1}^{n} e_{ij}^{T}(t)\frac{\partial s_{ij}(t)}{\partial x_{ij}(t)}\varepsilon_{ij} \le \frac{1}{2}\sum_{i=1}^{n}\left\|e_{ij}(t)\right\|^{2} M_{ij}^{2}+\frac{1}{2}\sum_{i=1}^{n}\bar{\varepsilon}_{ij}^{2}. \tag{33}$$

Combining (33) into (32), we obtain

$$\begin{aligned}\dot{V}_{\omega j} \le & \sum_{i=1}^{n} e_{ij}^{T}(t)\left[\frac{\partial s_{ij}(t)}{\partial x_{ij}(t)}\left(u_{ij}(t)+\omega_{ij}^{T}\Psi_{ij}\left(X_{ij}\right)\right)+U_{ij}(t)\right]+\frac{1}{2}\sum_{i=1}^{n} \nu q_{ij}^{2}\left(x_{ij}\left(t-\tau_{i}(t)\right)\right) \\ & -\sum_{i=1}^{n}\left(\tilde{\omega}_{ij}^{T}\Gamma_{ij}^{-1}\dot{\hat{\omega}}_{ij}\right)+\frac{1}{2}\sum_{i=1}^{n}\left\|e_{ij}(t)\right\|^{2} M_{ij}^{2}+\sum_{i=1}^{n}\frac{1}{2}\bar{\varepsilon}_{ij}^{2}.\end{aligned} \tag{34}$$

The Lyapunov–Krasovskii function is constructed to compensate uncertain time-varying delays as follows:

$$V_{\rho}(t)=\sum_{i=1}^{m} V_{\rho j}(t)=\frac{1}{2}\sum_{i=1}^{m}\sum_{i=1}^{n}\int_{t-\tau_{i}(t)}^{t}\beta_{ij}\left(x_{ij}(s)\right)ds, \tag{35}$$

where $\beta_{ij}(x_{ij}(s)) \le q_{ij}^{2}(x_{ij}(s))$ has been defined under Assumption 1.

Take the derivative of $V_{\rho j}(t)$. It obtains

$$\dot{V}_{\rho j}(t) \le \frac{1}{2}\sum_{i=1}^{n} q_{ij}^{2}\left(x_{ij}(t)\right)-\frac{1}{2}\nu\sum_{i=1}^{n} q_{ij}^{2}\left(x_{ij}\left(t-\tau_{i}(t)\right)\right). \tag{36}$$

The Lyapunov function candidate is chosen by combining (23) and (35) as follows:

$$\begin{aligned} V(t) &= V_{\omega}+V_{\rho}(t), \\ \sum_{j=1}^{m} V_{ij}(t) &= \sum_{j=1}^{m} V_{\omega j}+\sum_{i=1}^{m} V_{\rho j}(t), \\ \sum_{j=1}^{m} V_{ij}(t) &= \sum_{j=1}^{m}\left(\frac{1}{2}\sum_{i=1}^{n}\varsigma_{ij}^{T}(t) e_{ij}(t)+\frac{1}{2}\sum_{i=1}^{n}\left(\tilde{\omega}_{ij}^{T}\Gamma_{ij}^{-1}\tilde{\omega}_{ij}\right)\right)+\frac{1}{2}\sum_{j=1}^{m}\sum_{i=1}^{n}\int_{t-\tau_{i}(t)}^{t}\beta_{ij}\left(x_{ij}(s)\right)ds.\end{aligned} \tag{37}$$

According to (34) and (36), the derivative of $V_{ij}(t)$ can obtain

$$\dot{V}_{ij} \le \sum_{i=1}^{n} e_{ij}^{T}(t)\left[\frac{\partial s_{ij}(t)}{\partial x_{ij}(t)}\left(u_{ij}(t)+\omega_{ij}^{T}\Psi_{ij}\left(X_{ij}\right)\right)+U_{ij}(t)\right]+\frac{1}{2}\sum_{i=1}^{n} q_{ij}^{2}\left(x_{ij}(t)\right)-\sum_{i=1}^{n}\left(\tilde{\omega}_{ij}^{T}\Gamma_{ij}^{-1}\dot{\hat{\omega}}_{ij}\right)+\frac{1}{2}\sum_{i=1}^{n}\left\|e_{ij}(t)\right\|^{2} M_{ij}^{2}+\frac{1}{2}\sum_{i=1}^{n}\bar{\varepsilon}_{ij}^{2}. \tag{38}$$

The designed decentralized controller has been described as follows:

$$u_{ij}(t)=\begin{cases}\left(\dfrac{\partial s_{ij}(t)}{\partial x_{ij}(t)}\right)^{-1}\left[-k_{ij}(t) e_{ij}(t)-\hat{\omega}_{ij}^{T}\Psi_{ij}\left(X_{ij}\right)\right. \\ \left.-\dfrac{1}{2}\dfrac{\left\|e_{ij}(t)\right\| q_{ij}^{2}\left(x_{ij}(t)\right)}{\left\|e_{ij}(t)\right\|^{2}+\chi_{ij}}-U_{ij}(t)\right], & e_{ij}(t) \in \Omega_{\delta_{i}}^{c}, \\ 0, & e_{ij}(t) \in \Omega_{\delta_{i}},\end{cases} \tag{39}$$

where $\partial s_{ij}(t)/\partial x_{ij}(t)$ is a monotonically increasing function and the inverse must exist in Remark 1. $k_{ij}(t)$ is the controller gain that will be defined later. $\Omega_{\delta_i} = \{e_{ij}(t) | \|e_{ij}(t)\| < \delta_i\}$ is a compact set, $\Omega_{\delta_i}^c$ is its complement set, δ_i is an arbitrarily positive real number, and its definition will be given later. Once in Ω_{δ_i} near the origin, there is no need to impose on control. The piecewise function χ_{ij} satisfies the following:

$$\chi_{ij} = \begin{cases} 1, & e_{ij}(t) \in \Omega_{\delta_i}^c, \\ 0, & e_{ij}(t) \in \Omega_{\delta_i}. \end{cases} \tag{40}$$

Remark 6. Particularly, singularities may occur when $e_i(t) = [0]_m$ in cooperative control strategy in $1/2\|e_{ij}(t)\|^{-1} q_{ij}^2(x_{ij}(t))$. The function $\lim_{e_{ij}(t)\longrightarrow 0} e_{ij}^{-1}(t) = \infty$ means the limit of synchronization error function infinitely approaches the sphere near the origin. Even though it is not equal to zero and there is no singular value, it is still uncontrollable. Therefore, (40) is designed to prevent the occurrence and accelerate the convergence rate.

Figure 1 is the flow diagram of the control approach for a class of uncertain nonlinear MASs with state time-varying constraints and delays, which can clearly guide the construction process of the control strategy.

From Remark 3, the adaptive law for $\widehat{\omega}_{ij}$ is designed as follows:

$$\dot{\widehat{\omega}}_{ij} = \Gamma_{ij}\{e_{ij}(t)\Psi_{ij}(X_{ij}) - \kappa_{ij}\widehat{\omega}_{ij}\}, \tag{41}$$

where Γ_{ij} is a positive symmetric gain. κ_{ij} is the positive constant to improve the approximation error robustness of FLSs.

When $e_{ij}(t) \in \Omega_{\delta_i}^c$, combining (39), (40), and (41) into (38) yields

$$\dot{V}_{ij}(t) \le \sum_{i=1}^{n} -k_{ij}(t)\|e_{ij}(t)\|^2 + \sum_{i=1}^{n} \kappa_{ij}\widetilde{\omega}_{ij}^T\widehat{\omega}_{ij} + \frac{1}{2}\sum_{i=1}^{n}\|e_{ij}(t)\|^2 M_{ij}^2 + \frac{1}{2}\sum_{i=1}^{n}\bar{\varepsilon}_{ij}^2. \tag{42}$$

Using Young's inequality, it follows that

$$\widetilde{\omega}_{ij}^T\widehat{\omega}_{ij} = \widetilde{\omega}_{ij}^T(\omega_{ij} - \widetilde{\omega}_{ij}) \le \frac{1}{2}\omega_{ij}^2 - \frac{1}{2}\widetilde{\omega}_{ij}^T\widetilde{\omega}_{ij}. \tag{43}$$

According to (43) into (42), then $\dot{V}_{ij}(t)$ obtains

$$\dot{V}_{ij}(t) \le \sum_{i=1}^{n}\left[-k_{ij}(t)\|e_{ij}(t)\|^2 + \frac{1}{2}\sum_{i=1}^{n} M_{ij}^2\|e_{ij}(t)\|^2\right] - \frac{1}{2}\kappa_{ij}\widetilde{\omega}_{ij}^T\widetilde{\omega}_{ij} + \eta_{j2}, \tag{44}$$

where $\eta_{j2} = 1/2\sum_{i=1}^{n}\kappa_{ij}\omega_{ij}^2 + 1/2\sum_{i=1}^{n}\bar{\varepsilon}_{ij}^2$.

The definition of controller gain $k_{ij}(t)$ is described briefly as follows:

$$k_{ij}(t) = k_{ij}^0 + k_{ij}^1(t), \tag{45}$$

where $k_{ij}^0 \ge 1/2M_{ij}^2$, and $k_{ij}^1(t)$ satisfies

$$k_{ij}^1(t) = \frac{\gamma_{ij}}{2}\left[\lambda_{\max}(Q) + \frac{1}{\|e_{ij}(t)\|^2 + \chi_{ij}}\int_{t-\tau_{\max}}^{t}\beta_{ij}(x_{ij}(s))ds\right]. \tag{46}$$

Substitute (45) and (46) into (44); it yields

$$\dot{V}_{ij}(t) \le -\frac{1}{2}\sum_{i=1}^{n}\gamma_{ij}\lambda_{\max}(Q)\|e_{ij}(t)\|^2 - \frac{1}{2}\sum_{i=1}^{n}\frac{\kappa_{ij}}{\Gamma_{ij}^{-1}}(\widetilde{\omega}_{ij}^T\Gamma_{ij}^{-1}\widetilde{\omega}_{ij}) - \frac{1}{2}\sum_{i=1}^{n}\gamma_{ij}\int_{t-\tau_{\max}}^{t}\beta_{ij}(x_{ij}(s))ds + \eta_{j2}, \tag{47}$$

where $\beta_{ij}(x_{ij}(s)) > 0$ has been defined; therefore, the integral inequality satisfies

$$\frac{1}{2}\sum_{i=1}^{n}\int_{t-\tau_{\max}}^{t}\beta_{ij}(x_{ij}(s))ds \ge \frac{1}{2}\sum_{i=1}^{n}\int_{t-\tau_i(t)}^{t}\beta_{ij}(x_{ij}(s))ds. \tag{48}$$

By (48), $\dot{V}_{ij}(t)$ can obtain

$$\dot{V}_{ij}(t) \le -\frac{1}{2}\sum_{i=1}^{n}\gamma_{ij}\lambda_{\max}(Q)\|e_{ij}(t)\|^2 - \frac{1}{2}\sum_{i=1}^{n}\frac{\kappa_{ij}}{\Gamma_{ij}^{-1}}(\widetilde{\omega}_{ij}^T\Gamma_{ij}^{-1}\widetilde{\omega}_{ij}) - \frac{1}{2}\sum_{i=1}^{n}\gamma_{ij}\int_{t-\tau_i(t)}^{t}\beta_{ij}(x_{ij}(s))ds + \eta_{j2}. \tag{49}$$

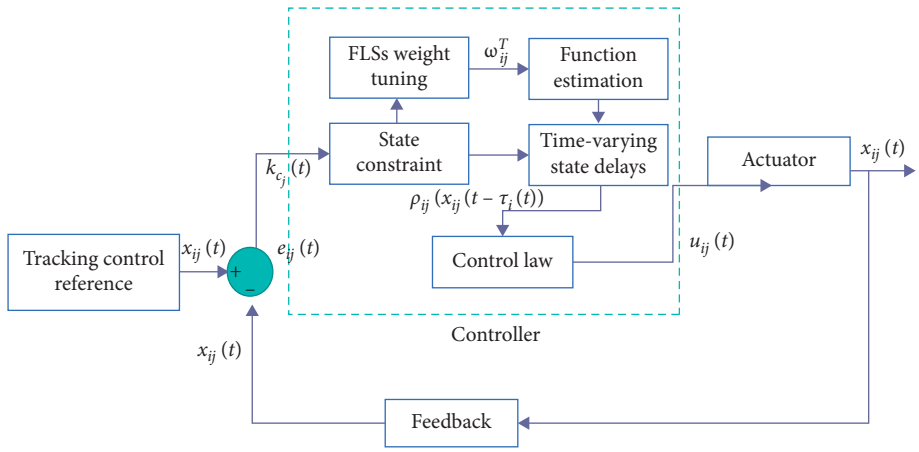

Figure 1: The block diagram illustrating the flow of the proposed control approach.

From (21), $\dot{V}_{ij}(t)$ yields

$$\dot{V}_{ij}(t) \leq -\eta_{j1} V_{ij}(t) + \eta_{j2}, \tag{50}$$

where $\eta_{j1} = \min_{1\leq i\leq n}\{\gamma_{ij}, \quad \kappa_{ij}/\Gamma_{ij}^{-1}$.

Then, compute this sum and integral of $\dot{V}_{ij}(t)$ obtained that

$$V(t) \leq V(0)e^{-\eta_1 t} + \left[\frac{\eta_2}{\eta_1}\left(1 - e^{-\eta_1 t}\right)\right], \tag{51}$$

where $\eta_1 = \min_{1\leq j\leq m} \eta_{j1}$, $\eta_2 = \sum_{j=1}^{m} \eta_{j2}$.

Theorem 1. *For nonlinear dynamics (1) and (3) with Assumptions 1–3 and the controller gains in (39), the adaptive law is given by (41). By selecting appropriate parameters, the adaptive fuzzy cooperative control strategy can guarantee the following:*

(1) The synchronization error converges to the desired small neighborhood near the origin

(2) The state time-varying constraints for agents given by (5) and (8) would not be violated

(3) The time-varying delays can be compensated by LKFs. The signals in the closed-loop systems can be verified SUUB

Proof. When $e_{ij}(t) \in \Omega_{\delta_i}^c$, choosing the Lyapunov function in (37), the derivative of $V(t)$ is as follows:

$$\begin{aligned}\dot{V}(t) \leq \sum_{j=1}^{m}\Bigg\{&\sum_{i=1}^{n} \bar{e}_{ij}^T(t)\left\{\frac{\partial s_{ij}(t)}{\partial x_{ij}(t)}\left[u_{ij}(t) + \rho_{ij}\left(x_{ij}(t-\tau_i(t)) + f_{ij}\left(x_{ij}t\right)\right)\right] + U_{ij}(t)\right\} \\ &- \sum_{i=1}^{n}\left(\tilde{\omega}_{ij}^T \Gamma_{ij}^{-1}\dot{\hat{\omega}}_{ij}\right) + \sum_{i=1}^{n} q_i^2(x_i(t)) - \frac{1}{2}\nu\sum_{i=1}^{n} q_i^2(x_i(t-\tau_i(t)))\Bigg\}.\end{aligned} \tag{52}$$

Applying the results in (28), (29), (30), (33), and (36) into (52), it obtains

$$\dot{V}(t) \leq \sum_{j=1}^{m}\left\{\sum_{i=1}^{n} e_{ij}^T(t)\left[\frac{\partial s_{ij}(t)}{\partial x_{ij}(t)}\left(u_{ij}(t) + \omega_{ij}^T\Psi_{ij}\left(X_{ij}\right)\right) + U_{ij}(t)\right] + \sum_{i=1}^{n}\frac{1}{2}q_{ij}^2\left(x_{ij}(t)\right) - \sum_{i=1}^{n}\left(\tilde{\omega}_{ij}^T\Gamma_{ij}^{-1}\dot{\hat{\omega}}_{ij}\right) + \frac{1}{2}\sum_{i=1}^{n} M_{ij}^2\left\|e_{ij}(t)\right\|^2 + \sum_{i=1}^{n}\frac{1}{2}\bar{\varepsilon}_{ij}^2\right\}. \tag{53}$$

Substitute (39), (41), controller gain (45), (46) into (53); then, it yields

$$\dot{V}(t) \leq \sum_{j=1}^{m}\left\{-\frac{1}{2}\sum_{i=1}^{n}\gamma_{ij}\lambda_{\max}(Q)\left\|e_{ij}(t)\right\|^2 - \frac{1}{2}\sum_{i=1}^{n}\gamma_{ij}\int_{t-\tau_{\max}}^{t}\beta_{ij}\left(x_{ij}(s)\right)ds - \frac{1}{2}\sum_{i=1}^{n}\frac{\kappa_{ij}}{\Gamma_{ij}^{-1}}\left(\tilde{\omega}_{ij}^T\Gamma_{ij}^{-1}\tilde{\omega}_{ij}\right) + \eta_{j2}\right\}. \tag{54}$$

From (21), given the integral inequality in (48), $\dot{V}(t)$ yields

$$\dot{V}(t) \le \sum_{j=1}^{m}\sum_{i=1}^{n}\left[-\frac{1}{2}\gamma_{ij}\lambda_{\max}(Q)\left\|e_{ij}(t)\right\|^2 - \frac{\gamma_{ij}}{2}\int_{t-\tau_i(t)}^{t}\beta_{ij}\left(x_{ij}(s)\right)ds - \frac{1}{2}\frac{\kappa_{ij}}{\Gamma_{ij}^{-1}}\left(\tilde{\omega}_{ij}^T\Gamma_{ij}^{-1}\tilde{\omega}_{ij}\right) + \eta_{j2}\right] \le -\eta_1 V(t) + \eta_2. \tag{55}$$

For $e_{ij} \in \Omega_{\delta_i}^c$, integrate the above $\dot{V}(t)$ over $[0, t]$; then, it can obtain

$$0 < V(t) \le \frac{\eta_2}{\eta_1} + \left(V(0) - \frac{\eta_2}{\eta_1}\right)e^{-\eta_1 t}. \tag{56}$$

From (21), (37), and (56), the inequality obtains

$$\sum_{j=1}^{m}\sum_{i=1}^{n}\frac{\lambda_{\min}(Q)}{2}\left\|e_{ij}(t)\right\|^2 \le V(t) \le \frac{\eta_2}{\eta_1} + \left(V(0) - \frac{\eta_2}{\eta_1}\right)e^{-\eta_1 t} \le \frac{\eta_2}{\eta_1} + V(0)e^{-\eta_1 t}\sum_{j=1}^{m}\sum_{i=1}^{n}\left\|e_{ij}(t)\right\|^2 \le \frac{2\eta_2}{\lambda_{\min}(D)\eta_1} + \frac{2}{\lambda_{\min}(D)}V(0)e^{-\eta_1 t}. \tag{57}$$

Given $\delta_i > \sqrt{2\eta_2/\lambda_{\min}(Q)\eta_1}$, there exists $T > 0$, for $i = 1, \ldots, n$, and all $t > T$:

$$\left\|e_{ij}(t)\right\| < \delta_i, \tag{58}$$

where δ_i is a small positive constant which determines tracking performance. The inequality can be obtained bounded by the Lyapunov Theory and selecting the appropriate parameters in the closed-loop MASs.

The proof is completed. □

Remark 8. For the uncertain nonlinear MASs (1) and (3), Assumptions 1–3, the actual controller is designed in (39) and the adaptive law (41) guarantees that all the signals in the closed-loop systems are SUUB. The parameters selection guidelines for controller design with state time-varying constraints and delays in MASs are demonstrated:

(i) Select appropriately designed parameters such that k_{ij}^0, ω_{ij}^T, β_{ij}, δ_i, Γ_{ij}, κ_{ij}, γ_{ij}, $\bar{\varepsilon}_{ij}$. Meanwhile, a positive matrix Q is needed to satisfy $Q = P\hat{\Lambda}^{-1}P^T$ and $P\Lambda P^T = \tilde{L} \otimes I_m$.

(ii) Decrease the control gain Γ_{ij}, ω_{ij}^2, and $\bar{\varepsilon}_{ij}$. Increasing the adaptive gain γ_{ij} and k_{ij}^0 would result in better consensus tracking performance. Other parameters are selected according to experience. Therefore, the parameter design of the controller should be adjusted according to the system performance and the tradeoff between tracking performance and constraints between agents such as collision avoidance.

4. Simulation Example

The following example is given to illustrate the effectiveness of the proposed adaptive fuzzy tracking control scheme for distributed uncertainties nonlinear MASs containing one leader with three followers. Assume that i^{th} agent with time-varying delays is as follows:

$$\begin{cases} \dot{x}_{i1} = x_{i2}(t)\sin\left(D_{i1}x_{i1}(t)\right) + \rho_{i1}\left(x_{i1}\left(t - \tau_i(t)\right)\right) + u_i(t), \\ \dot{x}_{i2} = x_{i1}(t)\cos\left(D_{i2}x_{i2}(t)\right) + \rho_{i2}\left(x_{i2}\left(t - \tau_i(t)\right)\right) + u_i(t). \end{cases} \tag{59}$$

The dynamic of the leader can be described as

$$\dot{x}_l(t) = \begin{bmatrix} 0.5\ \sin(0.8t) \\ 0.1 + 0.5\ \sin(t) \end{bmatrix}, \tag{60}$$

where u_i is the input of the cooperative tracking control, $x_l(t)$ is the state of the leader, the designed trajectories are $g_{l1} = 0.5\ \sin(0.8t)$, and $g_{l2} = 0.1 + 0.5\ \sin(t)$. The state variables $x_{i1}(t)$ and $x_{i2}(t)$ are bounded by time-varying state constraints as follows: $-k_{c_1}(t) < x_{i1}(t) < k_{c_1}(t)$, and $k_{c_1}(t) = 1 + 0.3\ \sin(2t)$; $-k_{c_2}(t) < x_{i2}(t) < k_{c_2}(t)$, and $k_{c_2}(t) = 1.8 + 0.4\ \sin(0.5t)$; C_{i1} and C_{i2} are defined in Table 1; and D_{i1} and D_{i2} are defined in Table 2, $i = 1, 2, 3$. The time-varying delays are $\tau_1(t) = 1.25 - 0.5\ \sin(0.5t)$, $\tau_2(t) = 1.3 - 0.6\ \sin(0.5t)\sin(t)$, $\tau_3(t) = 1.2 - 0.5\ \cos(0.5t)$, $\tau_{\max} = 2$.

The information interaction between agents is shown in Figure 2.

The topology illustrates the information interaction between agents in Figure 2 and $B = \text{diag}\{1, 1, 0\}$. The Laplacian matrix L is given as $L = \begin{pmatrix} 0.7 & -0.7 & 0.0 \\ -0.7 & 1.5 & -0.8 \\ 0.0 & -0.8 & 0.8 \end{pmatrix}$.

The initial of three agents are $x_1(0) = (0.05, 0.108)^T$, $x_2(0) = (-0.13, 0.1)^T$, and $x_3(0) = (0.038, -0.135)^T$. The designed parameters are chosen as $\Gamma_{i1} = \Gamma_{i2} = 1$, $\kappa_{11} = 0.7$, $\kappa_{21} = 0.4$, $\kappa_{31} = 0.4$, $\kappa_{12} = 0.6$, $\kappa_{22} = 0.6$, $\kappa_{32} = 0.6$, $k_{0_1} = k_{0_2} = 270$, $\delta_i = 10^{-7}$, and $\gamma_i = 0.9$, $i = 1, 2, 3$.

Apparently, Assumption 2 can be satisfied by choosing $q_i(x_i(t)) = \sqrt{(C_{i1}x_{i1}(t))^2 + (C_{i2}x_{i2}(t))^2}$. The adaptive FLSs

Table 1: Values of C_{i1} and C_{i2}, $i = 1, 2, 3$.

i	1	2	3
C_{i1}	1	3	−2
C_{i2}	1.5	2.7	0.8

Table 2: Values of D_{i1} and D_{i2}, $i = 1, 2, 3$.

i	1	2	3
D_{i1}	0.6	−3	6
D_{i2}	0.7	0.5	−5

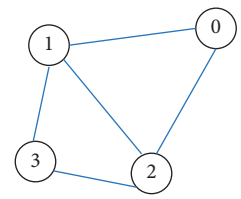

Figure 2: The communication topology for one leader and three followers.

controller u_i is given by (39), and the fuzzy rule numbers are $l_1 = l_2 = 10$. Choose the fuzzy membership functions as follows:

$$\begin{aligned}
\mu_{F_{i1}^{l_1}}(X_{i1}) &= \exp\left[-\frac{(x_{i1}-0.5l_1)^2}{8}-\frac{(x_{i2}-0.5l_1)^2}{8}-\frac{(k_{c_1}-0.5l_1)^2}{8}-\frac{(e_{i1}-0.5l_1)^2}{8}\right],\\
\mu_{F_{i2}^{l_2}}(X_{i2}) &= \exp\left[-\frac{(x_{i1}-0.5l_2)^2}{8}-\frac{(x_{i2}-0.5l_2)^2}{8}-\frac{(k_{c_2}-0.5l_2)^2}{8}-\frac{(e_{i2}-0.5l_2)^2}{8}\right],\\
\Psi_{i1}^{l_1}(X_{i1}) &= \frac{\mu_{F_{i1}^{l_1}}(X_{i1})}{\sum_{l_1=1}^{10}\mu_{F_{i1}^{l_1}}(X_{i1})},\\
\Psi_{i2}^{l_2}(X_{i2}) &= \frac{\mu_{F_{i1}^{l_2}}(X_{i2})}{\sum_{l_2}^{10}\mu_{F_{i1}^{l_2}}(X_{i2})}.
\end{aligned} \tag{61}$$

The simulation results are shown in Figures 3–7, and $i = 1, 2, 3$. The trajectories of the desired signal g_{l1} and full state $x_{i1}(t)$ with time-varying symmetrical barrier functions $-k_{c_1}(t)$ and $k_{c_1}(t)$ are shown in Figure 4. The full state $x_{i2}(t)$ constraints are bounded by time-varying symmetric functions $-k_{c_2}(t)$ and $k_{c_2}(t)$ and track the desired signal g_{l2} in Figure 5.

From Figures 3–5, it is easy to indicate that the tracking trajectory always holds within the time-varying constraints $-k_{c_j}(t) < x_{ij}(t) < k_{c_j}(t)$, $j = 1, 2$, and converges uniformly to the tracking signal. Figure 6 shows the synchronization errors. e_{i1} and e_{i2} fluctuate infinitely and approach the origin. Figure 7 shows the norms of the adaptive laws that can show that the effect of control is better. From the simulation, it is obvious that the proposed adaptive fuzzy distributed cooperative tracking control protocol is effective.

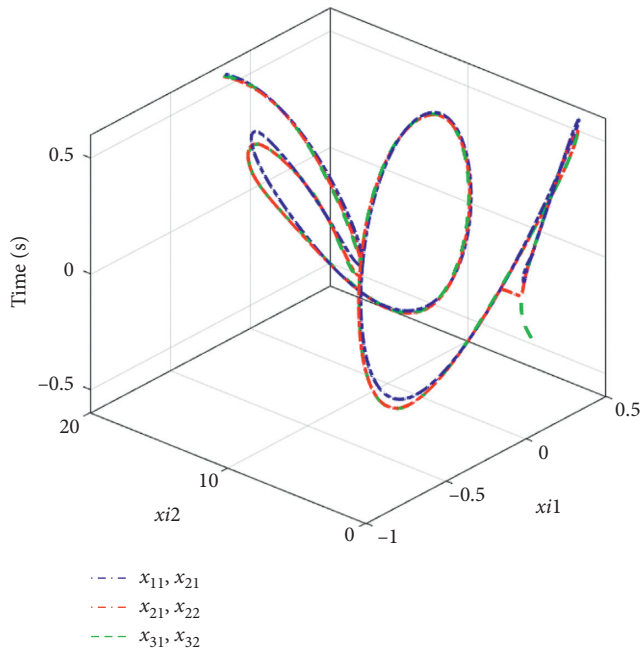

FIGURE 3: The three agents follow the trajectory of the leader.

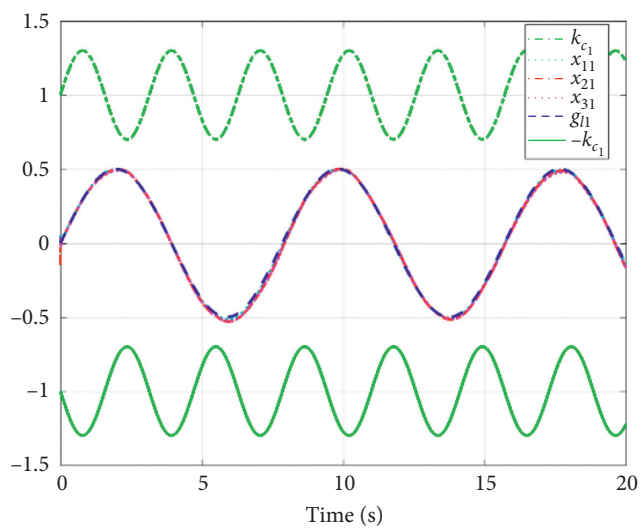

FIGURE 4: The trajectories of state x_{i1} with the reference signal g_{l1} in the time-varying constraint boundaries $-k_{c1}(t)$ and $k_{c1}(t)$.

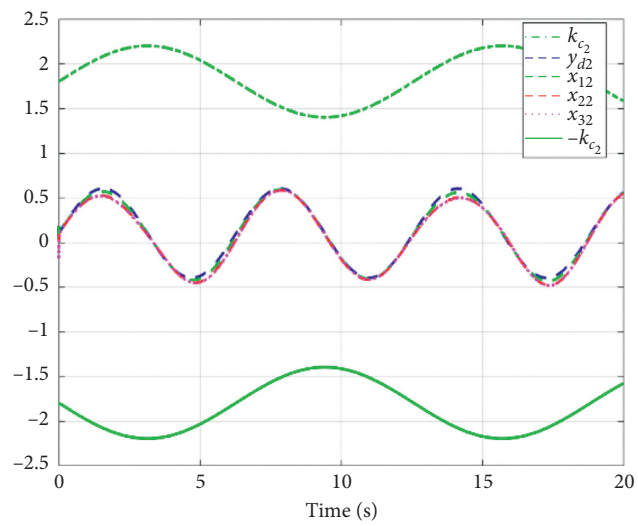

FIGURE 5: The trajectories of state x_{i2} with the reference signal g_{l2} in the time-varying constraint boundaries $-k_{c_2}(t)$ and $k_{c_2}(t)$.

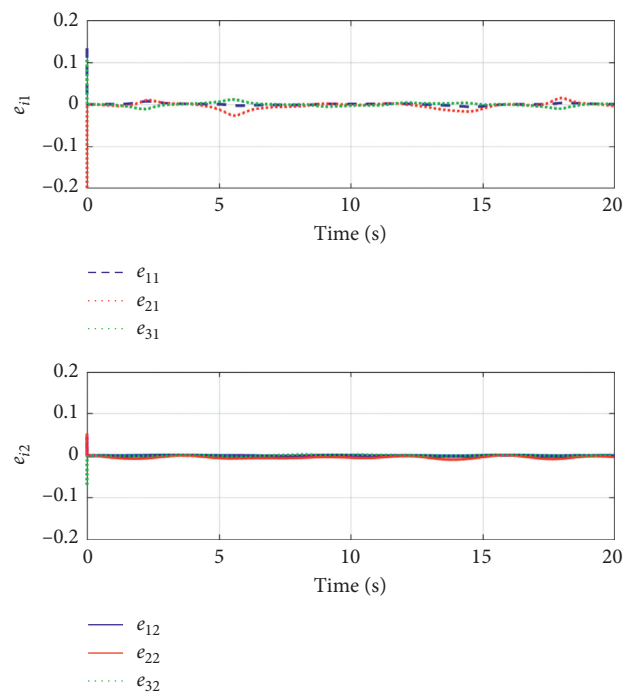

FIGURE 6: The trajectories of errors e_{i1} and e_{i2} with time-varying delays and constraints.

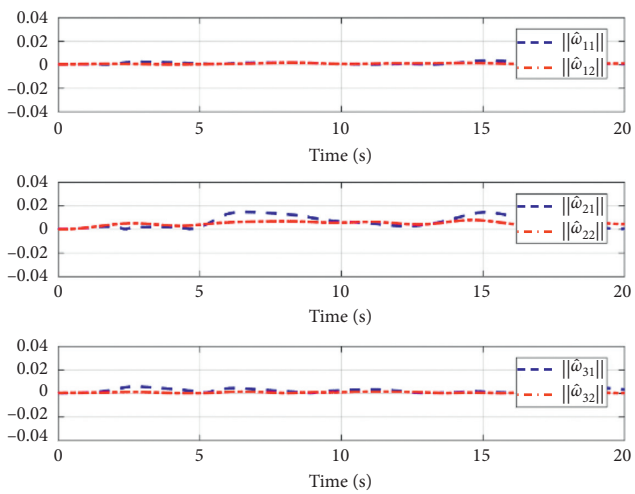

Figure 7: The boundedness of the adaptive laws.

5. Conclusion

An adaptive fuzzy cooperative tracking control has been presented for a class of uncertain nonlinear MASs with state time-varying delays and time-varying constraints. LKFs have been used to compensate for unknown time-varying delays and overcome the difficulty of employing the variable separation technique in the nonfeedback systems. To guarantee that time-varying delay states would not violate the time-varying bounds by constructing nonlinear coordinate transformations, ulteriorly, additional piecewise constructors can speed up convergence and avoid uncontrollability. The simulation results can be sufficiently demonstrated effective control. This paper further enriches the study of nonlinear state constrained systems. The simulation results provide theoretical support for further practical application.

Data Availability

The data used to support the findings of this study are included within the article.

Conflicts of Interest

The authors declare that they have no conflicts of interest.

Acknowledgments

This work was supported in part by the National Natural Science Foundation of China under Grants 61473139 and 61903168, Provincial Key Research and Development projects under JH2/10200002, and Provincial Scientific Research Fund of Education Department under JJL202015407.

References

[1] A. Abdessameud and A. Tayebi, "Attitude synchronization of a group of spacecraft without velocity measurements," *IEEE Transactions on Automatic Control*, vol. 54, no. 11, pp. 2642–2648, 2009.

[2] H. Zhang, P. Cheng, L. Shi, and J. Chen, "Optimal DoS attack scheduling in wireless networked control system," *IEEE Transactions on Control Systems Technology*, vol. 24, no. 3, pp. 843–852, 2015.

[3] N. Michael, J. Fink, and V. Kumar, "Cooperative manipulation and transportation with aerial robots," *Autonomous Robots*, vol. 30, no. 1, pp. 73–86, 2011.

[4] Y. Xu, W. Liu, and J. Gong, "Stable multi-agent-based load shedding algorithm for power systems," *IEEE Transactions on Power Systems*, vol. 26, no. 4, pp. 2006–2014, 2011.

[5] W. Meng, X. Wang, and S. Liu, "Distributed load sharing of an inverter-based microgrid with reduced communication," *IEEE Transactions on Smart Grid*, vol. 9, no. 2, pp. 1354–1364, 2016, to be published.

[6] B. Grocholsky, J. Keller, V. Kumar, and G. Pappas, "Cooperative air and ground surveillance," *IEEE Robotics and Automation Magazine*, vol. 13, no. 3, pp. 16–25, 2006.

[7] I.-S. Jeon, J.-I. Lee, and M.-J. Tahk, "Homing guidance law for cooperative attack of multiple missiles," *Journal of Guidance, Control, and Dynamics*, vol. 33, no. 1, pp. 275–280, 2010.

[8] F. De Rango, G. Potrino, M. Tropea, A. F. Santamaria, and P. Fazio, "Scalable and ligthway bio-inspired coordination protocol for FANET in precision agriculture applications," *Computers and Electrical Engineering*, vol. 74, pp. 305–318, 2019.

[9] H. Su, X. Wang, and Z. Lin, "Flocking of multi-agents with a virtual leader," *IEEE Transactions on Automatic Control*, vol. 54, no. 2, pp. 293–307, 2009.

[10] W. Ren, R. W. Beard, and E. M. Atkins, "Information consensus in multivehicle cooperative control," *IEEE Control Systems*, vol. 27, no. 2, pp. 71–82, 2007.

[11] Z. Li, X. Liu, W. Ren, and L. Xie, "Distributed tracking control for linear multiagent systems with a leader of bounded unknown input," *IEEE Transactions on Automatic Control*, vol. 58, no. 2, pp. 518–523, 2012.

[12] G. Shi and Y. Hong, "Global target aggregation and state agreement of nonlinear multi-agent systems with switching topologies," *Automatica*, vol. 45, no. 5, pp. 1165–1175, 2009.

[13] G. Wen, C. P. Chen, and Y. J. Liu, "Formation control with obstacle avoidance for a class of stochastic multiagent systems," *IEEE Transactions on Industrial Electronics*, vol. 65, no. 7, pp. 5847–5855, 2017.

[14] R. Olfati-Saber, J. A. Fax, and R. M. Murray, "Consensus and cooperation in networked multi-agent systems," *Proceedings of the IEEE*, vol. 95, no. 1, pp. 215–233, 2007.

[15] R. Olfati-Saber, "Flocking for multi-agent dynamic systems: algorithms and theory," *IEEE Transactions on Automatic Control*, vol. 51, no. 3, pp. 401–420, 2006.

[16] J. Gao, J. Liu, B. Rajan et al., "SCADA communication and security issues," *Security and Communication Networks*, vol. 7, no. 1, pp. 175–194, 2014.

[17] P. Ping Guo, C. L. P. Chen, and M. R. Lyu, "Cluster number selection for a small set of samples using the Bayesian Ying-Yang model," *IEEE Transactions on Neural Networks*, vol. 13, no. 3, pp. 757–763, 2002.

[18] W. Cao, Y. Zhou, C. L. P. Chen, and L. Xia, "Medical image encryption using edge maps," *Signal Processing*, vol. 132, pp. 96–109, 2017.

[19] S. Sui, C. L. P. Chen, and S. Tong, "Neural-Network-based adaptive DSC design for switched fractional-order nonlinear systems," *IEEE Transactions on Neural Networks and Learning Systems*, pp. 1–10, 2020.

[20] L. Liu, X. Li, Y.-J. Liu, and S. Tong, "Neural network based adaptive event trigger control for a class of electromagnetic suspension systems," *Control Engineering Practice*, vol. 106, Article ID 104675, 2021.

[21] S. Sui, C. L. P. Chen, and S. Tong, "Event-trigger-based finite-time fuzzy adaptive control for stochastic nonlinear system with unmodeled dynamics," *IEEE Transactions on Fuzzy Systems*, p. 1, 2020.

[22] H. A. Yousef, M. Hamdy, A. Saleem, K. Nashed, M. Mesbah, and M. Shafiq, "Enhanced adaptive control for a benchmark piezoelectric-actuated system via fuzzy approximation," *International Journal of Adaptive Control and Signal Processing*, vol. 33, no. 9, pp. 1329–1343, 2019.

[23] H. A. Yousef, M. Hamdy, and K. Nashed, "L1 adaptive fuzzy controller for a class of nonlinear systems with unknown backlash-like hysteresis," *International Journal of Systems Science*, vol. 48, no. 12, pp. 2522–2533, 2017.

[24] Q. Shen, B. Jiang, P. Shi, and J. Zhao, "Cooperative adaptive fuzzy tracking control for networked unknown nonlinear multiagent systems with time-varying actuator faults," *IEEE Transactions on Fuzzy Systems*, vol. 22, no. 3, pp. 494–504, 2013.

[25] G. X. Wen, C. L. P. Chen, Y. J. Liu, and Z. Liu, "Neural-network-based adaptive leader-following consensus control for second-order non-linear multi-agent systems," *IET Control Theory & Applications*, vol. 13, no. 9, pp. 1927–1934, 2015.

[26] H. Zhang and F. L. Lewis, "Adaptive cooperative tracking control of higher-order nonlinear systems with unknown dynamics," *Automatica*, vol. 48, no. 7, pp. 1432–1439, 2012.

[27] W. Wang and S. Tong, "Adaptive fuzzy containment control of nonlinear strict-feedback systems with full state constraints," *IEEE Transactions on Fuzzy Systems*, vol. 27, no. 10, pp. 2024–2038, 2019.

[28] S. S. Ge, F. Hong, and T. H. Lee, "Adaptive neural control of nonlinear time-delay systems with unknown virtual control coefficients," *IEEE Transactions on Systems, Man and Cybernetics, Part B (Cybernetics)*, vol. 34, no. 1, pp. 499–516, 2004.

[29] Z. Liu, G. Lai, Y. Zhang, and C. L. P. Chen, "Adaptive fuzzy tracking control of nonlinear time-delay systems with dead-zone output mechanism based on a novel smooth model," *IEEE Transactions on Fuzzy Systems*, vol. 23, no. 6, pp. 1998–2011, 2015.

[30] D. Yang, X. Li, J. Shen, and Z. Zhou, "State-dependent switching control of delayed switched systems with stable and unstable modes," *Mathematical Methods in the Applied Sciences*, vol. 41, no. 16, pp. 6968–6983, 2018.

[31] Y. Dan, X. D. Li, and J. L. Qiu, "Output tracking control of delayed switched systems via state-dependent switching and dynamic output feedback," *Nonlinear Analysis: Hybrid Systems*, vol. 32, pp. 294–305, 2019.

[32] C. L. P. Chen, G. X. Wen, Y. J. Liu, and F. Wang, "Adaptive consensus control for a class of nonlinear multiagent time-delay systems using neural networks," *IEEE Transactions on Neural Networks and Learning Systems*, vol. 25, pp. 1217–1226, 2017.

[33] G. Wen, C. L. P. Chen, Y.-J. Liu, and Z. Liu, "Neural network-based adaptive leader-following consensus control for a class of nonlinear multiagent state-delay systems," *IEEE Transactions on Cybernetics*, vol. 47, no. 8, pp. 2151–2160, 2017.

[34] K. P. Tee, S. S. Ge, and E. H. Tay, "Barrier Lyapunov functions for the control of output-constrained nonlinear systems," *Automatica*, vol. 45, no. 4, pp. 918–927, 2009.

[35] Z. Zhi Liu, G. Y. Guanyu Lai, Y. Yun Zhang, and C. L. P. Chen, "Adaptive neural output feedback control of output-constrained nonlinear systems with unknown output nonlinearity," *IEEE Transactions on Neural Networks and Learning Systems*, vol. 26, no. 8, pp. 1789–1802, 2015.

[36] S. Sui, C. L. P. Chen, and S. Tong, "A novel adaptive NN prescribed performance control for stochastic nonlinear systems," *IEEE Transactions on Neural Networks and Learning Systems*, pp. 1–10, 2020.

[37] Y.-J. Liu, Q. Zeng, S. Tong, C. L. P. Chen, and L. Liu, "Adaptive neural network control for active suspension systems with time-varying vertical displacement and speed constraints," *IEEE Transactions on Industrial Electronics*, vol. 66, no. 12, pp. 9458–9466, 2019.

[38] J. Lan, Y.-J. Liu, L. Liu, and S. Tong, "Adaptive output feedback tracking control for a class of nonlinear time-varying state constrained systems with fuzzy dead-zone input," *IEEE Transactions on Fuzzy Systems*, p. 1, 2020.

[39] Y. J. Liu, S. C. Tong, C. L. P. Chen, and D. J. Li, "Adaptive NN control using integral barrier Lyapunov functionals for uncertain nonlinear block-triangular constraint systems," *IEEE Transactions on Cybernetics*, vol. 47, no. 11, pp. 3747–3757, 2016.

[40] L. Liu, Y. J. Liu, A. Chen, S. C. Tong, and C. L. P. Chen, "Integral barrier Lyapunov function-based adaptive control for switched nonlinear systems," *Science China Information Sciences*, vol. 63, no. 3, pp. 1–14, 2020.

[41] L. Liu, T. Gao, Y.-J. Liu, S. Tong, C. L. P. Chen, and L. Ma, "Time-varying IBLFs-based adaptive control of uncertain nonlinear systems with full state constraints," *Automatica*, vol. 129, Article ID 109595, 2021.

[42] Y. Zhang, H. Liang, H. Ma, Q. Zhou, and Z. Yu, "Distributed adaptive consensus tracking control for nonlinear multi-agent systems with state constraints," *Applied Mathematics and Computation*, vol. 326, pp. 16–32, 2018.

[43] K. Zhao and Y. Song, "Removing the feasibility conditions imposed on tracking control designs for state-constrained strict-feedback systems," *IEEE Transactions on Automatic Control*, vol. 64, no. 3, pp. 1265–1272, 2019.

[44] W. Meng, Q. Yang, J. Si, and Y. Sun, "Consensus control of nonlinear multiagent systems with time-varying state constraints," *IEEE Transactions on Cybernetics*, vol. 47, no. 8, pp. 2110–2120, 2016.

[45] D.-P. Li, D.-J. Li, Y.-J. Liu, S. Tong, and C. L. P. Chen, "Approximation-based adaptive neural tracking control of nonlinear MIMO unknown time-varying delay systems with full state constraints," *IEEE Transactions on Cybernetics*, vol. 47, no. 10, pp. 3100–3109, 2017.

[46] D. Li, C. L. P. Chen, Y.-J. Liu, and S. Tong, "Neural network controller design for a class of nonlinear delayed systems with time-varying full-state constraints," *IEEE Transactions on Neural Networks and Learning Systems*, vol. 30, no. 9, pp. 2625–2636, 2019.

Hindawi
Complexity
Volume 2021, Article ID 9933472, 8 pages
https://doi.org/10.1155/2021/9933472

Research Article

Nonsingular Global Fixed-Time Stabilization for Nonlinear Systems

Wei Hu,[1,2] **Zhangyong Zhou**,[1,2] **and Junjun Tang**[1]

[1]*Stated-Owned Wuhu Machinery Factory, Wuhu 241007, China*
[2]*Nanjing University of Aeronautics and Astronautics, Nanjing 210000, China*

Correspondence should be addressed to Wei Hu; huwei9698@126.com

Received 10 March 2021; Accepted 8 June 2021; Published 21 June 2021

Academic Editor: Xiaodi Li

Since existing results about fixed-time stabilization are only applied to strict feedback systems, this paper investigates the nonsingular fixed-time stabilization of more general high-order nonlinear systems. Based on a novel concept named coordinate mapping of time domain, a control method is first proposed to transform the nonsingular fixed-time convergence problem into the finite-time convergence problem of a transformed time-varying system. By extending the existing, adding a power integrator technique into the considered time-varying system, a periodic controller is constructed to stabilize the original system in fixed time. The results of simulations verify the effectiveness of the proposed method.

1. Introduction

In recent years, more and more attention has been paid to the controller design of high-order nonlinear systems due to its wide application in modeling aerospace craft, rigid robotic systems, and machine systems with underactuation, weak coupling, and instability [1–4]. On the one hand, high-order nonlinear systems are more general forms of strict feedback nonlinear systems, which have been widely studied. More practical systems can be described, including rigid robots, aerospace vehicles, and hydraulic systems. On the other hand, the systems cannot be linearized at the origin or cannot be controlled after linearization when the power of the high-order nonlinear system is not 1, which makes it difficult to control [2].

For high-order nonlinear system, the finite-time stabilization is studied from different perspectives in [1–6]. However, the convergence time is decided by the initial state of the system in recent achievements. That is to say, the convergence time cannot be prespecified, since the state can be initialed at any point. Besides, when the initial state of the system tends to infinity, the time tends to infinity as well.

The concept of fixed-time stabilization is proposed in [7]. As a special finite-time stabilization method, it requires that the convergence time of the system be bounded and the upper bound be independent of the initial state, which can be set in advance. A primary method for fixed-time stabilization is proposed in [8], which successfully solved the problem of fixed-time stabilization for linear systems with only matching uncertainties. Most of the existing literature is limited to second-order linear systems [9–12]; only [13–15] have studied the fixed-time stabilization for high-order nonlinear systems. Based on the implicit Lyapunov function method, the fixed-time stability of high-order integrators is analyzed in [13]. A nonsmoothed controller is constructed by using the recursive design method to solve the fixed-time stabilization problem of high-order nonlinear interconnected systems [14]. The fixed-time stabilization of strict feedback nonlinear systems with only matching uncertainties is achieved by ingenious state transformation [15]. It should be pointed out that all the systems in [8–15] are merely special forms of higher-order systems. Therefore, it is of great significance to study the fixed-time stabilization of more general high-order nonlinear systems.

Based on the above, the nonsingular global fixed-time stabilization of high-order nonlinear systems is proposed. The main difficulty lies in the design complexity caused by various power terms. Particularly, this issue would be

intensified if we adopt traditional double-power-term law. The obstacle is partially avoided in this work by using the time-domain mapping, with which the nonsingular fixed-time stabilization problem of the original system is transformed into the finite-time stabilization problem of the corresponding time-varying system; by using the power integration method, the finite-time stabilization problem of the time-varying system is realized. The main innovations are summarized as follows:

(1) A control method based on time-domain mapping is proposed, which transforms the nonsingular fixed-time stabilization problem of the original system into the finite-time stabilization problem of the corresponding time-varying system and provides a new idea for the design of the fixed-time convergence control law. Compared with the traditional double-power-reaching law, the proposed method is designed with a single-power-reaching law, which is more effective and simpler.

(2) In essence, the fixed-time stabilization can be regarded as the optimal control with fixed terminal time, and the design of its control law is easy to produce singularity, while the control law of the proposed method is nonsingular.

(3) The existing method can only solve the problem of fixed-time stabilization for strict feedback systems with only matching uncertainties, while the proposed method can solve the fixed-time stabilization problem of high-order nonlinear systems with unmatched uncertainties. It is noted that the strict feedback systems are special cases of high-order nonlinear systems; the results of this paper greatly extend the research scope of fixed-time stabilization.

2. Description

For the convenience of description, we define $\mathbf{R}$, $\mathbf{R}_+$, and $\mathbf{R}^n$ as real number, positive real number, and n-dimensional real vectors, respectively, define $\mathbf{C}^i$ as i-order continuous differentiable function, and define $\mathbf{Q}_{\text{odd}}$ as rational number whose numerator and denominator are positive odd integers.

Consider the following high-order nonlinear systems:

$$\begin{cases} \dot{x}_1 = x_2^{p_1} + f_1(\overline{\mathbf{x}}_1, t), \\ \dot{x}_2 = x_3^{p_2} + f_2(\overline{\mathbf{x}}_2, t), \\ \vdots \\ \dot{x}_n = u^{p_n} + f_n(\overline{\mathbf{x}}_n, t), \end{cases} \tag{1}$$

where $\mathbf{x} = [x_1, x_2, \ldots, x_n]^T \in \mathbf{R}^n$ and $u \in \mathbf{R}$ represent the state of the system and the control input; $\overline{\mathbf{x}}_\mathbf{i}$ is defined as $[x_1, \ldots, x_i]^T \in \mathbf{R}^i$; p_i is a constant, which belongs to $\mathbf{Q}_{\text{odd}}$; f_i: $\mathbf{R}^i \times [0, +\infty) \longrightarrow \mathbf{R}$ is an uncertain nonlinear function that satisfies $f_i(\mathbf{0}, t) = 0$, $\forall t \in [0, +\infty)$. According to the mean value theorem, it means that there exists a function $\gamma_{ij}(\overline{\mathbf{x}}_i, t)$, which makes $f_i(\overline{\mathbf{x}}_i, t) = \sum_{j=1}^{i} x_j \gamma_{ij}(\overline{\mathbf{x}}_i, t)$, $i = 1, \ldots, n$. Furthermore, the following assumptions are given.

Hypothesis 1. There exists a function $\overline{\gamma}_i(\overline{\mathbf{x}}_i) \geq 0$, which makes $f_i(\overline{\mathbf{x}}_i, t) = \sum_{j=1}^{i} x_j \gamma_{ij}(\overline{\mathbf{x}}_i, t)$, $i = 1, \ldots, n$.

Hypothesis 2. For $p_i \in \mathbf{Q}_{\text{odd}}$, $i = 1, \ldots, n$, in formula (1), there exists a constant $\eta_i \in \mathbf{Q}_{\text{odd}}$, $i = 1, \ldots, n+1$, which is larger than 1, and it makes the following formulas hold:

$$0 < \frac{1}{\eta_1} - \frac{p_1}{\eta_2} \leq \frac{1}{\eta_2} - \frac{p_2}{\eta_3} \leq \cdots \leq \frac{1}{\eta_n} - \frac{p_n}{\eta_{n+1}}, \tag{2}$$

$$\frac{p_i}{\eta_{i+1}} \leq \min\left\{\frac{1}{\eta_1}, \frac{1}{\eta_2}, \ldots, \frac{1}{\eta_{i-1}}\right\}. \tag{3}$$

To accurately describe the concept of fixed-time stability, we give the following definitions.

Definition 1. If any solution $\mathbf{x}(t, \mathbf{x}_0)$ of formula (1) reaches the origin at a certain finite time $T(\mathbf{x}_0)$ and then remains at the origin, where T: $\mathbf{R}^n \mapsto \mathbf{R}_+ \cup 0$ is called the convergence time function, then the origin can be called globally finite-time stable. If the origin is globally finite-time stable and the convergence time function $T(\mathbf{x}_0)$ is bounded, that is, $\exists T_{\max} > 0$, such that $T(\mathbf{x}_0) \leq T_{\max}$, $\forall \mathbf{x}_0 \in \mathbf{R}^n$, then the origin is globally fixed-time stable.

The goal of the paper is to design a control input for system (1) to make all closed-loop signals globally bounded and the system state converges to the origin in a fixed time. To facilitate the controller design and stability analysis, the following lemma is introduced from [6, 16].

Lemma 1. *The Lyapunov function $V(t)$ is assumed to meet the following formula:*

$$\frac{\mathrm{d}V(t)}{\mathrm{d}t} \leq -\rho[V(t)]^v, \tag{4}$$

where ρ is a constant and $\rho > 0$ and $0 < v < 1$; then, the following formulas can be established:

$$\begin{cases} V(t) \le \left[V^{1-v}(t_0) - (1-v)\rho(t-t_0)\right]^{1/(1-v)}, & t_0 \le t < \dfrac{t_0 + V^{1-v}(t_0)}{\rho(1-v)}, \\ V(t) = 0, & t \ge t_0 + \dfrac{V^{1-v}(t_0)}{\rho(1-v)}. \end{cases} \tag{5}$$

Lemma 2. *For any positive real number x_i, $i = 1, \ldots, n$, $1 < b < 1$, the following inequality is established:*

$$\left(|x_1| + \cdots + |x_n|\right)^b \le |x_1|^b + \cdots + |x_n|^b. \tag{6}$$

When $b = (p/q) \le 1$ and $p > 0$ and $q > 0$, we can obtain

$$\left|x^b - y^b\right| \le 2^{1-b}|x-y|^b. \tag{7}$$

Lemma 3. *For any positive real number m, n, and function $a(x, y)$, the following inequality is established:*

$$\left|a(x,y)x^m y^n\right| \le c(x,y)|x|^{m+n} + \frac{n}{m+n} \times \left[\frac{m}{(m+n)c(x,y)}\right]^{m/n} |a(x,y)|^{(m+n)/n}|y|^{m+n}, \tag{8}$$

where $c(x, y) > 0$, $x \in R$, $y \in R$.

3. Design of Nonsingular Fixed-Time Controller

3.1. Time-Domain Mapping. In this section, the concept of time-domain mapping is proposed for the first time. The problem of nonsingular fixed-time stabilization of system (1) is transformed into the problem of finite-time stabilization of the time-varying system (12), which simplifies the analysis and design process of fixed-time stabilization.

Assume that the upper bound of the convergence time of system (1) is T; when $t \in [0, T)$, the following time-domain coordinate mapping is used to extend the finite-time domain to the infinite-time domain:

$$\tau = \mu + \sigma \tan\left[\frac{t((\pi/2) + \arctan(\mu/\sigma))}{T - \arctan(\mu/\sigma)}\right]. \tag{9}$$

The inverse transformation of it is as follows:

$$t = T\frac{\arctan((\tau-\mu)/\sigma) + \arctan(\mu/\sigma)}{(\pi/2) + \arctan(\mu/\sigma)} \triangleq t_0(\tau), \tag{10}$$

where $\mu \in R$ and $\sigma > 0$; according to equation (10), obviously there is $t_0(\tau)$: $[0, +\infty) \longrightarrow [0, T)$, and find the derivative on the left and right sides of formula; formula (10) can be transformed as follows:

$$\frac{\mathrm{d}t}{\mathrm{d}\tau} = \frac{T}{\sigma[(\pi/2) + \arctan(\mu/\sigma)]} \cdot \frac{1}{1 + [(\tau-\mu)/\sigma]} \triangleq \mathrm{K}(\tau). \tag{11}$$

When $t \in [0, T)$, multiplying both sides of formula (1) by formula (11) yields

$$\begin{cases} \dfrac{\mathrm{d}x_1}{\mathrm{d}\tau} = \kappa(\tau)\left[x_2^{p_1} + \widetilde{f}_1(\overline{\mathbf{x}}_1, \tau)\right], \\ \dfrac{\mathrm{d}x_2}{\mathrm{d}\tau} = \kappa(\tau)\left[x_3^{p_2} + \widetilde{f}_2(\overline{\mathbf{x}}_2, \tau)\right], \\ \vdots \\ \dfrac{\mathrm{d}x_n}{\mathrm{d}\tau} = \kappa(\tau)\left[u^{p_n} + \widetilde{f}_n(\overline{\mathbf{x}}_n, \tau)\right], \end{cases} \tag{12}$$

where $\widetilde{f}_i(\overline{\mathbf{x}}_i, \tau) = f_i(\overline{\mathbf{x}}_i, t) \in \mathbf{C}^1$; according to Hypothesis 1, the following inequality holds:

$$\left|\widetilde{f}_i(\overline{\mathbf{x}}_i, \tau)\right| \le \overline{\gamma}_i(\overline{\mathbf{x}}_i)\left(|x_1| + \cdots + |x_i|\right), \quad i = 1, \ldots, n. \tag{13}$$

Remark 1. For the converted time-varying system (12), $\kappa(\tau)$ can be regarded as the time-varying control coefficient of the system. Therefore, to stabilize system (12), the control law must contain unbounded gain terms $1/\kappa(\tau)$ to compensate for the effectiveness loss of the time-varying control factor $\kappa(\tau)$. This means that if system (12) is asymptotically stabilized in the time domain τ, although system (1) will achieve a fixed-time stabilization in the time domain t, the control input tends to infinity at the terminal time. To overcome the singularity of the control law, a natural method is to achieve finite-time stabilization in time domain τ so that system (1) can achieve fixed-time stabilization at a certain time $t_f < T$. As τ is boundless, the control law is nonsingular.

Remark 2. The coordinate mapping from time domain τ to t is not limited to the form of equation (10). Some coordinate maps such as exponential function and trigonometric function are also feasible when they satisfy the following conditions: (1) infinitely differentiable and monotonically increasing; (2) $t_0(0) = 0$ and $\lim_{\tau \longrightarrow +\infty} t_0(\tau) = T$. On the other hand, by adjusting μ and σ, a relatively smooth and practical control input can be obtained.

3.2. Design of Finite-Time Controller in Time Domain. In this section, a finite-time state feedback controller is designed in time domain τ for the time-varying system (12). Firstly, the control parameters are selected. According to Hypothesis 2, a constant $\nu_i \in \mathbf{Q}_{\mathrm{odd}}$, $i = 1, \ldots, n$, which is not less than 1 can be chosen to satisfy the following requirements:

$$\nu_1 + \frac{p_1}{\eta_2} = \nu_2 + \frac{p_2}{\eta_3} = \cdots = \nu_n + \frac{p_n}{\eta_{n+1}} \triangleq \omega. \tag{14}$$

Extending the power integral method to the time-varying system (12), the finite-time controller is designed in time domain τ recursively. It should be pointed out that $\dot{V}_i$ represents the derivative of V_i to τ.

3.2.1. Choosing the C^1 Positive Definite Lyapunov Function.

$$V_1(x_1) = \frac{1}{\eta_1\nu_1 + 1} x_1^{\eta_1\nu_1+1} \triangleq W_1(x_1). \tag{15}$$

Calculating derivation of equation (15), the following equation can be obtained according to formula (3):

$$\begin{aligned}\dot{V}_1(x_1) &= x_1^{\eta_1\nu_1}\kappa(\tau)\left[x_2^{p_1} + \tilde{f}_1(\overline{\mathbf{x}}_1, \tau)\right] \\ &\le \kappa(\tau)x_1^{\eta_1\nu_1}\left(x_2^{p_1} - x_2^{*\,p_1}\right) + \kappa(\tau)x_1^{\eta_1\nu_1}x_2^{*\,p_1} \\ &\quad + \kappa(\tau)x_1^{\eta_1(\nu_1+p_1/\eta_2)}\rho_1(x_1),\end{aligned} \tag{16}$$

where $\rho_1(x_1) \ge x_1^{1-(p_1\eta_1/\eta_2)}\overline{\gamma}_1(x_1) \ge 0$ is the C^1 function, which can be defined as $\rho_1(x_1) = (1 + x_1^2)\overline{\gamma}_1(x_1)$.

According to formula (16), the virtual control law x_2^* is defined as follows:

$$x_2^{*\,p_1} = -x_1^{p_1\eta_1/\eta_2}\left[\frac{n}{\mathrm{K}(\tau)} + \rho_1 x_1\right] \triangleq -\xi_1^{p_1/\eta_2}\beta_1^{p_1}(x_1, \tau), \tag{17}$$

where $\xi_1 = x_1^{\eta_1}$ and $\beta_1(x_1, \tau) = [(n/\kappa(\tau)) + \rho_1(x_1)]^{1/p_1} > 0$ are C^1 functions. Substituting equation (17) into equation (16), the following formula can be obtained:

$$\dot{V}_1(x_1) \le -nx_1^{\eta_1(\nu_1+(p_1/\eta_2))} + \kappa(\tau)x_1^{\eta_1\nu_1}\left(x_2^{p_1} - x_2^{*\,p_1}\right). \tag{18}$$

Suppose that, in step $k-1$, there exists a positive Lyapunov function, which satisfies the following equation:

$$V_{k-1}(\overline{\mathbf{x}}_{k-1}, \tau) \le 2\sum_{i=1}^{k-1}\xi_i^{\nu_i+(1/\eta_i)}. \tag{19}$$

Define virtual control law and error as follows:

$$\begin{aligned}&x_1^* = 0, \xi_1 = x_1^{\eta_1} - x_1^{*\,\eta_1}, \\ &x_2^* = -\xi_1^{1/\eta_2}\beta_1(x_1, \tau), \quad \xi_2 = x_2^{\eta_2} - x_2^{*\,\eta_2}, \\ &\quad\vdots \quad\quad \vdots \\ &x_k^* = -\xi_{k-1}^{1/\eta_k}\beta_{k-1}(\overline{\mathbf{x}}_{k-1}, \tau), \quad \xi_k = x_k^{\eta_k} - x_k^{*\,\eta_k},\end{aligned} \tag{20}$$

where $\beta_i(\overline{\mathbf{x}}_i, \tau) > 0$ and ξ_i are C^1 functions. Besides, $i = 1, \ldots, k-1$ and

$$\dot{V}_{k-1}(\overline{\mathbf{x}}_{k-1}, \tau) \le -(n-k+2)\sum_{i=1}^{k-1}\xi_i^{\omega} + \kappa(\tau)\xi_{k-1}^{\nu_{k-1}}\left(x_k^{p_{k-1}} - x_k^{*\,p_{k-1}}\right). \tag{21}$$

As ξ_{k-1} and $\beta_{k-1}(\overline{\mathbf{x}}_{k-1}, \tau) > 0$ are C^1 functions, $\eta_k \ge 1$; it can be easily obtained that $\xi_k = x_k^{\eta_k} + \xi_{k-1}\beta_{k-1}^{\eta_k}(\overline{\mathbf{x}}_{k-1}, \tau)$ is also a C^1 function.

Designing C^0 virtual control law x_{k+1}^*, which makes equations (19) and (21) hold in step k, the C^1 positive Lyapunov function (equation (22)) is considered.

$$V_k(\overline{\mathbf{x}}_k, \tau) = V_{k-1}(\overline{\mathbf{x}}_{k-1}, \tau) + \int_{x_k^*}^{x_k}\left(s^{\eta_k} - x_k^{*\,\eta_k}\right)^{\nu_k}\mathrm{d}s. \tag{22}$$

According to equations (7) and (19) and mean value theorem, it can be achieved that $V_k(\overline{\mathbf{x}}_k, \tau) \le 2\sum_{i=1}^{k}\xi_i^{\nu_i+(1/\eta_i)}$, which means that equation (19) is right in step k.

Defining that $W_k(\overline{\mathbf{x}}_k, \tau) = \int_{x_k^*}^{x_k}(s^{\eta_k} - x_k^{*\,\eta_k})^{\nu_k}\mathrm{d}s$, calculating derivation of $V_k(\overline{\mathbf{x}}_k, \tau)$ to τ, equation (23) can be achieved after combining formulas (20) to (22).

$$\begin{aligned}\dot{V}_k(\overline{\mathbf{x}}_k, \tau) \le &-(n-k+2)\sum_{i=1}^{k-1}\xi_i^{\omega} + \kappa(\tau)\xi_{k-1}^{\nu_{k-1}}\left(x_k^{p_{k-1}} - x_k^{*\,p_{k-1}}\right) + \kappa(\tau)\xi_k^{\nu_k}\left(x_{k+1}^{p_k} - x_{k+1}^{*p_k}\right) + \kappa(\tau)\xi_k^{\nu_k}x_{k+1}^{*p_k} + \kappa(\tau)\xi_k^{\nu_k}\tilde{f}_k(\overline{\mathbf{x}}_k, \tau) \\ &+ \sum_{i=1}^{k-1}\frac{\partial W_k}{\partial x_i}\frac{\mathrm{d}x_i}{\mathrm{d}\tau} + \frac{\partial W_k}{\partial \tau}.\end{aligned} \tag{23}$$

Let us estimate each term on the right side of equation (23); according to Lemma 2, it can be obtained that

$$\left|x_k^{p_{k-1}} - x_k^{*\,p_{k-1}}\right| \le 2^{1-(p_{k-1}/\eta_k)}\left|x_k^{\eta_k} - x_k^{*\,\eta_k}\right|^{p_{k-1}/\eta_k} \le 2\xi_k^{p_{k-1}/\eta_k}. \tag{24}$$

According to Lemma 3, there exists a C^1 function $c_k(\overline{\mathbf{x}}_{k-1}) \ge 0$ making the following inequality right:

$$\left|\kappa(\tau)\xi_{k-1}^{\nu_{k-1}}\left(x_k^{p_{k-1}} - x_k^{*\,p_{k-1}}\right)\right| \le \frac{1}{4}\xi_{k-1}^{\omega} + \kappa(\tau)c_k(\overline{\mathbf{x}}_{k-1})\xi_k^{\omega}. \tag{25}$$

For the convenience of narration, the following lemmas are given to estimate the residual terms on the right side of equation (23). The proof ideas of Lemmas 4 and 5 are similar to those of inequalities (17) and (18) in [4]. Readers can refer to [4] for proof. For simplicity, this paper omits the proof.

Lemma 4. *There exits C^1 function $\tilde{\gamma}_k(\overline{\mathbf{x}}_k, \tau) \ge 0$, $k = 2, \ldots, n$, which makes the following inequality hold:*

$$\left|\kappa(\tau)\xi_k^{\nu_k}\tilde{f}_k(\overline{\mathbf{x}}_k, \tau)\right| \le \frac{1}{4}\sum_{i=1}^{k-1}\xi_i^{\omega} + \kappa(\tau)\tilde{\gamma}_k(\overline{\mathbf{x}}_k, \tau)\xi_k^{\omega}. \tag{26}$$

Lemma 5. *There exists C^1 function $\tilde{\rho}_k(\bar{\mathbf{x}}_k, \tau) \geq 0$, $k = 2, \ldots, n$, which makes the following inequality hold:*

$$\left|\sum_{i=1}^{k-1} \frac{\partial W_k}{\partial x_i} \frac{\mathrm{d}x_i}{\mathrm{d}\tau}\right| \leq \frac{1}{4} \sum_{i=1}^{k-1} \xi_i^{\omega} + \kappa(\tau)\tilde{\rho}_k(\bar{\mathbf{x}}_k, \tau)\xi_k^{\omega}. \tag{27}$$

Lemma 6. *There exists C^1 function $\tilde{\varphi}_k(\bar{\mathbf{x}}_k, \tau) \geq 0$, $\tilde{\varphi}_k(\bar{\mathbf{x}}_k, \tau) \geq 0$, which makes the following inequality hold:*

$$\left|\frac{\partial W_k}{\partial \tau}\right| \leq \frac{1}{4} \sum_{i=1}^{k-1} \xi_i^{\omega} + \tilde{\varphi}_k(\bar{\mathbf{x}}_k, \tau)\xi_k^{\omega}. \tag{28}$$

3.2.2. Demonstration. It is noticed that the time after transformation is only explicitly included in $x_k^{*\eta_k}$ which belongs to the expression W_k $(k = 2, \ldots, n)$. So, we use mathematical induction to analyze $\partial x_k^{*\eta_k}/\partial \tau$.

According to $x_2^{*\eta_2} = -x_1\beta_1^{\eta_2}(x_1, \tau)$, where $\beta_1(x_1, \tau) > 0$ is a C^1 function, it can be concluded that the partial derivative about τ to $x_2^{*\eta_2}$ is available and that the following inequality can be obtained:

$$\left|\frac{\partial x_2^{*\eta_2}}{\partial \tau}\right| = \left|\xi_1 \frac{\partial \beta_1^{\eta_2}(x_1, \tau)}{\partial \tau}\right| \leq |\xi_1|\varphi_1(x_1, \tau), \tag{29}$$

where $\varphi_1(x_1, \tau) \geq 0$ is a designable C^1 function.

Assuming that when $k = 3, \ldots, n$, $x_{k-1}^{*\eta_{k-1}}$ is partially differentiable to τ, there exists a C^1 function $\varphi_{k-2}(\bar{\mathbf{x}}_{k-2}, \tau)$, which makes the following equality hold:

$$\left|\frac{\partial x_{k-1}^{*\eta_{k-1}}}{\partial \tau}\right| = \varphi_{k-2}(\bar{\mathbf{x}}_{k-2}, \tau) \sum_{i=1}^{k-2} |\xi_i|. \tag{30}$$

It should be noticed that $x_k^{*\eta_k} = -\xi_{k-1}\beta_{k-1}^{\eta_k}(\bar{\mathbf{x}}_{k-1}, \tau)$, where $\beta_{k-1}(\bar{\mathbf{x}}_{k-1}, \tau)$ is a C^1 function and $\xi_{k-1} = x_{k-1}^{\eta_{k-1}} - x_{k-1}^{*\eta_{k-1}}$; therefore, $x_k^{*\eta_k}$ is partially differentiable to τ, and

$$\begin{aligned}
\left|\frac{\partial x_k^{*\eta_k}}{\partial \tau}\right| &\leq \left|\xi_{k-1}\frac{\partial \beta_{k-1}^{\eta_k}(\bar{\mathbf{x}}_{k-1}, \tau)}{\partial \tau}\right| + \beta_{k-1}^{\eta_k}(\bar{\mathbf{x}}_{k-1}, \tau)\left|\frac{\partial x_{k-1}^{*\eta_{k-1}}}{\partial \tau}\right| \\
&\leq |\xi_{k-1}|\left|\frac{\partial \beta_{k-1}^{\eta_k}(\bar{\mathbf{x}}_{k-1}, \tau)}{\partial \tau}\right| + \beta_{k-1}^{\eta_k}(\bar{\mathbf{x}}_{k-1}, \tau)\varphi_{k-2}(\bar{\mathbf{x}}_{k-2}, \tau)\sum_{i=1}^{k-2}|\xi_i| \\
&\leq \varphi_{k-1}(\bar{\mathbf{x}}_{k-1}, \tau)\sum_{i=1}^{k-1}|\xi_i|,
\end{aligned} \tag{31}$$

where $\varphi_{k-1}(\bar{\mathbf{x}}_{k-1}, \tau) \geq 0$ is a designable C^1 function.

When $k = 2, \ldots, n$, W_k is continuous partial differentiable to τ. According to formula (2), we can also know that $\nu_k + (1/\eta_k) > \omega$; hence, we have the following:

$$\begin{aligned}
\left|\frac{\partial W_k}{\partial \tau}\right| &= \left|\frac{\partial x_k^{*\eta_k}}{\partial \tau}\int_{x_k^*}^{x_k} \nu_k\left(s^{\eta_k} - x_k^{*\eta_k}\right)^{\nu_k - 1}\mathrm{d}s\right| \\
&\leq 2\nu_k\varphi_{k-1}(\bar{\mathbf{x}}_{k-1}, \tau)|\xi_k|^{\nu_k - 1 + (1/\eta_k)}\sum_{i=1}^{k-1}|\xi_i| \\
&\leq \frac{1}{4}\sum_{i=1}^{k-1}\xi_i^{\omega} + \xi_k^{\omega}\tilde{\varphi}_k(\bar{\mathbf{x}}_k, \tau),
\end{aligned} \tag{32}$$

where $\tilde{\varphi}_k(\bar{\mathbf{x}}_k, \tau) \geq 0$ is a designable C^1 function.

Substituting formulas (25)–(28) into equation (23), the following inequality can be obtained:

$$\begin{aligned}
\dot{V}_k(\bar{\mathbf{x}}_k, \tau) \leq &-(n - k + 1)\sum_{i=1}^{k-1}\xi_i^{\omega} + \kappa(\tau)\xi_k^{\nu_k}\left(x_{k+1}^{p_k} - x_{k+1}^{*p_k}\right) \\
&+ \kappa(\tau)\xi_k^{\omega}\left[c_k(\bar{\mathbf{x}}_{k-1}) + \tilde{\gamma}_k(\bar{\mathbf{x}}_k, \tau) + \tilde{\rho}_k(\bar{\mathbf{x}}_k, \tau) + \frac{\tilde{\varphi}_k(\bar{\mathbf{x}}_k, \tau)}{\kappa(\tau)}\right] + \kappa(\tau)\xi_k^{\nu_k}x_{k+1}^{*p_k}.
\end{aligned} \tag{33}$$

The C^0 virtual control law in step k can be designed as follows:

$$x_{k+1}^* = -\xi_k^{1/\eta_{k+1}}\left[\frac{n-k+1+\tilde{\varphi}_k(\overline{x}_k,\tau)}{\kappa(\tau)} + c_k(\overline{x}_{k-1}) + \tilde{\gamma}_\kappa(\overline{x}_k,\tau) + \tilde{\rho}_\kappa(\overline{x}_k,\tau)\right]^{1/p_\kappa} \triangleq -\xi_k^{1/\eta_{k+1}}\beta_\kappa(\overline{x}_k,\tau), \tag{34}$$

where $\beta_k(\overline{\mathbf{x}}_k,\tau) > 0$ is a C^1 function. Substituting formula (34) into formula (33), the following inequality can be obtained:

$$\dot{V}_k(\overline{\mathbf{x}}_k,\tau) \le -(n-k+1)\sum_{i=1}^{k}\xi_i^{\omega} + \kappa(\tau)\xi_k^{\nu_k}\left(x_{k+1}^{p_k} - x_{k+1}^{*p_k}\right). \tag{35}$$

According to the above derivation process, the following C^0 state feedback controller can be designed in step n:

$$u = x_{n+1}^* = -\xi_n^{d_n}\beta_n(\mathbf{x},\tau), \tag{36}$$

which makes C^1 positive Lyapunov function $V_n(\mathbf{x},\tau)$ meet $V_n(\mathbf{x},\tau) \le 2\sum_{i=1}^{n}\xi_i^{\nu_i+(1/\eta_i)}$, and the following formula is established:

$$\dot{V}_n(\mathbf{x},\tau) \le -\sum_{i=1}^{n}\xi_i^{\omega}. \tag{37}$$

Considering that moment k contains the dynamic open set of origin $\overline{\Omega} = \{\mathbf{x} \in \mathbf{R}^n | |\xi_i| < 1,\ i = 1,\ldots,n\}$, we can choose $\varepsilon > 0$, which is small enough to make $\tilde{\Omega} = \{\mathbf{x} \in \mathbf{R}^n | V_n(\mathbf{x},\tau) < \varepsilon\}$ be a subset of $\overline{\Omega}$ in time k. From formulas (2) and (14), we can know that $\nu_i + (1/\eta_i) > \omega$, and combining (6) and (37), the following inequality can be achieved:

$$\frac{\mathrm{d}V}{\mathrm{d}\tau} \le -\frac{V^\rho}{2^\rho}, \quad \forall \mathbf{x} \in \tilde{\Omega}, \tag{38}$$

where $\rho\min_{i=1,\ldots,n}\{\nu_i + (1/\eta_i)\} = \omega$.

In the time domain τ and, according to equation (37), the solution trajectories of system (12) will enter the set $\tilde{\Omega}$ in finite time and the finite time can be marked as τ_s. It should be noted that τ_s cannot be calculated but can be obtained online by real-time detection of system errors. Furthermore, by using formula (38) and Lemma 1, the finite convergence time of system (12) in time domain τ can be estimated as follows:

$$\tau_f = \tau_s + \frac{2n^{1-\rho}}{1-\rho}. \tag{39}$$

Remark 3. From formula (37), we can know that x is bounded, and, according to the state feedback control law (36), it can be known that u is also bounded in the closed interval $[0,\tau_f]$ of time domain; that is to say, the actual control law (36) is not singular.

3.3. Design of Fixed-Time Controller in Time Domain t. Transform the mapping in (9) into the following compact form:

$$\tau = \tau_0(t) = \frac{\mu^2+\sigma^2}{\mu + \cot[t((\pi/2) + \arctan(\mu/\sigma))/T]}. \tag{40}$$

Consider that we have already made controller (36) of system (12) into finite-time stabilization in the last section. Let $t_f = t_0(\tau_f)$, and if the control law in time domain t is designed as

$$u(\mathbf{x},t) = -\xi_n^{1/\eta_{n+1}}\beta_n(\mathbf{x},\tau_0(t)), \quad 0 \le t < t_f. \tag{41}$$

Then, any solution trajectory of system (1) will reach the origin in finite time.

For the time set $[kt_f, kt_f + t_f)$, $k = 1,2,\ldots$ in time domain t, assume that the following time-domain coordinate mapping is adopted:

$$t = t_k(\tau) = t_0(\tau) + kt_f. \tag{42}$$

The control law can be designed as follows:

$$u(\mathbf{x},t) = -\xi_n^{1/\eta_{n+1}}\beta_n\left(\mathbf{x},\tau_0\left(t - kt_f\right)\right), \quad kt_f \le t < kt_f + t_f. \tag{43}$$

The solution trajectory of system (1) will always remain at the origin.

In conclusion, the fixed-time stabilization control law in time domain t can be designed as

$$u(\mathbf{x},t) = -\xi_n^{1/\eta_{n+1}}\beta_n\left(\mathbf{x},\tau_0\left(\mathrm{mod}\left(t,t_f\right)\right)\right), \tag{44}$$

where $\mathrm{mod}(t,t_f)$ denotes modular operation, the result of which is the remainder obtained by t dividing t_f.

Remark 4. The proposed control scheme provides a novel perspective of fixed-time stabilization. Compared with the traditional method composed of high-power and low-power terms [8–11], there exist only low-power terms in (44), which simplifies the design and analysis process to some degree. Besides, it is worth noticing that the setting times of [8–11, 17] depend on the control parameter, e.g., control gains and power terms. However, the setting time in this work can be directly specified in advance.

4. Simulation Experiment

4.1. System Scheme. To verify the effectiveness of the proposed control law, a practical example simulation is used to compare the proposed control method with recent literature.

To the best of our knowledge, existing fixed-time results consider at most so-called normal form systems [15], which is the trivial case of the high-order systems. Therefore, consider the following single link manipulator system:

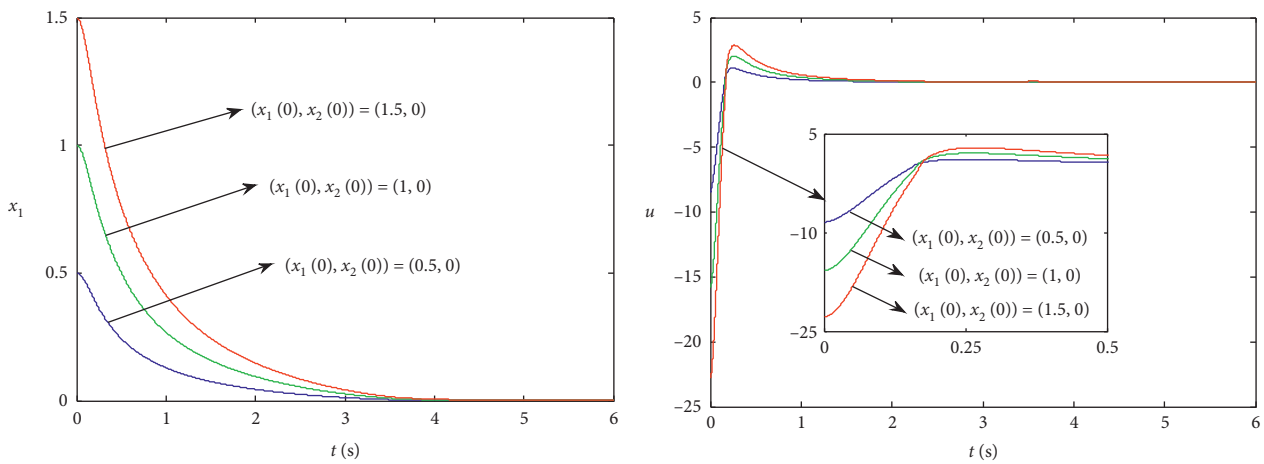

Figure 1: Response of system (46) to control law (44). (a) Equivalent angular displacement x_1. (b) Control input u.

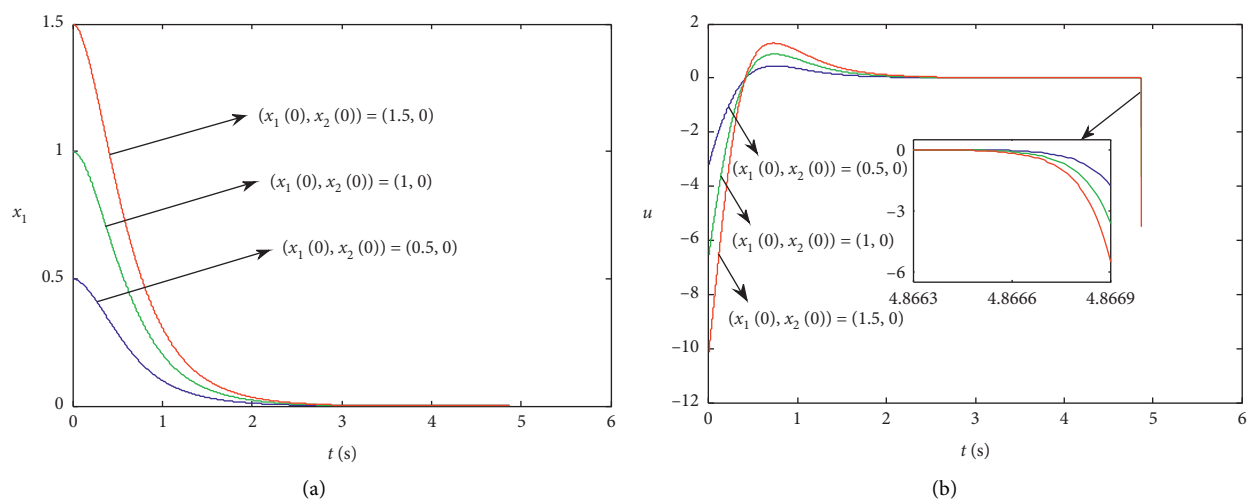

Figure 2: Response of system (46) to control law in [15]. (a) Equivalent angular displacement x_1. (b) Control input u.

$$ml\ddot{\varphi} + fl\dot{\varphi} + mg\sin\varphi = u, \tag{45}$$

where $\varphi \in (-(\pi/2), (\pi/2))$ is the rotation angular displacement, u is the external force acting on the manipulator, m is the mass of the manipulator, l is the distance from the center of mass of the manipulator to the rotating shaft, f is the unknown friction coefficient whose upper bound is known, and g is the acceleration of gravity. Assuming that the equivalent angular displacement is $x_1 = ml\varphi$ and the equivalent angular acceleration is $x_2 = ml\dot{\varphi}$, equation (45) can be written in the following form:

$$\begin{cases} \dot{x}_1 = x_2, \\ \dot{x}_2 = u - mg\sin\left(\dfrac{x_1}{ml}\right) - \dfrac{fx_2}{m}. \end{cases} \tag{46}$$

In the above formula, all physical quantities are in Si basic units, and the values of parameters in the simulation process are selected as $l = g$ and $m = \overline{f} = 1/g$.

For the fixed-time controller (44) designed in this paper, we can choose the parameters as follows: $\eta_1 = 13/11$, $\eta_2 = 11/9$, $\eta_3 = 9/7$, $\nu_1 = 1$, $\nu_2 = 103/99$, and $\mu = \sigma = 1$. For the controller designed in [15], we can choose corresponding parameters as follows: $\lambda = 0.1$, $k_1 = 1$, and $k = \theta = 2$.

Considering the value range of φ, the three following groups of initial conditions are selected in the simulation: $x_1(0) = 0.5,\ 1,\ 1.5$ and $x_2(0) = 0,\ 0,\ 0$. Figures 1(a) and 2(a) show the state changes of system (44) with the control law (46) proposed in this paper and with the control law proposed in [15]. It can be seen that, no matter what the initial conditions are, the said two methods achieve stabilization in a fixed time.

It can be seen from Figures 1(b) and 2(b) that the control input in this paper is nonsingular in the whole process; however, that of [15] diverges at the terminal moment. Therefore, from this point of view, the method proposed in this paper is more acceptable.

5. Conclusion

The problem of fixed-time stabilization for high-order nonlinear systems is studied in the paper. A control method based on time-domain mapping is firstly introduced. Compared with the existing literature, the paper proposes a new idea to realize fixed-time stabilization based on time-domain mapping, which greatly expands the research scope of fixed-time stabilization. Note that all the states should be accessible in this work; an interesting problem is the observer design in the case of partially unknown state, which will be considered in our further work.

Data Availability

The data used to support the findings of this study are included within the article. The original data ca be obtained from the corresponding author upon request.

Conflicts of Interest

The authors declare that there are no conflicts of interest regarding the publication of this paper.

Acknowledgments

The authors would like to acknowledge the Major Science and Technology Projects in Anhui Province (no. 18030901058).

References

[1] Y. J. Zhou, L. Wang, and C. Y. Sun, "Global asymptotic and finite-time stability for nonlinear systems," *ACTA Automatica Sinica*, vol. 39, no. 5, pp. 664–672, 2013.

[2] Z.-Y. Sun, M.-M. Yun, and T. Li, "A new approach to fast global finite-time stabilization of high-order nonlinear system," *Automatica*, vol. 81, no. 5, pp. 455–463, 2017.

[3] X. Huang, W. Lin, and B. Yang, "Global finite-time stabilization of a class of uncertain nonlinear systems," *Automatica*, vol. 41, no. 5, pp. 881–888, 2005.

[4] J. Back, S. G. Cheong, H. Shim, and J. H. Seo, "Nonsmooth feedback stabilizer for strict-feedback nonlinear systems that may not be linearizable at the origin," *Systems & Control Letters*, vol. 56, no. 11-12, pp. 742–752, 2007.

[5] J. Fu, T. Y. Chai, C. Y. Su et al., "Adaptive output tracking control of a class of nonlinear systems," *Control Engineering of China*, vol. 22, no. 4, pp. 731–736, 2015.

[6] J. Fu, R. Ma, and T. Chai, "Adaptive finite-time stabilization of a class of uncertain nonlinear systems via logic-based switchings," *IEEE Transactions on Automatic Control*, vol. 62, no. 11, pp. 5998–6003, 2017.

[7] V. Andrieu, L. Praly, and A. Astolfi, "Homogeneous approximation, recursive observer design, and output feedback," *SIAM Journal on Control and Optimization*, vol. 47, no. 4, pp. 1814–1850, 2008.

[8] A. Polyakov, "Nonlinear feedback design for fixed-time stabilization of linear control systems," *IEEE Transactions on Automatic Control*, vol. 57, no. 8, pp. 2106–2110, 2012.

[9] Y. Dvir and A. Levant, "Accelerated twisting algorithm," *IEEE Transactions on Automatic Control*, vol. 60, no. 10, pp. 2803–2807, 2015.

[10] J. P. Mishra, C. J. Li, X. H. Yu et al., "Fixed-time converging terminal surface with non-singular control design for second-order systems," in *Proceedings of IFAC World Congress*, pp. 5139–5143, Elsevier, Toulouse, France, July 2017.

[11] B. Tian, Z. Zuo, X. Yan, and H. Wang, "A fixed-time output feedback control scheme for double integrator systems," *Automatica*, vol. 80, no. 3, pp. 17–24, 2017.

[12] Y. Liu, Y. Zhao, W. Ren, and G. Chen, "Appointed-time consensus: accurate and practical designs," *Automatica*, vol. 89, no. 3, pp. 425–429, 2018.

[13] A. Polyakov, D. Efimov, and W. Perruquetti, "Finite-time and fixed-time stabilization: implicit Lyapunov function approach," *Automatica*, vol. 51, no. 1, pp. 332–340, 2015.

[14] C. Hua, Y. Li, and X. Guan, "Finite/fixed-time stabilization for nonlinear interconnected systems with dead-zone input," *IEEE Transactions on Automatic Control*, vol. 62, no. 5, pp. 2554–2560, 2017.

[15] Y. Song, Y. Wang, J. Holloway, and M. Krstic, "Time-varying feedback for regulation of normal-form nonlinear systems in prescribed finite time," *Automatica*, vol. 83, no. 7, pp. 243–251, 2017.

[16] J. Wu, D. Yang, X. He, and X. Li, "Finite-time stability for a class of underactuated systems subject to time-varying disturbance," *Complexity*, vol. 2020, Article ID 8704505, 7 pages, 2020.

[17] J. Hu, G. Sui, X. Lv, and X. Li, "Fixed-time control of delayed neural networks with impulsive perturbations," *Nonlinear Analysis: Modelling and Control*, vol. 23, no. 6, pp. 904–920, 2018.

Hindawi
Complexity
Volume 2021, Article ID 9956587, 11 pages
https://doi.org/10.1155/2021/9956587

Research Article

Bipartite Synchronization of Heterogeneous Signed Networks with Distributed Impulsive Control

Guizhen Feng,[1] **Jian Ding**,[2] **Jinde Cao**,[3,4] **and Qingqing Cao**[5]

[1]*Department of Basic Courses, Nanjing Vocational University of Industry Technology, Nanjing 210023, China*
[2]*College of Math and Statistics, Nanjing University of Information Science and Technology, Nanjing 210044, China*
[3]*School of Mathematics, Southeast University, Nanjing 210096, China*
[4]*Yonsei Frontier Lab, Yonsei University, Seoul 03722, Republic of Korea*
[5]*Aviation College, Nanjing Vocational University of Industry Technology, Nanjing 210023, China*

Correspondence should be addressed to Jian Ding; 416999448@qq.com

Received 5 March 2021; Revised 27 April 2021; Accepted 4 June 2021; Published 21 June 2021

Academic Editor: Dan Selisteanu

This study investigates the bipartite synchronization of heterogeneous signed networks with distributed impulsive control. Leader-follower bipartite synchronization within a nonzero error bound is analyzed when the average impulsive interval is $T_a < \infty$ or $T_a = \infty$. Some sufficient conditions to achieve the bipartite quasi-synchronization are presented, and the synchronization error level is estimated by the specific mathematical expression. The correctness of the theoretical results is verified by numerical examples.

1. Introduction

There are some cooperative behaviors of interconnected dynamic systems, such as image processing [1], pattern recognition [2], and secure communication [3], which have been eliciting increasing attention recently. In particular, synchronization, as a typical collective behavior, has been widely studied by many researchers through different control methods, for example, feedback control [4, 5], adaptive control [6–8], event-triggered control [9–11], and impulsive control [12–18]. Among these methods, impulsive control, as a form of discontinuous control [19], has advantages of low cost and high efficiency and so has been widely used in many fields, such as the population growth model [19] and neural networks [20]. Particularly, a distributed impulsive controller was proposed in [21] and successfully applied to synchronization of a leaderless network. Later, the method of distributed impulsive control was also used to investigate the consensus of multiagent systems [22, 23].

In most early studies, in order to make the system achieve the desired trajectory, the controller is usually applied to all nodes. However, this is difficult to implement or even is inapplicable, especially for large networks. Pinning control is a kind of control strategy which only needs control finite nodes of the system [24, 25]. Considering the advantages of pinning control and impulsive control, the pinning impulsive controller was proposed in [26]. Lu et al. [27] studied the synchronization of complex dynamic networks by using a pinning impulsive controller. In [28], a distributed pinning impulsive controller was developed to investigate the synchronization of heterogeneous networks.

In most of the aforementioned literature, the upper bound and lower bound of the impulsive interval determine the frequency of the impulse occurrence. Lu et al. [29] proposed the concept of average impulsive interval, and then it was used to describe a sparse impulsive sequence with an infinite average impulsive interval in [30]. On the contrary, most studies on interactions among individual systems are assumed to be unsigned, where the weights of the adjacency matrix are nonnegative. In fact, it is more reasonable to consider signed networks since the agents in a network may be cooperative or competitive so that interaction weights

between agents can either be positive or negative. Such weights are called signed interaction digraphs. Coordination control on signed networks has become a hot topic in recent years [31, 32]. Proskurnikov et al. [31] investigated opinion dynamics of social networks. Xia et al. [32] studied the separation of opinion in trust-mistrust social networks. Meng et al. [33] achieved bipartite consensus on a signed network. The concept of bipartite synchronization was presented in [34] under a signed network. In [35], bipartite synchronization under a pinning controller was studied on signed and switching networks.

Based on the aforementioned studies, we intend to study the bipartite synchronization of a signed network with distributed impulsive control. The following factors are integrated into our study: (i) interaction graphs are signed; in other words, the weights of the adjacency matrix can be positive or negative; (ii) two error levels are given for bipartite quasi-synchronization of asymmetric networks; (iii) more general impulsive sequences whose average impulsive interval is finite or infinite are considered. By designing a distributed impulsive controller, this study aims to develop the heterogeneous signed network that can be bipartitely quasi-synchronized.

The rest of the paper is organized as follows: in Section 2, we formulate the problem of bipartite quasi-synchronization between the leader and the heterogeneous systems under a distributed impulsive controller and give some necessary preparations. In Section 3, we establish some bipartite quasi-synchronization criteria for the signed network. In Section 4, we design numerical examples to verify the correctness of our theoretical results. In Section 5, we summarize all results in a conclusion.

Notations: throughout the paper, I_n denotes an n-dimensional identity matrix; we write $A > 0$ if matrix A is positive definite; $\sigma_{\max}(B)$ is the maximum singular value for matrix B; $\|\cdot\|$ is the Euclidean vector norm; $\otimes$ is the Kronecker product.

2. Problem Descriptions and Preliminaries

2.1. Problem Formulation. For a heterogeneous system, we use a signed graph $\mathscr{A}^s(\mathscr{U}, \mathscr{V}, \mathscr{G}^s)$ to denote its underlying topology, where $\mathscr{U} = \{1, 2, \ldots, N\}$ is the set of nodes, $\mathscr{V} \subseteq \mathscr{U} \times \mathscr{U}$ is the set of edges, $\mathscr{G}^s = (a_{ij}^s) \in \mathbb{R}^{\mathbb{N}\times\mathbb{N}}$: $a_{ij}^s \neq 0 \Leftrightarrow (j, i) \in \mathscr{V}$ is the weighted adjacency matrix, and a_{ij}^s can be positive or negative.

There are some necessary definitions and lemmas in the process of theoretical derivation.

Definition 1 (see [36]). The sighed graph $\mathscr{A}^s(\mathscr{U}, \mathscr{V}, \mathscr{G}^s)$ is called structurally balanced if its node set $\mathscr{U}$ can be partitioned into two disjoint subsets $\mathscr{U}_1$ and $\mathscr{U}_2$ such that their induced subgraphs $G(\mathscr{U}_1)$ and $G(\mathscr{U}_2)$ are both unsigned, and the weights of all links between $G(\mathscr{U}_1)$ and $G(\mathscr{U}_2)$ are negative.

Lemma 1 (see [36]). *If a signed graph $\mathscr{A}^s(\mathscr{U}, \mathscr{V}, \mathscr{G}^s)$ is structurally balanced, then there exists a diagonal matrix of form $\Sigma = diag(\sigma_1, \sigma_2, \ldots, \sigma_N), \sigma_i \in \{\pm 1\}$, $i = 1, 2, \ldots, N$, such that all entries of $\Sigma\mathscr{G}^s\Sigma$ are nonnegative.*

Assume that the nodes of the heterogeneous system have the following dynamics:

$$\dot{x}_i(t) = A_i x_i(t) + B_i f(x_i(t)) + u_i(t), \tag{1}$$

where $x_i(t) = (x_{i1}(t), \ldots, x_{in}(t))^T \in \mathbb{R}^n$ is the state of the ith node; $f(x) = (f_1(x), f_2(x), \ldots, f_n(x))^T$ is a nonlinear function on $\mathbb{R}^n$; $A_i, B_i \in \mathbb{R}^{n\times n}$ are constant matrices; and $u_i(t)$ is a control protocol.

The leader node of nonlinear system (1) is described by

$$\dot{s}(t) = As(t) + Bf(s(t)), \tag{2}$$

where $s(t) \in \mathbb{R}^n$ is bounded.

Assumption 1. The nonlinear function $f(x) = (f_1(x), f_2(x), \ldots, f_n(x))^T$ is odd and satisfies the Lipschitz condition. Specifically,

$$f_i(-x) = -f_i(x), \quad i, j = 1, 2, \ldots, n, \tag{3}$$

and there are nonnegative constants δ_{ij} such that, for any $x_1, x_2 \in \mathbb{R}^n$,

$$\left|f_i(x_1) - f_i(x_2)\right| \leq \sum_{j=1}^{n} \delta_{ij}\left|x_{1j} - x_{2j}\right|. \tag{4}$$

Since (1) is heterogeneous, it is difficult to realize full synchronization by a static controller. In recent years, quasi-synchronization about heterogeneous networks received wide attention [28, 35], but this is not applicable for signed heterogeneous networks. According to dynamic properties of network (1) and leader (2), a more general synchronization concept, called bipartite quasi-synchronization, is introduced below.

Definition 2. Suppose that the signed graph $\mathscr{A}^s(\mathscr{U}, \mathscr{V}, \mathscr{G}^s)$ of (1) is structurally balanced, $\Sigma = \mathrm{diag}(\sigma_1, \sigma_2, \ldots, \sigma_N), \sigma_i \in \{\pm 1\}$, $i = 1, 2, \ldots, N$, is a diagonal matrix such that all entries of $\Sigma\mathscr{G}^s\Sigma$ are nonnegative. Signed network (1) is said to achieve bipartite quasi-synchronization if the error $e_i(t) = x_i(t) - \sigma_i s(t)$ $(i = 1, 2, \ldots, N)$ converges to some compact set $M_1 = \{e_i(t) \in \mathbb{R}^n | \|e_i(t)\| \leq \epsilon, \epsilon > 0\}$ when $t \longrightarrow \infty$.

Obviously, when $\sigma_i = 1$ for $i = 1, 2, \ldots, n$, bipartite quasi-synchronization becomes quasi-synchronization.

Suppose that the signed graph $\mathscr{A}^s(\mathscr{U}, \mathscr{V}, \mathscr{G}^s)$ of (1) is structurally balanced, $\Sigma = \mathrm{diag}(\sigma_1, \sigma_2, \ldots, \sigma_N), \sigma_i \in \{\pm 1\}$, $i = 1, 2, \ldots, N$, is a fixed diagonal matrix such that all entries of $\Sigma\mathscr{G}^s\Sigma$ are nonnegative. The distributed impulsive protocol with pinning control of (1) is designed as

$$u_i(t) = \sum_{k=1}^{\infty}\left[-c\sum_{j=1}^{N}\left|a_{ij}^s\right|\left(x_i(t) - \operatorname{sign}\left(a_{ij}^s\right)x_j(t)\right) - cd_{ik}\left(x_i(t) - \sigma_i s(t)\right)\right]\delta(t - t_k), \tag{5}$$

where c is a constant and $d_{ik} > 0$ if node i is pinned; otherwise, $d_{ik} = 0$. δ is the Dirac function, and $\{t_k\}_{k=1}^{\infty}$ is the impulse sequence satisfying $0 = t_0 < t_1 < t_2 \cdots < t_k < \cdots$, $\lim_{k\longrightarrow\infty} t_k = \infty$.

Remark 1. Controller (5) indicates that if two nodes i and j are cooperative, $a_{ij}^s > 0$, and the coupling term is expressed as $a_{ij}^s(x_i(t) - x_j(t))$; if two nodes i and j are competitive, $a_{ij}^s < 0$, and the coupling term is expressed as $-a_{ij}^s(x_i(t) + x_j(t))$ [36]. On the contrary, if the graph $\mathscr{A}^s$ is unsigned, controller (5) degenerates into a traditional distributed impulsive controller defined by previous studies [21, 23, 28].

Based on the aforementioned control protocol (5), the impulsive signed network reads as

$$\begin{cases} \dot{x}_i(t) = A_i x_i(t) + B_i f\left(x_i(t)\right), \quad t \neq t_k, \\ \Delta x_i(t) = -c\sum_{j=1}^{N}\left|a_{ij}^s\right|\left(x_i(t_k^-) - \operatorname{sign}\left(a_{ij}^s\right)x_j(t_k^-)\right) - cd_{ik}\left(x_i(t_k^-) - \sigma_i s(t_k^-)\right), \end{cases} \tag{6}$$

where $\Delta x_i(t_k) = x_i(t_k^+) - x_i(t_k^-)$, $x_i(t_k^-) = \lim_{h\longrightarrow 0^-} x_i\ (t_k + h)$, and $x_i(t_k) = x_i(t_k^+) = \lim_{h\longrightarrow 0^+} x_i(t_k + h)$.

Remark 2. According to Lemma 2, it is necessary that $\mathscr{A}^s$ is structurally balanced during investigating the bipartite synchronization. In fact, Meng et al. [33] demonstrated that a network cannot obtain bipartite synchronization when the signed network is structurally unbalanced.

Definition 3. Let $\zeta \triangleq \{t_1, t_2, \ldots\}$ be an impulsive sequence on $(t_0, +\infty)$. For any $t \in (t_0, +\infty)$, $N_\zeta(t, t_0)$ denotes the impulsive times of ζ on the interval (t_0, t). Then, the average impulsive interval, denoted by T_a, is defined by

$$T_a = \lim_{t\longrightarrow+\infty}\frac{t - t_0}{N_\zeta(t, t_0)}. \tag{7}$$

Remark 3. Obviously, $0 \le T_a \le \infty$. For example, let $N_\zeta(t, t_0) = [t^{3/2}]$; then, $T_a = 0$; let $N_\zeta(t, t_0) = [t^{1/2}]$; then, $T_a = \infty$. When $0 < T_a < \infty$, it was proposed in [29] and then was applied in [19–23, 26–28]. The case of $T_a = \infty$ was proposed in [30] when impulses occur infinitely but sparsely.

2.2. Synchronization Error Dynamics. Let $\overline{L} = (\bar{l}_{ij})_{N\times N}$ be the Laplacian matrix of network (6); then, $\overline{L} = (\bar{l}_{ij})_{N\times N} = \mathscr{B} - \mathscr{G}^s$, where $\mathscr{B} = \operatorname{diag}(b_1, b_2, \ldots, b_N)$ with $b_i = \sum_{k=1}^{N}|a_{ik}^s|$. Let $\mathscr{A}(\mathscr{U}, \mathscr{V}, \mathscr{G})$ be the unsigned graph corresponding to $\mathscr{A}^s$. Then, $\mathscr{G} = (|a_{ij}^s|)_{N\times N}$, and so, the corresponding Laplacian matrix $L = (l_{ij})_{N\times N} = \mathscr{B} - \mathscr{G}$ with $l_{ij} = -|a_{ij}^s|$ for $i \neq j$ and $l_{ii} = \sum_{k=1,k\neq i}|a_{ik}^s|$.

Since $\mathscr{A}^s(\mathscr{U}, \mathscr{V}, \mathscr{G}^s)$ is structurally balanced and the diagonal matrix $\Sigma = \operatorname{diag}(\sigma_1, \sigma_2, \ldots, \sigma_N)$, $\sigma_i \in \{\pm 1\}$, $i = 1, 2, \ldots, N$, make sure that $\Sigma\mathscr{G}^s\Sigma = \mathscr{G}$. By $\overline{L} = \mathscr{B} - \mathscr{G}^s$ and $L = \mathscr{B} - \mathscr{G}$, it is easy to see that $L = \Sigma\overline{L}\Sigma$ holds with $l_{ij} = -|a_{ij}^s|$ for $i \neq j$ and $l_{ii} = \sum_{k=1,k\neq i}|a_{ik}^s|$.

Let $\overline{x}_i(t) = \sigma_i x_i(t)$, $i = 1, \ldots, N$, that is, $x_i(t) = \sigma_i\overline{x}_i(t)$. Then, it follows from (6) that

$$\begin{cases} \dot{\overline{x}}_i(t) = A_i\overline{x}_i(t) + B_i\sigma_i f\left(\sigma_i\overline{x}_i(t)\right), \quad t \neq t_k, \\ \Delta\overline{x}_i(t) = -c\sum_{j=1}^{N}\left|a_{ij}^s\right|\left(\overline{x}_i(t_k^-) - sign\left(a_{ij}^s\right)\overline{x}_j(t_k^-)\right) - cd_{ik}\left(\overline{x}_i(t_k^-) - s(t_k^-)\right). \end{cases} \tag{8}$$

By Assumption 1, $f_i(\cdot)$, $i \in \{1, \ldots, N\}$ is odd. Then, $\sigma_i f(\sigma_i\overline{x}_i(t)) = f(\overline{x}_i(t))$ holds for any $\sigma_i \in \{-1, 1\}$ and $i \in \{1, \ldots, N\}$. Then, from (8), we get

$$\begin{cases} \dot{\overline{x}}_i(t) = A_i\overline{x}_i(t) + B_i f\left(\overline{x}_i(t)\right), \quad t \neq t_k, \\ \Delta\overline{x}_i(t) = -c\sum_{j=1}^{N} l_{ij}\overline{x}_j(t_k^-) - cd_{ik}\left(\overline{x}_i(t_k^-) - s(t_k^-)\right). \end{cases} \tag{9}$$

From (2) and (9), based on the fact that L is a matrix with zero row sum, the following error system can be obtained:

$$\begin{cases} \dot{e}_i(t) = A_i e_i(t) + B_i g\left(e_i(t)\right) + W_i(s(t)), \quad t \neq t_k, \\ \Delta e_i(t) = -c\sum_{j=1}^{N} l_{ij}e_j(t_k^-) - cd_{ik}e_i(t_k^-), \end{cases} \tag{10}$$

where $e_i(t) = \overline{x}_i(t) - s(t)$, $g(e_i(t)) = f(e_i(t) + s(t)) - f(s(t))$, and $W_i(s(t)) = (A_i - A)s(t) + (B_i - B)f(s(t))$. Since $s(t)$ is bounded and $f(\cdot)$ is a Lipschitz function, it is easy to know that $W_i(s(t))$ is bounded. Suppose $\sup_{t\geq t_0}\|W_i(s(t))\| = w_i$, $i = 1, \ldots, n$.

Now, we rewrite the error system with a matrix form at the impulse instant $t = t_k$:

$$e(t_k) = ((I_N - c(L + D_k)) \otimes I_n)e(t_k^-), \tag{11}$$

where $e(t) = (e_1^T, e_2^T, \ldots, e_N^T)^T$ and $D_k = \mathrm{diag}(d_{1k}, d_{2k}, \ldots, d_{Nk})$.

Lemma 2 (see [37]; Schur complement). *Suppose that $Q(x)$ and $R(x)$ are both symmetric time-varying matrices; then, for any time-varying matrix $S(x)$,*

$$\begin{bmatrix} Q(x) & S(x) \\ S^T(x) & R(x) \end{bmatrix} > 0 \tag{12}$$

is equivalent to

(1) $Q(x) > 0$, $R(x) - S^T(x)Q^{-1}(x)S(x) > 0$,

or

(2) $R(x) > 0$, $Q(x) - S^T(x)R^{-1}(x)S(x) > 0$.

Definition 4. Symmetric time-varying matrix $P(t) \in \mathbb{R}^{n\times n}$ is called to be uniformly bounded and positive definite if there exist constants $\check{m} > 0$ and $\widehat{m} > 0$ such that

$$0 < \check{m} \leq \lambda_{\min}(P(t)) \leq \lambda_{\max}(P(t)) \leq \widehat{m}, \quad \forall t \geq 0. \tag{13}$$

Lemma 3 (see [38]). *Suppose that $0 \leq \tau_i(t) \leq \tau$, $i = 1, 2, \ldots, n$, $F(t, w, w_1, \ldots, w_n)$: $\mathbb{R}^+ \times \mathbb{R}^{n+1} \longrightarrow \mathbb{R}$ is nondecreasing in w_i for each fixed $(t, w, w_1, \ldots, w_{i-1}, w_{i+1}, \ldots, w_n)$, $i = 1, 2, \ldots, n$, and $I_k(w)$: $\mathbb{R} \longrightarrow \mathbb{R}$ is nondecreasing in w, $k \in \mathbb{N}^+$. If $u(t)$ and $v(t)$ satisfy*

$$\begin{cases} D^+u(t) \leq F(t, u(t), u(t-\tau_1(t)), \ldots, u(t-\tau_n(t))), & t \neq t_k, \\ u(t_k^+) \leq I_k(u(t_k^-)), & k \in \mathbb{N}^+, \end{cases}$$
$$\begin{cases} D^+v(t) \geq F(t, v(t), v(t-\tau_1(t)), \ldots, v(t-\tau_n(t))), & t \neq t_k, \\ v(t_k^+) \geq I_k(v(t_k^-)), & k \in \mathbb{N}^+, \end{cases} \tag{14}$$

then $u(t) \leq v(t)$ for $-\tau \leq t \leq 0$ implies that $u(t) \leq v(t)$ for $t \geq 0$.

3. Main Results

In this section, we derive some bipartite quasi-synchronization criteria for error system (10). As it is known, it is very difficult to achieve bipartite quasi-synchronization when we considered different average impulsive intervals. Here, we focus on two cases of average impulsive intervals. One is the case of $T_a < \infty$, and the other is the case of $T_a = \infty$.

3.1. The Case of $T_a < \infty$

Theorem 1. *Suppose that Assumption 1 holds and the average impulsive interval $T_a < \infty$. Let $P_i(t) \in \mathbb{R}^{n\times n}$, $i = 1, 2, \ldots, N$, be a sequence of symmetric time-varying matrices, which are uniformly bounded and positive definite, i.e., there exist positive numbers $\check{m}_i$ and $\widehat{m}_i$ satisfying $\check{m}_i \leq \lambda_{\min}(P_i(t)) \leq \lambda_{\max}(P_i(t)) \leq \widehat{m}_i$, $i = 1, 2, \ldots, N$. If there exist diagonal matrices $\Sigma_j > 0$ $(j = 1, 2)$, D_k $(k \in \mathbb{N}^+)$, and scalars α, μ_k $(k = 1, 2, \ldots, N_\zeta(t, s))$, $c > 0$, such that*

$$\begin{bmatrix} \dot{P}_i + P_iA_i + A_i^TP_i - \alpha P_i + \Delta^T\Sigma_1\Delta & P_iB_i & P_i \\ B_i^TP_i & -\Sigma_1 & 0 \\ P_i & 0 & -\Sigma_2 \end{bmatrix} < 0, \tag{15}$$

$$\begin{bmatrix} \mu_k P(t_k^-) & \Pi_k^T P(t_k^+) \\ P(t_k^+)\Pi_k & P(t_k^+) \end{bmatrix} > 0, \tag{16}$$

$$\eta \triangleq \frac{\ln \mu}{T_a} + \alpha < 0, \tag{17}$$

where $P(t) = diag(P_1(t), P_2(t), \ldots, P_N(t))$, $\Pi_k = (I_N - c(L + D_k)) \otimes I_n$, $\mu = \lim_{t\longrightarrow\infty}((|\mu_1| + |\mu_2| + \cdots |\mu_{N_\zeta(t,s)}|)/N_\zeta(t, s)) > 0$, and $\Delta = (\delta_{ij})_{n\times n}$, then the bipartite quasi-synchronization can be achieved. Specifically, for $0 > \eta_1 > \eta$, error system (10) between nonlinear system (1) and leader (2) exponentially converges into

$$S = \left\{ e \in \mathbb{R}^{n\times N} \,\middle|\, \|e\| \leq \sqrt{-\frac{\lambda_{\max}(\Sigma_2)\sum_{i=1}^N \omega_i^2}{\eta_1 \min_i\{\check{m}_i\}}} \right\}, \tag{18}$$

and the convergence rate is $-(\eta_1/2)$.

Construct the Lyapunov function

$$V(e(t)) = \sum_{i=1}^N e_i^T(t)P_i(t)e_i(t). \tag{19}$$

Then, the derivative of $V(e(t))$ is

$$\dot{V}(e(t)) = \sum_{i=1}^N e_i^T(t)\left[\dot{P}_i(t)e_i(t) + 2P_iA_ie_i(t) + 2P_iB_ig(e_i(t)) + 2P_iW_i(s(t))\right]. \tag{20}$$

By Assumption 1,

$$\begin{aligned}
&2\sum_{i=1}^{N} e_i^T(t)P_iB_ig(e_i(t)) \\
&\quad\le \sum_{i=1}^{N} e_i^T(t)P_iB_i\Sigma_1^{-1}B_i^TP_ie_i(t) + \sum_{i=1}^{N} g(e_i(t))^T\Sigma_1 g(e_i(t)) \\
&\quad\le \sum_{i=1}^{N} e_i^T(t)P_iB_i\Sigma_1^{-1}B_i^TP_ie_i(t) + \sum_{i=1}^{N} e_i^T(t)\Delta^T\Sigma_1\Delta e_i(t) \\
&\quad= \sum_{i=1}^{N} e_i^T(t)\left[P_iB_i\Sigma_1^{-1}B_i^TP_i + \Delta^T\Sigma_1\Delta\right]e_i(t),
\end{aligned} \tag{21}$$

$$\begin{aligned}
&2\sum_{i=1}^{N} e_i^T(t)P_iW_i(s(t)) \\
&\quad\le \sum_{i=1}^{N} e_i^T(t)P_i\Sigma_2^{-1}P_ie_i(t) + \sum_{i=1}^{N} W_i(s(t))^T\Sigma_2W_i(s(t)) \\
&\quad\le \sum_{i=1}^{N} e_i^T(t)P_i\Sigma_2^{-1}P_ie_i(t) + \lambda_{\max}(\Sigma_2)\sum_{i=1}^{N}\omega_i^2,
\end{aligned} \tag{22}$$

where $\Delta = (\delta_{ij})_{n\times n}$.

Substituting (21) and (22) into (20) yields

$$\dot{V}(e(t)) = \sum_{i=1}^{N} e_i^T(t)\left[\dot{P}_i(t) + 2P_iA_i + P_iB_i\Sigma_1^{-1}B_i^TP_i + \Delta^T\Sigma_1\Delta + P_i\Sigma_2^{-1}P_i\right]e_i(t) + \lambda_{\max}(\Sigma_2)\sum_{i=1}^{N}\omega_i^2. \tag{23}$$

By Lemma 2 and (15), we obtain

$$\dot{V}(e(t)) \le \alpha V(t) + \lambda_{\max}(\Sigma_2)\sum_{i=1}^{N}\omega_i^2. \tag{24}$$

When $t = t_k$, (11) gives

$$e(t_k) = ((I_N - c(L + D_k))\otimes I_n)e(t_k^-) = \Pi_k e_i(t_k^-). \tag{25}$$

By Lemma 2 and (16), we have $\mu_k P(t_k^-) - \Pi_k^T P(t_k^+)\Pi_k > 0$. Thus,

$$\begin{aligned}
V(t_k^+) &= e^T(t_k)P(t_k^+)e(t_k) \\
&= e^T(t_k^-)\Pi_k^TP(t_k^-)\Pi_k e(t_k^-) \\
&\le \mu_k e^T(t_k^-)P(t_k^-)e(t_k^-) \\
&\le \mu_k V(t_k^-).
\end{aligned} \tag{26}$$

For any $\varepsilon > 0$, consider the following comparison system:

$$\begin{cases}
\dot{v}(e(t)) = \alpha v(t) + \lambda_{\max}(\Sigma_2)\sum_{i=1}^{N}\omega_i^2 + \varepsilon, \quad t \ne t_k, \\
v(t_k^+) = \mu_k v(t_k^-). \\
v(0) = \max_i\{\hat{m}_i\}\|e(0)\|^2.
\end{cases} \tag{27}$$

Let $v(t)$ be the unique solution of (27); then, we obtain from Lemma 3 that $V(t) \le v(t)$ for all $t > 0$. Using the idea of the variation of parameters, we can write the form of $v(t)$ as

$$v(t) = W(t,0)v(0) + \int_0^t W(t,s)\left(\lambda_{\max}(\Sigma_2)\sum_{i=1}^{N}\omega_i^2 + \varepsilon\right)\mathrm{d}s, \tag{28}$$

where $W(t,s)$, $0 \le s \le t$, satisfies

$$\begin{aligned}
W(t,s) &= e^{\alpha(t-s)}\mu_1\mu_2\cdots\mu_{N_\zeta(t,s)} \\
&\le^{\alpha(t-s)}\left(\frac{|\mu_1| + |\mu_2| + \cdots |\mu_{N_\zeta(t,s)}|}{N_\zeta(t,s)}\right)N_\zeta(t,s) \\
&= e^{\alpha(t-s)}e^{N_\zeta(t,s)\ln\left(\left(|\mu_1|+|\mu_2|+\cdots|\mu_{N_\zeta(t,s)}|\right)/N_\zeta(t,s)\right)} \\
&= e^{\alpha(t-s)}e^{\frac{\ln\left(\left(|\mu_1| + |\mu_2| + \cdots |\mu_{N_\zeta(t,s)}|\right)/N_\zeta(t,s)\right)}{\left((t-s)/N_\zeta(t-s)\right)}(t-s)}.
\end{aligned} \tag{29}$$

Due to the construction of μ and the definition of T_a, for any η_1, $\eta < \eta_1 < 0$, there is $T > 0$ such that, for $t > T$ and $0 \le s \le t$,

$$\begin{aligned} W(t,s) &\le {}^{\alpha(t-s)} e^{\left((\ln \mu/T_a)+\eta_1-\eta\right)(t-s)} \\ &= e^{\left((\ln \mu/T_a)+\eta_1-\eta+\alpha\right)(t-s)} \\ &= e^{\eta_1(t-s)}. \end{aligned} \tag{30}$$

Substituting (30) into (28) yields

$$\begin{aligned} v(t) &\le {}^{\eta_1 t} v(0) + \int_0^t e^{\eta_1(t-s)} \left(\lambda_{\max}(\Sigma_2) \sum_{i=1}^N \omega_i^2 + \varepsilon \right) \mathrm{d}s \\ &\le {}^{\eta_1 t} v(0) + \frac{\lambda_{\max}(\Sigma_2) \sum_{i=1}^N \omega_i^2 + \varepsilon}{\eta_1} \left(e^{\eta_1 t} - 1 \right) \\ &\le {}^{\eta_1 t} v(0) - \frac{\lambda_{\max}(\Sigma_2) \sum_{i=1}^N \omega_i^2 + \varepsilon}{\eta_1}. \end{aligned} \tag{31}$$

Let $\varepsilon \longrightarrow 0$; one has

$$\begin{aligned} \min_i \{\check{m}_i\} \|e(t)\|^2 &\le \sum_{i=1}^N e_i(t) P_i(t) e_i(t) \\ &= V(t) \le v(t) \\ &\le {}^{\eta_1 t} v(0) - \frac{\lambda_{\max}(\Sigma_2) \sum_{i=1}^N \omega_i^2}{\eta_1}. \end{aligned} \tag{32}$$

Consequently,

$$\|e(t)\| \le \sqrt{\frac{v(0)}{\min_i \{\check{m}_i\}}} e^{(\eta_1/2)t} + \sqrt{-\frac{\lambda_{\max}(\Sigma_2) \sum_{i=1}^N \omega_i^2}{\eta_1 \min_i \{\check{m}_i\}}}, \tag{33}$$

which implies that (10) converges exponentially into $S = \left\{ e \in \mathbb{R}^{n\times N} \middle| \|e\| \le \sqrt{-(\lambda_{\max}(\Sigma_2) \sum_{i=1}^N \omega_i^2)/(\eta_1 \min_i \{\check{m}_i\})} \right\}$ at convergence rate $-(\eta_1/2)$ when $t \longrightarrow \infty$.

Remark 4. It is noticed that the impulses in Theorem 1 may be desynchronizing ($|\mu_k| > 1$), synchronizing ($|\mu_k| < 1$), or inactive ($|\mu_k| = 1$). However, most of the previous studies are devoted to investigate these impulses separately. The problem of bipartite quasi-synchronization is to find an impulsive interval T_a, a coupling strength c, and a pinning matrix D_k so that all stable or unstable isolated nodes in a network synchronize into a bounded region.

Corollary 1. *Suppose that Assumption 1 holds and the average impulsive interval $T_a < \infty$. If there exist matrix $P > 0$, diagonal matrices $\Sigma_j > 0$ ($j = 1, 2$), D, and scalars $c > 0$, $0 < \mu < \infty$, α, and $\check{m} > 0$ such that*

$$\begin{bmatrix} PA_i + A_i^T P - \alpha P + \Delta^T \Sigma_1 \Delta & PB_i & P \\ B_i^T P & -\Sigma_1 & 0 \\ P & 0 & -\Sigma_2 \end{bmatrix} < 0, \tag{34}$$

$$P \ge \check{m} I, \tag{35}$$

$$\eta \triangleq \frac{\ln \mu}{T_a} + \alpha < 0, \tag{36}$$

where $\Delta = (\delta_{ij}) n \times n$ and $\mu = \sigma_{\max}^2 (I_N - c(L + D))$, then (10) exponentially converges into

$$S = \left\{ e \in \mathbb{R}^{n\times N} \middle| \|e\| \le \sqrt{-\frac{\lambda_{\max}(\Sigma_2) \sum_{i=1}^N \omega_i^2}{\eta_1 \check{m}}} \right\} \tag{37}$$

at convergence rate $-(\eta_1/2)$ for $0 > \eta_1 > \eta$.

Proof. Let

$$V(e(t)) = \sum_{i=1}^N e_i^T(t) P e_i(t). \tag{38}$$

If $t = t_k$, one has

$$\begin{aligned} V(t_k^+) &= e^T(t_k)(I_N \otimes P) e(t_k) \\ &= e^T(t_k^-)\left(\left(I_N - c(L+D)^T\right) \otimes I_n\right)(I_N \otimes P)\left((I_N - c(L+D)) \otimes I_n\right) e(t_k^-) \\ &= e^T(t_k^-)\left(I_N - c(L+D)^T\right)(I_N - c(L+D)) \otimes P e(t_k^-) \\ &\le \sigma_{\max}^2 \left(I_N - c(L+D)^T\right) e^T(t_k^-) P e(t_k^-) \\ &\triangleq \mu V(t_k^-), \end{aligned} \tag{39}$$

where $\mu = \sigma_{\max}^2 (I_N - c(L + D))$.

Using a similar proof as Theorem 1, we have

$$W(t,s) = e^{\alpha(t-s)} \prod_{s \le t_k \le t} \mu \le {}^{\alpha(t,s)} \mu^{N_\zeta(t,s)} = e^{\alpha(t,s)} e^{N_\zeta(t,s) \ln \mu} = e^{\alpha(t,s)} e^{\left((\ln \mu/(t,s))/N_\zeta(t,s)\right)(t,s)}. \tag{40}$$

By the definition of T_a and (36), for any η_1, $\eta < \eta_1 < 0$, there exists sufficiently large T such that

$$\begin{aligned} W(t,s) &\le e^{\alpha(t,s)} e^{\left((\ln \mu/T_a)+\eta_1-\eta\right)(t-s)} \\ &= e^{\left((\ln \mu/T_a)+\eta_1-\eta+\alpha\right)(t-s)} \\ &= e^{\eta_1(t-s)}, \end{aligned} \tag{41}$$

when $t > T$ and $0 \le s \le t$.

Using Theorem 1, we obtain the conclusion. □

3.2. The Case of $T_a = \infty$. This section concerns the bipartite quasi-synchronization of system (1) with average impulsive interval $T_a = \infty$.

Theorem 2. *Suppose that Assumption 1 holds and the average impulsive interval $T_a = \infty$. Let $P_i(t)$ $(i = 1, 2, \ldots, N)$ be a sequence of time-varying matrices, which are uniformly bounded and positive definite, i.e., there exist positive numbers $\check{m}_i$ and $\hat{m}_i$ satisfying $\check{m}_i \le \lambda_{\min}(P(t)) \le \lambda_{\max}(P(t)) \le \hat{m}_i$ $(i = 1, 2, \ldots, N)$. If there exist diagonal matrices $\Sigma_j > 0$ $(j = 1, 2)$, D_k $(k \in \mathbb{N}_+)$, and scalars $\alpha < 0$, $c > 0$, and μ_i $(i = 1, 2, \ldots, N_\zeta(t,s))$ such that*

$$\begin{bmatrix} P_iA_i + A_i^TP_i - \alpha P_i + \Delta^T\Sigma_1\Delta & P_iB_i & P_i \\ B_i^TP_i & -\Sigma_1 & 0 \\ P_i & 0 & -\Sigma_2 \end{bmatrix} < 0, \tag{42}$$

$$\begin{bmatrix} \mu_k P(t_k^-) & \Pi_k^T P(t_k^+) \\ P(t_k^+)\Pi_k & P(t_k^+) \end{bmatrix} > 0, \tag{43}$$

where $P(t) = diag\{P_1(t), P_2(2), \ldots, P_N(t)\}$, $\Pi_k = (I_N - c(L + D_k)) \otimes I_n$, $\Delta = (\delta_{ij})n \times n$, and $\mu = \lim_{t\longrightarrow\infty}((|\mu_1| + |\mu_2| + \cdots + |\mu_{N_\zeta(t,s)}|)/N_\zeta(t,s)) > 0$, then error system (10) exponentially converges into

$$S = \left\{ e \in \mathbb{R}^{n\times N} \,\middle|\, \|e\| \le \sqrt{-\frac{\lambda_{\max}(\Sigma_2)\sum_{i=1}^N \omega_i^2}{\alpha_1 \check{m}}} \right\} \tag{44}$$

at convergence rate $-(\alpha_1/2)$ for $0 > \alpha_1 > \alpha$.

Proof. Using the similar proof of Theorem 1, we obtain

$$\begin{aligned} W(t,s) &= e^{\alpha(t-s)}\mu_1\mu_2\cdots + \mu_{N_\zeta(t,s)} \\ &\le e^{\alpha(t-s)} e^{\left(\ln\left(\left(|\mu_1|+|\mu_2|+\cdots|\mu_{N_\zeta(t,s)}|\right)/N_\zeta(t,s)\right)/\left((t-s)/N_\zeta(t,s)\right)\right)(t-s)}. \end{aligned} \tag{45}$$

Recalling the construction of μ and $T_a = \infty$, we can get

$$\lim_{t\longrightarrow\infty} \frac{\ln\left(\left(|\mu_1| + |\mu_2| + \cdots |\mu_{N_\zeta(t,s)}|\right)/N_\zeta(t,s)\right)}{(t-s)/N_\zeta(t,s)} = 0. \tag{46}$$

Thus, for any α_1, $\alpha < \alpha_1 < 0$, there exists sufficiently large T such that

$$\frac{\ln\left(\left(|\mu_1| + |\mu_2| + \cdots + |\mu_{N_\zeta(t,s)}|\right)/N_\zeta(t,s)\right)}{(t-s)/N_\zeta(t,s)} < \alpha_1 - \alpha, \tag{47}$$

when $t > T$.

Then, by (45) and (47), we have

$$\begin{aligned} W(t,s) &\le e^{(\alpha_1-\alpha)(t-s)} e^{\alpha(t-s)} \\ &= e^{\alpha_1(t-s)}. \end{aligned} \tag{48}$$

Using Theorem 1, we obtain the conclusion. □

Remark 5. From the conclusion of Theorem 2, we can observe that there is no relationship between the convergence rate and the average impulsive interval when $T_a = \infty$. In other words, the impulsive control, when it occurs infinitely but very sparsely, does not influence the bipartite quasi-synchronization of the networks, but it is necessary to put forward high requirements for their dynamics of the leader and five nodes, which can be seen from Example 2.

Corollary 2. *Suppose that Assumption 1 holds and the average impulsive interval $T_a = \infty$. If there exist matrix $P > 0$, diagonal matrices $\Sigma_j > 0$ $(j = 1, 2)$, D, and scalars $\alpha < 0$, $c > 0$, $\check{m} > 0$, and $0 < \mu < \infty$ such that*

$$\begin{bmatrix} PA_i + A_i^TP - \alpha P + \Delta^T\Sigma_1\Delta & PB_i & P \\ B_i^TP & -\Sigma_1 & 0 \\ P & 0 & -\Sigma_2 \end{bmatrix} < 0, \tag{49}$$

$$P \ge \check{m}I, \tag{50}$$

where $\Delta = (\delta_{ij})n \times n$ and $\mu = \sigma_{\max}^2(I_N - c(L + D))$, then error system (10) exponentially converges into

$$S = \left\{ e \in \mathbb{R}^{n\times N} \,\middle|\, \|e\| \le \sqrt{-\frac{\lambda_{\max}(\Sigma_2)\sum_{i=1}^N \omega_i^2}{\alpha_1 \check{m}}} \right\}. \tag{51}$$

at convergence rate $-(\alpha_1/2)$ for $0 > \alpha_1 > \alpha$.

4. Simulation Examples

In this section, two numerical examples are used to simulate the theoretical results in the above section.

Example 1. Bipartite quasi-synchronization with $T_a < \infty$.

Suppose that the leader $s(t)$ satisfies the following Chua's circuit:

$$\dot{s}(t) = As(t) + Bf(s(t)), \tag{52}$$

where $s(t) = (s_1(t), s_2(t), s_3(t))^T$, $A = \begin{bmatrix} -am_1 & a & 0 \\ 1 & -1 & 1 \\ 0 & -b & 0 \end{bmatrix}$, $B = \begin{bmatrix} a(m_1 - m_0) & 0 & 0 \\ 0 & 0 & 0 \\ 0 & 0 & 0 \end{bmatrix}$, parameters $m_0 = -(1/7)$, $m_1 = (2/7)$, $a = 9$, and $b = 14.286$, and $f(s(t)) = (0.5(|s_1 + 1| - |s_1 - 1|), 0, 0)^T$.

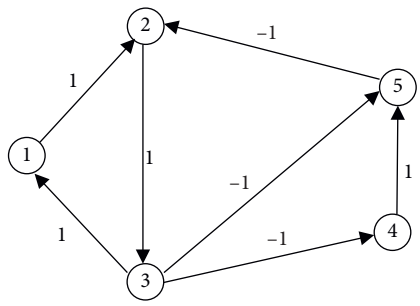

Figure 1: A signed network with five nodes.

Consider a signed network shown in Figure 1, consisting of five followers described by

$$\dot{x}_i(t) = A_i x_i(t) + B_i f(x_i(t)), \quad i = 1,2,3,4,5, \tag{53}$$

where $x_i(t) = (x_{i1}(t), x_{i2}(t), x_{i3}(t))^T$, $f(x_i(t)) = (0.5(|x_{i1}+1| - |x_{i1}-1|), 0, 0)^T$, and

$$\begin{aligned}
A_1 &= \begin{bmatrix} -am_1 + 0.3 & a + 0.1 & 0 \\ 1 & -1 & 1 \\ 0 & -b + 0.4 & 0 \end{bmatrix}, \\
B_1 &= \begin{bmatrix} a(m_1 - m_0) - 1 & 0 & 0 \\ 0 & 0.2 & 0 \\ 0 & 0 & 1 \end{bmatrix}, \\
A_2 &= \begin{bmatrix} -am_1 - 0.5 & a - 0.1 & 0 \\ 1 & -1 & 1 \\ 0 & -b - 0.2 & 0 \end{bmatrix}, \\
B_2 &= \begin{bmatrix} a(m_1 - m_0) + 1 & 0 & 0 \\ 0 & 0.5 & 0 \\ 0 & 0 & 1 \end{bmatrix}, \\
A_3 &= \begin{bmatrix} -am_1 + 0.1 & a - 0.1 & 0 \\ 1 & -1 - 0.1 & 1 \\ 0 & -b + 0.1 & 0 \end{bmatrix}, \\
B_3 &= \begin{bmatrix} a(m_1 - m_0) + 0.8 & 0 & 0 \\ 0 & 0.5 & 0 \\ 0 & 0 & 1 \end{bmatrix}, \\
A_4 &= \begin{bmatrix} -am_1 - 0.1 & a & 0 \\ 1 & -1 + 0.1 & 1 \\ 0 & -b - 0.1 & 0 \end{bmatrix}, \\
B_4 &= \begin{bmatrix} a(m_1 - m_0) - 0.6 & 0 & 0 \\ 0 & 1 & 0 \\ 0 & 0 & 1 \end{bmatrix}, \\
A_5 &= \begin{bmatrix} -am_1 - 0.1 & a - 0.1 & 0 \\ 1 & -1 & 1 \\ 0 & -b + 0.3 & -0.1 \end{bmatrix}, \\
B_5 &= \begin{bmatrix} a(m_1 - m_0) - 1 & 0 & 0 \\ 0 & -0.5 & 0 \\ 0 & 0 & -1 \end{bmatrix}.
\end{aligned} \tag{54}$$

The dynamics of the five followers may be chaotic, stable, or periodic. From Figure 1, one sees that the signed network is balanced with $\mathcal{U}_1 = \{1,2,3\}$ and $\mathcal{U}_2 = \{4,5\}$. Lemma 1 holds for $\Gamma = \mathrm{diag}\{1,1,-1,-1\}$, and the Laplacian matrix is

$$L = \begin{bmatrix} 1 & -1 & 0 & 0 & 0 \\ 0 & 2 & -1 & -1 & 0 \\ -1 & 0 & 2 & -1 & 0 \\ 0 & 0 & 0 & 1 & -1 \\ 0 & 0 & -1 & 0 & 1 \end{bmatrix}. \tag{55}$$

In addition, $s(0) = (0.2, 0.1, 0.1)^T$ is the initial condition of the leader node, and $[0.1, 0.2, 0.2; 0.1, 0.1, 0.2; -0.1, 0.1, 0.2; 0.1, 0.1, 0.2; 0.1, 0.1, 0.2]$ is the initial condition of the five nodes in the signed network. By simulation, one gets $\omega_1 = 0.7554$, $\omega_2 = 0.5447$, $\omega_3 = 1.0092$, $\omega_4 = 0.8248$, and $\omega_5 = 1.2946$.

Note that the node functions $f_k(\cdot)$ $(k = 1,2,3)$ are odd functions satisfying the Lipschitz condition with $\Delta = \mathrm{diag}\{1,0,0\}$. Hence, Assumption 1 is satisfied.

Let $D = \mathrm{diag}\{3, 0.9, 3, 0, 0\}$, i.e., agents 1, 2, and 3 are pinned. Let $c = 0.33$; then, it is found that $\mu = \sigma_{\max}^2(I_N - c(L+D)) = 0.8734$. According to Corollary 1, by solving generalized eigenvalue problems (34)–(36), we can find a feasible solution with $T_a = 0.01$, $\breve{m} = 3.13$, $\alpha = 23.812$, $P = \begin{bmatrix} 3.2067 & -0.2836 & -0.0563 \\ -0.0846 & 4.6926 & 1.4635 \\ -0.0376 & 1.3216 & 4.4915 \end{bmatrix}$, and $\Sigma_2 = \mathrm{diag}(0.446, 0.4376, 0.4419)$. Then, $\lambda_{\max}(\Sigma_2) = 0.446$. From (43), one obtains that $\eta_1 = -3.25$. Consequently, the error level is 0.4305. From Figures 2 and 3, one easily sees that the heterogeneous systems achieve bipartite leader-following quasi-synchronization with the distributed impulsive control, where $e_{1,2,3}(t) = (e_1^T, e_2^T, e_3^T(t))^T$ and $e_{4,5}(t) = (e_4^T, e_5^T)^T$.

Example 2. Bipartite quasi-synchronization with $T_a = \infty$.

According to the condition $\alpha < 0$ in Corollary 2, the dynamics of the leader and the five followers need to be stable. The leader $s(t)$ has the following parameters: $A = 10\begin{bmatrix} -am_1 & a & 0 \\ 1 & -1 & 1 \\ 0 & -b & 0 \end{bmatrix}$, $B = 0.01\begin{bmatrix} a(m_1 - m_0) & 0 & 0 \\ 0 & 0 & 0 \\ 0 & 0 & 0 \end{bmatrix}$, parameters $m_0 = -(1/7)$, $m_1 = (2/7)$, $a = 9$, and $b = 14.286$, and $f(s(t)) = (0.01(|s_1+1| - |s_1-1|), 0, 0)^T$.

The signed network is the same as that of Example 1, in which five followers have the following parameters:

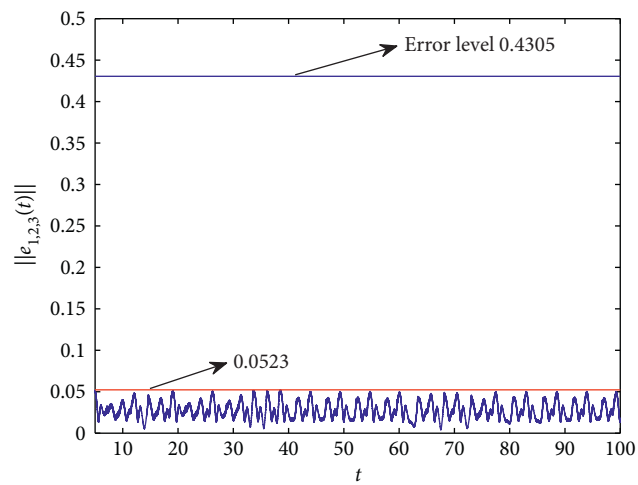

FIGURE 2: $\|e_{1,2,3}(t)\|$ on $\mathscr{U}_1 = \{1, 2, 3\}$ and the error level 0.4305 in the signed network.

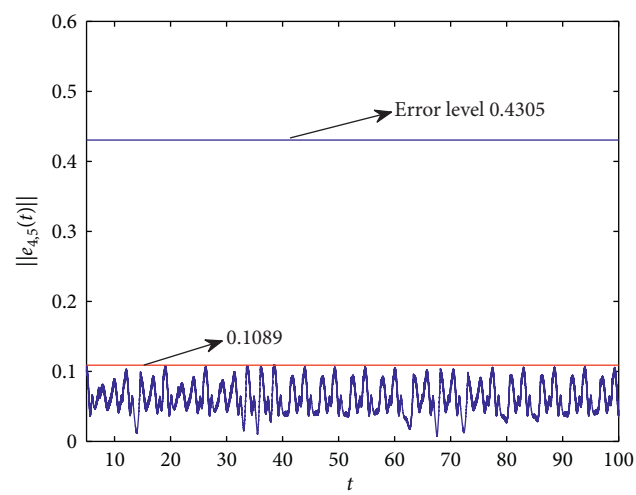

FIGURE 3: $\|e_{4,5}(t)\|$ on $\mathscr{U}_2 = \{4, 5\}$ and the error level 0.4305 in the signed network.

$$
\begin{aligned}
A_1 &= 8\begin{bmatrix} -am_1 - 1 & a-1 & 0 \\ 1 & -1 & 1 \\ 0 & -b-1 & -0.3 \end{bmatrix}, \\
B_1 &= 0.1\begin{bmatrix} a(m_1 - m_0) - 1 & 0 & 0 \\ 0 & -0.5 & 0 \\ 0 & 0 & -1 \end{bmatrix}, \\
A_2 &= 8\begin{bmatrix} -am_1 - 0.9 & a-0.1 & 0 \\ 1 & -1 & 1 \\ 0 & -b-1 & -0.2 \end{bmatrix}, \\
B_2 &= \begin{bmatrix} a(m_1 - m_0) - 0.9 & 0 & 0 \\ 0 & -0.5 & 0 \\ 0 & 0 & -0.9 \end{bmatrix}, \\
A_3 &= 8\begin{bmatrix} -am_1 - 0.8 & a-0.9 & 0 \\ 1 & -1 & 1 \\ 0 & -b-1 & -0.2 \end{bmatrix}, \\
B_3 &= 0.1\begin{bmatrix} a(m_1 - m_0) - 0.9 & 0 & 0 \\ 0 & -0.5 & 0 \\ 0 & 0 & -0.9 \end{bmatrix}, \\
A_4 &= 10\begin{bmatrix} -am_1 - 0.7 & a-1 & 0 \\ 1 & -1 & 1 \\ 0 & -b-0.8 & -0.2 \end{bmatrix}, \\
B_4 &= \begin{bmatrix} a(m_1 - m_0) - 0.8 & 0 & 0 \\ 0 & -0.5 & 0 \\ 0 & 0 & -0.9 \end{bmatrix}, \\
A_5 &= \begin{bmatrix} -am_1 - 0.6 & a-1 & 0 \\ 1 & -1 & 1 \\ 0 & -b-1 & -0.2 \end{bmatrix}, \\
B_5 &= \begin{bmatrix} a(m_1 - m_0) - 0.7 & 0 & 0 \\ 0 & -0.5 & 0 \\ 0 & 0 & -1 \end{bmatrix},
\end{aligned}
\tag{56}
$$

and $f(x_i(t)) = (0.5(|x_{i1} + 1| - |x_{i1} - 1|), 0, 0)^T$, $i = 1, 2, 3, 4, 5$.

By simulation, one gets $\omega_1 = 0.345$, $\omega_2 = 0.351$, $\omega_3 = 0.348$, $\omega_4 = 0.074$, and $\omega_5 = 0.099$. In addition, the node function satisfies the Lipschitz condition with $\Delta = \mathrm{diag}\{0.01, 0, 0\}$. By solving generalized eigenvalue problems (49) and (50) of Corollary 2, one can find a feasible solution with $T_a = \infty$ for $N_\zeta(t, t_0) = [t^{1/2}]$, $\check{m} = 3.3975$, $\alpha = -0.1$, $P = \begin{bmatrix} 15.3805 & -3.9822 & 6.4789 \\ -3.9822 & 83.6290 & -2.7129 \\ 6.4789 & -2.7129 & 6.9045 \end{bmatrix}$, $\Sigma_2 = I_3$, and $\alpha_1 = -0.099$. Theoretically, the error level is 0.0113. From Figures 4 and 5, we can observe that the heterogeneous systems achieve bipartite leader-following quasi-

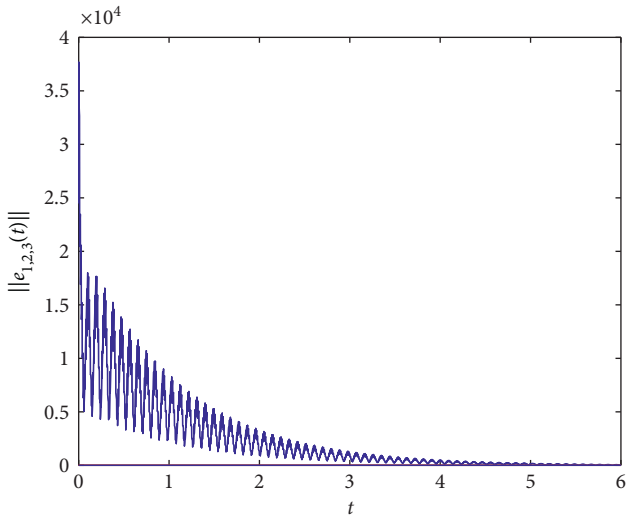

Figure 4: $\|e_{1,2,3}(t)\|$ on $\mathcal{U}_1 = \{1, 2, 3\}$.

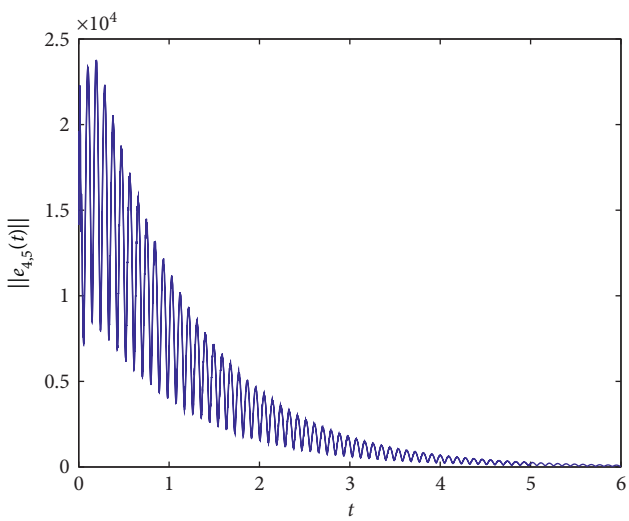

Figure 5: $\|e_{4,5}(t)\|$ on $\mathcal{U}_2 = \{4, 5\}$.

synchronization with lower level, where $e_{1,2,3}(t) = (e_1^T, e_2^T, e_3^T(t))^T$ and $e_{4,5}(t) = (e_4^T, e_5^T)^T$.

5. Conclusions

This work investigates bipartite synchronization of heterogeneous signed networks. A pinning impulsive control strategy is proposed to realize bipartite synchronization. A leader-follower system within a nonzero error bound is analyzed simultaneously with these two kinds of impulses $T_a < \infty$ and $T_a = \infty$ by using the concept on average impulsive gain. Sufficient conditions on bipartite quasi-synchronization are obtained, and synchronization error is derived to show the synchronization level. However, when $T_a = \infty$, synchronization is necessary to put forward high requirements for their dynamics of the leader and the followers with $\alpha < 0$. Simulation examples show that the theoretical results are effective.

Data Availability

The data used to support the findings of this study are available from the corresponding author upon request.

Conflicts of Interest

The authors declare that they have no conflicts of interest.

Acknowledgments

This work was supported by the National Natural Science Foundation of China (Grant no. 61807019) and Introduced Talents Startup Foundation of Nanjing Institute of Industry Technology (Grant no. YK18-03-05).

References

[1] V. I. Krinsky, V. N. Biktashev, and I. R. Efimov, "Autowave principles for parallel image processing," *Physica D: Nonlinear Phenomena*, vol. 49, no. 1-2, pp. 247–253, 1991.

[2] F. C. Hoppensteadt and E. M. Izhikevich, "Pattern recognition via synchronization in phase-locked loop neural networks," *IEEE Transactions on Neural Networks*, vol. 11, no. 3, pp. 734–738, 2000.

[3] G. D. VanWiggeren and R. Roy, "Communication with chaotic lasers," *Science*, vol. 279, no. 5354, pp. 1198–1200, 1998.

[4] C. Chai and L. O. Chua, "Synchronization in an array of linearly coupled dynamical systems," *IEEE Transactions on Circuits and Systems I: Fundamental Theory and Applications*, vol. 42, no. 8, pp. 430–447, 1995.

[5] D. Yang, X. Li, and J. Qiu, "Output tracking control of delayed switched systems via state-dependent switching and dynamic output feedback," *Nonlinear Analysis: Hybrid Systems*, vol. 32, pp. 294–305, 2019.

[6] J. Lu and J. Cao, "Adaptive synchronization of uncertain dynamical networks with delayed coupling," *Nonlinear Dynamics*, vol. 53, no. 1-2, pp. 107–115, 2008.

[7] Z. Zuo, J. Zhang, and Y. Wang, "Adaptive fault tolerant tracking control for linear and Lipschitz nonlinear multi-agent systems," *IEEE Transactions on Industrial Electronics*, vol. 62, no. 6, pp. 3923–3931, 2015.

[8] T. Wang, H. Gao, and J. Qiu, "A combined adaptive neural network and nonlinear model predictive control for multirate networked industrial process control," *IEEE Transactions on Neural Networks and Learning Systems*, vol. 27, no. 2, pp. 416–425, 2016.

[9] B. Liu, D. J. Hill, and Z. Sun, "Stabilisation to input-to-state stability for continuous-time dynamical systems via event-triggered impulsive control with three levels of events," *IET Control Theory & Applications*, vol. 12, no. 9, pp. 1167–1179, 2018.

[10] X. Li, D. Peng, and J. Cao, "Lyapunov stability for impulsive systems via event-triggered impulsive control," *IEEE Transactions on Automatic Control*, vol. 65, no. 11, pp. 4908–4913, 2020.

[11] B. Liu, Z. Sun, Y. Luo, and Y. Zhong, "Uniform synchronization for chaotic dynamical systems via event-triggered impulsive control," *Physica A: Statistical Mechanics and its Applications*, vol. 531, p. 121725, 2019.

[12] X. Yang, X. Li, X. Li, Q. Xi, and P. Duan, "Review of stability and stabilization for impulsive delayed systems,"

Mathematical Biosciences & Engineering, vol. 15, no. 6, pp. 1495–1515, 2018.

[13] X. Li, X. Yang, and T. Huang, "Persistence of delayed cooperative models: impulsive control method," *Applied Mathematics and Computation*, vol. 342, pp. 130–146, 2019.

[14] X. Ji, J. Lu, J. Lou, J. Qiu, and K. Shi, "A unified criterion for global exponential stability of quaternion-valued neural networks with hybrid impulses," *International Journal of Robust and Nonlinear Control*, vol. 30, no. 18, pp. 8098–8116, 2020.

[15] B. Liu and D. J. Hill, "Impulsive consensus for complex dynamical networks with nonidentical nodes and coupling time-delays," *SIAM Journal on Control And Optimization*, vol. 49, no. 2, pp. 315–338, 2011.

[16] Y. Li, "Impulsive synchronization of stochastic neural networks via controlling partial states," *Neural Processing Letters*, vol. 46, no. 1, pp. 59–69, 2017.

[17] J. Ding, J. Cao, G. Feng, A. Alsaedi, A. Al-Barakati, and H. M. Fardoun, "Stability analysis of delayed impulsive systems and applications," *Circuits, Systems, and Signal Processing*, vol. 37, no. 3, pp. 1062–1080, 2018.

[18] B. Jiang, J. Lu, and Y. Liu, "Exponential stability of delayed systems with average-delay impulses," *SIAM Journal on Control and Optimization*, vol. 58, no. 6, pp. 3763–3784, 2020.

[19] X. Liu, "Stability results for impulsive differential systems with applications to population growth models," *Dynamics and Stability of Systems*, vol. 9, no. 2, pp. 163–174, 1994.

[20] P. Wang, X. Li, N. Wang, Y. Li, K. B. Shi, and J. Lu, "Almost periodic synchronization of quaternion-valued fuzzy cellular neural networks with leakage delays, Fuzzy Sets and Systems," In press, 2021.

[21] Z. Guan, Z. Liu, G. Feng, and Y. Wang, "Synchronization of complex dynamical networks with time-varying delays via impulsive distributed control," *IEEE Transactions on Circuits and Systems I: Regular Papers*, vol. 57, no. 8, pp. 2182–2195, 2010.

[22] Z.-H. Guan, Z.-W. Liu, G. Feng, and M. Jian, "Impulsive consensus algorithms for second-order multi-agent networks with sampled information," *Automatica*, vol. 48, no. 7, pp. 1397–1404, 2012.

[23] Z. Li, J. a. Fang, Y. Tang, and T. Huang, "Consensus of linear discrete-time multi-agent systems: a low-gain distributed impulsive strategy," *IEEE Transactions on Systems, Man, and Cybernetics: Systems*, vol. 49, no. 6, pp. 1041–1052, 2019.

[24] X. Li, X. Wang, and G. Chen, "Pinning a complex dynamical network to its equilibrium," *IEEE Transactions on Circuits and Systems I: Regular Papers*, vol. 51, no. 10, pp. 2074–2087, 2004.

[25] Y. Li, J. Lou, Z. Wang, and F. E. Alsaadi, "Synchronization of dynamical networks with nonlinearly coupling function under hybrid pinning impulsive controllers," *Journal of the Franklin Institute*, vol. 355, no. 14, pp. 6520–6530, 2018.

[26] J. Lu, J. Kurths, J. Cao, N. Mahdavi, and C. Huang, "Synchronization control for nonlinear stochastic dynamical networks: pinning impulsive strategy," *IEEE Transactions on Neural Networks and Learning Systems*, vol. 23, no. 2, pp. 285–292, 2012.

[27] J. Lu, D. W. C. Ho, J. Cao, and J. Kurths, "Single impulsive controller for globally exponential synchronization of dynamical networks," *Nonlinear Analysis: Real World Applications*, vol. 14, no. 1, pp. 581–593, 2013.

[28] W. He, F. Qian, J. Lam, G. Chen, Q.-L. Han, and J. Kurths, "Quasi-synchronization of heterogeneous dynamic networks via distributed impulsive control: error estimation, optimization and design," *Automatica*, vol. 62, pp. 249–262, 2015.

[29] J. Lu, D. W. C. Ho, and J. Cao, "A unified synchronization criterion for impulsive dynamical networks," *Automatica*, vol. 46, no. 7, pp. 1215–1221, 2010.

[30] N. Wang, X. Li, J. Lu, and F. E. Alsaadi, "Unified synchronization criteria in an array of coupled neural networks with hybrid impulses," *Neural Networks*, vol. 101, pp. 25–32, 2018.

[31] A. V. Proskurnikov, A. S. Matveev, and M. Cao, "Opinion dynamics in social networks with hostile camps: consensus vs. polarization," *IEEE Transactions on Automatic Control*, vol. 61, no. 6, pp. 1524–1536, 2016.

[32] W. Xia, M. Cao, and K. H. Johansson, "Structural balance and opinion separation in trust-mistrust social networks," *IEEE Transactions on Control of Network Systems*, vol. 3, no. 1, pp. 46–56, 2016.

[33] D. Meng, M. Du, and Y. Jia, "Interval bipartite consensus of networked agents associated with signed digraphs," *IEEE Transactions on Automatic Control*, vol. 61, no. 12, pp. 3755–3770, 2016.

[34] F. Liu, Q. Song, G. Wen, J. Cao, and X. Yang, "Bipartite synchronization in coupled delayed neural networks under pinning control," *Neural Networks*, vol. 108, pp. 146–154, 2018.

[35] S. Zhai and Q. Li, "Pinning bipartite synchronization for coupled nonlinear systems with antagonistic interactions and switching topologies," *Systems & Control Letters*, vol. 94, pp. 127–132, 2016.

[36] C. Altafini, "Consensus problems on networks with antagonistic interactions," *IEEE Transactions on Automatic Control*, vol. 58, no. 4, pp. 935–946, 2013.

[37] S. Boyd, L. El. Ghaoui, E. Feron, and V. Balakrishnan, *Linear Matrix Inequalities in System and Control Theory*, SIAM, Philadelphia, PA, USA, 1994.

[38] Z. Ding, "Consensus output regulation of a class of heterogeneous nonlinear systems," *IEEE Transactions on Automatic Control*, vol. 58, no. 10, pp. 2648–2653, 2013.

Hindawi
Complexity
Volume 2021, Article ID 9991989, 16 pages
https://doi.org/10.1155/2021/9991989

Research Article

Terminal Sliding-Mode Control of Uncertain Robotic Manipulator System with Predefined Convergence Time

Yang Wang, Mingshu Chen, and Yu Song

School of Science, Xijing University, Xi'an, China

Correspondence should be addressed to Yang Wang; zjt219571@163.com

Received 5 March 2021; Revised 25 April 2021; Accepted 15 May 2021; Published 10 June 2021

Academic Editor: Xiaodi Li

This paper concentrates on the predefined-time trajectory tracking for an uncertain robotic manipulator system. First, a modified predefined-time control (PTC) algorithm is proposed. Subsequently, with the help of proposed modified PTC algorithm and the nonsingular design method of terminal sliding mode, a novel nonsingular terminal sliding-mode control (NTSMC) scheme is proposed for ensuring the predefined-time convergence of tracking errors. The advantages of the newly proposed control scheme are as follows. (i) Unlike the conventional predefined-time sliding-mode control (SMC) which only guarantees the predefined-time convergence of sliding-mode surface, the proposed scheme can guarantee the predefined-time convergence of tracking errors. (ii) Compared with the conventional PTC algorithm, the proposed modified PTC algorithm can reduce the initial control peaking and enhance the precision of convergence time. The performance and effectiveness of the proposed control scheme are illustrated by comparing with the existing methods.

1. Introduction

Trajectory tracking control of robot manipulators has been recognized as one of the most important control modes in the robot control field [1, 2]. As a classical control method, proportional-integral-derivative (PID) control has been widely used in engineering [3–6]. However, the tracking precision of these PID-based control schemes may be dramatically degraded by uncertainty. With the development of technology, the robotic manipulator is not only required to accomplish the repetitive labor missions in the structured factory environment but also expected to service in many unstructured environments, such as underwater environment [7], man-machine interaction environment [8], and space environment [9]. In these unstructured environments, many complex uncertainties may be brought by the unknown knowledge of the dynamic model, the model linearization error, and external environmental disturbance. To suppress the uncertainties, many classical robust control methods have been introduced, including linear matrix inequality (LMI) control [10], composite nonlinear feedback control [11], modified PID [12], and SMC [13]. Among these robust methods, based on the sample structure and the insensitivity property [14, 15], SMC was widely studied in literatures. However, the conventional SMC adopted the linear sliding-mode surface, which implies that the convergence time is infinite.

Combining with finite-time control [16–18] and SMC, the terminal sliding-mode control (TSMC) has been explored to achieve the finite convergence time [19–26]. In [19], for a one-order chaotic system, a global TSMC scheme was proposed. And the reaching period of the sliding-mode surface can be omitted. Thus, the high robust performance can be guaranteed from the initial time. In [20], for the uncertain robotic manipulator, a traditional TSMC was designed. However, for such two-order robotic manipulator system or higher-order uncertain systems, the control input of the traditional TSMC in [20] diverges to infinity when the tracking errors converge to zero. This is known as the singular problem of TSMC. To overcome this problem, the NTSMC schemes have been proposed by several different methods, including restricted sliding-mode surface method [21, 22], transformed sliding-mode surface method [23, 24], and integral TSMC method [25, 26]. However, these

NTSMC schemes in [19–26] are typical finite-time control methods, which means that the convergence times of these NTSMC schemes in [19–26] relate to the initial tracking errors. Especially, the convergence performance may be affected seriously when the initial tracking errors are large.

In recent years, to overcome the above shortage of finite-time control, the fixed-time control has been developed [27–30]. Unlike the finite-time stability achieved in [19–26], the convergence time of fixed-time control is bounded by a setting time constant, which is unrelated to the initial tracking errors [27–30]. Recognizing this advantage of fixed-time stability, the conventional TSMC has been extended to fixed-time TSMC in several contributions [31, 32]. And the design idea of fixed-time TSMC has been introduced to the trajectory tracking of a robotic manipulator system in [33–35]. Like the conventional TSMC, the singular problem also needs to be eliminated in the fixed-time TSMC. In [33, 34], the fixed-time NTSMC was proposed for the robotic manipulators and the approximate piecewise functions were utilized to avoid the potential singular problem. In [35], based on the bi-limit homogeneous technique, a fixed-time NTSMC with prescribed performance was developed for a n-DOF uncertain manipulator, and the singular problem was eliminated by designing integral sliding-mode surface. Although the fixed-time NTSMC has significantly improved the convergence performance of conventional TSMC, the setting time constant of fixed-time NTSMC cannot be simply adjusted by using control parameters [33, 34] or is completely unclear [35]. Actually, for many practice engineering cases, it is necessary to define the settling time constant in advance.

With the purpose of predefining the settling time constant of fixed-time control by parameters, the predefined-time control (PTC) has been introduced in [36–39]. Among these methods, the Lyapunov-function-based PTC algorithm proposed in [39] has the advantages of simple structure and easy implementation. Thus, in recent two years, the PTC algorithm of [39] has been applied to synchronization of chaotic systems [40–43] and trajectory tracking control of robotic manipulator systems [44]. In particular, for the uncertain robotic manipulator system, the authors in [44] combined the PTC algorithm of [39] with the SMC to construct a robust predefined-time SMC which has greatly promoted the development of predefined-time control for the uncertain robotic manipulator system. However, the control performance and the actual engineering feasibility of [44] can be improved if following two limitations can be eliminated: (i) the sliding-mode surface of [44] is linear, which means that predefined-time SMC of [44] only can guarantee the predefined-time convergence of sliding-mode surface rather than the tracking errors; (ii) the PTC algorithm proposed in [44] is too conservative, which does not consider any information of initial system conditions. According to engineering practice of the robotic manipulator system, even if the exact value of initial system conditions is unknown, we can know the upper bound of initial system conditions.

By designing a novel NTSMC and modifying the conventional PTC algorithm, a novel predefined-time NTSMC which can eliminate above two limitations is proposed in this paper. The contributions are as follows:

(1) Compared with the recent predefined-time SMC in [44], the main contribution of the proposed method is that the proposed NTSMC guarantees the predefined-time convergence of tracking errors rather than the predefined-time convergence of sliding-mode surface.

(2) In comparison with the existing PTC algorithm in [44], the proposed modified PTC algorithm can achieve higher precision of convergence time and smaller initial control peaking.

The rest of this paper is organized as follows. In Section 2, the preliminaries including the dynamic model of robot manipulators, assumption, design objective, and motivation are given. In Section 3, the controller and its stability analysis are presented. In Section 4, the simulation is given to compare the proposed control scheme and the related works. In Section 5, the conclusion is given.

Notations: in this paper, t denotes the time and the initial time is 0.

2. Preliminaries

2.1. Dynamic Model of Uncertain Robotic Manipulator System. An uncertain robotic manipulator system with n-DOF can be described by the following Euler–Lagrange equation:

$$J(\phi)\ddot{\phi} + L(\phi,\dot{\phi})\dot{\phi} + G(\phi) = \tau + D, \tag{1}$$

where $\phi \in R^{n\times 1}$ is the joint angle, $\dot{\phi} \in R^{n\times 1}$ is the angular velocity, $\ddot{\phi}$ is the angular acceleration, $J(\phi) \in R^{n\times n}$ is the inertia matrix, $\mathbf{L}(\phi,\dot{\phi}) \in R^{n\times n}$ is the centrifugal-Coriolis forces matrix, $G(\phi) \in R^{n\times 1}$ is the gravitational torque, $\tau \in R^{n\times 1}$ is the control torque, and $\mathbf{D}$ is the uncertainty, respectively.

Let the position tracking error be $\mathbf{e}_1 = \phi - \phi_d = [e_{11},\ldots,e_{1n}]^T$. Then, we have

$$\ddot{e}_1 = \ddot{\phi} - \ddot{\phi}_d. \tag{2}$$

Let $\dot{e}_1 = \mathbf{e}_2 = [e_{21},\ldots,e_{2n}]^T$, $\varphi = -(\mathbf{J}(\phi))^{-1}(\mathbf{L}(\phi,\dot{\phi})\phi + \mathbf{G}(\phi)) - \ddot{\phi}_d$, $(\mathbf{J}(\phi))^{-1}\tau = \mathbf{u}$, and $\overline{D} = (\mathbf{J}(\phi))^{-1}\mathbf{D}$; then, the error dynamic equation can be established as

$$\begin{cases} \dot{e}_1 = \mathbf{e}_2, \\ \dot{e}_2 = \boldsymbol{\varphi} + u + \overline{D}, \end{cases} \tag{3}$$

where

$$\boldsymbol{\varphi} = [\,\varphi_1 \;\ldots\; \varphi_n\,]^T \in R^{n\times 1}, \tag{4}$$

$$\mathbf{u} = [\,u_1 \;\ldots\; u_n\,]^T \in R^{n\times 1}, \tag{5}$$

$$\overline{D} = [\,\overline{D}_1 \;\; \ldots \;\; \overline{D}_n\,]^T \in R^{n\times 1}. \tag{6}$$

Assumption 1. The uncertain vector $\overline{D} = [\,\overline{D}_1 \;\; \ldots \;\; \overline{D}_n\,]^T \in R^{n\times 1}$ is bounded as $|\overline{D}_i| \le \overline{D}_{i\max}$, $(i = 1, \ldots, n)$, where $\overline{D}_{i\max}$ is a positive constant.

For e_{1i} and e_{2i}, $(i = 1, \ldots, n)$, according to (3)–(6), the error dynamic equation can be rewritten as

$$\begin{cases} \dot{e}_{1i} = e_{2i}, \\ \dot{e}_{2i} = \varphi_i + u_i + \overline{D}_i. \end{cases} \tag{7}$$

2.2. Predefined-Time Stability. Consider following dynamic system:

$$\dot{y} = \mathbf{f}(\mathbf{y}), \tag{8}$$

where $\mathbf{y} \in R^{n\times 1}$ is the system state and $\mathbf{f}(\mathbf{y})$ denotes a nonlinear function. For system (8), the system state $\mathbf{y}$ can reach the equilibrium point at the time $T_y(\mathbf{y}(0))$. $T_y(\mathbf{y}(0))$ denotes the convergence time function and $\mathbf{y}(0)$ is the initial system state. Then, the related stability definitions are given as follows.

Definition 1 (finite-time stability). For system (8), the finite-time stability is guaranteed if $T_y(\mathbf{y}(0))$ is finite.

Definition 2 (fixed-time stability). For system (8), the fixed-time stability is guaranteed if $T_y(\mathbf{y}(0))$ is bounded by a constant T_F, i.e., $\exists T_F > 0$: $\forall \mathbf{y}(0) \in R^n$: $T_y(\mathbf{y}(0)) \le T_F$. T_F is the settling time constant.

Definition 3 (predefined-time stability). For system (8), the predefined-time stability is guaranteed if $T_y(\mathbf{y}(0))$ is bounded by a settling time constant T_c, i.e., $\forall \mathbf{y}(0) \in R^n$: $T_y(\mathbf{y}(0)) \le T_c$. And the settling time constant T_c is a predefined control parameter.

2.3. Motivation of This paper. As stated in the Introduction section, for uncertain robotic manipulator system (1), the NTSMC schemes in [19–26] can not only suppress the uncertainties but also guarantee that the convergence time is finite. However, according to Definition 1, we know that the convergence time function of finite-time stability is related to the initial system state. Especially, the convergence performance may be affected seriously when the initial system state is large. According to Definition 2, we know that the convergence time function of fixed-time stability is bounded by a settling time constant. Thus, the fixed-time stability can guarantee the fast convergence performance even if the initial system state is large. Based on fixed-time stability and SMC, several fixed-time NTSMC schemes have been proposed in [33–35] for uncertain robotic manipulator systems. However, the settling time constant of fixed-time NTSMC schemes in [33–35] cannot be simply adjusted by using control parameters or is completely unclear. Recently, with the purpose of predefining the settling time constant of fixed-time control by control parameters, the predefined-time SMC scheme has been developed in [44]. The predefined-time SMC in [44] provides a novel way to predefine the convergence rate of the uncertain robotic manipulator system. Inspired by the result of [44], to further improve the control performance of predefined-time control, we mainly focus on two research objectives: (i) designing a new NTSMC scheme to achieve the predefined-time stability of tracking errors rather than the predefined-time stability of sliding-mode surface in [44] and (ii) modifying the PTC algorithm used in [44] to reduce initial control peaking and enhance the precision of convergence time of conventional PTC algorithm.

3. Main Result

3.1. Modified Predefined-Time Control. For convenience, considering the vector $\xi = [\xi_1, \ldots, \xi_n]^T \in R^n$ and constant $\alpha > 0$, in this paper, the vector function $\overrightarrow{\mathbf{Sig}}(\xi)^\alpha \in R^n$ and function $\mathrm{Sig}(\xi_i)^\alpha \in R\,(i = 1, 2 \ldots, n)$ are defined as follows:

$$\begin{aligned} \overrightarrow{\mathbf{Sig}}(\xi)^\alpha &= \left[\,|\xi_1|^\alpha + (\xi_1), \ldots, |\xi_n|^\alpha + (\xi_n)\,\right]^T, \\ \mathrm{Sig}(\xi)^\alpha &= |\xi_i|^\alpha + (\xi_i). \end{aligned} \tag{9}$$

The PTC algorithm used in [44] is given as follows.

Lemma 1 (see [44]). *Consider a dynamic system as follows:*

$$\dot{x} = v, \tag{10}$$

where $x \in R$ denotes the system state and v denotes the control input. If the control input is designed as

$$v = v_1 = -\frac{\pi/2}{T_s\alpha}\left(\mathrm{Sig}(x)^{1-\alpha} + \mathrm{Sig}(x)^{1+\alpha}\right), \tag{11}$$

where T_s is the predefined time parameter and $1 > \alpha > 0$, then $x = 0$ is predefined-time stable with the predefined time T_s, and x converges to zero at time t_{f1}:

$$x(t) = 0, \quad \text{if } t \ge t_{f1}, \tag{12}$$

$$\begin{aligned} t_{f1} &= \frac{T_s}{\pi/2}\arctan\left(|x(0)|^\alpha\right), \\ t_{f1} &\le T_s. \end{aligned} \tag{13}$$

Proof See [44].

Then, the PTC algorithm is modified as follows. □

Lemma 2. *Consider a dynamic system given as follows:*

$$\dot{x} = v, \tag{14}$$

where $x \in R$ denotes the system state and v denotes the control input. If the control input is designed as

$$v = v_2 = -\frac{\arctan\left(x_{\max}^{\alpha} + \kappa_x\right)}{T_s\alpha}\left(\mathrm{Sig}(x)^{1-\alpha} + \mathrm{Sig}(x)^{1+\alpha}\right), \tag{15}$$

where T_s is the predefined time parameter, $1 > \alpha > 0$, and $\kappa_x > 0$ (the parameter $x_{\max}$ is selected as $|x(0)| \le x_{\max}$), then $x = 0$ is predefined-time stable with the predefined time T_s, and x converges to zero at time t_{f2}:

$$x(t) = 0, \quad \text{if } t \ge t_{f2}, \tag{16}$$

$$t_{f2} = \frac{\arctan\left(|x(0)|^{\alpha}\right)}{\arctan\left(x_{\max}^{\alpha} + \kappa_x\right)}T_s, \quad t_{f2} \le T_s. \tag{17}$$

Proof. A Lyapunov function V_x is defined as

$$V_x = x^2. \tag{18}$$

Calculating the time derivative of V_x and substituting the expressions of v given in (15) into (19), we get

$$\begin{aligned}\dot{V}_x &= 2x\dot{x} \\ &= -\frac{2\arctan\left(x_{\max}^{\alpha} + \kappa_x\right)}{T_s\alpha}\left(V_x^{1-\alpha/2} + V_x^{1+\alpha/2}\right).\end{aligned} \tag{19}$$

Then, we have

$$\frac{T_s\alpha}{2\arctan\left(x_{\max}^{\alpha} + \kappa_x\right)}\frac{V_x^{\alpha/2-1}}{\left(1 + V_x^{\alpha}\right)}\mathrm{d}V_x = -\mathrm{d}t. \tag{20}$$

The convergence time is defined as t_{f2}. Then, integrating (20) from $t = 0$ to $t = t_{f2}$, we have

$$\begin{aligned}t_{f2} &= -\frac{T_s\alpha}{2\arctan\left(x_{\max}^{\alpha} + \kappa_x\right)}\int_{V_x(0)}^{V_x(t_{f2})}\frac{V_x^{\alpha/2-1}}{\left(1 + V_x^{\alpha}\right)}\mathrm{d}V_x \\ &= -\frac{T_s}{\arctan\left(x_{\max}^{\alpha} + \kappa_x\right)}\left(\arctan\left(V_x^{\alpha/2}(t_{f2})\right) - \arctan\left(V_x^{\alpha/2}(0)\right)\right) \\ &= -\frac{T_s}{\arctan\left(x_{\max}^{\alpha} + \kappa_x\right)}\left(\arctan\left(\left|x(t_{f2})\right|^{\alpha}\right) - \arctan\left(|x(0)|^{\alpha}\right)\right).\end{aligned} \tag{21}$$

Considering $V_x(t_{f2}) = x(t_{f2}) = 0$, $\kappa_x > 0$ and $|x(0)| \le x_{\max}$, then (16) and (17) can be satisfied.

The proof is finished. □

Remark 1. According to (13) and (17), for the exact convergence time t_{f1} and t_{f2}, we have

$$\frac{t_{f1}}{t_{f2}} = \frac{\arctan\left(x_{\max}^{\alpha} + \kappa_x\right)}{\pi/2} < 1. \tag{22}$$

Then, considering $t_{f1} \le T_s$ and $t_{f2} \le T_s$, we have

$$t_{f1} < t_{f2} \le T_s. \tag{23}$$

Thus, we know that t_{f2} is closer to the predefined time T_s. And according to (11) and (15), we have

$$\frac{v_1(0)}{v_2(0)} = \frac{\pi/2}{\arctan\left(x_{\max}^{\alpha} + \kappa_x\right)} > 1. \tag{24}$$

Thus, we know that initial control input $v_2(0)$ is smaller than $v_1(0)$. Although it is difficult to achieve the initial system conditions in advance, we can achieve the upper bound of initial system condition according to the engineering practice. The parameter $x_{\max}$ is closer to the exact value of $|x(0)|$, and more accurate convergence time and smaller initial control peaking can be achieved.

3.2. Predefined-Time Nonsingular Sliding-Mode Control. The PTC algorithm (11) is adopted in [44] to design the reaching law to guarantee the predefined-time convergence of sliding-mode surface. To extend the result of Muñoz-Vázquez et al. [44] to achieve the predefined-time convergence of tracking errors, it is necessary not only to use PT algorithm to design the reaching law but also to use PTC algorithm to design the sliding-mode surface. However, the sliding-mode surface is directly designed by the PTC algorithm (11) or (15) can cause the singular problem. To avoid this problem, a novel predefined-time NTSMC scheme will be developed in this section.

First, inspired by the nonsingular method of Zhao et al. [21] and based on the modified PTC algorithm (15), the predefined-time nonsingular sliding-mode surface is developed for system (7) as follows:

$$s_i = e_{2i} + \frac{\arctan\left(e_{1i\max}^{\alpha_{e_i}} + \kappa_{e_i}\right)}{\left(T_{e_i} - T_{s_i}\right)\alpha_{e_i}}\left(f_{e_{1i}} + \mathrm{Sig}(e_{1i})^{1+\alpha_{e_i}}\right), \tag{25}$$

where T_{e_i} and T_{s_i} are the predefined time parameters, and they satisfy $T_{e_i} > T_{s_i} > 0$. κ_{e_i} is a positive constant. $e_{1i\max}$ and α_{e_i} satisfy $e_{1i\max} \ge |e_{1i}(T_{s_i})|$ and $0 < \alpha_{e_i} < 1$. The nonlinear function $f_{e_{1i}}$ is defined as

$$f_{e_{1i}} = \begin{cases} \dfrac{-1 - \ln\delta_{e_i}}{1 - \alpha_{e_i} - \delta_{e_i}\ln\delta_{e_i}}\mathrm{Sig}(e_{1i})^{2-\alpha_{e_i}} + \dfrac{\delta_{e_i}^{-2\alpha_{e_i}}\delta_{ei}^{|e_{1i}|}}{1 - \alpha_{e_i} - \delta_{e_i}\ln\delta_{e_i}}e_{1i}, & \text{if } |e_{1i}| \le \delta_{e_i}, \\ \mathrm{Sig}(e_{1i})^{1-\alpha_{e_i}}, & \text{if } |e_{1i}| > \delta_{e_i}, \end{cases} \tag{26}$$

where $\delta_{e_i} \in (0, 1/e) = (0, 0.36)$ and $\delta_{e_i} = \alpha_{e_i}$.

It can be known that $f_{e_{1i}}$ is differentiable and its derivative is given as

$$\frac{\mathrm{d}f_{e_{1i}}}{\mathrm{d}t}=\begin{cases}\dfrac{-1-\ln\delta_{e_i}}{1-\alpha_{e_i}-\delta_{e_i}\ln\delta_{e_i}}\left(2-\alpha_{e_i}\right)\left|e_{1i}\right|^{1-\alpha_{e_i}}e_{2i}+\dfrac{\delta_{e_i}^{-2\alpha_{e_i}}\delta_{e_i}^{\left|e_{1i}\right|}}{1-\alpha_{e_i}-\delta_{e_i}\ln\delta_{e_i}}\left(\left|e_{1i}\right|\ln\delta_{e_i}+1\right)e_{2i}, & \text{if } \left|e_{1i}\right|\le\delta_{e_i},\\ \left(1-\alpha_{e_i}\right)\left|e_{1i}\right|^{-\alpha_{e_i}}e_{2i}, & \text{if } \left|e_{1i}\right|>\delta_{e_i}.\end{cases}\tag{27}$$

From (27), we have $(\mathrm{d}f_{e_{1i}}/\mathrm{d}t)=(\delta_{e_i}^{-2\alpha_{e_i}}/1-\alpha_{e_i}-\delta_{e_i}\ln\delta_{e_i})e_{2i}$ if $e_{1i}=0$. Thus, we can know that there is no singular term existing in $(\mathrm{d}f_{e_{1i}}/\mathrm{d}t)$ if $e_{1i}=0$. We also can know that $(\mathrm{d}f_{e_{1i}}/\mathrm{d}t)$ is continuous according to (27).

Then, the control input is designed based on the sliding-mode surface (25), and the modified PTC algorithm (15) is given as follows:

$$\begin{aligned}u_i=&-\left(\varphi_i+\frac{\arctan\left(e_{1i\max}^{\alpha_{e_i}}+\kappa_{e_i}\right)}{\left(T_{e_i}-T_{s_i}\right)\alpha_{ei}}\left(\frac{\mathrm{d}f_{e_{1i}}}{\mathrm{d}t}+\left(1+\alpha_{ei}\right)\left|e_{1i}\right|^{\alpha_{e_i}}e_{2i}\right)\right)\\&-\frac{\arctan\left(s_{i\max}^{\alpha_{s_i}}+\kappa_{s_i}\right)}{T_{s_i}\alpha_{s_i}}\left(\mathrm{Sig}\left(s_i\right)^{1-\alpha_{s_i}}+\mathrm{Sig}\left(s_i\right)^{1+\alpha_{s_i}}\right)-\overline{D}_{i\max}\left(s_i\right),\end{aligned}\tag{28}$$

where $\overline{D}_{i\max}$ is given by Assumption 1. The parameters satisfy $s_{i\max}\ge|s_i(0)|$, $\kappa_{s_i}>0$ and $0<\alpha_{s_i}<1$.

The input torque τ can be calculated by following equation:

$$\boldsymbol{\tau}=\mathbf{J}(\boldsymbol{\varphi})\mathbf{u}.\tag{29}$$

Then, the predefined-time stability analysis of the proposed controller (28) is given as follows.

Theorem 1. *For uncertain robotic manipulator system (7), if Assumption 1 is satisfied, then control scheme (28) can guarantee that the tracking errors e_{1i}, $(i=1,2)$ converge to the following small region in predefined time T_{e_i}:*

$$e_{1i}\le\delta_{e_i},\quad \text{if } t\ge T_{e_i}.\tag{30}$$

Then, e_{1i} can arrive at the origin asymptotically.

Proof. Calculating the time derivative of s_i, we have

$$\dot{s}_i=\varphi_i+u_i+\overline{D}_i+\frac{\arctan\left(e_{1i\max}^{\alpha_{e_i}}+\kappa_{e_i}\right)}{\left(T_{e_i}-T_{s_i}\right)\alpha_{ei}}\left(\frac{\mathrm{d}f_{e_{1i}}}{\mathrm{d}t}+\left(1+\alpha_{ei}\right)\left|e_{1i}\right|^{\alpha_{e_i}}e_{2i}\right).\tag{31}$$

Substituting controller (28) into (31), we have

$$\dot{s}_i=-\frac{\arctan\left(s_{i\max}^{\alpha_{s_i}}+\kappa_{s_i}\right)}{T_{s_i}\alpha_{s_i}}\left(\mathrm{Sig}\left(s_i\right)^{1-\alpha_{s_i}}+\mathrm{Sig}\left(s_i\right)^{1+\alpha_{s_i}}\right)-\overline{D}_{i\max}\left(s_i\right)+\overline{D}_i.\tag{32}$$

A Lyapunov function V_1 is defined as

$$V_1=s_i^2.\tag{33}$$

Calculating the time derivative of V_1, we get

$$\dot{V}_1=2\dot{s}_is_i.\tag{34}$$

Substituting (32) into (34), we get

$$\begin{aligned}\dot{V}_1&=2\left(-\frac{\arctan\left(s_{i\max}^{\alpha_{s_i}}+\kappa_{s_i}\right)}{T_{s_i}\alpha_{s_i}}\left(\mathrm{Sig}\left(s_i\right)^{1-\alpha_{s_i}}+\mathrm{Sig}\left(s_i\right)^{1+\alpha_{s_i}}\right)-\overline{D}_{i\max}\left(s_i\right)+\overline{D}_i\right)s_i\\&=-\frac{2\arctan\left(s_{i\max}^{\alpha_{s_i}}+\kappa_{s_i}\right)}{T_{s_i}\alpha_{s_i}}\left(V_1^{1-\alpha_{s_i}/2}+V_1^{1+\alpha_{s_i}/2}\right)+\left(\overline{D}_i-\overline{D}_{i\max}\left(s_i\right)\right)s_i\\&\le-\frac{2\arctan\left(s_{i\max}^{\alpha_{s_i}}+\kappa_{s_i}\right)}{T_{s_i}\alpha_{s_i}}\left(V_1^{1-\alpha_{s_i}/2}+V_1^{1+\alpha_{s_i}/2}\right)+\left(\left|\overline{D}_i\right|-\overline{D}_{i\max}\right)\left|s_i\right|.\end{aligned}\tag{35}$$

Considering Assumption 1, we have

$$\dot{V}_1 \le -\frac{2\arctan\left(s_{i\max}^{\alpha_{s_i}}+\kappa_{s_i}\right)}{T_{s_i}\alpha_{s_i}}\left(V_1^{1-\alpha_{s_i}/2}+V_1^{1+\alpha_{s_i}/2}\right). \quad (36)$$

Then, according to the proof of Lemma 2, we know that

$$V_1 = s_i = 0, \quad \text{if } t \ge \frac{\arctan\left(\left|s_i(0)\right|^{\alpha_{s_i}}\right)}{\arctan\left(s_{i\max}^{\alpha_{s_i}}+\kappa_{s_i}\right)}T_{s_i}. \quad (37)$$

Then, combining (25) and (37), we have

$$e_{2i} = -\frac{\arctan\left(e_{1i\max}^{\alpha_{e_i}}+\kappa_{e_i}\right)}{\left(T_{e_i}-T_{s_i}\right)\alpha_{ei}}\left(f_{e_{1i}}+\mathrm{Sig}\left(e_{1i}\right)^{1+\alpha_{ei}}\right), \quad \text{if } t \ge \sigma_{s_i}T_{s_i}, \quad (38)$$

where $\sigma_{s_i} = (\arctan(|s_i(0)|^{\alpha_{s_i}})/\arctan(s_{i\max}^{\alpha_{s_i}}+\kappa_{s_i}))$.

For $|e_{1i}| \ge \delta_{e_i}$, we have

$$e_{2i} = -\frac{\arctan\left(e_{1i\max}^{\alpha_{ei}}\right)}{\left(T_{e_i}-T_{s_i}\right)\alpha_{ei}}\left(\mathrm{Sig}\left(e_{1i}\right)^{1-\alpha_{e_i}}+\mathrm{Sig}\left(e_{1i}\right)^{1+\alpha_{ei}}\right), \quad \text{if } t \ge \sigma_{s_i}T_{s_i}. \quad (39)$$

Then, according to Lemma 2, we know that e_{1i} will converge to following region:

$$\left|e_{1i}\right| < \delta_{e_i}, \quad \text{if } t \ge \sigma_{s_i}T_{s_i}+\sigma_{e_i}\left(T_{e_i}-T_{s_i}\right), \quad (40)$$

where $\sigma_{e_i} = (\arctan(|e_{1i}(T_{s_i})|^{\alpha_{e_i}})/\arctan(e_{1i\max}^{\alpha_{e_i}}+\kappa_{e_i}))$. Since $s_{i\max}^{\alpha_{s_i}}+\kappa_{s_i} > |s_i(0)|^{\alpha_{s_i}}$ and $e_{1i\max}^{\alpha_{e_i}}+\kappa_{e_i} > |e_{1i}(T_{s_i})|^{\alpha_{e_i}}$, we have $0 < \sigma_{e_i} < 1$ and $0 < \sigma_{s_i} < 1$. Then, combining $T_{e_i} > T_{s_i}$, we have

$$\left|e_{1i}\right| \le \delta_{e_i}, \quad \text{if } t \ge T_{e_i}. \quad (41)$$

According to (37), $0 < \sigma_{s_i} < 1$ and $T_{e_i} > T_{s_i}$, and we have

$$s_i = 0, \quad \text{if } t \ge T_{e_i}. \quad (42)$$

Then, combining (25), (26), (41), and (42), we have

$$\begin{aligned} e_{2i} = &-\frac{\arctan\left(e_{1i\max}^{\alpha_{e_i}}\right)}{\left(T_{e_i}-T_{s_i}\right)\alpha_{e_i}}\left(\frac{-1-\ln\delta_{e_i}}{1-\alpha_{e_i}-\delta_{e_i}\ln\delta_{e_i}}\mathrm{Sig}\left(e_{1i}\right)^{2-\alpha_{e_i}}\right) \\ &-\frac{\arctan\left(e_{1i\max}^{\alpha_{e_i}}\right)}{\left(T_{e_i}-T_{s_i}\right)\alpha_{e_i}}\left(\frac{\delta_{e_i}^{-2\alpha_{e_i}}\delta_{ei}^{|e_{1i}|}e_{1i}}{1-\alpha_{e_i}-\delta_{e_i}\ln\delta_{e_i}}+\mathrm{Sig}\left(e_{1i}\right)^{1+\alpha_{e_i}}\right), \quad \text{if } t \ge T_{e_i}. \end{aligned} \quad (43)$$

We define a new Lyapunov function as

$$V_2 = \frac{e_{1i}^2}{2}. \quad (44)$$

Then, calculating the time derivative of V_2 and considering (43), we get

$$\begin{aligned} \dot{V}_2 &= e_{1i}e_{2i} \\ &= -\frac{\arctan\left(e_{1i\max}^{\alpha_{e_i}}\right)}{\left(T_{e_i}-T_{s_i}\right)\alpha_{e_i}}\left(\frac{\left(-1-\ln\delta_{e_i}\right)}{1-\alpha_{e_i}-\delta_{e_i}\ln\delta_{e_i}}\right)\left|e_{1i}\right|^{3-\alpha_{e_i}} \\ &\quad -\frac{\arctan\left(e_{1i\max}^{\alpha_{e_i}}\right)}{\left(T_{e_i}-T_{s_i}\right)\alpha_{e_i}}\left(\frac{\delta_{e_i}^{-2\alpha_{e_i}}\delta_{ei}^{|e_{1i}|}}{1-\alpha_{e_i}-\delta_{e_i}\ln\delta_{e_i}}\left|e_{1i}\right|^2+\left|e_{1i}\right|^{2+\alpha_{e_i}}\right), \quad \text{if } t \ge T_{e_i}. \end{aligned} \quad (45)$$

Since $\delta_{e_i} \in (0, 1/e)$ and $0 < \alpha_{e_i} < 1$, we have

$$\frac{-1-\ln\delta_{e_i}}{1-\alpha_{e_i}-\delta_{e_i}\ln\delta_{e_i}} > 0, \quad (46)$$

$$\frac{\delta_{e_i}^{-2\alpha_{e_i}}}{1-\alpha_{e_i}-\delta_{e_i}\ln\delta_{e_i}} > 0. \quad (47)$$

Considering (41) and $\delta_{e_i} \in (0, 1/e)$, we have

$$\delta_{ei}^{|e_{1i}|} \ge \delta_{ei}^{\delta_{ei}} > 0, \quad \text{if } t \ge T_{e_i}. \quad (48)$$

Then, combining (45), (46), (47), and (48), we have

$$\dot{V}_2 \le -k_{e_i}V_2, \quad \text{if } t \ge T_{e_i}, \quad (49)$$

where the constant $k_{e_i} = (\delta_{e_i}^{-2\alpha_{e_i}}/2(1-\alpha_{e_i}-\delta_{e_i}\ln\delta_{e_i}))\delta_{ei}^{\delta_{ei}} > 0$.

From (49), we have

$$V_2 \le V_2\left(T_{e_i}\right)e^{-k_{e_i}\left(t-T_{e_i}\right)}, \quad \text{if } t \ge T_{e_i}. \quad (50)$$

Thus, we have $V_2(\infty) = 0$. Combining $|e_{1i}| \le \delta_{e_i}$, if $t \ge T_{e_i}$ (see (41)), and $V_2(\infty) = 0$, the proof is finished. □

Remark 2. From the above analysis, to guarantee the predefined-time stability, we need $s_{i\max} > |s_i(0)|$ and $e_{1i\max} > |e_{1i}(T_{s_i})|$. In the practical cases, the upper bounds of initial states $e_{1i}(0)$ and $e_{2i}(0)$ can be obtained by considering physical constraint. However, the upper bounds of $e_{1i}(T_{s_i})$ and $s_i(0)$ cannot be obtained directly. To obtain the upper bound parameters $s_{i\max}$ and $e_{1i\max}$, an estimation method is given in the Appendix.

Remark 3. The predefined-time performance (setting time constant is T_{e_i}) must be satisfied by selecting $T_{e_i} > T_{s_i} > 0$, $\kappa_{e_i} > 0$, $\delta_{e_i} \in (0, 1/e) = (0, 0.36)$, $\delta_{e_i} = \alpha_{e_i}$, $0 < \alpha_{e_i} < 1$, $\kappa_{s_i} > 0$, and $0 < \alpha_{s_i} < 1$, and the upper bound parameters $s_{i\max}$ and $e_{1i\max}$ satisfy the estimation methods given in Appendix. Although the predefined-time convergence performance must be guaranteed if parameters satisfy these conditions, we can select the parameters appropriately to achieve a smaller initial control input. For example, κ_{e_i} is a positive constant, and the purpose of defining κ_{e_i} is to estimate the upper bound of $|e_{1i}|$ (see (b) of Appendix) and achieve small initial control input. To achieve exact upper bound of $|e_{1i}|$ and small initial control input, κ_{e_i} should be large. However, large κ_{e_i} may cause a large initial control input, and thus we

need to balance the choice of κ_{e_i}. Fortunately, even if the selection of κ_{e_i} can affect the initial control input, by defining an arbitrary κ_{e_i} still can achieve a smaller initial control input than conventional PTC (see Remark 1).

Remark 4. Although this paper focuses on the predefined-time control of rigid manipulator system, the proposed predefined-time NTSMC scheme can be directly applied to the one-order or two-order matched uncertain system. For example, since many chaotic systems are typical one-order or two-order systems (such as Lorenz system, Rossler system, and chaotic gyros system) and we usually only consider that these systems are affected by matched uncertainties, the proposed method can directly enhance the convergence performance of the synchronization control and the chaos anti-control for these complex chaotic systems. Similarly, the proposed scheme also can be applied to many complex engineering systems, including the formation control system of autonomous underwater vehicles, the aircraft attitude control system, and the angle constrained guidance system.

4. Simulation Results

The effectiveness of proposed predefined-time NTSMC will be illustrated by simulating in this section. We consider that system (1) is a two-DOF robot manipulator. The system parameters are given as follows:

$$\begin{aligned}
\vec{J}(\vec{\phi}) &= \begin{bmatrix} (\varepsilon_1+\varepsilon_2)\sigma_1^2+\varepsilon_2\sigma_2^2+2\varepsilon_2\sigma_1\sigma_2\cos(\phi_2)+P_1 & \varepsilon_2\sigma_2^2+\varepsilon_2\sigma_1\sigma_2\cos(\phi_2) \\ \varepsilon_2\sigma_2^2+\varepsilon_2\sigma_1\sigma_2\cos(\phi_2) & \varepsilon_2\sigma_2^2+P_2 \end{bmatrix}, \\
\vec{L}(\vec{\phi},\dot{\vec{\phi}}) &= \begin{bmatrix} -\varepsilon_2\sigma_1\sigma_2\sin(\phi_2)\dot{\phi}_1 & -2\varepsilon_2\sigma_1\sigma_2\sin(\phi_2)\dot{\phi}_1 \\ 0 & \varepsilon_2\sigma_1\sigma_2\sin(\phi_2)\dot{\phi}_2 \end{bmatrix}, \\
\vec{G}(\vec{\phi}) &= [(\varepsilon_1+\varepsilon_2)\sigma_1 g_1\cos(\phi_1)+\varepsilon_2\sigma_2 g_1\cos(\phi_1+\phi_2), \varepsilon_2\sigma_2 g_1\cos(\phi_1+\phi_2)]^T,
\end{aligned} \tag{51}$$

where $\varepsilon_1 = 0.7$, $\varepsilon_2 = 0.7$, $\sigma_1 = 0.5$, $\sigma_2 = 0.5$, $P_1 = P_2 = 1.5$, and $g_1 = 9.8$. The desired joint position $\vec{\phi}_d$ is chosen as

$$\vec{\phi}_d = [0.7-\cos(t/3), -0.3-\sin(t/2)]^T \text{ rad}. \tag{52}$$

The initial joint angle and angular velocity are chosen as

$$\begin{aligned}
\phi(0) &= [\,1 \;\; 1\,]^T \text{ rad}, \\
\dot{\phi}(0) &= [\,0 \;\; -0.5\,]^T \text{ rad/s}.
\end{aligned} \tag{53}$$

The uncertainty is chosen as

$$\mathbf{D} = [3\cos(t/3), 2.5\sin(t/2)]^T. \tag{54}$$

To remove the chattering problem, the chattering term in the proposed control (28) is replaced by the sigmoid function $\mathrm{sigmf}(\cdot)$ (see [37]) given as

$$\begin{aligned}
\overline{D}_{i\max}\mathrm{sign}(s_i) &= \overline{D}_{i\max}\mathrm{sigmf}(s_i), \\
\mathrm{sigmf}(s_i) &= 2\left(\frac{1}{1+\exp^{-\varpi s_i}}-\frac{1}{2}\right),
\end{aligned} \tag{55}$$

where ϖ is chosen as 30.

4.1. Comparison of the Proposed Predefined-Time NTSMC and Existing Methods. For comparison, the finite-time NTSMC in [27], the fixed-time NTSMC in [33], the predefined-time linear sliding-mode control (LSMC) in [44], and the proposed predefined-time NTSMC (28) will be considered in this section.

According to [27], the finite-time NTSMC scheme can be designed as

$$\tau = \tau_0 + \tau_{eq} + \tau_r, \tag{56}$$

where the sliding-mode surface s_T and the control components τ_0, τ_{eq}, and τ_r are given as

$$\begin{cases}
s_T = e_2 + \displaystyle\int_0^t \left(\Omega_1\, S(e_1)^{\zeta_1} + \Omega_2 S(e_2)^{\zeta_2}\right)dv\,, \\
\tau_0 = J(\phi)\ddot{\phi}_d + L(\phi,\dot{\phi})\dot{\phi} + G(\phi), \\
\tau_{eq} = -M(q)\left(\Omega_1 S(e_1)^{v_1} + \Omega_2 S(e_2)^{v_2}\right), \\
\tau_r = \left(-\dfrac{1}{1-\overline{\delta}_f}\left(k_f + b_0 + b_2\|\dot{q}\|^2 + \varpi_f\left\|\tau_0+\tau_{eq}\right\|\right)\right)\dfrac{s_T}{\|s_T\|+s_f}.
\end{cases} \tag{57}$$

$S(e_1)^{\zeta_1}$ and $S(e_2)^{\zeta_2}$ are defined as

$$\begin{aligned}
S(e_1)^{\zeta_1} &= \left[\,S(e_{11})^{\zeta_1} \;\; S(e_{12})^{\zeta_1}\,\right]^T, \\
S(e_2)^{\zeta_2} &= \left[\,S(e_{21})^{\zeta_2} S(e_{22})^{\zeta_2}\,\right]^T.
\end{aligned} \tag{58}$$

According to [33], the fixed-time NTSMC can be given as

$$\boldsymbol{\tau} = \boldsymbol{\tau}_1 + \boldsymbol{\tau}_2 + \boldsymbol{\tau}_3, \tag{59}$$

where

$$\begin{aligned}
\boldsymbol{\tau}_1 &= \mathbf{J}(\phi)\ddot{\phi}_d + \mathbf{L}(\phi,\dot{\phi})\dot{\phi} + \mathbf{G}(\phi),\\
\boldsymbol{\tau}_2 &= -\mathbf{K}_0\mathbf{Sig}(\mathbf{s}_F)^r - \mathbf{J}(\phi)\left(\mathbf{K}_1\mathbf{F}^{v_1}(\mathbf{e}_1) + v_2\mathbf{K}_2\mathbf{H}^{v_2}(\mathbf{e}_1)\right)\mathbf{e}_2,\\
\boldsymbol{\tau}_3 &= \left(-\frac{1}{1-\bar{\delta}}\left(k_0 + k_1 + k_2\|\dot{\phi}\|^2 + \varpi\|\boldsymbol{\tau}_1 + \boldsymbol{\tau}_2\|\right)\right)\frac{\mathbf{s}_F}{\|\mathbf{s}_F\| + s_{F0}},\\
\mathbf{s}_F &= \mathbf{e}_2 + \mathbf{K}_1\mathbf{S}^{v_1}(\mathbf{e}_1) + \mathbf{K}_2\overrightarrow{\mathbf{Sig}}^{v_2}(\mathbf{e}_1).
\end{aligned} \tag{60}$$

The vector $\overrightarrow{S}^{v_1}(\overrightarrow{e}_1)$ and the matrixes $\overrightarrow{H}^{v_2}(\overrightarrow{e}_1)$ and $\overrightarrow{F}^{v_1}(\overrightarrow{e}_1)$ are defined as

$$\begin{aligned}
S^{v_1}(e_1) &= \left[\, S(e_{11})^{v_1} \;\; S(e_{12})^{v_1} \,\right]^T,\\
H^{v_2}(e_1) &= \mathrm{diag}\left(|e_{11}|^{v_2-1}, |e_{12}|^{v_2-1}\right),\\
F^{v_1}(e_1) &= \mathrm{diag}\left(f(e_{11})^{v_1}, f(e_{12})^{v_1}\right),
\end{aligned} \tag{61}$$

where the functions $S(e_{1i})^{v_1}$ and $f(e_{1i})^{v_1}$, $(i = 1, 2)$, are defined as

$$S(e_{1i})^{v_1} = \begin{cases} |e_{1i}|^{v_1}\mathrm{sign}(e_{1i}), & |e_{1i}| \geq \delta_{Fi},\\ \delta_{Fi}^{v_1-1}e_{1i}, & |e_{1i}| < \delta_{Fi}, \end{cases} \tag{62}$$

$$f(e_{1i})^{v_1} = \begin{cases} v_1|e_{1i}|^{v_1-1}, & |e_{1i}| \geq \delta_{Fi},\\ \delta_{Fi}^{v_1-1}, & |e_{1i}| < \delta_{Fi}. \end{cases} \tag{63}$$

According to [44], the predefined-time LSMC is designed as

$$\boldsymbol{\tau} = \overline{\tau}_1 + \overline{\tau}_2 + \widehat{\overline{Y}}_r, \tag{64}$$

where

$$\begin{aligned}
\overline{\overrightarrow{\tau}}_1 &= \begin{cases} -\dfrac{\pi}{\eta T_c}\left(\gamma^{1-\eta/2}\|\mathbf{s}_r\|^{-\eta} + \gamma^{1+\eta/2}\|\mathbf{s}_r\|^{\eta}\right)\mathbf{s}_r, & \text{if } \|\mathbf{s}_r\| \geq \delta_r,\\ -\dfrac{\pi}{\eta T_c}\left(\gamma^{1-\eta/2}\delta_r^{-\eta} + \gamma^{1+\eta/2}\delta_r^{\eta}\right)\mathbf{s}_r, & \text{if } \|\mathbf{s}_r\| < \delta_r, \end{cases}\\
\overline{\tau}_2 &= \begin{cases} -k_\tau\dfrac{\mathbf{s}_r}{\|\overrightarrow{s}_r\|}, & \text{if } \|\mathbf{s}_r\| \geq \delta_r,\\ -k_\tau\dfrac{\mathbf{s}_r}{\delta_r}, & \text{if } \|\mathbf{s}_r\| < \delta_r, \end{cases}\\
\widehat{Y}_r &= \widehat{J}(\phi)\ddot{\phi}_m + \widehat{L}(\phi,\dot{\phi})\dot{\phi}_m + \widehat{G}(\phi),\\
\dot{\phi}_m &= \dot{\phi}_d - k_\alpha(\phi - \phi_d),\\
\ddot{\phi}_m &= \ddot{\phi}_d - k_\alpha\left(\dot{\phi} - \dot{\phi}_d\right),\\
s_r &= e_2 + k_\alpha e_1.
\end{aligned} \tag{65}$$

Then, we consider the following two cases.

Case 1-1: we desire the convergence time which is bounded by 2.5 s. In this case, we consider four control schemes including finite-time NTSMC, fixed-time NTSMC, predefined-time LSMC, and predefined-time NTSMC. First, we consider the following initial system state.

The initial joint angle and angular velocity are chosen as

$$\phi(0) = \left[\, 1 \;\; 1 \,\right]^T \text{ rad}, \tag{66}$$

$$\dot{\phi}(0) = \left[\, 0 \;\; -0.5 \,\right]^T \text{ rad/s}. \tag{67}$$

Then, the initial tracking error can be calculated as

$$e_1 = \left[\, 1.3 \;\; 1.3 \,\right]^T \text{ rad}, \tag{68}$$

$$e_2 = \left[\, 0 \;\; 0 \,\right]^T \text{ rad/s}. \tag{69}$$

It is assumed that we can use the trial-and-error method to adjust the parameters. The predefined-time parameters of predefined-time LSMC and predefined-time NTSMC are set as $T_c = 2.5$ and $T_{e_1} = T_{e_2} = 2.5$, respectively. For the fixed-time NTSMC, the gain matrix $\overrightarrow{K}_2$ is selected as $\overrightarrow{K}_2 = \begin{bmatrix} 2 & 0 \\ 0 & 2.4 \end{bmatrix}$. The other parameters of the three schemes are given in Table 1. The simulation results are shown in Figures 1–3 . From Figure 1, we know that the four schemes can guarantee that the convergence time is bounded by the desired time (2.5s) under these parameters. From Figure 3, it can be known that the input torques of fixed-time NTSMC have the problem of large switching. The reason is that the derivative of nonsingular function (63) in fixed-time NTSMC is discontinuous. The nonsingular function and its derivative of the proposed NTSMC are continuous, and thus the problem can be avoided by the proposed scheme.

Then, without changing the control parameters, we chose a new kind of initial system state.

The initial joint angle and angular velocity are chosen as

$$\begin{aligned}
\phi(0) &= \left[\, 3.6 \;\; 3.6 \,\right]^T \text{ rad},\\
\dot{\phi}(0) &= \left[\, 0 \;\; -0.5 \,\right]^T \text{ rad/s}.
\end{aligned} \tag{70}$$

Then, the initial tracking error can be calculated as

$$e_1 = \left[\, 3.9 \;\; 3.9 \,\right]^T, \tag{71}$$

$$e_2 = \left[\, 0 \;\; 0 \,\right]^T. \tag{72}$$

By comparing equations (68) and (71), we can know that the second kind of initial tracking error is much bigger than the first kind of initial tracking error. The simulation results are shown in Figures 4–6 . From Figure 4, we can know that the convergence performance of finite-time NTSMC is greatly affected by the increase of initial system state. The convergence performances of fixed-time NTSMC, predefined-time LSMC, and proposed predefined-time NTSMC are not affected even if the initial system states are greatly increased. As stated in Introduction section and Section 2,

Table 1: Control parameters.

Control scheme	Control parameters
Finite-time NTSMC	$\zeta_1 = 0.5, \zeta_2 = 2/3, \vec{\Omega}_1 = \begin{bmatrix} 23 & 0 \\ 0 & 19 \end{bmatrix}, \vec{\Omega}_2 = \begin{bmatrix} 16 & 0 \\ 0 & 12 \end{bmatrix}, k_f = 2, b_0 = 12, b_2 = 2.8, s_f = 0.01, \bar{\delta}_f = 0.5, \varpi_f = 0.4$
Fixed-time NTSMC	$\upsilon_1 = 0.5, \upsilon_2 = 3/2, K_0 = \begin{bmatrix} 1 & 0 \\ 0 & 1 \end{bmatrix}, K_1 = \begin{bmatrix} 1 & 0 \\ 0 & 1 \end{bmatrix}, \nu_1 = 0.5, \nu_2 = 1.5, \delta_{F1} = \delta_{F2} = 0.2, k_0 = 2, k_1 = 12, k_2 = 2.8,$ $r = 1.5, s_{F0} = 0.01, \bar{\delta} = 0.5, \varpi = 0.4$
Predefined-time LSMC	$\eta = 0.5, \delta_r = 0.2, k_\alpha = 5, k_\tau = 5, \gamma = 0.03$
Proposed predefined-time NTSMC	$\alpha_{e1} = \alpha_{e2} = 0.35, \delta_{e_1} = \delta_{e_2} = 0.35, \alpha_{s1} = \alpha_{s2} = 0.55, e_{11\max} = e_{12\max} = 3, \kappa_{s1} = \kappa_{s2} = 1, \kappa_{e1} = \kappa_{e2} = 1,$ $\overline{D}_{1\max} = \overline{D}_{2\max} = 3, T_{s_1} = T_{s_2} = 0.3, s_{1\max} = s_{2\max} = 35$

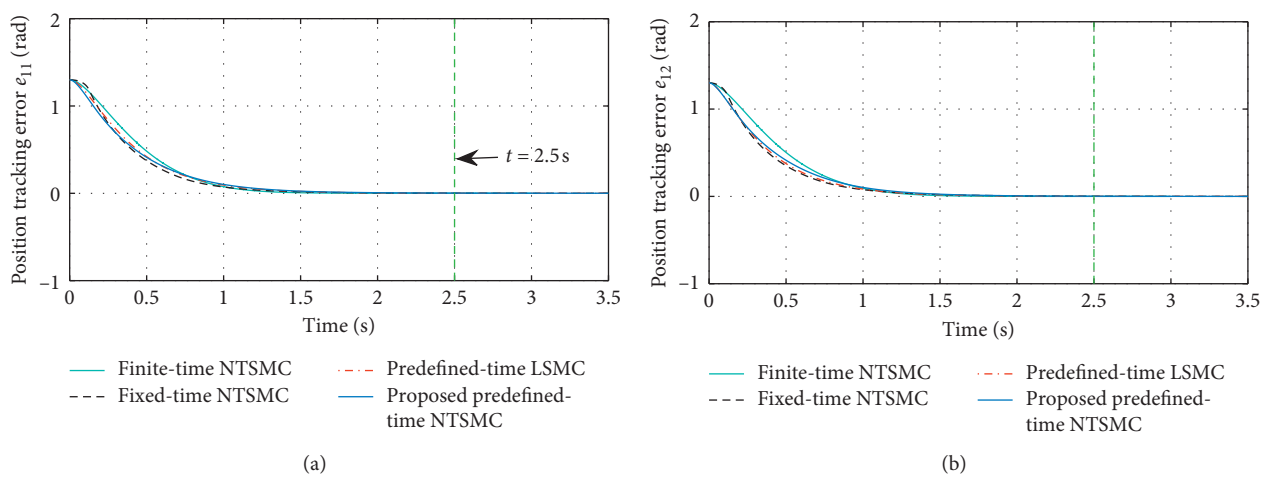

Figure 1: Position tracking errors e_{11} and e_{12} in Case 1-1 (first kind of initial system state).

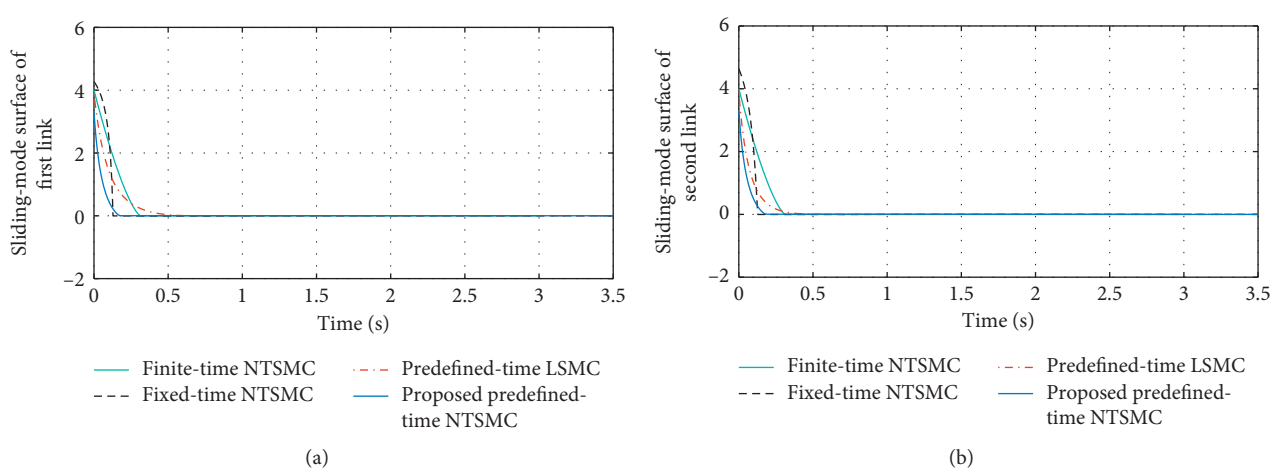

Figure 2: Sliding-mode surfaces s_1 and s_2 in Case 1-1 (first kind of initial system state).

the reason is that convergence time function of finite-time stability is related to the initial system state.

Case 1-2: compared with Case 1-1, we desire a new convergence time which is bounded by 0.7s. It is assumed that we cannot use the trial-and-error method. We can only change the parameters once in this case. In this case, we consider three control schemes including fixed-time NTSMC, predefined-time LSMC, and predefined-time NTSMC. The initial system states are chosen as in (66) and (67). Then, the predefined-time parameters of predefined-time LSMC and proposed predefined-time NTSMC are set as $T_c = 0.7$ and $T_{e_1} = T_{e_2} = 0.7$. However, for the fixed-time

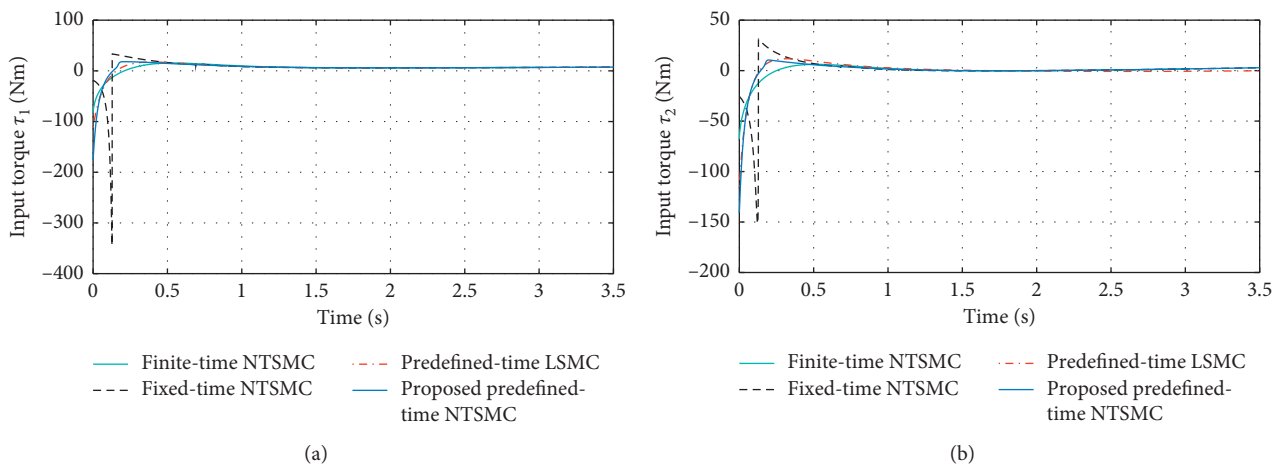

Figure 3: Input torques τ_1 and τ_2 in Case 1-1 (first kind of initial system state).

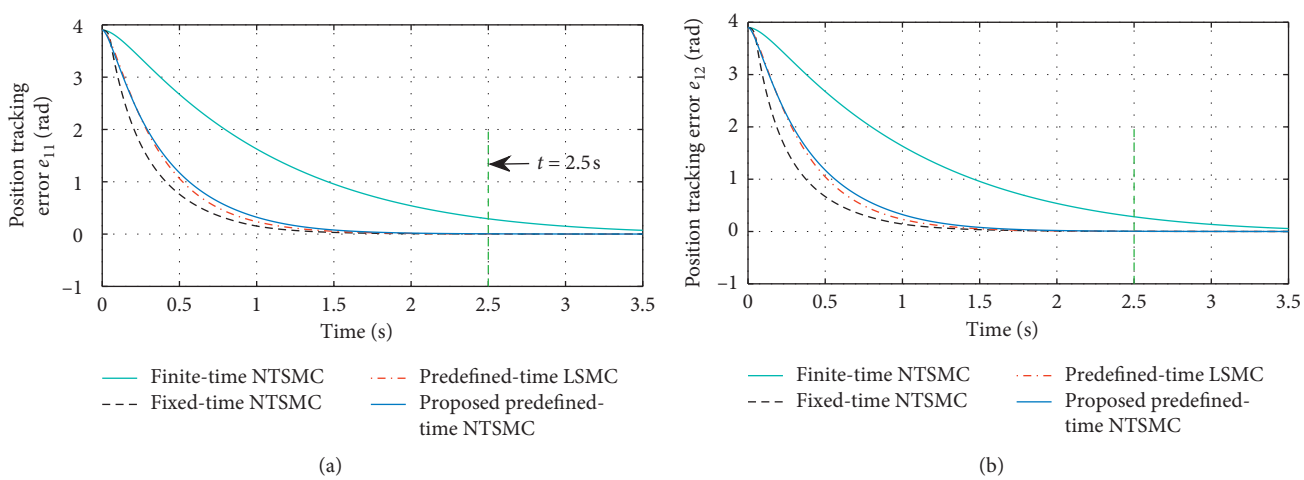

Figure 4: Position tracking errors e_{11} and e_{12} in Case 1-1 (second kind of initial system state).

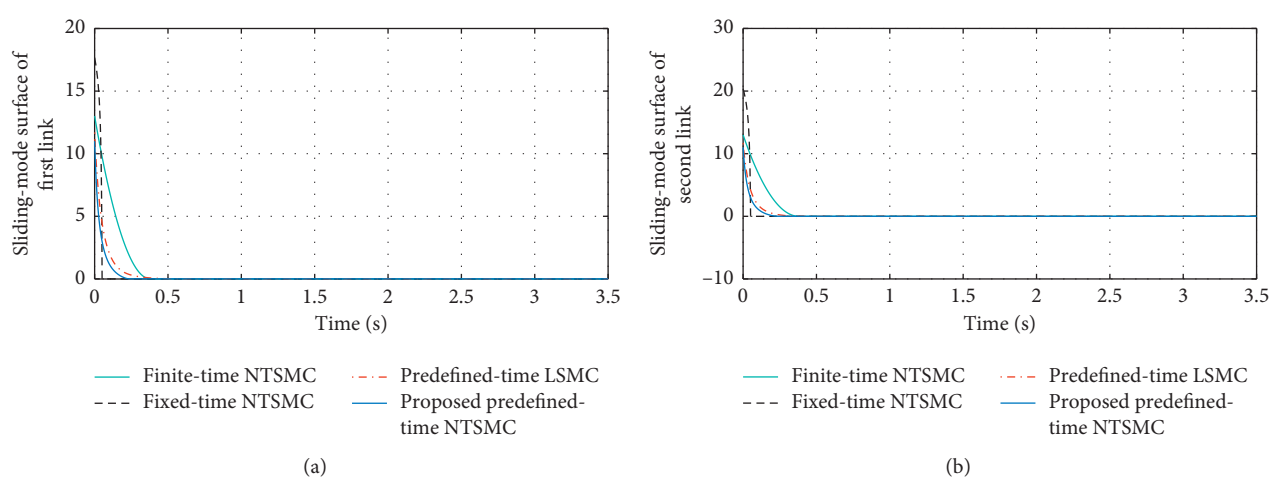

Figure 5: Sliding-mode surfaces s_1 and s_2 in Case 1-1 (second kind of initial system state).

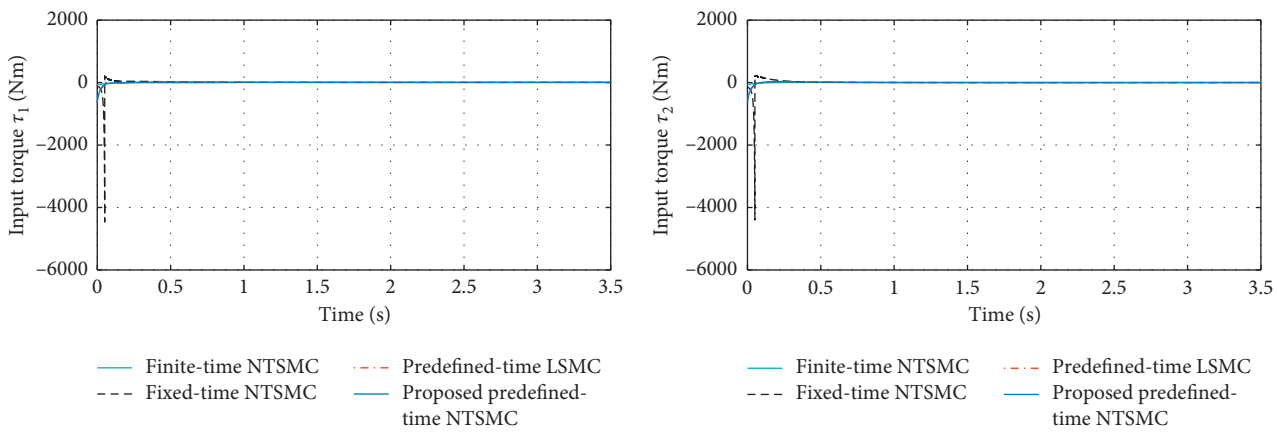

(a) (b)

Figure 6: Input torques τ_1 and τ_2 in Case 1-1 (second kind of initial system state).

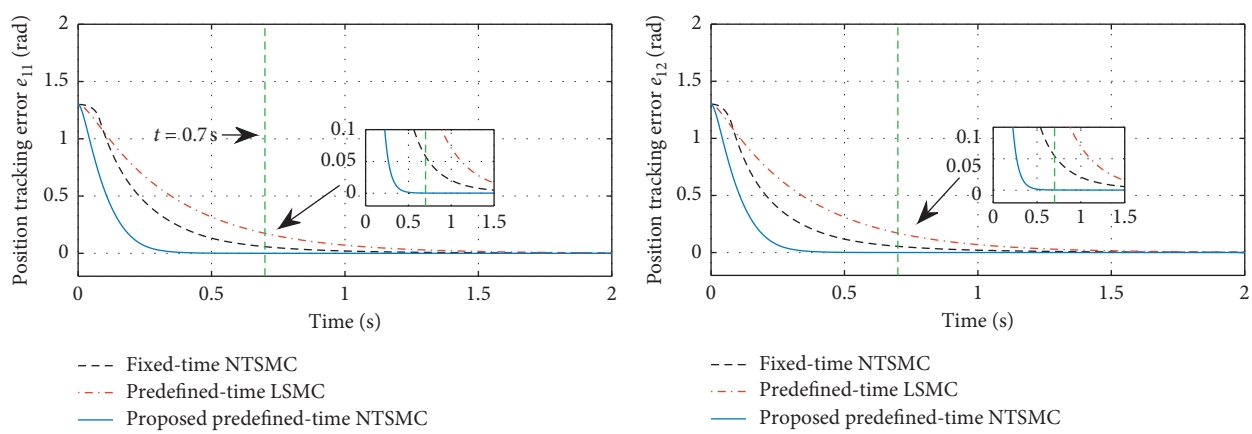

(a) (b)

Figure 7: Position tracking errors e_{11} and e_{12} in Case 1-2.

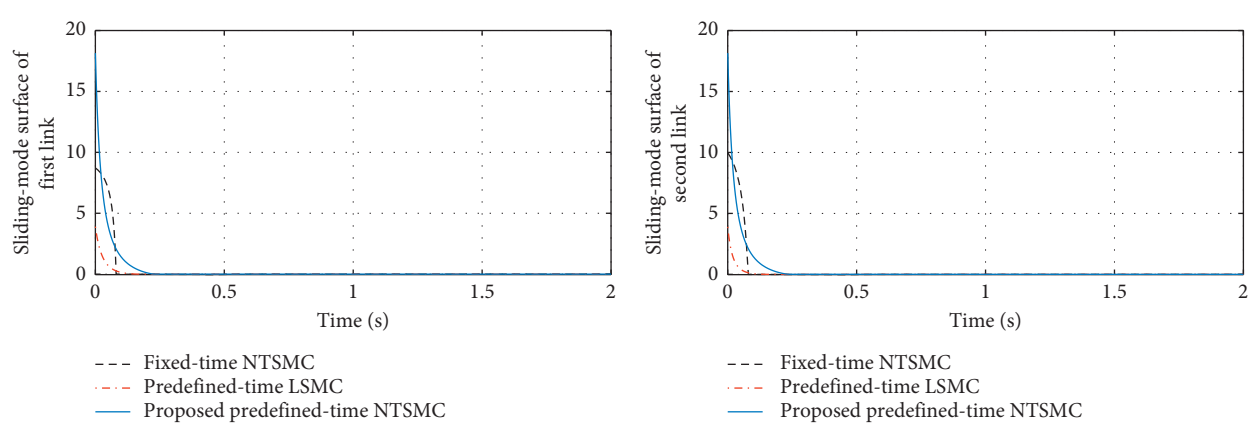

(a) (b)

Figure 8: Sliding-mode surfaces s_1 and s_2 in Case 1-2.

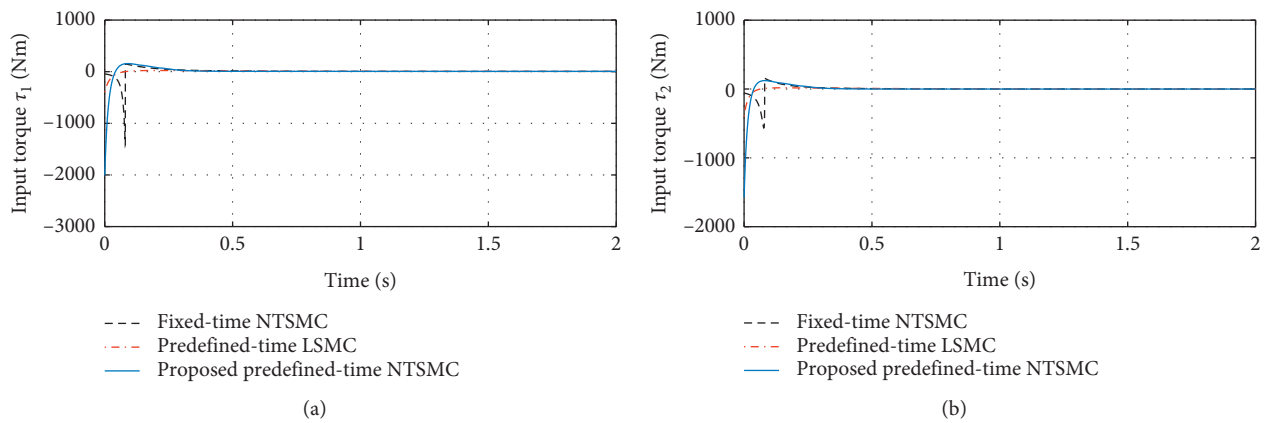

Figure 9: Input torques τ_1 and τ_2 in Case 1-2.

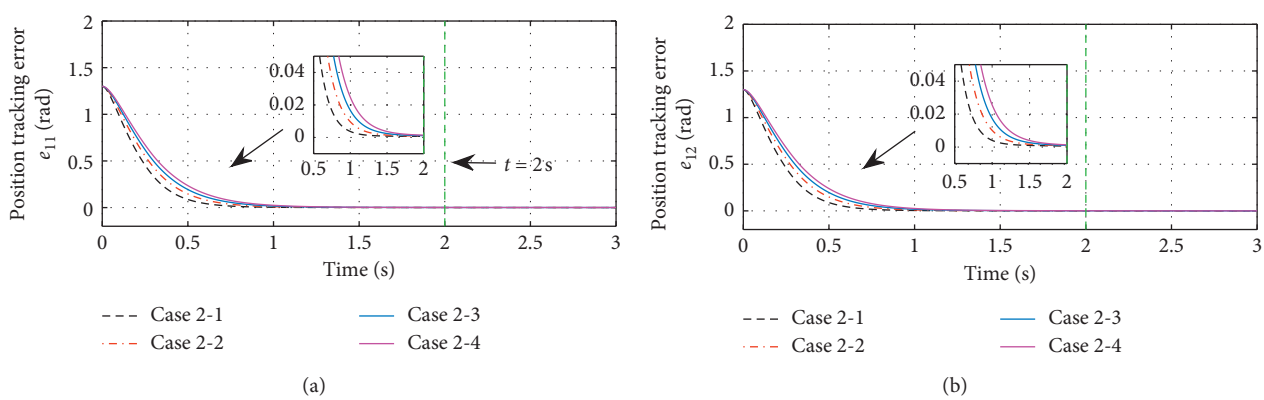

Figure 10: Position tracking errors e_{11} and e_{12} described in Section 4.2.

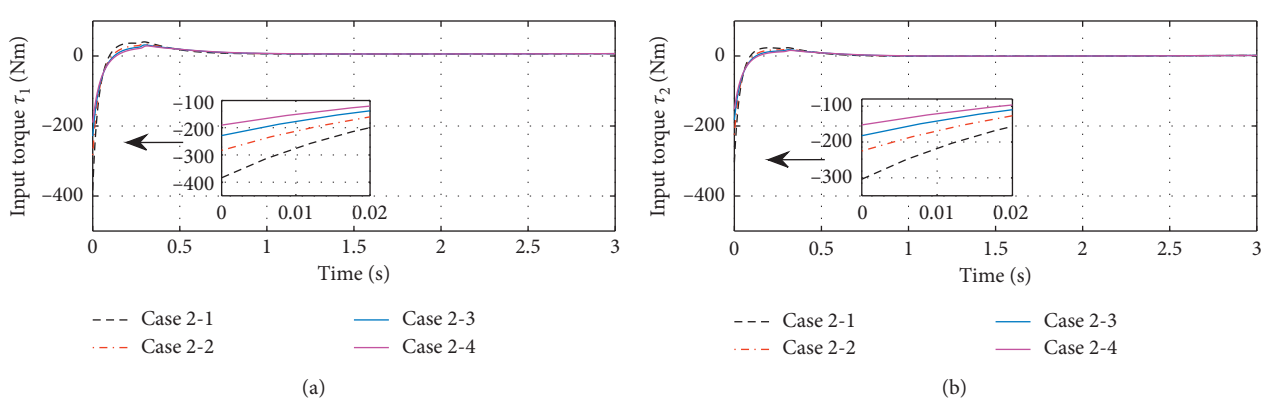

Figure 11: Position tracking errors e_{11} and e_{12} described in Section 4.2.

NTSMC, the relationship between the parameters and the settling time constant is complex and nonlinear. Since the new desired time is smaller than the value of Case 1-1, we try to increase the gain matrix $\vec{K}_2$ to $\vec{K}_2 = \begin{bmatrix} 5 & 0 \\ 0 & 6 \end{bmatrix}$. The other parameters of the three schemes are given in Table 1. Then, the simulation results of Case 1-2 are shown in Figures 7–9. From Figure 7, we know that only the proposed predefined-time NTSMC can guarantee that the convergence time is bounded by the new desired time (0.7s). Thus, according to Definition 3, the predefined-time stability is only achieved by the proposed scheme. As stated in Introduction section and Section 2, the reasons are as follows. (i) The sliding-mode surface of predefined-time LSMC is linear, which means that predefined-time LSMC only can guarantee the predefined-time convergence of sliding-mode surface (see Figure 8) rather than the predefined-time convergence of tracking errors. (ii) For the fixed-time NTSMC, the relationship between parameters and the setting time constant is complex and nonlinear. Thus, for the fixed-time NTSMC, it is difficult to adjust the parameters to achieve the predefined-time convergence without using the trial-and-error method.

4.2. Comparison of the Proposed Modified PTC and Conventional PTC Scheme. In this section, we consider the initial system state chosen as in (66) and (67). The predefined-time parameters are set as $T_{e_1} = T_{e_2} = 2$. In this section, we consider four kinds of upper bound of initial tracking errors $e_{1i}(0)$ and $e_{2i}(0)$. We assume that $|e_{1i}(0)| \le k_{1i}$ and $|e_{2i}(0)| \le k_{2i}$. From Case 2-1 to Case 2-4, the upper bounds are gradually approaching the exact values:

Case 2-1 (conventional PTC algorithm): $k_{11} = k_{12} = \infty$, $k_{21} = k_{22} = \infty$.

Case 2-2: $k_{11} = k_{12} = 20$, $k_{21} = k_{22} = 10$.

Case 2-3: $k_{11} = k_{12} = 5$, $k_{21} = k_{22} = 2.5$.

Case 2-4: $k_{11} = k_{12} = 2$, $k_{21} = k_{22} = 1$.

For Case 2-1, the proposed PTC algorithm is equivalent to the conventional PTC algorithm. We select $\kappa_{e1} = \kappa_{e2} = 1$. Then, according to Appendix, for the above cases, the upper bound parameters can be estimated as follows.

Case 2-1 (conventional PTC algorithm): $e_{11\max} = e_{12\max} = \infty$, $s_{1\max} = s_{2\max} = \infty$.

Case 2-2: $e_{11\max} = e_{12\max} = 37.9979$, $s_{1\max} = s_{2\max} = 253.7187$.

Case 2-3: $e_{11\max} = e_{12\max} = 10.9008$, $s_{1\max} = s_{2\max} = 46.2597$.

Case 2-4: $e_{11\max} = e_{12\max} = 5.0891$, $s_{1\max} = s_{2\max} = 15.6292$.

The other parameters are chosen as $\alpha_{e1} = \alpha_{e2} = 0.35$, $\delta_{e_1} = \delta_{e_2} = 0.35$, $\alpha_{s1} = \alpha_{s2} = 0.55$, $\kappa_{s1} = \kappa_{s2} = 1$, $\overline{D}_{1\max} = \overline{D}_{2\max} = 3$, and $T_{s_1} = T_{s_2} = 0.3$. The simulation results are shown in Figures 7 and 8. From Figures 10 and 11 , compared with the conventional PTC algorithm, the proposed modified PTC algorithm can achieve more accurate convergence time and smaller initial control input torques. Moreover, if the upper bounds k_{1i} and k_{2i} are closer to the exact values of initial values $|e_{1i}(0)|$ and $|e_{2i}(0)|$, more accurate convergence time and smaller initial control input torques can be achieved.

5. Conclusion

A novel predefined-time NTSMC was developed for the uncertain robotic manipulator system. The conventional PTC algorithm was modified such that the initial control peaking was reduced and the precision of convergence time was enhanced. Moreover, the proposed control scheme constructed a predefined-time nonsingular sliding-mode surface rather than the linear sliding-mode surface used in the conventional predefined-time SMC scheme. Thus, the proposed scheme can strictly guarantee the predefined-time stability of tracking error rather than only the predefined-time convergence of sliding-mode surface. The performance of the proposed control scheme has been illustrated by simulation. The proposed method of this paper focuses on the predefined-time convergence of the rigid manipulator system with uncertainties. The rigid manipulator system is a typical two-order matched uncertain system. However, some manipulator systems such as the flexible joint manipulator system are high-order systems (four order) and are affected by mismatched uncertainties. In the future work, we will extend the proposed predefined-time NTSMC scheme to higher-order and mismatched uncertain systems.

Appendix

In practical cases, the upper bound of initial tracking errors $e_{1i}(0)$ and $e_{2i}(0)$ can be obtained by considering the physical constraint. Thus, we assume that $|e_{1i}(0)| \le k_{1i}$ and $|e_{2i}(0)| \le k_{2i}$. Then, $s_{i\max}$ and $e_{1i\max}$ can be estimated by the following methods:

(a) Estimation of the upper bound parameter $s_{i\max}$: according to the definition of sliding-mode surface in (25) and considering (46), (47), and (48), the initial sliding-mode surface satisfies the following inequations:

$$\begin{aligned}
|s_i 0| &\le |e_{2i}0| + \frac{\arctan e_{1i\max}^{\alpha_{e_i}} + \kappa_{e_i}}{T_{e_i} - T_{s_i}\alpha_{e_i}} \times |e_{1i}0|^{1-\alpha_{e_i}} + |e_{1i}0|^{1+\alpha_{e_i}} \le k_{2i} + \frac{\pi}{2T_{e_i} - T_{s_i}\alpha_{e_i}} \times k_{1i}^{1-\alpha_{e_i}} + k_{1i}^{1+\alpha_{e_i}}, \quad \text{if } |e_{1i}| \ge \delta_{e_i}, \\
|s_i 0| &\le |e_{2i}0| + \frac{\arctan e_{1i\max}^{\alpha_{e_i}} + \kappa_{e_i}}{T_{e_i} - T_{s_i}\alpha_{e_i}} \times \frac{-1 - \ln \delta_{e_i}}{1 - \alpha_{e_i} - \delta_{e_i} \ln \delta_{e_i}} |e_{1i}0|^{2-\alpha_{e_i}} + \frac{\arctan e_{1i\max}^{\alpha_{e_i}} + \kappa_{e_i}}{T_{e_i} - T_{s_i}\alpha_{e_i}} \times \frac{\delta_{e_i}^{-2\alpha_{e_i}}}{1 - \alpha_{e_i} - \delta_{e_i} \ln \delta_{e_i}} \delta_{ei}^{|e_{1i}|} |e_{1i}0| + |e_{1i}0|^{1+\alpha_{e_i}} \\
&\le k_{2i} + \frac{\pi}{2T_{e_i} - T_{s_i}\alpha_{e_i}} \times \frac{-1 - \ln \delta_{e_i}}{1 - \alpha_{e_i} - \delta_{e_i} \ln \delta_{e_i}} k_{1i}^{2-\alpha_{e_i}} + \frac{\pi}{2T_{e_i} - T_{s_i}\alpha_{e_i}} \times \frac{\delta_{e_i}^{-2\alpha_{e_i}}}{1 - \alpha_{e_i} - \delta_{e_i} \ln \delta_{e_i}} \delta_{ei}^{\delta_{e_i}} k_{1i} + k_{1i}^{1+\alpha_{e_i}}, \quad \text{if } |e_{1i}| < \delta_{e_i}.
\end{aligned} \tag{A.1}$$

Then, the upper bound of initial sliding-mode surface can be obtained as

$$s_{i\max} = \max\{\bar{s}_{1i\max}, \bar{s}_{2i\max}\}, \tag{A.2}$$

where

$$\begin{cases} \bar{s}_{1i\max} = k_{2i} + \dfrac{\pi}{2T_{e_i} - T_{s_i}\alpha_{e_i}} \times k_{1i}^{1-\alpha_{e_i}} + k_{1i}^{1+\alpha_{e_i}}, \\ \bar{s}_{2i\max} = k_{2i} + \dfrac{\pi}{2T_{e_i} - T_{s_i}\alpha_{e_i}} \times \dfrac{-1 - \ln \delta_{e_i}}{1 - \alpha_{e_i} - \delta_{e_i} \ln \delta_{e_i}} k_{1i}^{2-\alpha_{e_i}} + \dfrac{\pi}{2T_{e_i} - T_{s_i}\alpha_{e_i}} \times \dfrac{\delta_{e_i}^{-2\alpha_{e_i}}}{1 - \alpha_{e_i} - \delta_{e_i} \ln \delta_{e_i}} \delta_{ei}^{\delta_{e_i}} k_{1i} + k_{1i}^{1+\alpha_{e_i}}. \end{cases} \tag{A.3}$$

(b) Estimation of upper bound parameter $e_{1i\max}$: if $|e_{1i}| \geq \delta_{e_i}$, according the definition of sliding-mode surface (25), we have

$$e_{2i} = s_i - \frac{\arctan\left(e_{1i\max}^{\alpha_{e_i}} + \kappa_{e_i}\right)}{\left(T_{e_i} - T_{s_i}\right)\alpha_{e_i}} \left(\mathrm{Sig}\left(e_{1i}\right)^{1-\alpha_{e_i}} + \mathrm{Sig}\left(e_{1i}\right)^{1+\alpha_{e_i}}\right), \quad \text{if } \left|e_{1i}\right| \geq \delta_{e_i}. \tag{A.4}$$

Then, for the Lyapunov function $V_2 = e_{1i}^2/2$ defined in (44), we have

$$\begin{aligned} \dot{V}_2 &= e_{1i} e_{2i} \\ &= e_{1i}\left(s_i - \frac{\arctan\left(e_{1i\max}^{\alpha_{e_i}} + \kappa_{e_i}\right)}{\left(T_{e_i} - T_{s_i}\right)\alpha_{e_i}} \left(\mathrm{Sig}\left(e_{1i}\right)^{1-\alpha_{e_i}} + \mathrm{Sig}\left(e_{1i}\right)^{1+\alpha_{e_i}}\right) \right) \\ &= e_{1i} s_i - \frac{\arctan\left(e_{1i\max}^{\alpha_{e_i}} + \kappa_{e_i}\right)}{\left(T_{e_i} - T_{s_i}\right)\alpha_{e_i}} \left(\left|e_{1i}\right|^{2-\alpha_{e_i}} + \left|e_{1i}\right|^{2+\alpha_{e_i}}\right) \\ &\leq \left|e_{1i}\right|\left|s_i\right| - \frac{\arctan\left(\kappa_{e_i}\right)}{\left(T_{e_i} - T_{s_i}\right)\alpha_{e_i}} \left(\left|e_{1i}\right|^{2-\alpha_{e_i}} + \left|e_{1i}\right|^{2+\alpha_{e_i}}\right), \quad \text{if } \left|e_{1i}\right| \geq \delta_{e_i}. \end{aligned} \tag{A.5}$$

From (35), we know that the sliding-mode surface s_i is always bounded from the initial time, i.e., $|s_i| \leq |s_i(0)| \leq s_{i\max}$. Then, we have

$$\dot{V}_2 \leq \left|e_{1i}\right| s_{i\max} - \frac{\arctan\left(\kappa_{e_i}\right)}{\left(T_{e_i} - T_{s_i}\right)\alpha_{e_i}} \left(\left|e_{1i}\right|^{2-\alpha_{e_i}} + \left|e_{1i}\right|^{2+\alpha_{e_i}}\right), \quad \text{if } \left|e_{1i}\right| \geq \delta_{e_i}. \tag{A.6}$$

Then, we have

$$\begin{aligned} \dot{V}_2 &\leq \left|e_{1i}\right|\left(s_{i\max} - \xi_i \left|e_{1i}\right|^{1-\alpha_{e_i}}\right), \quad \text{if } \left|e_{1i}\right| \geq \delta_{e_i}, \\ \dot{V}_2 &\leq \left|e_{1i}\right|\left(s_{i\max} - \xi_i \left|e_{1i}\right|^{1+\alpha_{e_i}}\right), \quad \text{if } \left|e_{1i}\right| \geq \delta_{e_i}, \end{aligned} \tag{A.7}$$

where the constant $\xi_i = (\arctan(\kappa_{e_i})/(T_{e_i} - T_{s_i})\alpha_{e_i}) > 0$. Then, we know that $\dot{V}_2 < 0$ if $|e_{1i}| > (s_{i\max}/\xi_i)^{1/(1-\alpha_{e_i})}$ or $|e_{1i}| > (s_{i\max}/\xi_i)^{1/(1+\alpha_{e_i})}$. Thus, we know that e_{1i} is bounded as

$$\left|e_{1i}\right| \leq \min\left(\left(\frac{s_{i\max}}{\xi_i}\right)^{1/\left(1-\alpha_{e_i}\right)}, \left(\frac{s_{i\max}}{\xi_i}\right)^{1/\left(1+\alpha_{e_i}\right)} \right), \quad \text{if } \left|e_{1i}\right| \geq \delta_{e_i}. \tag{A.8}$$

Thus, the upper bound parameter $e_{1i\max}$ can be obtained as

$$e_{1i\max} = \max\left\{\min\left(\left(\frac{s_{i\max}}{\xi_i}\right)^{1/\left(1-\alpha_{e_i}\right)}, \left(\frac{s_{i\max}}{\xi_i}\right)^{1/\left(1+\alpha_{e_i}\right)}\right), \delta_{e_i}\right\}. \tag{A.9}$$

Data Availability

All data generated or analysed during this study are included within the article.

Conflicts of Interest

The authors declare that there are no conflicts of interest regarding the publication of this paper.

Acknowledgments

This study was supported by the Natural Science Basic Research Program of Shaanxi (2021JQ-880, 2021JM-533, and 2020JM-646), the National Natural Science Foundation of China (11974289), the Key Research and Development Program of Shaanxi Province (2019SF-103), the Support Plan for Sanqin Scholars Innovation Team in Shaanxi Province of China (2020), the Innovation Capability Support Program of Shaanxi (2018GHJD-21), the Science and Technology Program of Xi'an (2019218414GXRC020CG021-GXYD20.3), the Fund of Excellent Doctoral Innovation of Xi'an University of Technology, and the Scientific Research Foundation of Xijing University (XJ200202).

References

[1] M. Yin, Z. Xu, Z. Zhao, and H. Wu, "Mechanism and position tracking control of a robotic manipulator actuated by the tendon-sheath," *Journal of Intelligent and Robotic Systems*, vol. 100, pp. 849–862, 2020.

[2] B. Xiao, S. Yin, and O. Kaynak, "Tracking control of robotic manipulators with uncertain kinematics and dynamics," *IEEE Transactions on Industrial Electronics*, vol. 63, no. 10, pp. 6439–6449, 2016.

[3] J. L. Meza, V Santib, R. Soto et al., "Fuzzy self-tuning PID semiglobal regulator for robot manipulators," *IEEE Transactions on Industrial Electronics*, vol. 59, no. 6, pp. 2709–2717, 2011.

[4] W. Yu and J. Rosen, "Neural PID control of robot manipulators with application to an upper limb exoskeleton," *IEEE Transactions on Cybernetics*, vol. 43, no. 2, pp. 673–684, 2013.

[5] C. Q. Huang, X. F. Peng, and J. P. Wang, "Robust nonlinear PID controllers for anti-windup design of robot manipulators with an uncertain jacobian matrix," *Acta Automatica Sinica*, vol. 34, no. 9, pp. 1113–1121, 2008.

[6] Y. Cao and Y. D. Song, "Adaptive PID-like fault-tolerant control for robot manipulators with given performance specifications," *International Journal of Control*, vol. 93, no. 3, pp. 377–386, 2020.

[7] T. Salloom, X. Yu, W. He, and O. Kaynak, "Adaptive neural network control of underwater robotic manipulators tuned by a genetic algorithm," *Journal of Intelligent and Robotic Systems*, vol. 97, pp. 657–672, 2020.

[8] E. Kobayashi, K. Masamune, I. Sakuma, T. Dohi, and D. Hashimoto, "A new safe laparoscopic manipulator system with a five-bar linkage mechanism and an optical zoom," *Computer Aided Surgery*, vol. 4, no. 4, pp. 182–192, 1999.

[9] E. G. Papadopoulos, *On the Dynamics and Control of Space Manipulators*, Massachusetts Institute of Technology, Cambridge, MA, USA, 1990.

[10] A. H. Mary and T. Kara, "Robust proportional control for trajectory tracking of a nonlinear robotic manipulator: LMI optimization approach," *Arabian Journal for Science and Engineering*, vol. 41, no. 12, pp. 5027–5036, 2016.

[11] Y. Jiang, K. Lu, C. Gong et al., "Robust composite nonlinear feedback control for uncertain robot manipulators," *International Journal of Advanced Robotic Systems*, vol. 17, no. 2, 2020.

[12] A. Khodabakhshian and M. Edrisi, "A new robust PID load frequency controller," *Control Engineering Practice*, vol. 16, no. 9, pp. 1069–1080, 2008.

[13] S. Mobayen, "A novel global sliding mode control based on exponential reaching law for a class of underactuated systems with external disturbances," *Journal of Computational and Nonlinear Dynamics*, vol. 11, no. 2, 2016.

[14] M. Zhihong and D. Habibi, "A robust adaptive sliding-mode control for rigid robotic manipulators with arbitrary bounded input disturbances," *Journal of Intelligent & Robotic Systems*, vol. 17, no. 4, pp. 371–386, 1996.

[15] M. R. Soltanpour, S. Zaare, M. Haghgoo, and M. Moattari, "Free-chattering fuzzy sliding mode control of robot manipulators with joints flexibility in presence of matched and mismatched uncertainties in model dynamic and actuators," *Journal of Intelligent & Robotic Systems*, vol. 100, no. 1, pp. 47–69, 2020.

[16] S. P. Bhat and D. S. Bernstein, "Geometric homogeneity with applications to finite-time stability," *Mathematics of Control, Signals, and Systems*, vol. 17, no. 2, pp. 101–127, 2005.

[17] X. Li, X. Yang, and S. Song, "Lyapunov conditions for finite-time stability of time-varying time-delay systems," *Automatica*, vol. 103, pp. 135–140, 2019.

[18] S. P. Bhat and D. S. Bernstein, "Finite-time stability of continuous autonomous systems," *SIAM Journal on Control and Optimization*, vol. 38, no. 3, pp. 751–766, 2000.

[19] S. Mobayen, "Adaptive global terminal sliding mode control scheme with improved dynamic surface for uncertain nonlinear systems," *International Journal of Control, Automation and Systems*, vol. 16, no. 4, pp. 1692–1700, 2018.

[20] M. Zhihong, A. P. Paplinski, and H. R. Wu, "A robust MIMO terminal sliding mode control scheme for rigid robotic manipulators," *IEEE Transactions on Automatic Control*, vol. 39, no. 12, pp. 2464–2469, 1994.

[21] D. Zhao, S. Li, and F. Gao, "A new terminal sliding mode control for robotic manipulators," *International Journal of Control*, vol. 82, no. 10, pp. 1804–1813, 2009.

[22] L. Zhang, Y. Su, and Z. Wang, "A simple non-singular terminal sliding mode control for uncertain robot manipulators," *Proceedings of the Institution of Mechanical Engineers, Part I: Journal of Systems and Control Engineering*, vol. 233, no. 6, pp. 666–676, 2019.

[23] L. Yang and J. Yang, "Nonsingular fast terminal sliding-mode control for nonlinear dynamical systems," *International Journal of Robust and Nonlinear Control*, vol. 21, no. 16, pp. 1865–1879, 2011.

[24] S. Yu, X. Yu, B. Shirinzadeh, and Z. Man, "Continuous finite-time control for robotic manipulators with terminal sliding mode," *Automatica*, vol. 41, no. 11, pp. 1957–1964, 2005.

[25] L. Zhang, L. Liu, Z. Wang, and Y. Xia, "Continuous finite-time control for uncertain robot manipulators with integral sliding

mode," *IET Control Theory & Applications*, vol. 12, no. 11, pp. 1621–1627, 2018.

[26] Y. Su and C. Zheng, "A new nonsingular integral terminal sliding mode control for robot manipulators," *International Journal of Systems Science*, vol. 51, pp. 1–11, 2020.

[27] A. Polyakov and L. Fridman, "Stability notions and Lyapunov functions for sliding mode control systems," *Journal of the Franklin Institute*, vol. 351, no. 4, pp. 1831–1865, 2014.

[28] Y. Wang, M. Chen, and Y. Song, "Robust fixed-time inverse dynamic control for uncertain robot manipulator system," *Complexity*, vol. 2021, Article ID 6664750, 12 pages, 2021.

[29] A. Polyakov, D. Efimov, and W. Perruquetti, "Finite-time and fixed-time stabilization: implicit Lyapunov function approach," *Automatica*, vol. 51, pp. 332–340, 2015.

[30] B. Tian, H. Lu, Z. Zuo, and H. Wang, "Fixed-time stabilization of high-order integrator systems with mismatched disturbances," *Nonlinear Dynamics*, vol. 94, no. 4, pp. 2889–2899, 2018.

[31] Z. Zuo, "Nonsingular fixed-time consensus tracking for second-order multi-agent networks," *Automatica*, vol. 54, pp. 305–309, 2015.

[32] Z. Zuo, "Non-singular fixed-time terminal sliding mode control of non-linear systems," *IET Control Theory and Applications*, vol. 9, no. 4, pp. 545–552, 2014.

[33] Y. Su, C. Zheng, and P. Mercorelli, "Robust approximate fixed-time tracking control for uncertain robot manipulators," *Mechanical Systems and Signal Processing*, vol. 135, Article ID 106379, 2020.

[34] L. Zhang, Y. Wang, Y. Hou, and H. Li, "Fixed-time sliding mode control for uncertain robot manipulators," *IEEE Access*, vol. 7, pp. 149750–149763, 2019.

[35] Y. Zhang, C. Hua, and K. Li, "Disturbance observer-based fixed-time prescribed performance tracking control for robotic manipulator," *International Journal of Systems Science*, vol. 50, no. 13, pp. 2437–2448, 2019.

[36] A. J. Muñoz-Vázquez, G. Fernández-Anaya, J. D. Sánchez-Torres, and F. Meléndez-Vázquez, "Predefined-time control of distributed-order systems," *Nonlinear Dynamics*, vol. 103, no. 3, pp. 2689–2700, 2021.

[37] Y. Wang, Z. Wang, M. Chen, and L. Kong, "Predefined-time sliding mode formation control for multiple autonomous underwater vehicles with uncertainties," *Chaos, Solitons & Fractals*, vol. 144, Article ID 110680, 2021.

[38] J. D. Sánchez-Torres, M. Defoort, and A. J. Muñoz-Vázquez, "Predefined-time stabilisation of a class of nonholonomic systems," *International Journal of Control*, vol. 93, no. 12, pp. 2941–2948, 2020.

[39] E. Jiménez-Rodríguez, A. J. Muñoz-Vázquez, J. D. Sánchez-Torres, and A. G. Loukianov, "A note on predefined-time stability," *IFAC-PapersOnLine*, vol. 51, no. 13, pp. 520–525, 2018.

[40] C. A. Anguiano-Gijón, A. J. Muñoz-Vázquez, J. D. Sánchez-Torres, G. Romero-Galván, and F. Martínez-Reyes, "On predefined-time synchronisation of chaotic systems," *Chaos, Solitons & Fractals*, vol. 122, pp. 172–178, 2019.

[41] A. J. Muñoz-Vázquez, J. D. Sánchez-Torres, and C. A. Anguiano-Gijón, "Single-channel predefined-time synchronisation of chaotic systems," *Asian Journal of Control*, vol. 23, pp. 190–198, 2019.

[42] Q. Li and C. Yue, "Predefined-time modified function projective synchronization for multiscroll chaotic systems via sliding mode control technology," *Complexity*, vol. 2020, Article ID 6590502, 11 pages, 2020.

[43] Q. Li and C. Yue, "Predefined-time polynomial-function-based synchronization of chaotic systems via a novel sliding mode control," *IEEE Access*, vol. 8, pp. 162149–162162, 2020.

[44] A. J. Muñoz-Vázquez, J. D. Sánchez-Torres, E. Jiménez-Rodríguez, and A. G. Loukianov, "Predefined-time robust stabilization of robotic manipulators," *IEEE/ASME Transactions on Mechatronics*, vol. 24, no. 3, pp. 1033–1040, 2019.

Hindawi
Complexity
Volume 2021, Article ID 5207154, 8 pages
https://doi.org/10.1155/2021/5207154

Research Article

Finite-Time Impulsive Control of Financial Risk Dynamic System with Chaotic Characteristics

Li Ziyan,[1] **Tao Ke**,[2] **Xia Qing**,[3] **Xie Chengrong**,[4] **and Xu Yuhua**[2]

[1]*School of Politics and Public Administration, Soochow University, Suzhou 215000, China*
[2]*School of Finance, Nanjing Audit University, Nanjing 211815, Jiangsu, China*
[3]*School of Economics, Wuhan Donghu University, Wuhan 430212, China*
[4]*School of Statistics and Mathematics, Nanjing Audit University, Nanjing 211815, Jiangsu, China*

Correspondence should be addressed to Xia Qing; 77218434@qq.com

Received 10 April 2021; Revised 5 May 2021; Accepted 31 May 2021; Published 10 June 2021

Academic Editor: Xiaodi Li

The control of financial risk has always been one of the important topics in financial research. Based on the theory of finance, this paper proposes a kind of financial risk dynamic system. By analyzing some properties of the dynamic system, the system shows obvious coexisting chaotic oscillations. In order to control the financial risk dynamic system effectively, this paper proposes a finite-time impulse controller to control the financial risk dynamic system. Simulation results show that the finite-time impulse controller has faster convergence speed than the impulse controller.

1. Introduction

Since Lorenz discovered the strange attractor for the first time, various chaotic systems have been discovered one after another. Although there are a large number of chaotic systems, the development of chaotic dynamic models is relatively slow in the economic field [1]. Akhmet et al. investigated the generation of chaos in economic models through exogenous shocks [2]. Liu discussed the two-stage multiplier acceleration econometric model of the capitalist market and the investment model depicting the growth of socialist planned economy. Liu described the instability of the market economy, the cyclical change, and even chaos of the central planned socialist economy [3]. Peters, an American scholar, puts forward the fractal market hypothesis, which makes up for the serious deficiency of the efficient market hypothesis. In particular, it focused on the analysis of the impact of market liquidity and investment duration on investors' behavior, which directly established a model for the changes of investment behavior and price [4]. Liu and Wan discussed the bifurcation and control of the real-estate dynamic model based on the famous logistic wormhole model [5]. Du et al. took the two-dimensional dynamic production game model as an example, taking the form of one participant taking control and two participants participating in control at the same time, and successfully realized the control of chaos in the model [6]. Yu and Yu studied stability of Bayesian Nash equilibrium of the dynamic Cournot duopoly model [7]. Ma and Wang analyzed the bifurcation behavior of a new financial chaotic system [8]. Ding et al. discussed the bifurcation behavior of a class of nonlinear financial delay systems [9]. Ma and Bangura discussed the dynamic behavior of the economic system under the condition of parameter change [10]. We can see that most of the researchers discussed the evolution behavior of the discrete economic and financial chaotic dynamic model. In the economic and financial system, the continuous economic and financial dynamic model may better simulate the real economic and financial world in some extent because of the continuity of economic activities.

At present, many scholars had made extraordinary explorations on the control of economic and financial chaotic systems. For example, Du et al. discussed control of economic dynamical systems by adding upper bound or lower bound to state variables, which is different from the chaos stabilization in engineering or physics systems [11]. Wen

and Yang analyzed the stability of equilibrium solution of the fractional-order chaotic financial system and explored the complexity evolution law of the financial system [12]. Bella and Mattana proposed a suitable policy algorithm to eliminate or control the chaotic dynamics [13]. Sun et al. applied impulse control to the economic chaotic system, paying more attention to the feasibility of the control method. They achieved good results by saving money and improving efficiency through these methods [14].

Generally speaking, the simulation of economic phenomena based on dynamic principles and the effective control of nonlinear financial complex systems is always attracting in real world. In recent years, a variety of methods has been proposed to realize the effective control of nonlinear complex systems. For example, in [15–20], the authors proposed the impulse control method, which greatly saves the control cost. In [21–25], the authors proposed the finite-time control method, which saves the control time. Therefore, the finite-time impulse control method not only saves the control cost but also reduces the control cost. At the same time, it also saves control time, which will be an effective control method for the economic system [16, 26, 27]. Although some effort has been made in this field, the research on the evolution behavior of financial complex dynamic system based on finite-time impulse control has not received enough attention in recent years.

2. Chaotic Financial Model and its Basic Analysis

In [28], the author puts forward a three-stage cycle structure financial system risk model:

$$\begin{cases} \dot{x} = yz - ax, \\ \dot{y} = xz - by, \\ \dot{z} = cz - xy, \end{cases} \tag{1}$$

where x represents the total risk value of the system under the external or internal impact of the first stage, y represents the total risk value of the system under the infection effect of the second stage, z represents the value of the system risk control in the third stage, a represents the degree of risk, b represents the degree of control, and c represents the control strength. When $a = 4, b = 8$, and $c = 2$, system (1) shows chaotic phenomenon.

Since external or internal shocks directly affect the intensity of contagion effect, the financial system risk model (1) can be modified as follows:

$$\begin{cases} \dot{x} = yz - ax, \\ \dot{y} = xz - by + \mathrm{d}x, \\ \dot{z} = -xy + cz, \end{cases} \tag{2}$$

when $a = 4$, $b = 1$, $c = 1$, and $d = 1$, the system is in a chaotic state. The corresponding pair of attractors is shown in Figure 1. It can be seen that when the initial values of the system are different, the chaotic attractors have rotational symmetry, which can be proved by the transformation invariance of the system equation. When $x \longrightarrow -x$, $y \longrightarrow -y$, and $z \longrightarrow z$, the system equation remains unchanged.

Figure 2 shows that the financial system risk model has initial value sensitivity when $a = 4$, $b = 1$, $c = 1$, and $d = 1$. It can be seen from Figure 2 that the slight change of initial value has a great impact on the solution of the system.

3. Bifurcation Analysis

Due to the rotational symmetry of the system and the existence of a pair of coexisting chaotic attractors under the above parameters, the system presents coexistence bifurcation behavior when the system parameters evolve in a certain interval. As shown in Figure 3, when $b = 1$, $c = 1$, and $d = 1$, a changes in the interval [1.57, 9.57]. The system has two bifurcation paths. At the same time, the Lyapunov exponent of the system has the same evolution law. The left plot shows a pair of symmetrical bifurcations under two sets of initial conditions, while the right one shows that coexisting bifurcations obey unified Lyapunov exponents.

When $a = 4$, $c = 1$, and $d = 1$, b changes in the interval [0.1, 2.1], and the system has two similar bifurcation paths, as shown in Figure 4.

When $a = 4$, $b = 1$, and $d = 1$, c changes in the interval [0.75, 3], and the system has two similar bifurcation paths, as shown in Figure 5.

It is interesting that the parameter d of system (1) can vary in a large range of positive and negative ranges when the system presents different chaotic motions. Figure 6 shows the bifurcation diagram and Lipschitz exponent spectrum of the system when d changes in the interval [−25, 25].

Typically, when $d = 0, -1, -10, -12, -18, 20$, the solution of the system is shown in Figure 7.

In system (1), the x feedback term of the second dimension can be negative. When $b = 1$, $c = 1$, and $d = -1$, the bifurcation diagram and Lipschitz exponent spectrum of the system are shown in Figure 8. It can be seen that the system also presents a pair of coexisting bifurcations.

The above analysis shows that system (2) has the property of coexisting chaos, which brings great risk in real financial world. Therefore, in the following section, an effective method is explored to control the stability of system (2). Among many schematics, we select finite-time impulsive control, which is one of the effective methods to save control cost [13].

4. Finite-Time Impulsive Control of Chaotic Financial System

Lemma 1 (see [26]). *For $\delta_i \geq 0, i = 1, \ldots, n$, $0 < \varsigma \leq 1$, there are*

$$\sum_{i=1}^{n} \delta_i^{\varsigma} \geq \left(\sum_{i=1}^{n} \delta_i \right)^{\varsigma}. \tag{3}$$

Lemma 2 (see [29]). *Suppose a continuous positive definite function satisfies the following differential inequalities:*

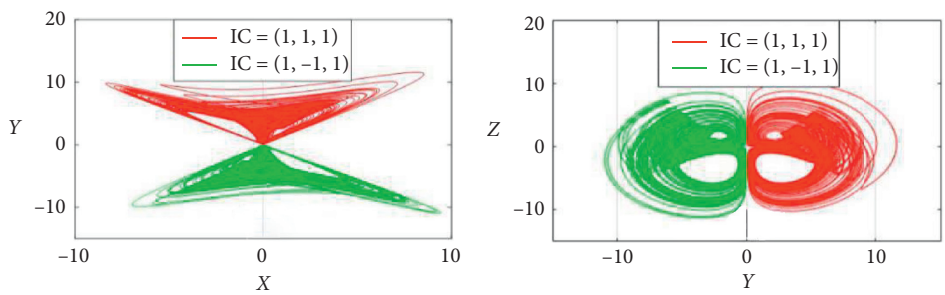

(a) (b)

Figure 1: Projections of chaotic attractors from system (1) with $a = 4$, $b = 1$, $c = 1$, and $d = 1$: (a) plane $x - y$; (b) plane $y - z$. IC represents the initial condition.

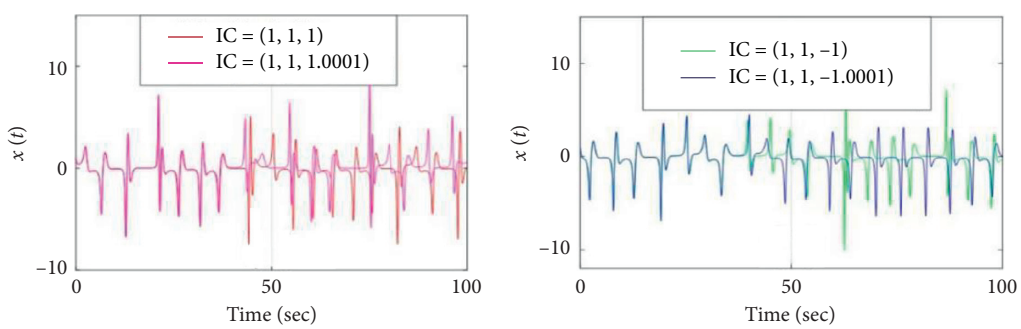

(a) (b)

Figure 2: Initial value sensitivity of system (2) with $a = 4$, $b = 1$, $c = 1$, and $d = 1$: (a) $x(t)$ in positive attractor and (b) $x(t)$ in negative attractor.

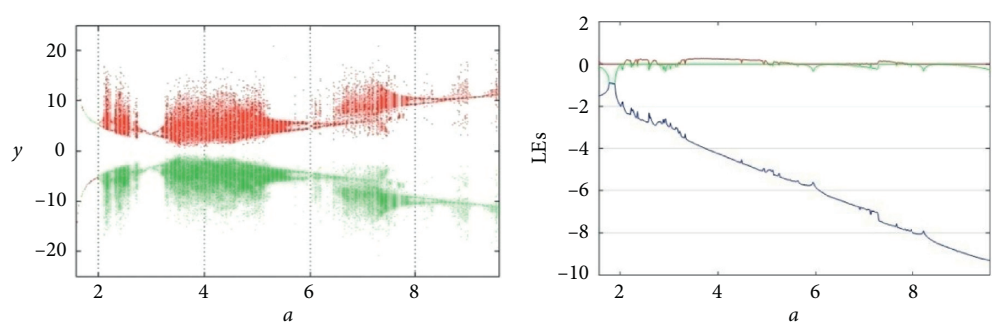

(a) (b)

Figure 3: Dynamical behavior of system (1) with $b = 1$, $c = 1$, and $d = 1$, and a varies in [1.57, 9.57]: (a) bifurcation diagram ($z = 0$), (x_0, y_0, z_0) = (1, 1, 1) is red, and (x_0, y_0, z_0) = (−1, −1, 1) is green; (b) Lyapunov exponents (LEs).

$$\begin{aligned} &\dot{v}(t) \le -kv^{\eta}(t), \\ &v(t_0) \ge 0, \quad \forall t \ge t_0, k > 0, 0 < \eta < 1. \end{aligned} \tag{4}$$

Then, for any given t_0, $v(t)$ satisfies the following inequality:

$$v(t) \le e^{l(t-t_0)}\left(v^{1-\eta}(t_0) + \frac{k}{l} - \frac{k}{l}e^{l(1-\eta)(t-t_0)}\right)^{1/(1-\eta)}, \quad t_0 \le t \le T, \tag{5}$$

and $v(t) = 0, t \ge T$ with T is given by

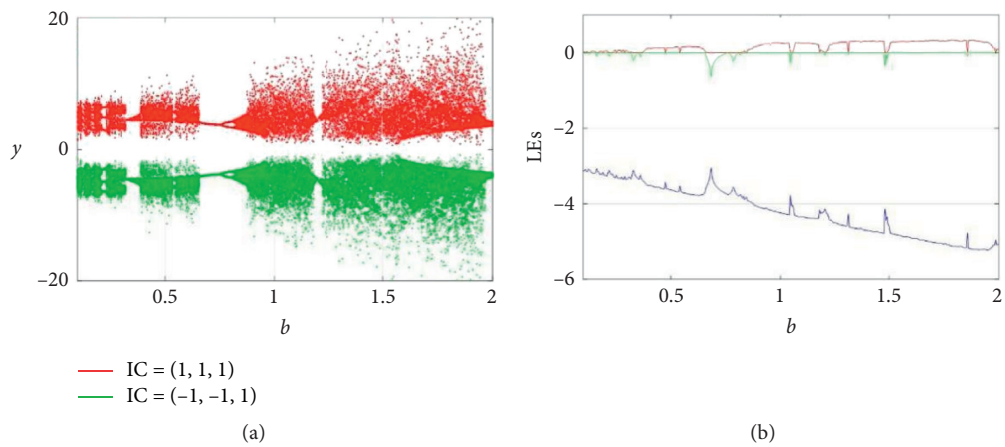

Figure 4: Dynamical behavior of system (1) with $a = 4$, $c = 1$, and $d = 1$, and b varies in [0.1, 2.1]: (a) bifurcation diagram ($z = 0$), (x_0, y_0, z_0) = (1, 1, 1) is red, and (x_0, y_0, z_0) = (−1, −1, 1) is green; (b) Lyapunov exponents.

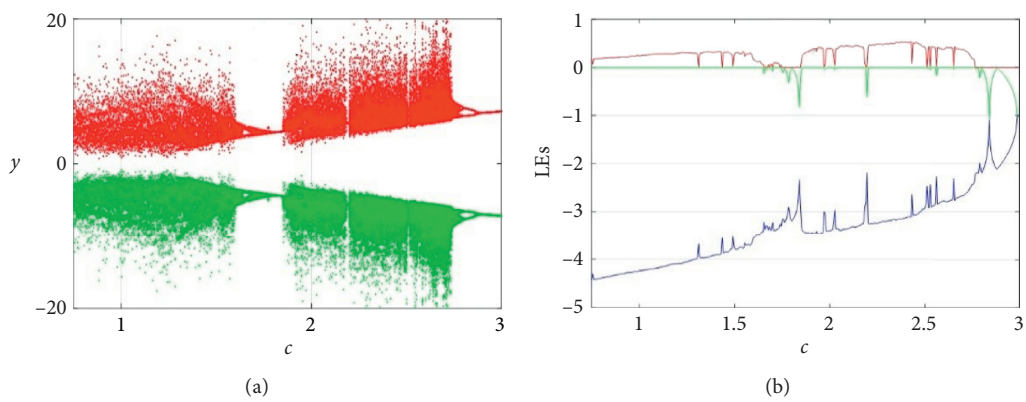

Figure 5: Dynamical behavior of system (1) with $a = 4$, $b = 1$, and $d = 1$, and c varies in [0.75, 3]: (a) bifurcation diagram ($z = 0$), (x_0, y_0, z_0) = (1, 1, 1) is red, and (x_0, y_0, z_0) = (−1, −1, 1) is green; (b) Lyapunov exponents.

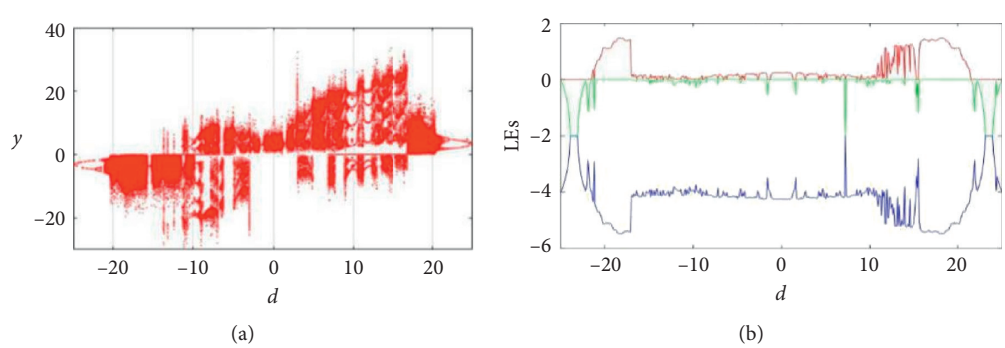

Figure 6: Dynamical behavior of system (1) with $a = 4$, $b = 1$, and $c = 1$, (x_0, y_0, z_0) = (1, 1, 1), and d varies in [−25, 25]: (a) bifurcation diagram ($x = 0$); (b) Lyapunov exponents.

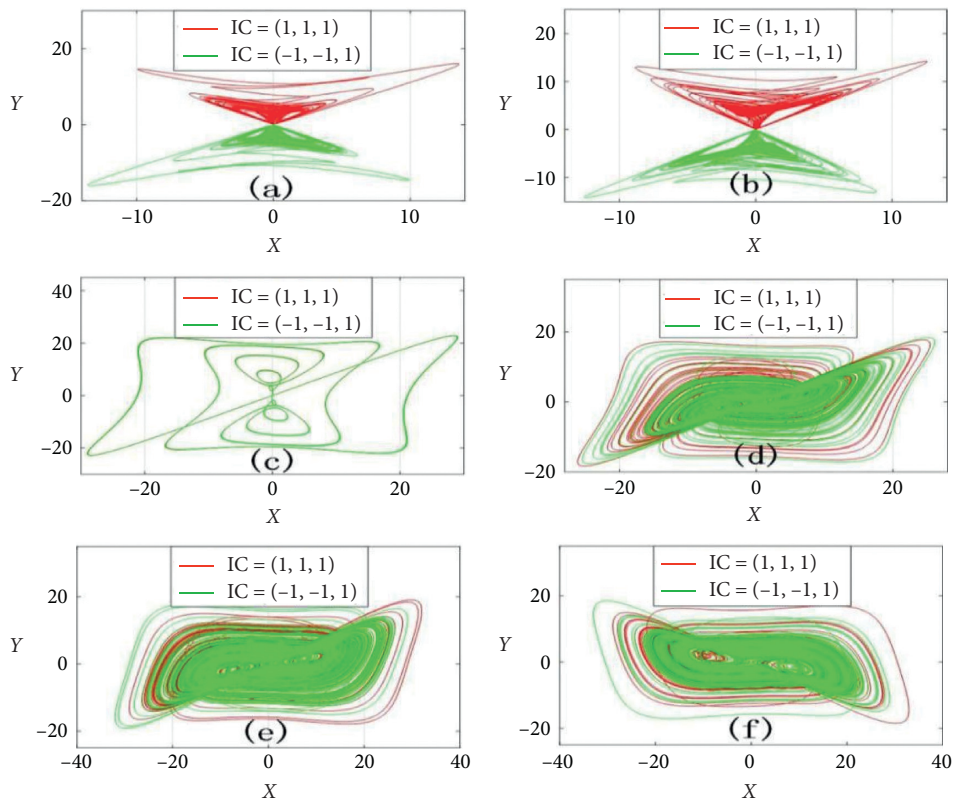

Figure 7: Typical attractors of system (1) with $a = 4$, $b = 1$, and $c = 1$: (a) $d = 0$, (b) $d = -1$, (c) $d = -10$, (d) $d = -12$, (e) $d = -18$, and (f) $d = 20$.

$$T \le t_0 + \frac{v^{1-\eta}(t_0)}{l(1-\eta)}. \tag{6}$$

Remark 1. For an impulsive system, if it is stable in a finite time, we call it impulsive stable in a finite time.

We consider coupled impulsive control of the chaotic financial system as follows:

$$\begin{cases} \dot{x}_1 = x_2x_3 - ax_1 + u_1, & t \ne t_k, \\ \dot{x}_2 = x_1x_3 - bx_2 + \mathrm{d}x_1 + u_2, & t \ne t_k, \\ \dot{x}_3 = -x_1x_2 + cx_3 + u_3, & t \ne t_k, \\ \Delta x = B(x-y) = -Bw, & t = t_k. \end{cases} \tag{7}$$
$$\begin{cases} \dot{y}_1 = y_2y_3 - ay_1 + u_1, & t \ne t_k, \\ \dot{y}_2 = y_1y_3 - by_2 + \mathrm{d}y_1 + u_2, & t \ne t_k, \\ \dot{y}_3 = -y_1y_2 + cy_3 + u_3, & t \ne t_k, \\ \Delta y = B(y-x) = Bw, & t = t_k, \end{cases}$$

where $x = (x_1, x_2, x_3)^T \in R^3$ and $y = (y_1, y_2, y_3)^T \in R^3$.

The finite-time controller is

$$\begin{cases} u_1 = x_2x_3 - y_2y_3 - kw_1 - l\mathrm{sgn}(w_1)w_1^{\delta}, \\ u_2 = x_1x_3 - y_1y_3 - kw_2 - l\mathrm{sgn}(w_2)w_2^{\delta}, \\ u_3 = y_1y_2 - x_1x_2 - kw_3 - l\mathrm{sgn}(w_3)w_3^{\delta}, \end{cases} \tag{8}$$

where $w = (w_1, w_2, w_3)^T = (y_1 - x_1, y_2 - x_2, y_3 - x_3)^T$ and $0 < \delta < 1$.

So, the error impulsive systems is

$$\begin{cases} \dot{w}_1 = y_2y_3 - x_2x_3 - aw_1 + u_1, & t \ne t_k, \\ \dot{w}_2 = y_1y_3 - x_1x_3 - bw_2 + \mathrm{d}y_1 + u_2, & t \ne t_k, \\ \dot{w}_3 = -y_1y_2 + x_1x_2 + cw_3 + u_3, & t \ne t_k, \\ \Delta w = 2Bw, & t = t_k, \end{cases} \tag{9}$$

where $w = (w_1, w_2, w_3)^T = (y_1 - x_1, y_2 - x_2, y_3 - x_3)^T$.

The objective is to find some conditions on the control gains, B, and the impulsive distances $t_k - t_{k-1}$, $k = 1, 2, \ldots$, such that the impulsive system (9) is asymptotical stable.

Theorem 1. *If there exists two constants $\alpha \ge 1$, $\rho > 0$, and $\beta = \lambda_{\max}[(I + 2B)^T(I + 2B)]$, then the error impulsive system (9) can realize finite-time stable under impulsive condition $\ln \alpha\beta + \rho(t_k - t_{k-1}) \le 0$.*

Proof. Let

$$v(w) = w^Tw = w_1^2 + w_2^2 + w_3^2. \tag{10}$$

The time derivative along trajectory (9) is

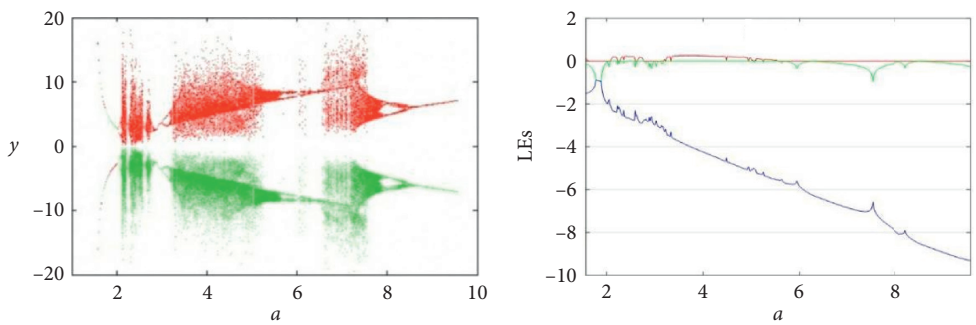

(a) (b)

Figure 8: Dynamical behavior of system (1) with $b = 1$, $c = 1$, and $d = -1$, and a varies in [1.57, 9.57]: (a) bifurcation diagram ($z = 0$), (x_0, y_0, z_0) = (1, 1, 1) is red, and (x_0, y_0, z_0) = (−1, −1, 1) is green; (b) Lyapunov exponents.

$$\begin{aligned}\dot{v}(w) &= 2\dot{w}_1 w_1 + 2\dot{w}_2 w_2 + 2\dot{w}_3 w_3 \\ &= 2w_1\left[-aw_1 - kw_1 - l\operatorname{sgn}(w_1)w_1^{\delta}\right] \\ &\quad + 2w_2\left[-bw_2 - kw_2 - l\operatorname{sgn}(w_2)w_2^{\delta}\right] \\ &\quad + 2w_3\left[cw_3 - kw_3 - l\operatorname{sgn}(w_3)w_3^{\delta}\right] \\ &\le -2(a+k)w_1^2 - 2(b+k)w_2^2 - 2(k-c)w_3^2 \le \rho v(w(t)),\end{aligned} \tag{11}$$

where $\rho = \max\{a + k, b + k, k - c\}$.

So,

$$\begin{aligned}&v(w(t)) \le v(w(t_{k-1}^+))\exp(\rho(t - t_{k-1})), \\ &\qquad t \in (t_{k-1}, t_k], k = 1, 2, \ldots, \\ &v(w(t_k^+)) = [(I + B)w]^T (I + 2B)w \\ &\qquad = w^T\left[(I + 2B)^T (I + 2B)\right]w \le \beta w^T w = \beta v(w(t_k)).\end{aligned} \tag{12}$$

For $t \in (t_0, t_1]$, $v(w(t)) \le v(w(t_0^+))\exp(\rho(t - t_0))$; then,

$$v(w(t_1)) \le v(w(t_0^+))\exp(\rho(t_1 - t_0)). \tag{13}$$

So,

$$v(w(t_1^+)) \le \beta v(w(t_1)) \le \beta v(w(t_0^+))\exp(\rho(t_1 - t_0)). \tag{14}$$

In the same way, for $t \in (t_1, t_2]$, we have

$$\begin{aligned}v(w(t)) &\le v(w(t_1^+))\exp(\rho(t - t_1)) \\ &\le \beta v(w(t_0^+))\exp(\rho(t - t_0)).\end{aligned} \tag{15}$$

In general, for any $t \in (t_k, t_{k+1}]$, one finds that

$$v(w(t)) \le v(w(t_0^+))\beta^k \exp(\rho(t - t_0)). \tag{16}$$

So, $\forall t \in (t_k, t_{k+1}]$, $k = 1, 2, \ldots$, and we have

$$\begin{aligned}v(w(t)) &\le v(w(t_0^+))\beta^k \exp(\rho(t - t_0)) \\ &\le v(w(t_0^+))\beta^k \exp(\rho(t_{k+1} - t_0)) \\ &= v(w(t_0^+))\beta \exp(\rho(t_2 - t_1))\beta \exp(\rho(t_3 - t_2)) \\ &\quad \cdots \beta \exp(\rho(t_{k+1} - t_k))\exp(\rho(t - t_0)).\end{aligned} \tag{17}$$

As

$$\beta \exp(\mu(t_{k+1} - t_k)) \le \frac{1}{\alpha}, \quad k = 1, 2, \ldots, \tag{18}$$

we have

$$v(w(t)) \le v(w(t_0^+))\frac{1}{\alpha^k}\exp(\rho(t - t_0)), \tag{19}$$

so

$$v(w(t)) \le v(w(t_0^+))\frac{1}{\alpha^k}\exp(\rho(t - t_0)), \quad t \ge t_0. \tag{20}$$

For $\alpha \ge 1$, from [30], it implies that the origin in system (9) is impulsive stable.

On the contrary,

$$\begin{aligned}\dot{v}(w) &= 2\dot{w}_1 w_1 + 2\dot{w}_2 w_2 + 2\dot{w}_3 w_3 \\ &= 2w_1\left[-aw_1 - kw_1 - l\operatorname{sgn}(w_1)w_1^{\delta}\right] \\ &\quad + 2w_2\left[-bw_2 - kw_2 - l\operatorname{sgn}(w_2)w_2^{\delta}\right] \\ &\quad + 2w_3\left[cw_3 - kw_3 - l\operatorname{sgn}(w_3)w_3^{\delta}\right] \\ &= -2(a+k)w_1^2 - 2(b+k)w_2^2 - 2(k-c)w_3^2 \\ &\quad - 2lw_1\operatorname{sgn}(w_1)w_1^{\delta} - 2lw_2\operatorname{sgn}(w_2)w_2^{\delta} \\ &\quad - 2lw_3\operatorname{sgn}(w_3)w_3^{\delta} \\ &\le -2lw_1\operatorname{sgn}(w_1)w_1^{\delta} - 2lw_2\operatorname{sgn}(w_2)w_2^{\delta} \\ &\quad - 2lw_3\operatorname{sgn}(w_3)w_3^{\delta} \\ &= -2l\left(|w_1|^{\delta+1} + |w_2|^{\delta+1} + |w_2|^{\delta+1}\right).\end{aligned} \tag{21}$$

From Lemma 1,

$$\begin{aligned}&\left(|w_1|^{\delta+1} + |w_2|^{\delta+1} + |w_2|^{\delta+1}\right) \\ &\quad = \left(\left(w_1^2\right)^{(\delta+1/2)} + \left(w_2^2\right)^{(\delta+1/2)} + \left(w_3^2\right)^{(\delta+1/2)}\right) \\ &\quad \ge \left(w_1^2 + w_2^2 + w_3^2\right)^{(\delta+1/2)},\end{aligned} \tag{22}$$

so

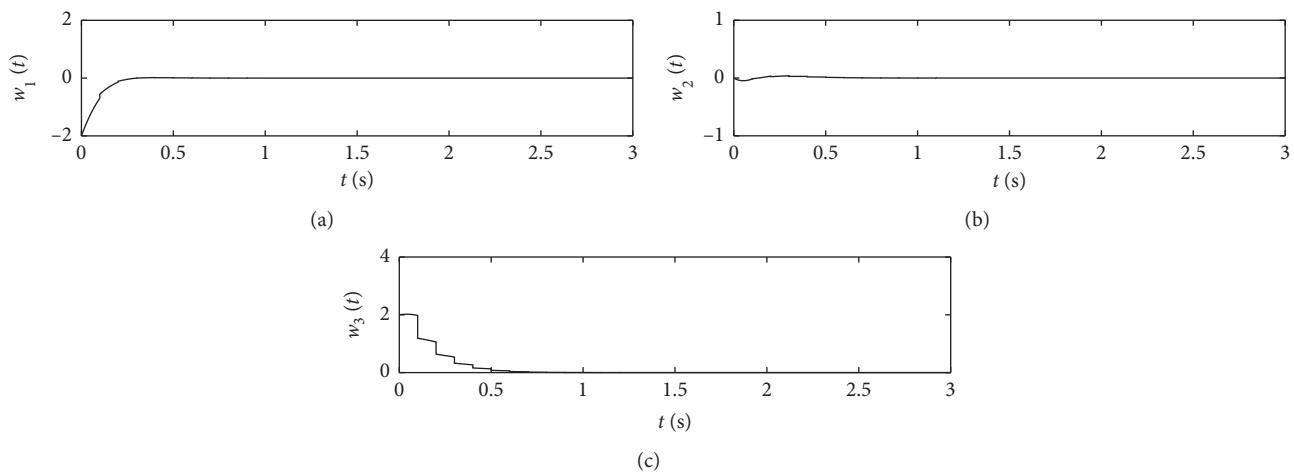

Figure 9: Finite-time impulsive synchronization errors.

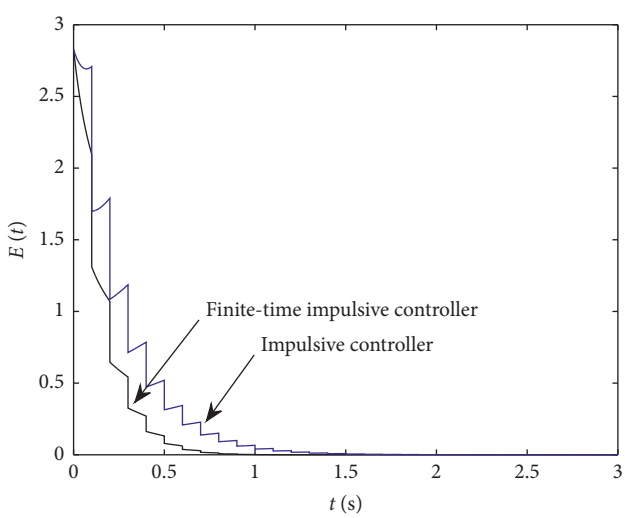

Figure 10: Comparison between finite-time impulsive controller and impulsive controller.

$$\dot{v}(w) \leq -2l\left(w_1^2 + w_2^2 + w_3^2\right)^{(\delta+1/2)} = -2lv^{(\delta+1/2)}. \quad (23)$$

From Lemma 2, system (9) is finite-time stable.

To sum up, system (9) can realize finite-time stable under impulsive condition. □

Remark 2. In [15, 16, 18], the authors put forward the principle of impulsive control in nonlinear systems, and their conclusions provide the basic theoretical foundation for this paper. However, the exact finite-time impulsive controller of financial systems needs to be designed.

In the following simulation, we set $a = 4$, $b = 1$, $c = 1$, $d = 1$, $B = \mathrm{diag}(-0.2, -0.3, -0.4)$, $\rho = 6$, $k = 2$, and $l = 1$; then, $\beta = 0.36$. Let $\alpha = 1.2$, from $\ln \alpha\beta + \rho(t_k - t_{k-1}) \leq 0$; then, $t_k - t_{k-1} \leq 0.1399$ and we let $t_k - t_{k-1} = 0.1$. The initial conditions of the master and slave systems are (1, 2, 3) and (3, 2, 1). In Figure 9, three state errors versus time are shown and the state errors tend to zero asymptotically as time evolves under finite-time impulsive controller. Let $E(t) = \sqrt{w_1^2 + w_2^2 + w_3^2}$; Figure 10 shows the finite-time impulsive controller has faster convergence speed than impulsive controller.

5. Conclusion and Discussion

The paper has presented a new chaotic financial system and discussed some basic dynamic behavior of the new system. Although many approaches have been reported for chaos control, many of them are associated with amplitude control [31, 32] and offset boosting [33–35] without removing the inherent chaos. In this work, based on finite-time control theory, the finite-time impulsive synchronization criterion of the new chaotic financial system has been studied and proposed. The results of numerical simulation prove that they are feasible for the new financial system, and finite-time impulse control of the economic system provides a helpful reference scheme for real economic world. As the coexisting chaos-embedded bifurcations of economic system brings great risk to the economy, if the bifurcation behavior of economic system can be controlled by the finite-time impulse method, the instability of the system will be reduced, which will be our next research topic.

Data Availability

No data were used to support this study.

Conflicts of Interest

The authors declare that there are no conflicts of interest regarding the publication of this paper.

Acknowledgments

The authors are grateful to J. C. Sprott for helping with parameter selection that led to this work. This work was supported by the National Natural Science Foundation of China (61871230), the Major Natural Science Foundation of Jiangsu Higher Education Institutions (20KJA120002), the

Natural Science Foundation of Jiangsu Higher Education Institutions (19KJB120007), the Natural Science Foundation of Jiangsu Province (BK20181418), and the Six Talent Peaks Project in Jiangsu Province (DZXX-019).

References

[1] Y. Xu, Z. Ke, W. Zhou, and C. Xie, "Dynamic evolution analysis of stock price fluctuation and its control," *Complexity*, vol. 2018, Article ID 5728090, 9 pages, 2018.

[2] M. Akhmet, Z. Akhmetova, and M. O. Fen, "Chaos in economic models with exogenous shocks," *Journal of Economic Behavior & Organization*, vol. 106, pp. 95–108, 2014.

[3] H. Liu, *Chaos Theory and Method of Economic System Prediction*, Science Press, Beijing, China, 2003.

[4] E. E. Peters, *Fractal Market Analysis: Applying Chaos Theory to Investment and Economics*, Wiley Finance, Hoboken, NJ, USA, 1994.

[5] J. Liu and W. Han, "OGY chaos control strategy for real estate investment bubble," *Systems Engineering*, vol. 3, pp. 41–43, 2002.

[6] J. Du, Z. Sheng, and H. Yao, "Threshold control method for a class of chaotic economic model," *Systems Engineering—Theory & Practice*, vol. 10, pp. 27–32, 2004.

[7] W. Yu and Y. Yu, "The stability of Bayesian Nash equilibrium of dynamic cournot duopoly model with asymmetric information," *Communications in Nonlinear Science and Numerical Simulation*, vol. 63, pp. 101–116, 2018.

[8] C. Ma and X. Wang, "Hopf bifurcation and topological horseshoe of a novel finance chaotic system," *Communications in Nonlinear Science and Numerical Simulation*, vol. 17, no. 2, pp. 721–730, 2012.

[9] Y. Ding, W. Jiang, and H. Wang, "Hopf-pitch fork bifurcation and periodic phenomenain nonlinear financial system with delay," *Chaos, Solitons & Fractals*, vol. 45, no. 8, pp. 1048–1057, 2012.

[10] J. Ma and H. I. Bangura, "Complexity analysis research of financial and economic system under the condition of three parameters' change circumstances," *Nonlinear Dynamics*, vol. 70, no. 4, pp. 2313–2326, 2012.

[11] J. Du, T. Huang, Z. Sheng, and H. Zhang, "A new method to control chaos in an economic system," *Applied Mathematics and Computation*, vol. 217, no. 6, pp. 2370–2380, 2010.

[12] C. Wen and J. Yang, "Complexity evolution of chaotic financial systems based on fractional calculus," *Chaos, Solitons & Fractals*, vol. 128, pp. 242–251, 2019.

[13] G. Bella and P. Mattana, "Chaos control in presence of financial bubbles," *Economics Letter*, vol. 193, Article ID 109314, 2020.

[14] J. Sun, F. Qiao, and Q. Wu, "Impulsive control of a financial model," *Physics Letters A*, vol. 335, no. 4, pp. 282–288, 2005.

[15] X. Li, X. Yang, and T. Huang, "Persistence of delayed cooperative models: impulsive control method," *Applied Mathematics and Computation*, vol. 342, pp. 130–146, 2019.

[16] X. Li, J. Shen, and R. Rakkiyappan, "Persistent impulsive effects on stability of functional differential equations with finite or infinite delay," *Applied Mathematics and Computation*, vol. 329, pp. 14–22, 2018.

[17] X. Li, J. Shen, H. Akca, and R. Rakkiyappan, "LMI-based stability for singularly perturbed nonlinear impulsive differential systems with delays of small parameter," *Applied Mathematics and Computation*, vol. 250, pp. 798–804, 2015.

[18] R. Rao and S. Zhong, "Impulsive control on delayed feedback chaotic financial system with Markovian jumping," *Advances in Difference Equations*, vol. 2020, no. 1, 2020.

[19] P. Li, X. Li, and J. Lu, "Input-to-state stability of impulsive delay systems with multiple impulses," *IEEE Transactions on Automatic Control*, vol. 66, no. 1, pp. 362–368, 2020.

[20] Y. Wang, J. Lu, and Y. Lou, "Halanay-type inequality with delayed impulses and its applications," *Science China Information Sciences*, vol. 62, no. 9, Article ID 192206, 2019.

[21] Y. Xu, X. Wu, N. Li, L. Liu, C. Xie, and C. Li, "Fixed-time synchronization of complex networks with a simpler nonchattering controller," *IEEE Transactions on Circuits and Systems II: Express Briefs*, vol. 67, no. 4, pp. 700–704, 2020.

[22] Y. Xu, X. Wu, B. Mao, and C. Xie, "A unified finite-/fixed-time synchronization approach to multi-layer networks," *IEEE Transactions on Circuits and Systems II: Express Briefs*, vol. 68, no. 1, pp. 311–315, 2021.

[23] Y. Xu, X. Wu, B. Mao, J. Lü, and C. Xie, "Fixed-time synchronization in pth moment for time-varying delay stochastic multilayer networks," *IEEE Transactions on Systems, Man, and Cybernetics: Systems*, vol. 99, pp. 1–10, 2020.

[24] Y. Xu, X. Wu, B. Mao, J. Lü, and C. Xie, "Finite-time intra-layer and inter-layer quasi-synchronization of two-layer multi-weighted networks," *IEEE Transactions on Circuits and Systems I: Regular Papers*, vol. 68, no. 4, pp. 1589–1598, 2021.

[25] J. Lu, Y. Wang, X. Shi, and J. Cao, "Finite-time bipartite consensus for multi-agent systems under detail-balanced antagonistic interactions," *IEEE Transactions on Systems, Man, and Cybernetics: Systems*, vol. 51, no. 6, pp. 3867–3875, 2021.

[26] X. Li, D. W. C. Ho, and J. Cao, "Finite-time stability and settling-time estimation of nonlinear impulsive systems," *Automatica*, vol. 99, pp. 361–368, 2019.

[27] Q. Xi, Z. Liang, and X. Li, "Uniform finite-time stability of nonlinear impulsive time-varying systems," *Applied Mathematical Modelling*, vol. 91, pp. 913–922, 2021.

[28] Y. Xu, C. Xie, and Y. Wang, "Evolution mechanism of financial system risk," *Statistics and Decision Making*, vol. 1, pp. 172–175, 2016.

[29] Y. Xu, W. Zhou, J. a. Fang, C. Xie, and D. Tong, "Finite-time synchronization of the complex dynamical network with non-derivative and derivative coupling," *Neurocomputing*, vol. 173, pp. 1356–1361, 2016.

[30] B. Jiang, J. Lu, and Y. Liu, "Exponential stability of delayed systems with average-delay impulses," *SIAM Journal on Control and Optimization*, vol. 58, no. 6, pp. 3763–3784, 2020.

[31] C. Li, J. Clinton Sprott, A. Akgul, H. H. C. Iu, and Y. Zhao, "A new chaotic oscillator with free control," *Chaos*, vol. 27, Article ID 083101, 2017.

[32] C. Li, W. Joo-Chen Thio, H. Ho-Ching Iu, and T. Lu, "A memristive chaotic oscillator with increasing amplitude and frequency," *IEEE Access*, vol. 6, pp. 12945–12950, 2018.

[33] C. Li, T. Lei, X. Wang, and G. Chen, "Dynamics editing based on offset boosting," *Chaos*, vol. 30, Article ID 063124, 2020.

[34] T. Lu, C. Li, X. Wang, C. Tao, and Z. Liu, "A memristive chaotic system with offest-boostable conditional symmetry," *European Physical Journal Special Topics*, vol. 229, no. 6-7, pp. 1059–1069, 2020.

[35] C. Li, G. Chen, J. Kurths, T. Lei, and Z. Liu, "Dynamic transport: from bifurcation to multistability," *Communications in Nonlinear Science and Numerical Simulation*, vol. 95, Article ID 105600, 2021.